Role of fascin in regulating microtubule and focal adhesion dynamics in carcinoma cells

Villari, Giulia

Awarding institution:
King's College London

Role of fascin in regulating microtubule and focal adhesion dynamics in carcinoma cells

A thesis submitted to King's College London for the degree of Doctor in Philosophy, October 2013

by

Giulia Villari

Randall Division of Cell and Molecular Biophysics
King's College London

Acknowledgements

I would like to thank my supervisors, Dr Maddy Parsons and Prof Gareth Jones for their support in this thesis. In particular, I would like to thank Maddy for being an enthusiastic and inspiring supervisor. I would also like to thank everyone in Parsons' lab and the Randall Cell Motility groups for giving me help and advice. A special thank goes to Asier for being the most helpful and supportive colleague but above all a good friend. I also thank James for helping me with the molecular biology. Thanks to Karl, Rumena, Mali, John, Christina, Pat, Rachael, Richard, Louise and all the students who shared this experience with me. I would also like to thank the all Randall Division for being such a welcoming and friendly work environment.

Thanks to my London 'family': Flavia, Eleonora, Stefano, Luca, Dario, Andrea and Nicola. Thanks to the beautiful 'Finniha' girl team, Viviane, Eleonora, Cecilia, and Barbara for the chat and laughter. Thanks to my friend and flat-mate Joe for being so present and cheerful.

Finally, I would like to thank my family and friends in Italy for always giving me strength and motivation.

Abstract

Fascin is an actin-bundling protein whose upregulation is correlated with poor prognosis in cancer. Previous studies have shown a role for fascin in regulating assembly of actin bundles and stability of adhesion structures. Fascin has not previously been localised at focal adhesions and the mechanisms by which it contributes to adhesion dynamics and assembly is still unknown. The aim of this thesis is to investigate whether fascin regulates focal adhesion (FA) dynamics and tumour cell invasion through control of actin and microtubule (MT) crosstalk. To analyse this, MT network integrity and focal adhesion area were quantified in control, fascin knockdown (KD) and fascin mutant rescued breast carcinoma cells treated with the MT-depolymerising agent nocodazole or following washout of this drug. Fascin KD cells showed a delay in the recovery of MT re-growth, increased MT stability and an increase in FA area following drug washout, compared to control cells. Both events were rescued by the re-expression of WT and S39A fascin (which constitutively associates with F-actin), but also by S39D fascin (is unable to bind F-actin). Interestingly, MT and FA assembly were increased compared to controls in cells re-expressing fascin that is mutated within a recently identified additional c-terminal actin-binding domain (S274D). To investigate whether there is a direct binding between MT and fascin that may explain these altered MT dynamics, I performed *in vitro* MT polymerisation/binding assays, in absence and presence of actin. WT and all fascin mutants showed association with tubulin in biochemical co-sedimentation assays. Interestingly, S274D fascin soluble fraction was not increased in the presence of actin, suggesting mutations in this actin-binding site are preferentially involved in controlling association with MT. To elucidate the mechanism regulating fascin binding to MT and its role in FA dynamics, I considered the Focal Adhesion Kinase (FAK) as a possible downstream effector. I found fascin to form a complex with FAK. In addition I showed fascin-FAK complex formation to be dependent on MT cytoskeleton integrity/stability and fascin-binding to F-actin and MT. Thus, fascin regulates MT and adhesion dynamics coordinating the actin-MT crosstalk and contributing towards carcinoma cell invasion.

Table of Contents

Table of Figures

Table of Tables

List of Movies

Movie1	mcherry-α-tubulin HeLa control cells	Figure 3.2e
Movie 2	mcherry-α-tubulin HeLa fascin knockdown cells	Figure 3.2e
Movie 3	MDA-MB-231 control cells during the nocodazole treatment and washout assay (Intereference Reflection Microscopy, IRM)	Figure 3.10, first row
Movie 4	MDA-MB-231 fasKD cells during the nocodazole treatment and washout assay (IRM)	Figure 3.10, second row
Movie 5	MDA-MB-231 fasKD rescued for GFP-WT fascin expression during the nocodazole treatment and washout assay (IRM)	Figure 3.10, third row

Abbreviations

2D	2-dimensional
3D	3-dimensional
30’ or 60’W	30 or 60 minute nocodazole washout
A	Alanine
ADP	Adenosine diphosphate
APS	Ammonium persulphate
Arp2	Actin related protein 2
Arp3	Actin related protein 3
ATP	Adenosine triphosphate
BSA	Bovine Serum Albumin
Control or ctrl cells	Cells stably expressing a shRNA targeting a scramble sequence – expressing endogenous human fascin
COL I or COL	Collagen type I
D	Aspartic acid
DMEM	Dulbecco’s Modified Eagle’s Medium
DMSO	Dimethyl sulfoxide
DNTPs	Deoxynucleosides
ECM	Extracellular matrix
EM	Electron microscopy
F-actin	Filamentous actin
FA	Focal adhesion
FACS	Fluorescence-activated cell sorting
FAK	Focal Adhesion Kinase
FasKD cells	Cells stably expressing a shRNA targeting human fascin expression
Fas WT	Fascin wild type
Fas S39A	Fascin serine 39 fascin mutated into Alanine
Fas S39D	Fascin serine 39 fascin mutated into Aspartic Acid
Fas S274A	Fascin serine 274 fascin mutated into Alanine

Fas S274D	Fascin serine 274 mutated into Aspartic acid
FAT	FA-targeting
FB	Fibrillar adhesion
FBS	Fetal Bovine Serum
FC	Focal complexes
FERM	Protein 4.1, Ezrin, Radixin, Moesin
FMN	Formin
FN	Fibronectin
FSCN	Fascin gene
G-actin	Monomeric actin
GAPs	GTPase-activated protein
GDP	Guanosine diphosphate
GEFs	Guanine nucleotide exchange factors
GFs	Growth factors
GFP	Green fluorescent protein
GTB	General Tubulin Buffer
GTP	Guanosine triphosphate
GTPases	Guanosine triphosphate-binding proteins
hFascin	Human fascin
h	Hour(s)
HRP	Horseradish peroxidase
IF	Immunofluorescence
Ig	Immunoglobulin
IP	Immunoprecipitation
IRM	Interference Reflection Microscopy
KCL	King's College London
KD	Kinase domain
LB	Luria Bertani
MAPK	Mitogen-activated protein kinase
MAPs	Microtubule-associated proteins

MT	Microtubules
MT+TIPs	Microtubule plus-end tracking proteins
MTOC	MT organising centre
N-WASP	Neural Wiskott-Aldrich syndrome protein
NOC	Nocodazole
OD	Optical density
P-FAK Y397	FAK phosphorylated on Tyrosine 397
PBS	Phosphate Buffer Saline
PFA	Paraformaldheyde
PH domain	Pleckstrin homology domain
PI3K	Phosphatidylinositol 3-kinase
PI	Protease inhibitor
PIP2	Phosphatidylinositol (4,5)-biphosphate
PKA	Protein Kinase A
PKC	Protein Kinase C
PTB	Phosphotyrosine binding
PY	Phosphotyrosine
ResGFP-WT or mutant fascin	FasKD cells transiently re-expressing GFP-tagged WT or mutant fascin
SDS	Sodium dodecyl phosphate
S.E.M.	Standard error of the mean
Ser or S	Serine
TAX	Taxol (paclitaxel)
TEMED	Tetramethylethylenediamine
TIRF	Total Interference Reflection Fluorescence
TM	Transmembrane
VT	Vitronectin
WASP	Wiskott-Aldrich syndrome proiten
WB	Western blotting
WT	Wild-type

1 INTRODUCTION.

1.1. Overview of cell migration

Cell migration is a complex process executed by all nucleated cell types and it is central in tissue formation and development. Indeed, embryonic development, wound healing and immune responses all require the orchestrated movement of cells towards a specific direction to a precise site of the tissue/organism (Friedl et al. 2012). Disruptions in the maintenance of these processes results in different pathological states such as vascular diseases, mental retardation, cancer formation and metastasis. Thus, a better understanding of the molecular mechanisms driving cell migration may provide therapeutic strategies to controlling some of these diseases such as tumour progression.

Cells respond to a variety of external and internal signals to acquire the capability to move. Chemical and mechanical signals coming from the environment together with cell-specific features contribute to the complexity of movement acquisition (Wolf et al. 2003). Moreover, different modes and mechanisms of motility have been studied and describe the movement of a single cell or the collective motion of several cells as a group (Van Zijl et al. 2011). Although these molecular features are specific for certain types of cells and tissue environment, they represent multiple variants of the same cytoskeletal dynamics (Lämmermann & Sixt 2009).

1.1.1. Molecular models for cell migration

Cells must dynamically modify their interactions with other cells and/or the extracellular environment to acquire motile capabilities. A single cell modifies its shape and stiffness to interact with the surrounding extracellular matrix (ECM) (Geiger et al. 2001). Live cell imaging experiments have shown a moving cell undergoes several cell shape changes, but also generally displays a prominent leading edge with a characteristic behavior. It is generally accepted that the leading

edge of the cell provides a polarized protruding force to push the cell and enable it to move forward (Insall & Machesky 2009; Ridley 2011).

Two models have been proposed to explain how cells move: the cytoskeletal model and the membrane flow model (Bretscher 1996)(Figure 1.1). The cytoskeletal model proposes that cells become elongated and organise flat sheets of membrane enriched in highly dynamic polymerised actin filaments at the front known as lamellipodia (Small et al. 2002) (Figure 1.1a). These membrane protrusions increase adhesion and promote increased mechanical tension within the cell that act to stabilise adhesions and increase contraction of the cell rear (Small et al. 2002). More structured, parallel actin filaments known as filopodia and stress fibers also act to drive the coupling of adhesions and the actin cytoskeleton at the leading edge (Ridley et al. 2003). ECM ligands are linked to the cell membrane via interactions with the integrin family of heterodimeric transmembrane receptors. These ECM receptors, together with multiple adhesion components (red circles in Figure 1.1a), form a strong bond between the cell and the ECM, which generate traction forces and a molecular flow towards the leading edge (Insall and Machesky 2009; Parsons et al. 2010). Surface proteases are then recruited to disrupt ECM contacts and provide a focal degradation point for the cell to move into (Baldassarre et al. 2006). Finally, the disassembly of focal contacts at the rear results in directed cell movement (Friedl & Wolf 2003). In this model, actin polymerisation is critical in driving formation of cellular protrusion and adhesion, force generation, cell body movement and ECM degradation. Indeed, actin bundle (F-actin) polymerisation at the leading edge (blue filaments in Figure 1.1a) pushes the cellular front to move forward, while actin depolymerisation at the trailing edge generates actin subunits (G-actin, blue circles in Figure 1.1a). Cell movement in fibroblasts and other cell types relies on the coordinated actin polymerisation/depolymerisation cycle (yellow arrows in Figure 1.1a), membrane and adhesion systems (Schäfer et al. 2010; Tamariz and Grinnell 2002).

The membrane flow model proposes the membrane to be site of a polarized endocytic cycles (Fig 1.1b). Endocytosis generates a vesicle flow in the plasma membrane (Figure 1.1), which decreases towards the cellular trailing edge. Therefore, exocytosis/endocytosis cycles (green arrows in Figure 1.1b) promote cell polarization and drive cell movement. Although both models likely contribute to migration in cells, in this thesis I will focus on elucidating mechanisms that drive cytoskeleton remodeling rather than control of endocytic compartments.

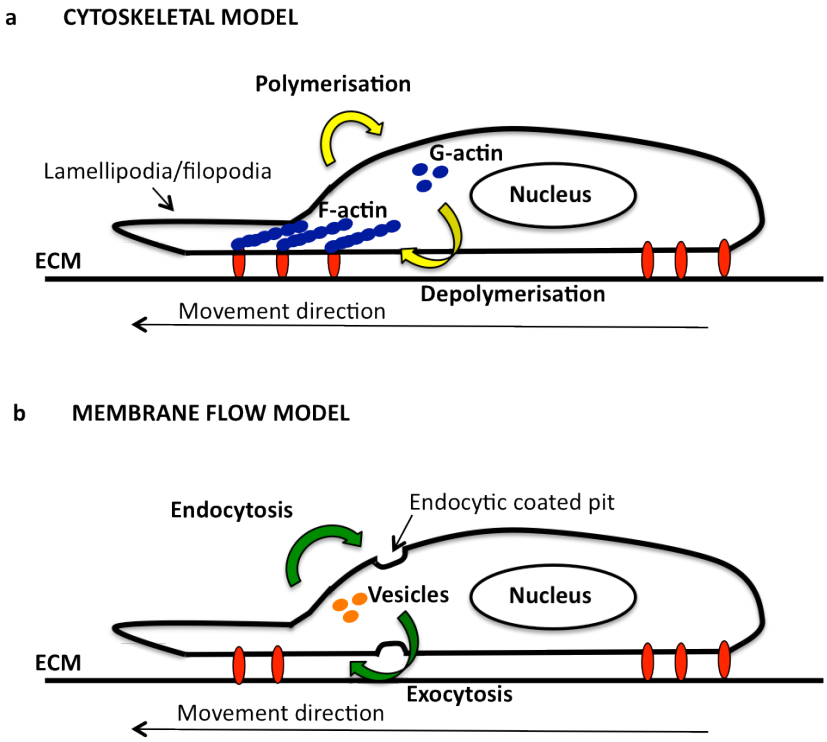

Figure 1.1. Schematic for migration models

(a) Cytoskeletal model for cell migration. Cell is moving to the left. Yellow arrows in Figure a show actin polymerisation/depolymerisation cycle, which is driven by F-actin filaments (blue filaments) assembly at the cellular leading edge and the depolymerisation and G-actin (blue circles) production at the trailing edge. (b) Membrane flow model for cell migration. Cell is moving to the left. Figure b shows endocytic-coated pits formation, which decreased with the increased distance from the leading edge, generating an exocytosis/endocytosis vesicle (in orange) flow (shown by green arrows), which in turn drives cell migration.

1.1.2. Cell migration modes

Different migration strategies have been studied to describe movement acquisition by a single cell or collective motion of several cells (Friedl & Wolf 2010). Actomyosin contractility-dependent cell shape changes and extracellular soluble and ECM-specific cues are all important in co-ordination of efficient cell migration in both single cells and groups (Ridley et al. 2003; MacKay et al. 2012).

Single cell movement is usually classified in two different migration modes: amoeboid and mesenchymal. Amoeboid migration describes the movement of rounded cells with immature focal adhesions and a lack of stress fibers (Friedl 2004; Lämmermann & Sixt 2009). The amoeboid migration mode can be divided into two subtypes. The first is the 'blebby' migration of cells, which do not adhere to the substrate and they rather move in a propulsive manner (Sanz-Moreno & Marshall 2009). The second occurs in more elongated amoeboid cells, which form actin-rich protrusions at the leading edge with a weak adhesion to the substrate (Friedl & Wolf 2010). Integrins are almost absent on the surface of these cells and their movement is mainly dependent on cellular shape changes, driven by actin-based cellular contractility (Friedl 2004). Hematopoietic stem cells, such as leukocytes, and certain tumour cells move with amoeboid or pseudo-amoeboid mode. These cellular types use a 'crawling' mechanism to migrate along the surface (Wolf et al. 2003). Cells with low contractility and strong adhesion to the substrate develop mesenchymal migration mode (Friedl 2004). Mesenchymal cells in vivo show elongated shape and fibroblast-morphology. Fibroblasts, myoblasts, single endothelial cells and tumour cells show the characteristic spindle morphology and move in a mesenchymal manner (Tamariz & Grinnell 2002; van Zijl et al. 2011). The elongated shape is dependent on integrin activation and generation of traction forces throughout the cell body. Both β1 and β3 integrin subtypes are known to be recruited to regulate adhesion to different ECM proteins in most adherent cells (Ballestrem et al. 2001;

Askari et al. 2010). The mesenchymal migration mode shows typical molecular features of the integrin-dependent movement described in section 1.1.1. (Wolf et al. 2003; Nagano et al. 2012). Depending on levels of key signaling molecules such as RhoA, Rac, Cdc42, matrix degradation and ECM architecture cells can establish one of the two described migration modes. Indeed, amoeboid migratory style requires high levels of RhoA/ROCK-driven actomyosin contractility, whereas elongated mesenchymal modes are primarily driven by Rac-dependent F-actin based leading lamellipodia/filopodial formation in an integrin-dependent manner (Sanz-Moreno et al. 2011; Calvo et al. 2011).

Additionally, chemokine or morphogenic gradients and/or extracellular tissue structures promote directed movement of cells moving together, in multicellular streams or chains (Friedl et al. 2012). The resulting collective cell migration occurs when junctions between cells are retained over prolonged time periods so that cells interact with their neighbours (Rørth 2009). When cells move collectively, the cytoskeleton of each cell acts independently to generate traction force on the matrix (Kraning-Rush et al. 2010). Therefore, a complex synchronization of cell-cell junction structures with cytoskeletal components is necessary to complement different adhesion types and drive collective migration (F. Huber et al. 2013). Figure 1.2 gives an overview of the described cell morphology changes and different migration modes. Black arrows in Figure 1.2 show plasticity of different migration modes. Indeed, each migration type, although driven by distinct mechanical and molecular mechanisms, may undergo transition towards another migration type. These transitions are central in processes such as macrophages and endothelial cell differentiation (Friedl 2004). Moreover, cancer cell progression and differentiation provides useful insights to understand molecular mechanisms driving cellular migration mode transitions. Epithelial-mesenchymal transition (EMT) is a key event in driving tumour invasion and metastasis (Thiery 2002).

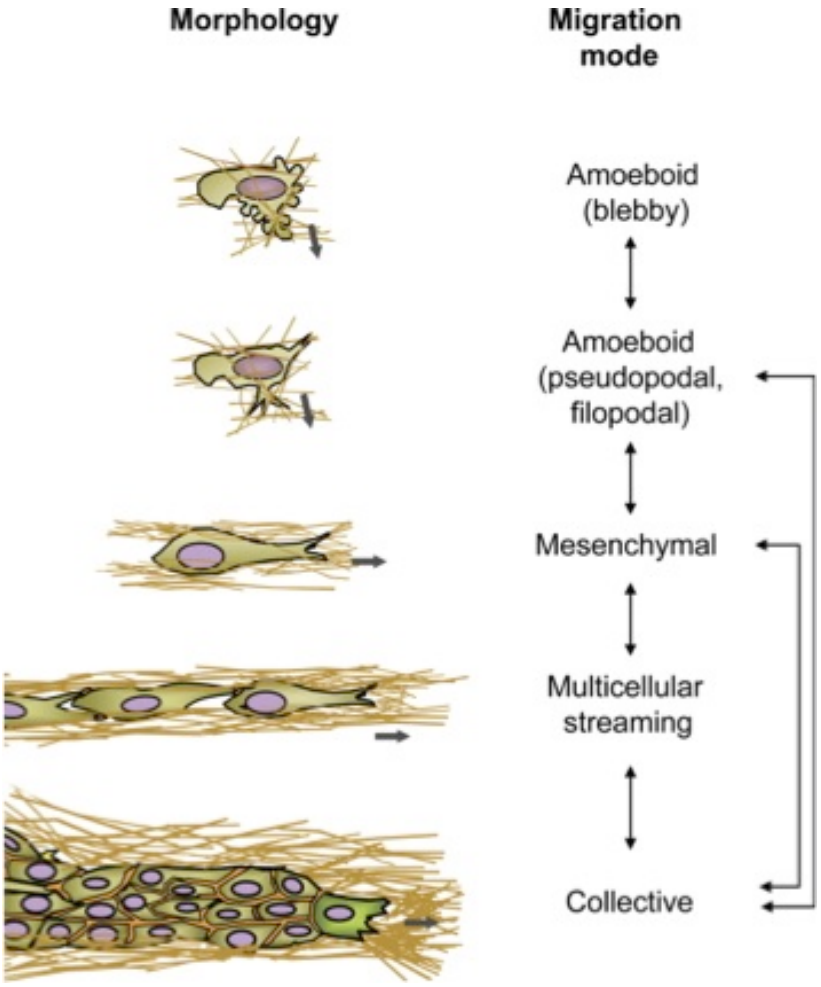

Figure 1.2. Cell morphology and migration modes (Friedl & Wolf 2010)
Single cells movement is usually classified in amoeboid and mesenchymal migration modes. Single cells migrating towards the same directions increase their cell-cell interaction, promoting multicellular streaming and collective migration. In Figure 1.2 thin black arrows show how migration styles can be converted in others to highlight plasticity of migration modes. Thick gray arrows show direction of movement.

1.1.3. Pathological cell migration

Single or collective cell movement is central in processes such as embryonic development, wound healing and immune response (Friedl et al. 2012). The actin cytoskeleton proteins play a fundamental role in all of the mechanical steps driving

global cell migration during tissue development and formation (Kurosaka and Kashina 2009). Furthermore, cytoskeletal proteins are implicated in many human pathological conditions, including cancer, infection and cardiovascular, inflammatory and neurodegenerative diseases (Rørth 2009; Friedl et al. 2012). Defects in neural crest cell migration lead to cognitive and motor disabilities as well as neurological disorders such as mental retardation (Perris & Perissinotto 2000). Dysregulated migration of endothelial cells directs abnormal angiogenesis causing processes such inflammation and cardiovascular diseases (Reinhart-King 2008).

One of the most described examples of cell migration in pathology is in the context of cancer cell metastasis. Cancer cells must acquire motile capabilities to colonize distant sites and give rise to metastases (Van Zijl et al. 2011). Many molecules involved in actin dynamics are dysregulated in invasive cancer cells (Parri & Chiarugi 2010; Nagano et al. 2012). For instance, GAPs, GEFs and many GTPase effector proteins have been shown to exhibit altered activation in cancer cells (Vega & Ridley 2008). Rho and Rac opportunistically regulate each other in cancer cells to modify cell shape and promote metastatic dissemination (Parri & Chiarugi 2010). Integrins and main adhesion components such as Focal Adhesion Kinase (FAK) drive cancer cell adhesion and invasion (Felding-Habermann et al. 2001; Provenzano and Keely 2009). Lastly, actin structures such as invadopodia are essential for tumour cell matrix degradation (Buccione et al. 2009). Cancer cells show high GTPase-dependent cell plasticity. Indeed, cancer cell invasion is tightly dependent on Rho- and Rac-dependent determination of movement mode (Sanz-Moreno et al. 2008). In particular, the switch from epithelial to mesenchymal migration mode (EMT) is proposed to be used by cancer cells to escape from the primary tumour and promote metastasis (Micalizzi et al. 2010).

1.2. The cellular cytoskeleton

The cytoskeleton of eukaryotic cells is composed of three kinds of filaments: microfilaments, intermediate filaments and microtubules. Together, these filaments contribute to cellular shape, integrity and homeostasis as well as dynamic changes during tissue remodelling or migration (Doherty & McMahon 2008). Microfilaments are composed of linear filaments of actin, intermediate filaments are formed of different proteins, such as keratin and vimentin, whereas microtubules are polymers of α and β tubulin.

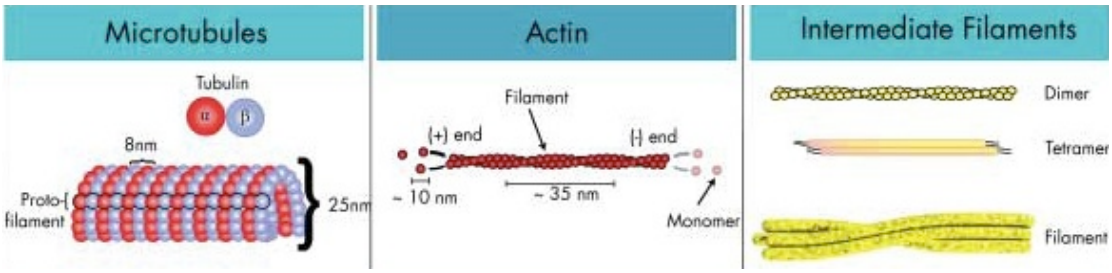

Figure 1.3. The cellular cytoskeleton components (adapted from (Huber et al. 2013) Three kinds of filaments form the cellular cytoskeleton: Microtubules, Microfilaments (F-actin filaments) and Intermediate filaments.

1.2.1. Actin

Actin is a 42 kDa- globular protein and is highly conserved across species. Three isoforms exist: α, β and γ. The α isoform is predominantly found in muscle whereas the β and γ isoforms are ubiquitous and co-exist in the cytoskeleton contributing to diverse cellular structures (Khaitlina 2001). The main function of actin is to form filaments that comprise the actin cytoskeleton (microfilaments, also known as filamentous or F-actin, in Figure 1.3). Actin filaments act as scaffolds for myosin motors during cytoskeletal contraction as well as being important in driving vesicle trafficking in many cell types (Doherty & McMahon 2008). Under physiological

conditions, monomeric G-actin is transformed into the polymeric F-actin by ATP-phosphorylation; the ATP on the F-actin polymer is then hydrolysed to promote the actin treadmilling. Nucleation factors are involved in F-actin filament polymerization. One example is the Arp2/3 complex, which enhances actin filament polymerization and promotes the initiation of new branches from existing ones (Egile et al. 2005). Figure 1.3 (middle panel) shows polarity of a growing actin filament, which is given by continuous growth from the plus end (+) and G-actin release from the minus end (–). Filament nucleation and directional growth are fundamental to cell shape and expansion, as well as to phagocytosis and internal vesicle motility (Bannigan & Baskin 2005).

Several cross-linking and bundling proteins bind actin to stabilize filaments and regulate cell mechanics. Examples of these are α-actinin and fascin, which are involved in the assembly and maintenance of filopodia and stress fibres (Small et al. 2002). α-actinin and fascin are both actin bundling proteins; the former binds actin filaments in any orientation to provide crosslinking stability, whereas fascin is more selective and only binds parallel-oriented polymers (Courson and Rock 2011). Fascin is known to regulate cytoskeletal structures for maintenance of cell adhesions and the promotion of invasive protrusions (Adams 2004; Jayo and Parsons 2010). The loss of fascin or α-actinin leads to a decrease in cell spreading, adhesion and migration, underlining the importance of actin crosslinkers in these processes (Friedl & Wolf 2003). Rho family of small guanosine triphosphate (GTP)-binding proteins (GTPases) are key regulators of actin filament formation (Ridley et al. 2003). GTPases are bound to GTP in their active state and they then interact with a wide array of molecular downstream effectors. GTPases are activated by guanine exchange factor (GEFs) and inactivated by GTP-activating proteins (GAPs). Rac and Cdc42 are the best characterized family members and are the GTPases mainly involved in lamellipodia and filopodia formation. Their preferential targets are the Arp2/3 complex activators, WASP and WAVE family proteins as well as p21-activated kinases (PAKs)

(Zalevsky et al. 2001; Stradal et al. 2004). Similarly, WASP and WAVE bind to GEFs and GAPs regulating Cdc42 and Rac activity (Rohatgi et al. 1999). Cdc42 is one of the master regulators of cell migration. It drives cell polarity through restricting the area where the lamellipodia form (Itoh et al. 2002). Cdc42 also directs the microtubule organizing centre (MTOC) and the Golgi apparatus towards movement direction (Cau & Hall 2005). Cdc42 is in turn maintained at the leading edge by several signals, such as its effector PAR6 activation and integrin clustering at adhesion sites (Etienne-Manneville & Hall 2001).

Another important determinant of cell polarity is the activity of the phosphoinositide(3,4,5)P_3 (PIP3) kinase (PI3K) and the PI3K phosphatase (PTEN). PI3K produces and localises PIP3 at the leading edge, while the phosphatase PTEN brings its dephosphorylated form (PIP2) to the rear, contributing to chemo-attractant agent response (Kölsch et al. 2009). Cdc42 is known to be involved in removing PTEN from the leading edge and PIP3 appears to be involved in localising Cdc42 at the cellular front (Van Keymeulen et al. 2006). Rac is one of the key molecules in maintaining directional F-actin protrusions. Rac activation induces integrin clustering and activation, promoting new adhesion formation (Kiosses et al. 2001). Mesenchymal cell migration is dependent on Rac1-mediated cell polarization and lamellipodia formation and its reciprocal regulation with Rho GTPases drives cancer cell invasion (Parri & Chiarugi 2010). Furthermore, Rac recruits and activates PI3K at the plasma membrane, promoting PIP3-dependent cell polarity (Cho et al. 2012). Rac can also drive a positive feedback loop to control microtubule targeting and stability (Rodriguez et al. 2003).

1.2.2. Microtubules

Microtubules (MTs) have a diameter of 25 nm and their length varies between 200 nm and 25 μm. MTs are polymers made up of α and β tubulin (left panel in Figure 1.3). These subunits dimerize in an end-to-end conformation to form protofilaments,

exposing one minus end (-) and one plus end (+). Parallel protofilaments bind each other, forming MT bundles, creating a strong polarity between the + and - ends. Ends are named according to the direction of filament elongation and shrinking (Figure 1.4). The – end is capped and MTs assemble and disassemble at the + end, promoting catastrophe and rescue of the bundles (Jiang and Akhmanova 2011). MTs are nucleated from the MTOCs (microtubules-organizing centre) as basal bodies and centrosomes. These structures contain γ tubulin subunits, which together form a scaffold ring to the – end that grows in the + end direction (Heald & Nogales 2002). During polymerization, both α and β subunits of the tubulin are bound to GTP; the binding at the – end is stable, while GTP at the + end may be hydrolyzed to GDP after assembly leading to depolymerisation (Drechsel & Kirschner 1994).

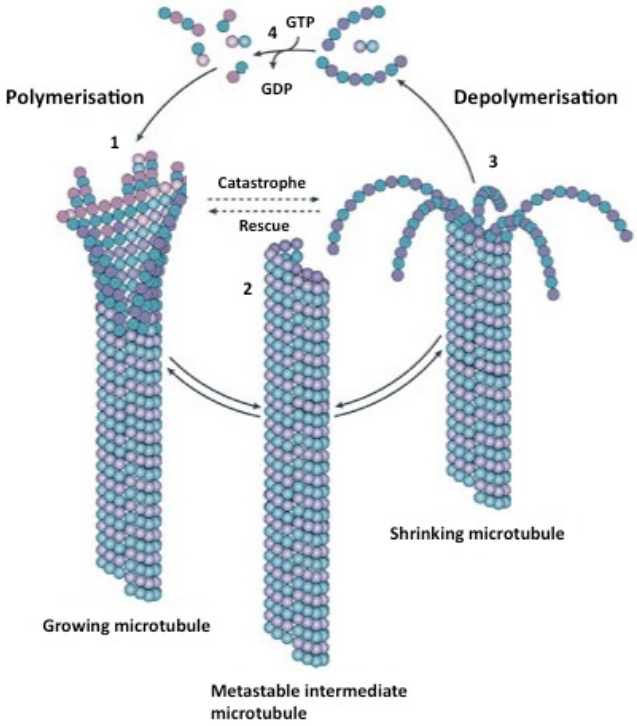

Figure 1.4. MT structure and dynamic instability (Akhmanova & Steinmetz 2008) MT structure is highly dynamic. (1-4) α and β subunits of the tubulin are bound to GTP during MT growth. (3) GTP hydrolysis to GDP induces MT shrinking. (2) An intermediate metastable form of MT exists due to a cycle of GTP binding and hydrolysis (2).

Assembly and disassembly of MTs are not only associated to GTP/GDP binding but also capping proteins. Proteins known as microtubules-associated proteins (MAPs) directly bind tubulin, cross-link MT bundles together or mediate interactions with other proteins. Different proteins are involved in MAP-MT binding and dynamics. One class of these are known as the +TIPs (plus-end tracking) proteins because they are associated with the growth of the + end. Additionally, motor proteins such as kinesin and dynein can 'walk' on MT bundles and drive vesicle movement through interactions with tubulin. Most kinesins walk in the + end direction, while dynein is a – end motor protein. They are vital for chromosome separation during mitosis and meiosis, for intracellular trafficking and regulation of cell shape. They are fundamental components of structures such as cilia and flagella (Walcott and Sun 2010) that generate forces from the cell surface to protect it from the environment. Post-translational modifications of tubulin such as acetylation, detyrosination, polyglutamylation and polyglycylation modify the binding between +TIP proteins and the MTs to permit specialized functions and enhanced stability (Ikegami and Setou 2010).

+TIP proteins do not track microtubule tips processively, instead they exchange rapidly by recognizing some specific structural features at the growing ends (Jiang & Akhmanova 2010). They are seen as rapidly moving, comet-like dots that can be visualized and used to quantify MT dynamics. +TIP proteins are separated into two subclasses: those that directly interact with the microtubules + end and those that interact with proteins belonging to this first group (Akhmanova & Steinmetz 2008). The prototypic +TIPs, are comprised of EB protein family (EB1, EB2 and EB3) (Juwana et al. 1999), CLIP-170 and CLIP-115 (Perez et al. 1999; Hoogenraad et al. 2000). These proteins have been used in studies as markers for monitoring MT dynamics (Matov et al. 2010). Motor proteins such as kinesin and dynein are considered in the second subclass of TIPs with CLASP1, CLASP2 (Akhmanova et al. 2001), the Diaphanous-related formins (DRF) (Tominaga 2005), the spectroplakin ACF7 (Kodama et al. 2003)

and the adenomatous polyposis coli (APC) tumour suppressor protein (Mimori-Kiyosue et al. 2000).

The majority of the EB proteins contain highly conserved N- and C terminal domains that are separated by a less conserved linker sequence. The N-terminal domain is necessary and sufficient for MT binding (Lansbergen & Akhmanova 2006). This domain globular structure is characteristic of calponin homology domains, which are formed by α-helical repetitions and typically found in actin-binding and signalling proteins (Gimona et al. 2002). Other +TIPs and MT motor proteins, such as some EB family proteins and dynein share an α helical coiled coil domain, which mediates the binding with MT (Akhmanova & Steinmetz 2008; Redwine et al. 2012). Several large and complex multidomain +TIPs contain extensive sequence regions that are enriched with basic and serine residues. These regions, which are predicted to be flexible, often mediate the interaction with MT and other EB proteins. Examples of serine-rich MT binding proteins are APC and the microtubule-actin crosslinking factor ACF7 (Jefferson et al. 2004; Bamburg et al. 1999). Other +TIP proteins such as CLIPs contain cytoskeleton-associated protein glycine-rich domains at their N-termini. These domains mediate their interaction with MT and EB proteins (Perez et al. 1999).

The key role for MT in many cellular functions, including migration and mitosis, make them potential targets for cancer treatment. Indeed, β tubulin isotypes are differentially up-regulated in many types of cancer and tubulin-binding agents (TBAs) are already used as anti-cancer drugs (Wilson & Jordan 2004). Interestingly, both types of TBAs, whether destabilizing or stabilizing, have an effect on actin-network. For instance, it is known that nocodazole, an anti-neoplastic drug that inhibits MTs polymerization, induces stress fibres formation and cell contractile morphology (Chang et al. 2008). Conversely, changes in actin organization or in its regulators are associated to MT-drugs sensitivity (Kavallaris 2010).

1.2.3. Intermediate filaments

Intermediate filaments (IF) are cytoskeletal components composed of a family of related proteins with similar structure and sequence. They have been designated as intermediate because their average diameter (10 nm) is larger than actin microfilaments, but narrower than myosin bundles, found in muscle cells (Herrmann et al. 2007). Most types of IF are cytoplasmic, except for lamins, which are nuclear. All IF proteins have a central α-helical rod domain composed with four α-helical segments (C.-H. Lee et al. 2012). The basal structure of an IF is a parallel homo/hetero dimer, which is formed through the interaction of the rod domains to form a coiled coil (right panel in Figure 4.1). The C and N termini of IF proteins are not α-helical regions and the N terminus of nuclear IF proteins binds DNA (Wang et al. 2001). Vimentin heads are able to alter nuclear architecture and nuclear distribution (Shoeman et al. 2001). Cytoplasmic IF do not show a polar orientation and unlike microfilament and microtubules, they do not play a key role in cell motility and cellular transport (Kreplak & Fudge 2007). In addition, IF do not show any binding sites for nucleoside triphosphate.

IF are classified in six types based on similarities in amino acid sequence and protein structure. Type I and II are the most diverse IF proteins and the keratin family is the most representative (C.-H. Lee et al. 2012). Vimentin belongs to the class III and it is the most distributed IF proteins in cells (Qin et al. 2009). IF proteins are deformable and stretched, which contribute to cytoskeletal functions in cells. They interact with cell-cell adhesion structures such as desmosomes and cell-matrix adhesion structures such as hemidesmosomes (Quinlan et al. 1995).

1.3. The role of actin and microtubule cytoskeletons in cell motility

As principal components of the cellular cytoskeleton, actin and MT regulate cell motility. The role of actin filament assembly/disassembly in regulating cytoskeleton reorganization has been known for years. Moreover, recent studies have focused on the contribution of MT to controlling adhesion dynamics and cell migration.

1.3.1. The role of actin in adhesion and migration

As mentioned in previous sections, cell migration requires a dynamic reorganization of the actin cytoskeleton. Actin-based protrusions formation is one of the main events promoting cell polarity and migration. The main role for the actin cytoskeleton is to provide mechanical stability to protrusions originating from the plasma membrane (Ridley 2011). There are different types of plasma membrane protrusions, with diverse complexity and molecular activators. Their specific activation allows cells to respond dynamically to the EC environment with the most appropriate type of protrusion (Keren 2011).

1.3.1.1. Lamellipodia

The elongation of flat sheets of membrane called lamellipodium is one example of actin-based protrusion (Small et al. 2002). The lamellipodium is a large area forming at the leading edge of motile cells and is formed by a dense network of F-actin filaments. The edge of the lamellipodium in fibroblasts and other cellular types shows a ruffling appearance. This is due to the dynamic activity of the actin filaments, which push the cell edge forward and quickly detach from the substrate. A myriad of molecules become active in response to stimuli, which activate

lamellipodia formation. Some of them are shown in the model for lamellipodia (Figure 1.5). Rho, Rac and Cdc42 are critical in the formation of structures, connecting the plasma membrane with the motility machinery (Ridley 2011). New actin filament nucleation is central in giving directionality to the lamellipodia. The localisation of the Arp 2/3 complex and its activators at the plasma membrane activate GTPases which in turn drive protrusion formation (Lai et al. 2008). Membrane receptor proteins are also critical in coupling the cellular cytoskeleton to the EC environment. For instance, integrin activation stabilizes actin filaments in early adhesion sites and promotes actin depolymerisation at the trailing edge (Ridley et al. 2003).

Integrin-dependent adhesion turnover requires the cooperation of many molecular players, which will be described in more detail in the next section. Other proteins have also been shown to contribute to actin filaments stabilization in the lamellipodia. For instance, formin family proteins protect actin filaments from capping (Goode & Eck 2007). Molecules, such as VASP and cofilin, involved in F-actin bundle elongation and severing respectively, also contribute to lamellipodia function (Van Rheenen et al. 2009; Bear & Gertler 2009). Moreover, cofilin and other ADF family proteins are involved in F-actin depolymerisation and severing (Bamburg et al. 1999).

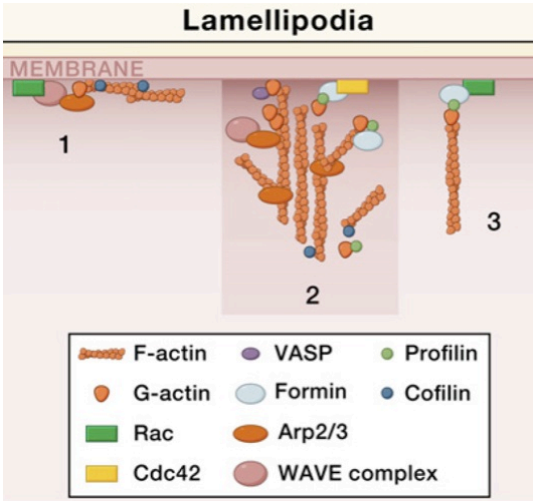

Figure 1.5. Lamellipodia (Ridley 2011)
Model for lamellipodia formation: (1) Free-actin filaments barbed ends stabilized by cofilin promote Arp2/3 complex-dependent new actin filaments nucleation. (2) WAVE complex proteins and VASP contribute to actin nucleation and Rac/Cdc42-dependent protrusion formation. Actin monomers are originated by the depolymerizing activity of cofilin and profilin. (3) Formins can also generate unbranched actin filaments, independently on Arp2/3 complex nucleation.

1.3.1.2. Filopodia

Filopodia are long protrusions formed by parallel F-actin bundles (Insall & Machesky 2009). Recent studies have shown mDia proteins of the formin family to promote actin polymerisation in filopodia formation (Mellor 2010). Several proteins have been shown to promote filopodia formation and function (Figure 1.6). For instance, Ena/VASP proteins localise at the tips of filopodia, showing an anti-capping activity and promoting filopodia elongation (Mejillano et al. 2004). Proteins containing I-BAR domains, such as IRSp53, have shown to induce filopodia formation in particular conditions through induction of membrane curvature (Ahmed et al. 2010). Furthermore, Myosin X localises at the tips of filopodia and induces their assembly (Sousa and Cheney 2005). Cdc42 activates N-WASP, IRSp53 and mDia2 promoting their localisation and elongating activity of filopodia (Figure 1.6; (Ahmed et al. 2010). In addition to Cdc42, other GTPases have been shown to play a role in filopodia

assembly. For example, RhoF/Rif induces filopodia formation via mDia2 in early stages of dendritic spine formation in neurons (Mellor 2010). Actin filaments are held together to form filopodia by cross-linking proteins. Fascin localises in filopodia and promotes their formation and stability (Vignjevic et al. 2006b). Fascin provides invasive capabilities to filopodia contributing to its role in cancer metastasis (Machesky & Li 2010).

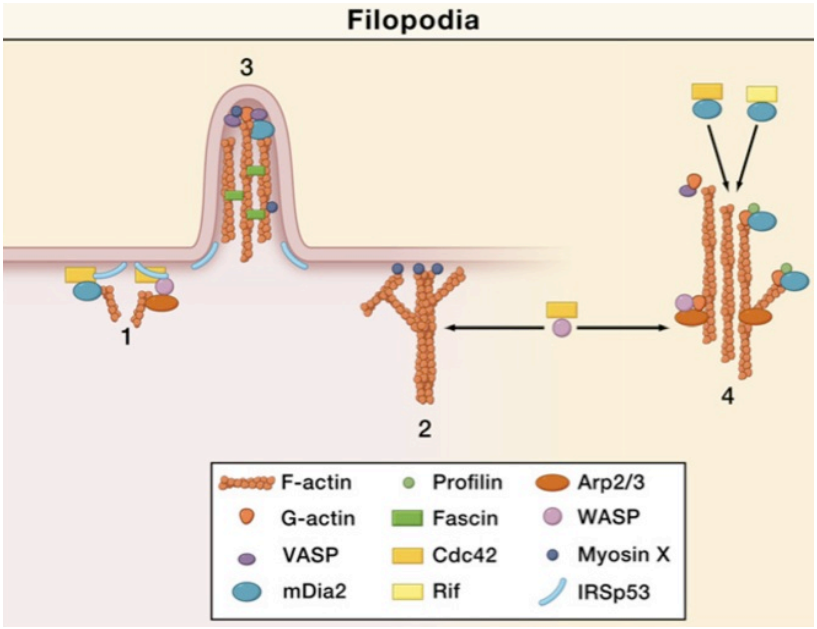

Figure 1.6. Filopodia (Ridley 2011)
Model for filopodia formation: (1) IRSp53 bends the membrane and induces Cdc42 to recruit targets such as mDia2 and VASP. These molecules induce actin polymerisation. (2) Actin filaments can also be provided by Myosin X activity. (3) F-actin filaments grow towards the movement direction and proteins, such as VASP, mDia2 and Myosin X, localising at filopodia tips mediate their assembly and stability. (4) mDia2 and VASP deliver actin monomers to the growing ends of actin filaments, while profiin contribute to the WASP/Arp2/3-driven nucleation of new branches.

1.3.1.3. Stress fibres

Actomyosin contractility in non-muscle cells is principally driven by myosin II-containing contractile actin filament structures called stress fibres. Stress fibres are

F-actin filaments with alternate polarity, held together by α-actinin and other actin binding proteins (Tojkander et al. 2012). Stress fibres in non-motile cells are usually thick and stable, while highly motile cells show thiner, more dynamic actin stress fibres (Pellegrin & Mellor 2007). Stress fibre assembly is critical in connecting the cytoskeleton to the ECM at adhesion sites called Focal Adhesions (FA). FA are adhesion structures that act as platforms for recruitment of different molecular players that ultimately contribute to the generation of mechanical stability and forces required for cell movement (Hayakawa et al. 2012; Schäfer et al. 2010). Forces created by stress fibres allow cells to 'sense' the ECM and to develop different protrusion or migration modes. ECM mechano-sensing is also determinant in other cellular processes such as cell fate and differentiation (Walcott & Sun 2010). In contrast to the well-characterised lamellipodia and filopodia structures, stress fibre assembly and formation mechanisms remain relatively poorly characterised. However, three classes of stress fibres have been distinguished (Hotulainen & Lappalainen 2006). Ventral and dorsal stress fibres and transverse arcs are shown in Figure 1.7. Ventral stress fibres are contractile actin filaments and have both ends associated with FA. They are found in the ventral part of the cell and they are central to the co-ordination of cell adhesion and contraction. Transverse arcs are not directly associated with FA and elongate from the leading edge to the center of the cell. Dorsal stress fibres are connected to FA at both ends and they follow the dorsal cortex of the cell, sometimes crosslinking with transverse arcs (Small et al. 1998).

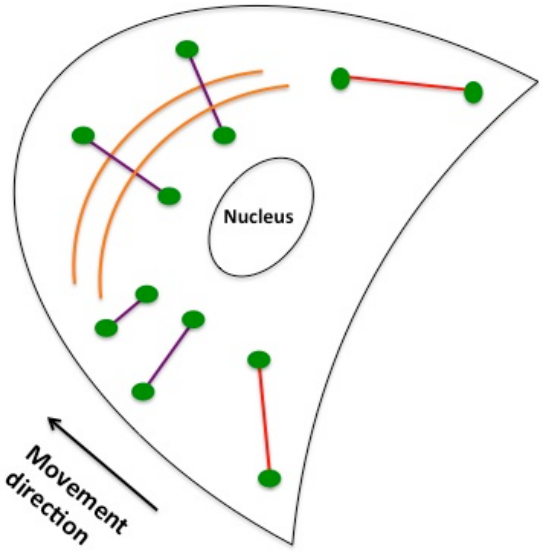

Figure 1.7. Schematic of stress fibre types
Red lines represent ventral stress fibres, orange lines represent transverse arcs and purple lines represent dorsal stress fibres. Green circles are FA localised at the ends of ventral and dorsal stress fibres. Direction of movement is shown.

Stress fibre assembly is regulated by signaling pathways involving the small GTPase RhoA (Ridley et al. 2003). Activated RhoA promotes Rho kinase (ROCK)-mediated contractility, which induces stress fibre formation by inhibiting actin depolymerisation via LIMK-dependent cofilin inactivation (Pritchard et al. 2004) or inducing myosin II phosphorylation (Kaneko-Kawano et al. 2012). Moreover RhoA activates formins, which are known to induce actin filament assembly (Goode & Eck 2007).

1.3.1.4. Integrins

Integrins are heterodimeric transmembrane receptors consisting of an α- and β-subunit. In mammals there are 24 different integrins formed by the combination of 18 α-subunits and 8 β-subunits, the combination of which dictates ligand-binding specificity (Figure 1.8). The amino-terminal domain in the α- and β- subunit forms the ligand-binding site in the extracellular domain. Integrin subunits also contain a single transmembrane domain and a short cytoplasmic tail, among which there is a

relatively high degree of conservation across α or β subunits (S. Shattil et al. 2010). Integrin affinity for their ECM ligands such as fibronectin, vitronectin, laminin and collagen is regulated by 'inside-out' signalling or activation events. During this process, intracellular effectors, such as talin or kindlin proteins bind to the β-integrin cytoplasmic tail, triggering conformational changes within the extracellular domain and thus promote clustering of integrins (Harburger & Calderwood 2009). This results in an increased affinity for the extracellular ligands (integrin activation) potentially through displacement of the integrin cytoplasmic tails.

Talin is a well characterised integrin binding and activating protein, but how talin co-operates with kindlin family members to maximally activate integrins remains unclear (Anthis et al. 2009; Lai-Cheong et al. 2009). Inside-out signalling controls adhesion strength and ensures that there is sufficient force for cell migration and ECM remodelling (E. Brown 2002). An integrin 'outside-in' signalling also exists, driven by the binding of integrins to extracellular ligands (Hynes 2002). Conformational changes in the extracellular domains of different α/β subunits combinations determine a high specificity of each integrin dimer for its own ligand. For example, active $\alpha_v\beta_3$ integrins can bind either fibronectin or vitronectin with different affinities (Harjanto and Zaman 2010). Outside-in signalling pathways can be triggered in different integrin heterodimers by binding to ECM ligands. For example, binding to fibronectin activates both β_1 and β_3 integrins, whereas adhesion to collagen leads to $\alpha_1\beta_1$ or $\alpha_2\beta_1$ activation (Harjanto and Zaman 2010).

The main function of integrins is to assemble adhesion structures between cells and the ECM regulating cell shape, polarity and migration (Askari et al. 2010). Intracellular adaptors and enzymes such as Rho family GTPases, tyrosine and serine/threonine kinases and phosphatases are all activated by integrin engagement (Brown 2002; Zaidel-Bar 2009). Their activation and interaction with other transmembrane receptor systems drives many cellular processes, including cell-fate

decisions, survival or apoptosis, cell cycle phase progression or senescence and tissue-specific gene expression (Streuli & Akhtar 2009). ECM signalling, together with the action of growth factors (GFs), hormones and cytokines compose a complex signalling network. Moreover, both β1 and β3 integrins have been associated with increased cancer cell invasion and metastasis (Felding-Habermann et al. 2001) and they have been proposed to be involved in different types of migration (Brockbank et al. 2005).

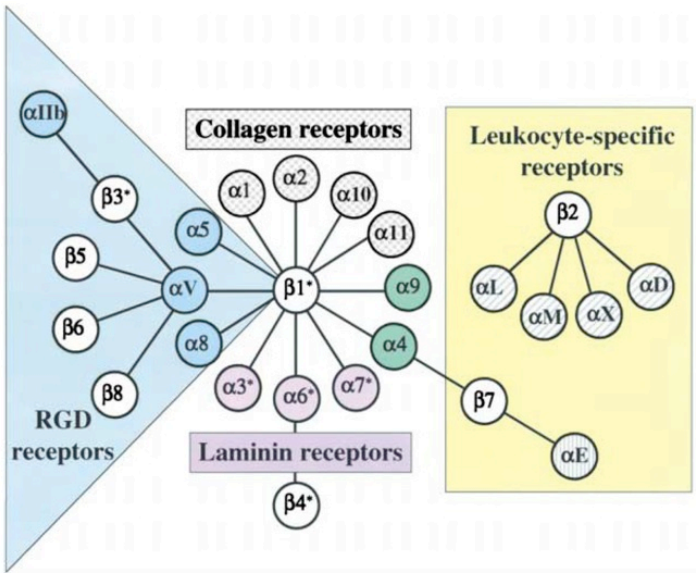

Figure 1.8. The integrin receptor family (Hynes 2002)
The combination of 18 α-subunits and 8 β-subunits dictates ligand-binding specificity of integrins.

1.3.1.5. Extracellular matrix adhesion types

Integrin clustering recruits many molecules to the membrane, which then form large multi-molecular adhesion complexes. Different types of adhesion structures have been classified and divided in terms of function, size, temporal activation and signalling. Classifications have divided these structures into the following categories: nascent adhesions, focal complexes, focal adhesions, fibrillar adhesions, invadopodia and podosomes. The first four types are known to regulate cell contact during

normal cell motility such as during development or tissue repair processes as well as pathological settings (Worth and Parsons 2010), whilst invadopodia/podosomes are involved in mediating adhesion-dependent invasion or ECM degradation (Gimona & Buccione 2006).

Nascent adhesions form underneath the protruding lamellipodium at the leading edge of the cell and undergo very rapid assembly and disassembly. Through an unknown mechanism, a proportion of these adhesions can undergo stabilisation to form focal complexes (FCs), which persist for tens of seconds and are thought to 'sample' the local ECM environment (left panel in Figure 1.9). FCs become elongated and then give rise to larger, more classical adhesive structures known as focal adhesions (T. Parsons et al. 2010). FA are more stable and reside at the ends of actin stress fibre bundles to provide mechanical stability and rigidity during cell motility (centre panel in Figure 1.9). A further subclass known as fibrillar adhesions (FBs) are rich in $\alpha 5\beta 1$ integrin and are predominantly found in cells aligning along fibronectin fibrils (right panel in Figure 1.9). FAs and FBs are also involved in the 'inside-out' signalling of integrins, transmitting signals linked for instance to matrix fibrillogenesis and reorganization (Askari et al. 2010).

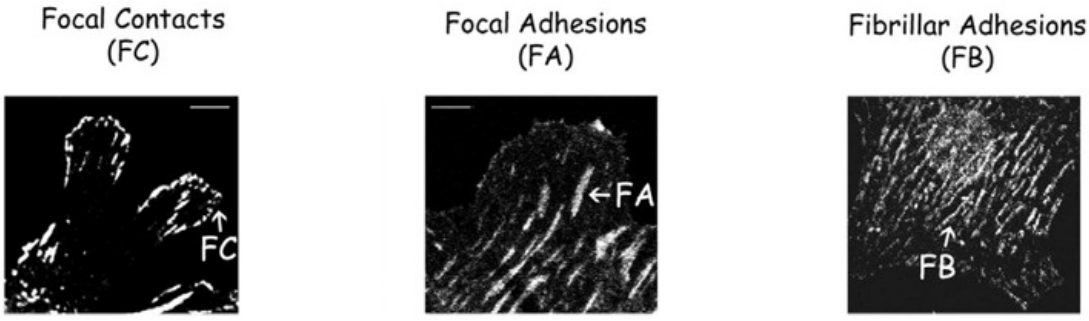

Figure 1.9. ECM adhesion types (adapted from Worth and Parsons 2010)
Different types of classified adhesion structures. They are divided in terms of function, size, temporal activation and signalling.

A further class of 'invasive' adhesions known as podosomes and invadopodia show some molecular similarities but also some differences between the adhesion sites previously described. The main difference lies in the focal degradation of the ECM by proteinases at these sites (Gimona et al. 2008). Both podosomes and invadopodia contain actin-rich cores and are involved in protease secretion (such as membrane-type matrix metalloproteinases 1 and 2). While the structure of podosomes has recently been characterized at high resolution, the one of invadopodia is still not completely understood (Caldieri et al. 2009). Podosomes are highly dynamic, actin-rich cores surrounded by a ring of adhesion proteins. They form adhesion structures of osteoclasts, macrophages, as well as epithelial, endothelial and vascular smooth muscle cells (Evans & Matsudaira 2006). They are involved in physiological cell attachment to solid surfaces and govern tissue invasion and matrix remodelling during development and immune responses. Similar functions have been attributed to invadopodia that are predominantly found in transformed cells or those derived from tumours. These are extended, specialized, proteolytically active plasma membrane protrusions responsible for the focal degradation of the matrix in cancer cells (Buccione et al. 2009).

Adhesions and invasive structures here described are all required for various steps to control the dynamic processes leading to cell movement. This is achieved by striking a dynamic balance between early FA maturation and the formation of new adhesive structures (T. Parsons et al. 2010). Two processes are fundamentally coupled in this dynamic balance: actin polymerization and myosin-II-generated tension. The assembly of the nascent adhesions in the lamellipodium is proportional to the protrusion rate of the leading edge and requires Arp2/3-complex-mediated actin polymerization (Small et al. 2002). As adhesions mature and disassemble at the leading edge, adhesions disassemble at the cell rear, leading it to move forward (Webb et al. 2002). A key regulator of the maturation is the myosin-II-activity, which mediates contraction of actin fibres and rearrangement of the actin cytoskeleton

(Kaneko-Kawano et al. 2012). Moreover, not all the adhesion sites share the same amount and types of these proteins. They are highly specific for adhesion types and their maturation timing (Harjanto and Zaman 2010; Worth and Parsons 2010). Similar proteins are involved in FCs and in FAs formation, while a few proteins such as tensin are involved in stabilising FBs.

1.3.1.6. Focal adhesions

Integrins drive the formation of focal adhesions (FA) at the ends of actin fibres. Over 150 molecules are proposed to participate in integrin-dependent adhesion formation and signaling (Costa and Parsons 2010; Webb et al. 2002; Zaidel-Bar 2009). Each step of the formation of adhesion structures is characterised by phosphorylation of different effectors, and these dictate a range of diverse cellular processes such as proliferation and differentiation, matrix remodeling, angiogenesis, tissue formation and cell migration. It results in a dynamic network of cellular pathways regulated by integrins and promoting FA assembly and maturation (Harburger & Calderwood 2009). Arp2/3 complex and Rho family GTPase activation induce FA formation by their actin nucleating and stabilising activities (Etienne-Manneville & Hall 2001; Villalonga & Ridley 2006). Furthermore, actin-binding proteins such as cofilin and α-actinin can also contribute to different steps of the FA maturation process (Hayakawa et al. 2012).

Not all of the FA components are able to bind integrins directly (Figure 10). Proteins such as talin and kindlins can bind integrins directly and they act as linkers between the receptor and other adaptor proteins. During FA formation, the interaction between talin and vinculin drives the binding of paxillin that triggers the autophosphorylation of focal adhesion kinase (FAK). This phosphorylation provides a docking site for the non-receptor tyrosine kinase Src and other signal mediator proteins (Webb et al. 2004). Molecular scaffold proteins like paxillin are signal

transduction adaptors with a large number of protein-protein interaction sites that connect integrins with intracellular effectors (Turner 2000). Paxillin is phosphorylated by tyrosine kinases such as Src, PI3K and the FAK. Src is crucial to invadopodia formation and the Src-FAK complex is central in the regulation of FA dynamics during cell migration (Balzer et al. 2010; Webb et al. 2004). FA are dynamically regulated to drive normal cell migration, but their turnover is also critical in disease progression such as cancer. Indeed, both ECM and mechanical microenvironment contribute to cancer progression and metastasis (Seong et al. 2013). Moreover different FA components are disregulated in multiple human tumours (Nagano et al. 2012).

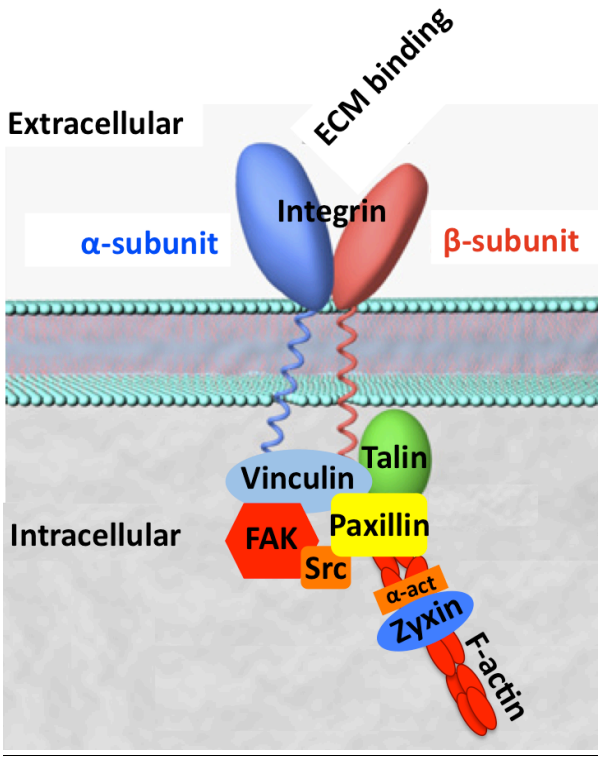

Figure 1.10. Schematic of the main FA components

ECM binding recruits and activates integrins, which in turn promote FA components assembly and activity. Talin, vinculin, paxillin, zyxin and FAK are main FA components.

The Rho GTPase family acts as a regulatory downstream convergence node that drives signals coming from Integrins (Etienne-Manneville & Hall 2002; Ridley 2006). Indeed, Rac, Cdc42 and RhoA regulate FA assembly and disassembly together (Nobes and Hall 1995; T. Parsons et al. 2010). Furthermore RhoB, another component of the Rho GTPase family, has been recently shown to regulate directional cell migration controlling β1 integrin surface levels and activity (Vega et al. 2012). Actin binding and cross-linking proteins such zyxin and α-actinin link FA structures to the actin cytoskeleton transmitting forces coming from the ECM and acting as 'mechanosensors' (C. K. Choi et al. 2008; Yoshigi et al. 2005). Some of the described molecules, such as talin, are able to translate mechanical cues and activate intracellular chemical pathways (Hayakawa et al. 2012). A nanoscale model of FA architecture proposed a protein-specific strata organisation of FA. In particular, talin binding to integrin and its orientation towards actin filaments appeared to be critical in straightening and stretching FA structures (Kanchanawong et al. 2010). Moreover, vinculin and FAK have been associated with increased strengthening FA (Dumbauld et al. 2011). Similarly, cell movement generates ECM components remodeling (Kirmse et al. 2011). Thus, FA turnover is a result of the complex coordinated activity of F-actin, myosin II and FA components (Gallant et al. 2005). In addition, microtubules are know to target FA and drive their dynamics modulating contraction forces at the cell membrane (Stehbens & Wittmann 2012; Small et al. 2002). Moreover, the asymmetry of the MT network coordinates the distribution of FA disassembly in motile cells (Broussard et al. 2008).

1.3.1.7. Focal Adhesion Kinase (FAK)

FAK is an intracellular non-receptor tyrosine kinase identified as one of the most relevant players in integrin-dependent adhesion formation. FAK-mediated FA-actin crosstalk generates traction forces promoting normal and cancer cell migration (Tilghman & Parsons 2008; Schober et al. 2007). FAK drives invadopodia formation

and thus initiation, progression and metastasis of many types of tumours including breast carcinomas (Chan et al. 2009; M. Luo and Guan 2010). Indeed, FAK expression and activity is up-regulated in different cancer cell types (Provenzano and Keely 2010). Inhibition of FAK interaction with growth factor receptors such as cMET and IGF-R has been associated with decreased cancer cell growth *in vitro* and *vivo* (Ucar et al. 2012) and it has been proposed as a therapeutic target (Mitra & Schlaepfer 2006). Upon activation by integrins, FAK undergoes auto-phosphorylation at tyrosine 397 (Y397) to generate docking sites for SH2-domain-containing proteins such as Src that in turn phosphorylate FAK. This promotes FAK kinase activity and interactions with other proteins such as paxillin (Brown et al. 2005). FAK triggers signalling pathways, which regulate the remodelling of the actin cytoskeleton, including the Arp2/3-complex and facilitates the cyclic activation of GEFs and GAPs in the regulation of the Rho subfamily of small GTPases (Tomar & Schlaepfer 2009; Tomar et al. 2012). FAK interactions with actin-related proteins includes its ability to bind cortactin and thus regulate cortical F-actin dynamics (Tomar et al. 2012). The cartoon shown in Figure 1.11 shows the three main domains of the FAK protein: the N-terminus FERM domain, a central kinase domain and a C-terminal focal adhesion-targeting (FAT) region. The FERM domain at the N terminus of FAK is known to bind integrins, growth factor receptors and scaffolding FA proteins that indirectly link to the actin cytoskeleton such as ezrin (Frame et al. 2010). The kinase domain, which contains Y397, is essential for FAK phosphorylation activity (Schober et al. 2007) and the C terminus contains the Focal Adhesion Targeting (FAT) domain, which is critical to recruit FAK and other proteins such as talin and paxillin (Hamadi et al. 2005).

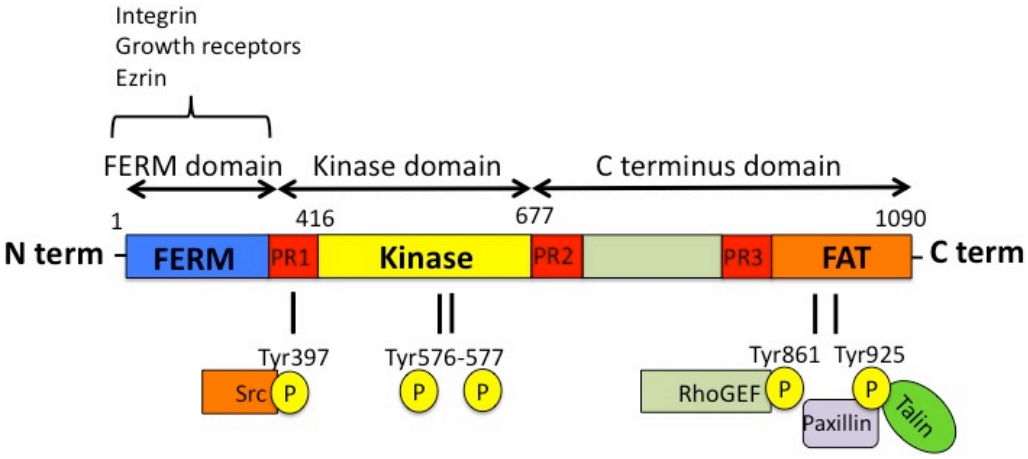

Figure 1.11. Main FAK domains and binding regions

Schematic representation of the three regulatory domains of FAK. The N-terminus FERM domain (in blue) binds integrin, growth factor receptors and FA components such as ezrin. The kinase domain (in yellow) is essential for FAK kinase activity as it contains Tyr 397 phosphorylated by Src. Lastly, the C-terminus FAT domain (in orange) recruits components such as talin and paxillin to FA. Moreover, the FAT domain contains the phosphorylation site for RhoGEF. Moreover, FAK structure contains three proline-rich domains (in red).

Src-dependent FAK phosphorylation recruits proteins that drive FA assembly. I previously mentioned FAK-paxillin interaction (Brown et al. 2005). Moreover, FAK recruits talin at nascent adhesions promoting their maturation to more stable adhesion structures (Lawson et al. 2012). FAK-Src activation regulates FA dynamics also through direct binding to dynamin, whose Tyr-phosphorylation activates integrin endocytosis (Wang et al. 2011). Although the mechanism is still not fully understood, FAK-dynamin interaction contributes to MT-dependent FA disassembly in the nocodazole treatment and washout assays (Ezratty et al. 2005). Other FA components, such as ZF21, have been shown to phosphorylate FAK at Y397 and collaborate in disassembling FA when MT have been depolymerised by nocodazole treatment (Nagano et al. 2010). Moreover, FAK-Src interaction controls FA disassembly driving a signaling pathway controlled by paxillin, the extracellular signal-regulated kinase (ERK) and myosin light-chain kinase (MLCK) (Webb et al. 2004). Lastly, the integrin-FAK signaling pathway facilitates Rho-mDia MT stabilising activity (Palazzo et al. 2004). Although several studies focused on identifying

molecules and signaling pathways driving MT-FA crosstalk, especially during FA disassembly, how MT triggers FAK activity and/or other FA components during their regrowth is still under investigation. A Rac1 independent signaling cascade may be activated in coupling MT with FAK activity during FA disassembly.

1.4. Fascin

Fascin is a 55kDa actin-binding and bundling protein. The known role of fascin is to regulate cytoskeletal structures for promotion of stable F-actin bundles and invasive protrusions (Adams 2004; Jayo and Parsons 2010). Therefore, fascin is critical in processes such as embryogenesis and adult tissue formation (Zhang et al. 2008). Furthermore, both fascin mRNA and protein have been shown to be over-expressed in a range of different types of cancer and it has been suggested as a potential prognostic biomarker of disease progression (Hashimoto et al. 2005; Tan et al. 2013).

1.4.1. Fascin gene

The human genome displays three fascin genes: *FSCN1, FSCN2* and *FSCN3*. *FSCN1* is expressed in mesenchymal and nervous tissues, *FSCN2* in retinal cells and *FSCN3* in testis. In humans, *FSCN1* and *FSCN3* genes reside on chromosome 7, while *FSCN2* is found on the chromosome 17. Expression of the fascin gene is required during both embryogenesis and adult tissue formation, in regions where cell migration is required (Zanet et al. 2009; De Arcangelis et al. 2004). In particular, it has been shown that fascin-1 expression during mouse embryonic development is principally associated with neuronal development and formation, migration of dendritic cells and differentiation of muscle somites. Fascin is not expressed in terminally differentiated epithelial cells (Zhang et al. 2008). Thus, fascin expression is time specific and highly tissue specific.

1.4.2. Fascin protein structure and actin-binding

Fascin belongs to the β-trefoil fold domain family of proteins and has four β trefoil domains (Ponting & Russell 2000). Each β-trefoil fold consists of six two-stranded β-hairpins, three of which form a barrel structure, while the remaining three form a triangular cap on the barrel. Another feature of this fold is that it is composed of three structural repeats, which appear to be highly conserved. Fascin was initially characterised as an actin-bundling protein 20 years ago (Cant et al. 1994). The four β-trefoil domains of fascin fold in a pseudo-symmetric globular protein, which account both for the actin-bundling property of fascin and for the approximate 1:4 stoichiometry of fascin:F-actin bundles, assuming each domain possesses an actin-binding activity (Ponting & Russell 2000).

Several studies have shown both actin-binding and bundling properties of fascin are regulated by phosphorylation (Anilkumar et al. 2003; Ono 1996). In particular, it has been shown that fascin associates both *in vivo* and *in vitro* with Protein Kinase Cα (PKCα) and that this kinase can directly phosphorylate serine39 in human fascin (Anilkumar et al. 2003). When the fascin-PKCα interaction is inhibited, cellular protrusion development and FA remodelling are increased. Although several mutagenesis and phospho-mapping experiments have been recently attempted to identify actin binding and/or phosphorylated sites on fascin protein (Yang et al. 2012; Jansen et al. 2011), only one actin-binding site has been so far fully characterised. Indeed, the best-characterized actin-binding site is located at the amino terminus in the first beta-trefoil domain (between aa29 and aa47). This domain also contains the phosphorylation site for PKCα. PKCα phosphorylates fascin at serine 39 resulting in loss of actin binding, reduced formation of filopodia and decreased cell migration (Anilkumar et al. 2003; Adams 2004). Recently, another potential actin-binding site has been determined (Zanet et al. 2012) and it lies

between residues 277 and 493 within the C terminus of fascin. The C terminal actin-binding site has been identified in both *Drosophila* fascin (singed) as well as human fascin. A phospho-mimetic mutation on serine 289 in *Drosophila* fascin disrupted the actin-bundling capacity of fascin. Unexpectedly, the same mutation was able to fully rescue filopodia formation in macrophages in fascin mutant flies (Zanet et al. 2012). Moreover, mutations in the corresponding conserved human site (S274) similarly affected fascin-actin bundling and altered filopodia formation. The mechanisms regulating this second actin-binding site in cells are still unclear. An actin-bundling independent activity has been suggested to explain filopodia formation in mutant cells (Zanet et al. 2012). This hypothesis was also supported by a recent study that shows mutation on serine 274 and others to have a moderate effect on actin bundling compared to S39D (Yang et al. 2012). Therefore an alternative mechanism regulating the other actin binding sites would explain an actin-independent role for fascin in filopodia formation. The regulation of phosphorylation at serine 274 is still under investigation. Unpublished data and i*n silico* analysis from our lab has shown S274 is phosphorylated in cells (through phospho mass spec analysis) and the phosphorylation may be dependent on protein kinase A (PKA). Figure 1.12 shows a schematic of the two known actin-binding sites and their regulation.

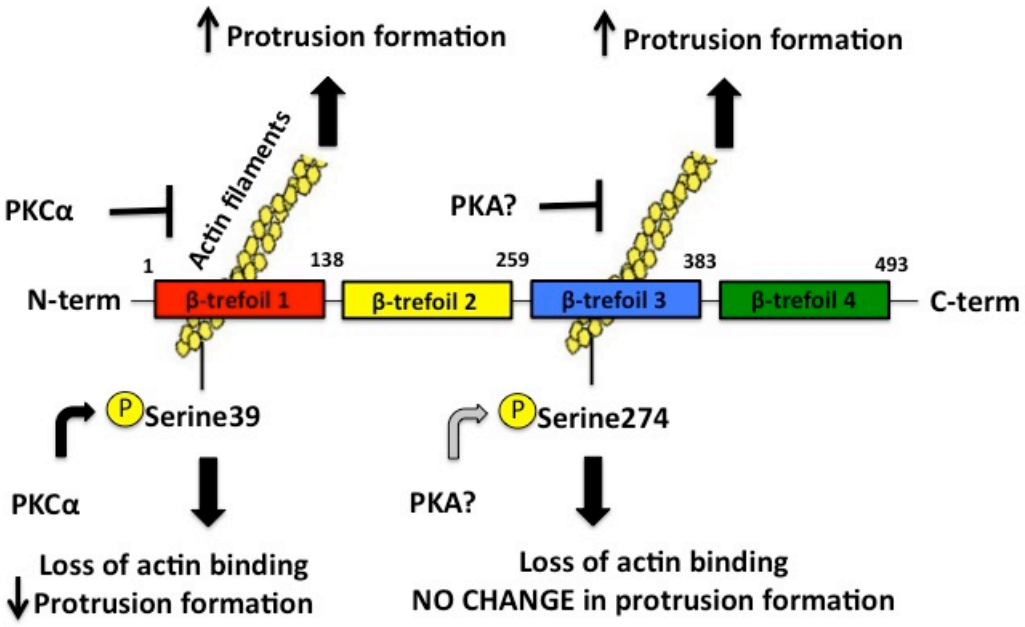

Figure 1.12. Schematic of fascin actin binding sites and their regulators

The four β trefoil domains of fascin are shown. The best-characterised actin-binding site lies on the Serine 39 in the first β trefoil domain (in red). PKCα regulates the binding between fascin and actin filaments (yellow filaments). Fascin binding to actin promotes protrusion formation. PKCα phosphorylation on the Serine 39 results in loss of actin binding and decrease in protrusion formation. A second actin-binding site has been identified and in the third β trefoil domain (in blue). The mechanism regulating this actin-binding site is not clear yet, but serine 274 residue within this region plays a key role. It is known that its binding to actin promotes protrusion formation and a phospho-dead mutation promotes the loss of the actin binding without obvious change in protrusion formation. S274A fascin also localises to the tips of filopodia, but does not colocalise with F-actin in these regions. Therefore, an actin-independent activity for this mutant is suggested. Unpublished data proposes PKA as a potential kinase promoting Serine 274 phosphorylation. Note the model does not depict protein real sizes.

1.4.3. Function of fascin

Fascin plays a critical role in cell adhesion, motility and invasion through binding and bundling actin filaments to stabilise them. Fascin, together with other actin cross-linking proteins, is involved in the assembly and maintenance of lamellipodia, filopodia and stress fibres (Small et al. 2002). Fascin binds actin filaments selectively, cross-linking parallel-orientated polymers only (Courson and Rock 2010). Serine 39-

PKC-dependent phosphorylation on fascin allows efficient and dynamic coordination of filopodia elongation/invasiveness and bundling (Vignjevic et al. 2006b). Fascin also localizes in F-actin containing structures such as podosomes and invadopodia, promoting their stability (Li et al. 2010; Quintavalle et al. 2010). Fascin mRNA and protein are both highly up-regulated in many types of cancer and this acts to promote invasiveness of cancer cells (Machesky & Li 2010). Fascin role in promoting cancer invasion and metastasis is also dependent on PKC-phosphorylation (Li et al. 2010; Hashimoto et al. 2007). Loss of fascin is associated with a decrease in cell spreading, adhesion and migration (Adams 2004). Fascin knockdown expression in human carcinoma cell lines has previously been shown by our lab to decrease focal adhesion dynamics, suggesting it may play a role in adhesion site stability (Hashimoto et al. 2007). However, fascin has not been found to localise in focal adhesions and thus the way in which fascin may contribute to adhesion stability and dynamics is still unknown.

PKC-binding and phosphorylation of fascin has previously been shown to depend in part on the small GTPase Rac1 and its downstream effector PAK1 (Hashimoto et al. 2008). Fascin also cooperates with the Arp2/3 complex and formins to assemble filopodia and invadopodia, but this is not thought to be via direct associations between these proteins and fascin (Baldassarre et al. 2006; Lizárraga et al. 2009). More recently, RhoA has been suggested as another regulator of fascin function in the assembly of F-actin structures (Jayo et al. 2012). In particular, fascin-F-actin binding is regulated by Rho kinase (ROCK) activity, but independent of myosin II or fascin/PKC complex formation. RhoA activation promotes fascin complex formation with LIM kinase (LIMK), which regulates filopodia stability. Furthermore, cofilin, an actin-depolymerising molecule, has been shown to cooperate with fascin in disassembling filopodia filaments (Breitsprecher et al. 2011). Figure 1.13 shows a schematic of fascin regulation and functions.

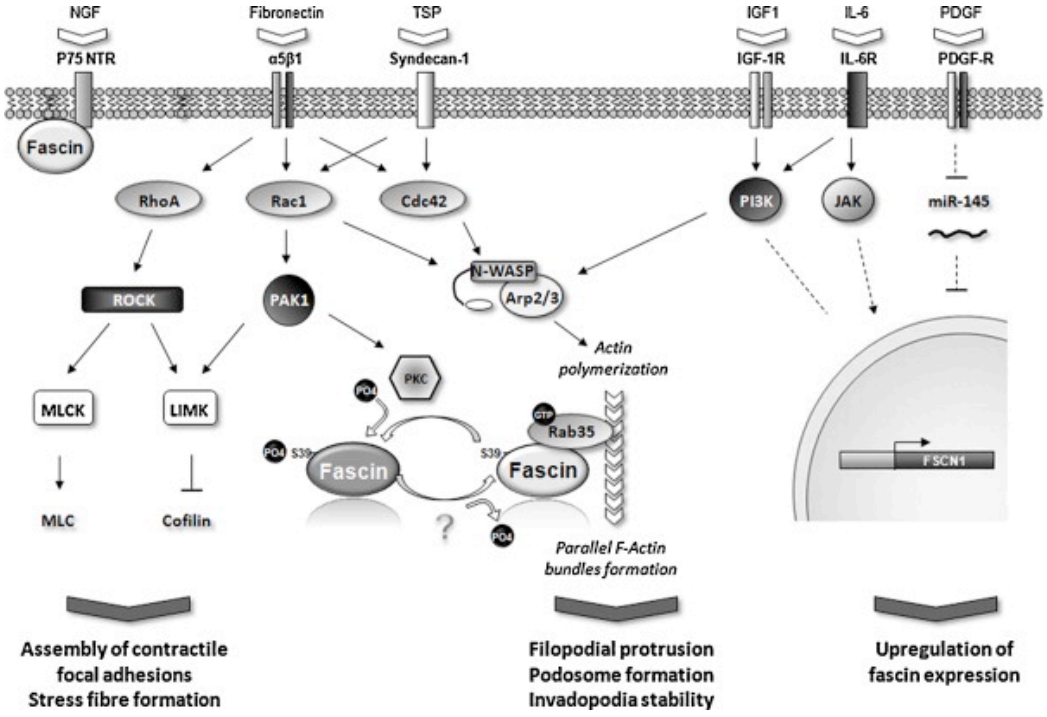

Figure 1.13. Regulation and functions of fascin (Jayo and Parsons 2010)
Fascin role in regulating stress fiber and FA formation together with filopodia and invading protrusion assembly is downstream of RhoA-driven ROCK activity and Rac1-dependent PAK1 regulation of PKC-fascin complex formation.

1.5. Microtubule-actin crosstalk in cell adhesion and motility

Many studies have shown MT to play a positive role in migration by regulating actin polymerisation, transport membrane vesicles to the leading edge and facilitating the turnover of adhesion sites (Small et al. 2002; Ridley 2011). The first studies of the role of MT role in migration showed cells treated with MT-depolymerising drugs results in increased cell migration speed (Ueda et al. 1997). Recently, mutations in β tubulin have been associated with abnormal cell migration (Keays et al. 2007) and

MT-targeting drugs have shown to increase actin protrusions formation and induce FA assembly. For instance, treatment of cells with nocodazole, a drug which de-polymerises MT, results in increased stress fibre formation and cell contractility (Chang et al. 2008). On the other hand, the MT-stabilising agent Taxol prevents the strengthening effect on FA promoted by nocodazole (Ganguly et al. 2012). It has also been shown that both increased cell contractility and FA assembly are rescued to normal levels by MT repolymerisation (Ezratty et al. 2005). Moreover, MT assembly exerts a pushing force that can act to counterbalance the contractile forces exerted by the actin fibres. Although the molecular details of how actin-MT crosstalk regulates cell adhesion and migration are still not fully understood, the current concept is that protrusion initiation signals may be driven by the actin network, whereas adhesion turnover and protrusion elongation may be due to crosstalk and co-operation between actin and microtubules (Schoumacher et al. 2011; Small et al. 2002). Two zones within cells have been distinguished: an actin-rich region with lamellipodia and filopodia and a MT-rich region where actin polymerisation is limited (Etienne-Manneville 2004) (Figure 1.14). The relative extension of the actin/MT rich regions depends on cell and protrusion types. Indeed, lamellipodia formation does not require dynamic MT, but these are essential for cell body movement and rear retraction (Webb et al. 2002). MT co-operate with stress fibres promoting maturation and turnover of FA at both the leading and trailing edge (Stehbens & Wittmann 2012). In some cell types, MT have also been shown to mediate filopodia reorganization (Schober et al. 2007).

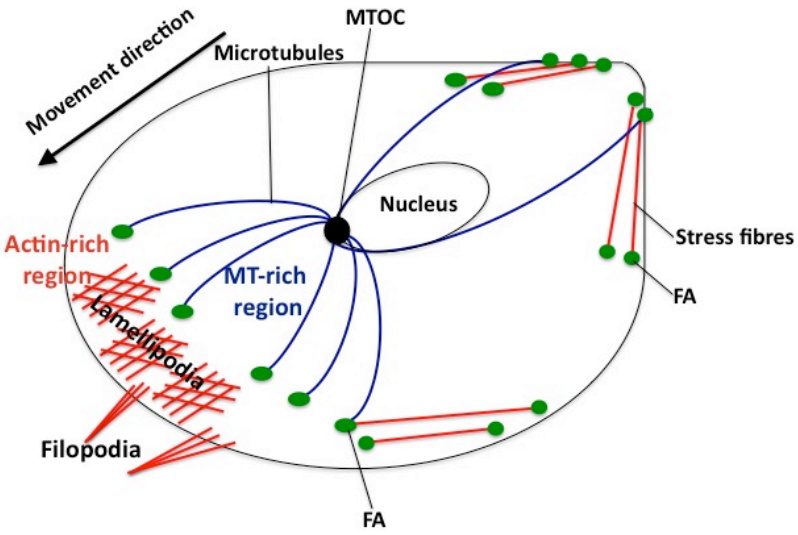

Figure 1.14. Actin and MT rich-regions in the regulation of stress fibre and FA dynamics

Two regions can be distinguished in the cellular leading edge: an actin-rich region (in red) and a MT-rich region (in blue). The first one comprises actin-based structures such as lamellipodia and filopodia, while the second shows MT (in blue) radiating from the MTOC (in black) and growing with their +ends towards the leading edge. MT target and stabilise FA (green circles). Actin structures in the MT-rich region are limited to stress fibres (red lines) co-operating with MT in FA assembly. Stress fibres and MT are also critical in regulating FA and trail retraction at the back of the cell. Direction of the movement is shown.

The role of MT in cell motility became more complex when studies observed different effects on cell migration depending on the concentration of MT-depolymerising drugs used (Ganguly & Cabral 2011). Low concentrations of nocodazole induces loss of MT dynamics and thus decreased fibroblast motility, without evident changes in MT assembly/polymerisation (Liao et al. 1995). On the other hand, high concentrations of the drug promote cell contractility and migration, affecting MT polymerisation (Ganguly & Cabral 2011). Therefore, MT polymerisation and/or dynamic integrity have different effects on cell motility. Additionally, tubulin post-translation modifications have been associated with changes in F-actin stability and cell motility. For instance, increased levels of tubulin acetylation after histone deacetylase 6 (HDAC6) inhibition results in decreased FA dynamics (Tran et al. 2007).

Furthermore the mechanism may involve the HDAC6 acetylation of cortactin, which alters the ability of cortactin to bind and stabilise F-actin (Zhang et al. 2007).

The actin-MT crosstalk can be classified as either 'regulatory' or 'structural' (Rodriguez et al. 2003). The structural interactions are the ones where actin and MT are physically linked. Some molecules regulating the assembly and/or stability of the two major cytoskeleton components have been demonstrated to directly interact with each other (Rodriguez et al. 2003). For instance, MT +TIP proteins can co-operate with actin-dependent adhesion structures to drive protrusion formation and generate forces to push the leading edge forward (Lansbergen & Akhmanova 2006; Morrison 2007). EB1 has been shown to interact with PKC in maintaining cell polarity (Schober et al. 2012). Additionally, EB3 has been shown to directly bind to the F-actin-associated protein drebrin and both proteins co-localize in the filopodia protrusions during neuritogenesis (Geraldo et al. 2008). Formins, such as INF2, mDia 1 and mDia2, have been shown to have different interaction with MT and thus different effects on either MT growth or catastrophe rate (Gaillard et al. 2011). The MAP CLIP-170 has been shown to interact with the actin-binding protein IQGAP1 in regulating dendrite morphology (Swiech et al. 2011).

Additionally, proteins that directly link actin and MT together have been reported. For instance, ACF7 is both a MT +TIP and actin-binding protein and has been shown to regulate both cytoskeletons through different mechanisms (Jefferson et al. 2004; Wu et al. 2011). The MAP doublecortin promotes lamellipodia formation in brain development inducing F-actin reorganisation and decreasing MT bundling (Toriyama et al. 2012). LIM kinase 1 promotes actin polymerisation both inhibiting cofilin actin depolymerising activity but also promoting MT destabilisation via complex formation with tubulin (Gorovoy at al 2006). Lastly, proteins which activate the Arp2/3 complex, called WHAMM (WASP homolog associated with actin, membranes and

microtubules), have been shown to alter membrane dynamics modifying the interplay between actin and MT (Campellone et al. 2008).

The regulatory cooperation is the one in which actin and MT indirectly crosstalk, via activation of common signalling cascades. The Rho family GTPases regulation of actomyosin contractility together with MT stability is one of the best cited examples (Wittmann & Waterman-Storer 2001). MT can alter actomyosin contractility via the small GTPase RhoA, by locally modulating its activation (Stehbens & Wittmann 2012). Nocodazole treatment induces the MT-associated guanine nucleotide exchange factor GEF-H1 to be released from binding to MT and thus RhoA activation (Chang et al. 2008). RhoA activation results in increased FA assembly and cell contractility observed after nocodazole treatment and inhibition of Rac1-dependent effects on cell contractility (Etienne-Manneville 2004). In contrast, MT re-growth following nocodazole washout results in rapid FA disassembly in a signaling cascade pathway involving the endocytic GTPase dynamin and FAK (Ezratty et al. 2005). Although MT-dependent FA disassembly has been shown to be driven by the GEF STEF-dependent Rac1 activation (Rooney et al. 2010), Rac1 inhibition does not disrupt MT-dependent FA disassembly (Ezratty et al. 2005). Therefore, the precise MT-dependent FA disassembly mechanisms are not known. However it is clear that MT together with GTPases act coordinately to promote FA dynamics (Wittmann & Waterman-Storer 2001) (Figure 15).

Interactions between +TIPs and Rho family GTPases and other actin regulatory proteins has been shown to occur in a number of different contexts (Lansbergen & Akhmanova 2006). The depletion of a +TIP protein known as GTSE1 has been shown to inhibit FA disassembly following nocodazole washout (Scolz et al. 2012). APC regulate cell polarization connecting EB1 to Rho family GTPases (Etienne-Manneville 2004). CLIP-170 is captured by both Rac1 and Cdc42 to stabilize MTs at the cellular leading edge (Fukata et al. 2002) and the formin mDia2, Rho-downstream effector

protein, has been found to stabilize microtubules and promote cell migration by interacting with EB1 and APC (Wen et al. 2004). Moreover, the MT-stabilising protein Calpain-6 has been shown to mediate the Rac1-dependent increased cell contractility via interaction with GEF-H1 (Tonami et al. 2011).

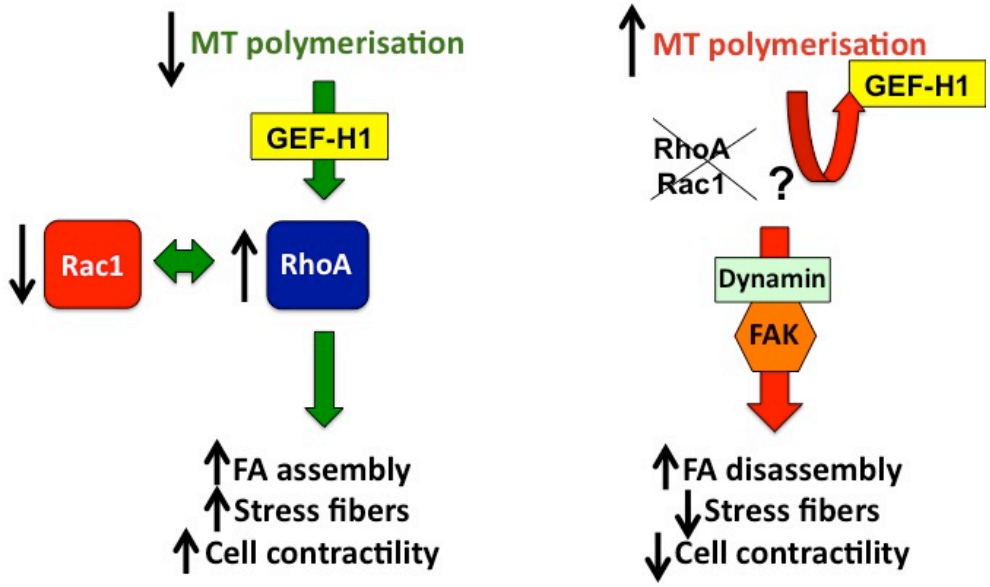

Figure 1.15. Signalling cascades regulating FA assembly and disassembly
MT depolymerisation after nocodazole treatment induces GEF-H1 release from MT and RhoA activation. RhoA activity promotes increased FA assembly, stress fibre formation and cell contractility in a Rac1-independent way. Conversely, MT re-growth following nocodazole washout re-captures GEF-H1 and somehow promotes FA disassembly and decreased stress fibre formation and cell contractility. MT-dependent FA disassembly is known to be driven by dynamin and FAK. However, how MT trigger this signaling cascade is still unknown.

Actin-MT crosstalk involves a feedback control of microtubules dynamics by actin-based structures. For instance, stress fibres emanating from FAs can act to stabilize the MT network (Small et al. 2002; Palazzo et al. 2004) and FA components such as paxillin regulate MT growing/shortening in adhesion sites (Andrey Efimov et al. 2008). MT stability is also regulated by actin-capping protein such as the formin mDia (Bartolini et al. 2012). Moreover, the Cdc42-MRCK regulation of actomyosin contractility establishes MTOC polarisation during nuclear movement (Gomes et al. 2005). Other studies have focused on the MT regulation of contacts with the ECM.

MTs may interfere with the affinity of integrins to ECM-components and thereby regulate cell polarity and migration (Small et al. 1999). In turn, MTs stability and dynamics are modified by integrin activation and ECM compliance (Lei et al. 2012; Myers et al. 2011). The mutual regulation of actin and microtubules is central in processes such as neuronal cone development (Zhou et al. 2002) and metastasis dissemination in cancer progression (Hall 2009). Although the identification of shared pathways between actin and MT have been the focus of much interest in the field, mechanisms driving their interactions are still poorly defined; particularly in the context of cancer cell invasion.

HYPOTHESIS

The hypothesis leading to this thesis is that fascin controls cell adhesion dynamics through association with microtubules, and acts to co-ordinate actin and microtubule networks to promote cancer cell adhesion and invasion.

AIMS

The work conducted in this thesis is designed to address the following aims:

- Determine the role of fascin-actin binding in controlling focal adhesion assembly and size in human cancer cells.
- Investigate whether fascin-actin binding contributes to microtubule-induced focal adhesion dynamics or vice versa.
- Determine whether fascin associates directly or indirectly with the microtubule network.
- Examine the role of fascin-actin binding in possible crosstalk with the microtubule cytoskeleton.
- Investigate whether fascin forms a complex with focal adhesions-associated proteins and whether this plays a role in fascin-dependent control of adhesion dynamics.

2 MATERIAL AND METHODS.

2.1. Reagents

Table 2.1. Cell culture reagents

Reagent	*Source*
Bovine Collagen, Type I	BD Biosciences
Calyculin A (10 µM final)	Calbiochem
Dimethyl sulphoxide (DMSO)	Sigma
Foetal Bovine Serum	Sera Laboratories International Ltd.
High Glucose Dulbecco's modified Eagle's media (DMEM)	Sigma Aldrich
Human Plasma Fibronectin Purified Protein	Millipore
L-Glutamine	PAA
Lipofectamine	Invitrogen
MG132 (20 µM final)	Calbiochem
Nocodazole	Sigma Aldrich
OptiMEM	Gibco
Paclitaxel (taxol)	Sigma Aldrich
Penicillin/ Streptomycin	Gibco
Phosphate Buffered Saline (PBS)	Lonza
Polybrene (hexadimethrine bromide)	Sigma Aldrich
Protease inhibitor (PI) cocktail set 1 (stock 100X, dilute to 1X)	Calbiochem
Containing:	
AEBSF, Hydrochloride - 500 µM	
Aprotinin, Bovine lung, crystalline – 150 nM	
E-64 Protease Inhibitor - 1 µM	
EDTA Disodium – 0.5 mM	
Leupeptin, Hemisulphate – 1 µM	

Rat Plasma Vitronectin	Sigma Aldrich
Trypsin/EDTA	PAA

Table 2.2. Molecular biology reagents

Reagent	***Source***
Agarose	Sigma Aldrich
Ampicillin	Sigma Aldrich
BL21 (DE3) competent cells	Agilent Technologies
Bovine serum albumin (BSA)	New England Biolabs
Deoxynucleosides (DNTPs)	Bioline
Hyperladder I	Biolabs
Hypperladder V	Biolabs
Imidazole	Sigma Aldrich
Kanamycin	Sigma Aldrich
Linear Polyethylenimine (PEI)	Polysciences, Inc
Luria Bertani (LB) agar and broth	Sigma Aldrich
Midiprep kit	Qiagen
Miniprep kit	Qiagen
NEbuffers	New England Biolabs
One Shot TOP10 chemically competent E.Coli	Invitrogen
Phusion Hot Start DNA polymerase	Finnzymes
Phusion buffer (10X)	New England Biolabs
Phusion polymerase	New England Biolabs
QIAquick gel extraction kit	Qiagen
Quickchange Site-directed mutagenesis kit	Stratagene
Restriction enzymes	New England Biolabs
Safeview	NBS Biologicals
T4 DNA Ligase and Buffer	New England Biolabs

Zero Blunt PCR Cloning Kit	Invitrogen

Table 2.3. Biochemical assay reagents

Reagent	***Source***
1.5 mm Cassettes	Invitrogen
1,4-Piperazineethanesulfonate (PIPES)	Sigma Aldrich
2-mercaptoethanol	Sigma Aldrich
30% Acrylamide/Bis solution	Biorad
A/G agarose affinity matrix	Alpha Diagnostic International
Adenosine-5'-triphosphate (ATP)	Sigma Aldrich
Ammonium persulphate (APS)	Sigma Aldrich
Bovine Brain Tubulin Protein	Cytoskeleton
Bovine Serum Albumin	PAA the cell culture company
Bromophenol blue	Sigma Aldrich
Calcium Chloride	Sigma Aldrich
Calyculin A	Sigma Aldrich
Coomasie blue	Fluka Chemika
Chromatography disposable columns	Thermo Scientific
Dithiothreitol (DTT)	Sigma Aldrich
ECL Plus western blotting detection system	GE Healthcare
EDTA (EGTA)	Sigma Aldrich
Fluorsave Mounting media	Calbiochem
G-actin	Sigma Aldrich
Glutathione Sepharose 4 Fast Flow beads	Amersham
Glycine	Sigma Aldrich

Glycerol	VWR International
Guanosine 5'-Triphosphate Sodium Salt Hydrate (GTP)	Sigma Aldrich
Hybond ECL Nitrocellulose membrane	Amersham Biosciences
Immersol 510 Immersion oil	Zeiss
Isopropyl β-D-1-thiogalactopyranoside (IPTG)	Sigma Aldrich
Magnesium Chloride	Fluka Analytical
Medical X-Ray film	Fuji
Milk Powder	MERCK
Ni-NTA Agarose Beads	Qiagen
Paraformaldehyde (PFA)	Sigma Aldrich
PeqGOLD protein marker V	PeqLab
Pierce BCA protein assay kit	Thermo Scientific
PBS tablets	Oxoid
Pierce ECL western blotting substrate	Thermo Scientific
Ponceau S solution	Sigma Aldrich
Porcine Brain Tubulin Protein (Rhodamine)	Cytoskeleton
Potassium Chloride	Sigma Aldrich
Sodium Chloride	Sigma Aldrich
Sodium Phosphate	Sigma Aldrich
Tetramethylethylenediamine (TEMED)	Sigma Aldrich
Tissue-Tek OCT compound	VWR international
Tris-Base	Sigma Aldrich
Tris-HCL	Sigma Aldrich
Triton X-100	Sigma Aldrich
Tween-20	Sigma Aldrich

Table 2.4. Solutions for biochemical assays

Buffers/Solutions	***Composition***
5% stacking acrylamide gel	5% 30%-acrylamide mix, 125mM Tris-HCl (pH6.8), 0.1% Sodium dodecyl sulphate (SDS), 0.1% ammonium persulphate (APS), 1% TEMED
8% resolving acrylamide gel	8% 30%-acrylamide mix, 400 mM Tris (pH 8.8), 0.1% SDS, 0.1% APS, 0.05% TEMED
10% resolving acrylamide gel	10% 30%-acrylamide mix, 400 mM Tris (pH 8.8), 0.1% SDS, 0.1% APS, 0.05% TEMED
Coomassie staining solution	0.025% Coomassie brilliant blue R250, 40%methanol, 7% acetic acid
Destaining solution	50% methanol, 10% acetic acid
F-Actin Polymerisation Buffer	50 mM Potassium Chloride, 2 mM Magnesium Chloride, 1 mM ATP
G-Actin Resuspension Buffer (KME 10x)	500 mM Potassium Chloride, 10 mM Magnesium Chloride, 10 mM
General Tubulin Buffer (GTB)	EGTA, 100 mM imidazole (pH 7)
	50 mM PIPES (pH 6.8), 1 mM EGTA, 1 mM Magnesium Chloride
His_6 tagged Protein Purification Lysis Buffer	50 mM Sodium Phosphate, 10 mM imidazole, 300 mM Sodium Chloride (pH 8)
His_6 tagged Protein Wash Buffer 1	50 mM Sodium Phosphate, 20 mM imidazole, 300 mM Sodium Chloride

	(pH 8)
His_6 tagged Protein Wash Buffer 2	50 mM Sodium Phosphate, 50 mM imidazole, 300 mM Sodium Chloride (pH 8)
His_6 tagged Protein Elution Buffer	50 mM Sodium Phosphate, 250 mM imidazole, 300 mM Sodium Chloride (pH 8)
His_6 tagged Protein Storage Buffer	PBS 1x, 10 mM imidazole, 10% Glycerol (pH 8)
Lysis Buffer	50 mM Tris (pH7.2), 500 mM NaCl, 10mM MgCl, 0.5% sodium deoxycholate, 1% Triton X-100, PI cocktail, Phosphatase inhibitors: 50 mM Sodium Fluoride and 1 µM Calyculin A
PBS-Tween (1x)	10 tablets of Phosphate buffered saline, 0.1% Tween-20
PlusOne Silver Staining Kit	GE Healthcare
Running Buffer (10x)	0.25 M Tris base, 1.92 M glycine, 1% SDS
SDS Sample Loading Buffer (2x)	60mM Tris-HCl (pH 6.8), 25% Glycerol, 2.5% SDS, 0.02% Bromophenol blue
TBS-Tween (10x)	20 mM Tris-base (pH 7.5), 150 mM NaCl, 0.1% Tween-20
Tubulin Polymerisation Buffer (TB1)	General Tubulin Buffer, 10% Glycerol, 5 mM Magnesium Chloride, 1 mM GTP
Tubulin Pelleting Buffer (TB2)	General Tubulin Buffer, 50%

	Glycerol, 1mM GTP, 80 uM Taxol
Tubulin Resuspension Buffer (TB3)	General Tubulin Buffer, 1 mM GTP, 80 uM Taxol
Transfer buffer (10x)	0.25 M Tris base, 1.86 M glycine, 10% methanol

2.2. Antibodies

Table 2.5. Antibodies

Target	***Dilution***	***Species***	***Source***
α/β Tubulin	1/2000 (WB) 1/50 (IF)	Rabbit	Cell signalling Technology
β Tubulin	1/200 (IF) 1/2000 (WB)	Mouse	Sigma Alrich
Acetylated tubulin	1/200 (IF) 1/500 (WB)	Mouse	Sigma Aldrich
Fascin	1/200 (IF) 1/2000 (WB)	Mouse	DAKO
Focal Adhesion Kinase (FAK)	1/200 (IF) 1/1000 (WB)	Rabbit	Santa Cruz Biotechnology

	1 μg (IP)		
Phospho-Tyrosine (PY)	1/200 (IF)	Mouse	Sigma Aldrich
Tyrosine-379-Phosporylated FAK	1/200 (IF) 1/2000 (WB)	Rabbit	Invitrogen
Vinculin	1/200 (IF) 1/500 (WB)	Mouse	Sigma Aldrich
Anti-Mouse HRP	1/1000 (WB)	Goat	DAKO
Anti-Rabbit HRP	1/1000 (WB)	Goat	DAKO
Anti-Mouse Alexa 488	1/400 (IF)	Goat	Molecular Probes
Anti-Mouse Alexa 568	1/200 (IF)	Goat	Molecular Probes
Anti-Mouse Alexa647	1/200 (IF)	Goat	Invitrogen
Anti-Mouse Alexa633	1/100 (IF)	Goat	Molecular Probes
Anti-Rabbit Alexa 488	1/400 (IF)	Goat	Molecular Probes
Anti-Rabbit Alexa 568	1/200 (IF)	Goat	Molecular Probes
Anti-Rabbit Alexa 633	1/100 (IF)	Goat	Molecular Probes
Phallodin 488	1/400 (IF)		Invitrogen
Phalloidin 568	1/200 (IF)		Invitrogen
Phalloidin 633	1/100 (IF)		Invitrogen

Abbreviations: Western blotting (WB), immunoflourescence (IF) and immunoprecipitation (IP).

2.3. Methods

2.3.1. Molecular biology and cloning

2.3.1.1. Generation of lentiviral vector to target fascin expression

Human lentiviral short hairpin RNA (shRNA) targeting fascin was cloned into the pLentiLox 3.7 (LL3.7), kindly donated by Dr Monypenny (King's College London). The vector map is shown in Figure 2.1.

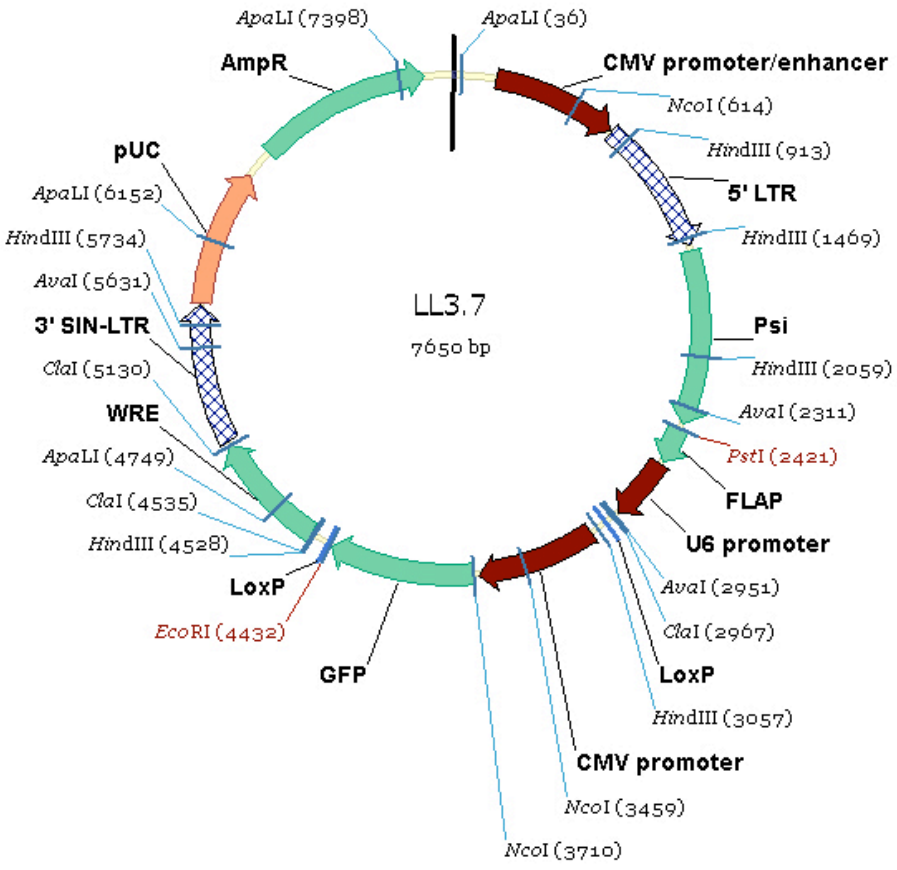

Figure 2.1. Map of the pLentiLox (LL3.7) lentiviral vector

The sequence of the shRNA (gift from Dr Adams, University of Bristol, UK) used to knock down fascin was 5'-GCCTGAAGAAGAAGCAGAT-3' directed to the first exon of the human fascin gene, isoform 1 (FSCN1) (Figure 2.2). Additionally, a scrambled sequence of the shRNA was cloned into the LL3.7 vector and used as a control.

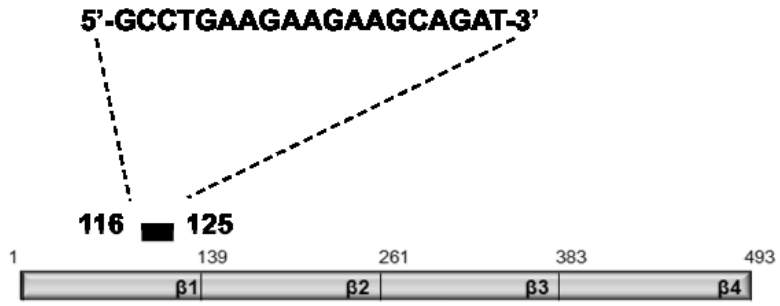

Figure 2.2. The target sequence of the shRNA is located in the first exon of human fascin gene

ShRNA-resistant hFascin cDNA in which the shRNA target sequence was changed to 5'-GCCTGAA**A**AA**A**AA**A**CAGAT-3' (bold letter indicate changes) by site directed mutagenesis and its wild type and mutant forms were generated and tagged in the N terminal site with EGFP (pEGFP vector, Takara Bio Inc).

The four Fascin mutant forms studied in this thesis were Ser39 and 274 mutated to either a non-phosphorylatable Alanine (A) or a phosphorylatable Aspartic Acid (D) and were generated as described in (Zanet et al. 2012). For recombinant fascin purification, the cDNA encoding hfascin wild type and mutants were cloned between *NotI* and *XhoI* restriction sites in the p-ET30a(+) vector (Novagen). Scrambled and fascin targeting shRNA sequences were also cloned into a pLKO lentiviral vector (RNAi Consortium) between the *AgeI* and *EcoRI* sites (Dr Jayo, King's College London). Antiparallel oligonucleotides containing the shRNA target sequence and flanking *AgeI* and *EcoRI* restriction sites used were:

Sense: 5'-CCG GGC CTG AAG AAG AAG CAG ATC TCT CGA GAG ATC TGC TTC TTC TTC AGG CTT TTT G-3'
Antisense: 5'-AAT TCA AAA AGC CTG AAG AAG AAG CAG ATC TCT CGA GAG ATC TGC TTC TTC TTC AGG C-3'

The human α-tubulin cDNA was cloned in m-Cherry tagged lentiviral vector pLVX (gift from Dr Monypenny, KCL) between *XhoI* and *BamHI-HF* sites. The following primers were used for PCR:

Sense: 5'-CTC GAG GGA GGT GGA ATG CGT GAG TGC ATC TCC AT-3'
Antisense: 5'-GGA TCC TTA GTA TTC CTC TCC TCT T-3'

The cDNAs encoding the GST tagged FERM domain, Kinase domain and C terminal domain of Focal Adhesion Kinase were kindly donated by Dr Frame (University of Edinburgh, UK).

2.3.1.2. Transformation of pGEX GST vectors

2 µl of DNA was added into 25 µl of BL21 competent cells, left on ice for 30 min and heat shocked at 42°C in a waterbath for 45 seconds and then left in ice for 2 min. 250 µl SOC media was added and placed in a 37 C shaking incubator for 1 h. Finally the solution was streaked on an agar plate with the appropriate selection antibiotic (Ampicillin 100 µg/mL for the pGEX system) and left in the 37 °C incubator overnight for growth.

2.3.1.3. Bacterial Transformation

Transformations were performed according to protocols provided by Invitrogen. Briefly, One Shot Top10 E.coli were thawed on ice, then 1-5 µl DNA was added to each vial (50 µl) of competent cells and were incubated for 30 min on ice. This was followed by incubation at 42 °C for 45 seconds and then immediate incubation on ice for 2 min. 250 µl S.O.C. media was then added and incubated for 1-2 h shaking at 37 °C. LB agar plates containing Kanamycin (50 µg/mL) were then spread with the solution. Plates were inverted and incubated at 37°C overnight.

2.3.1.4. Restriction digests

Restriction digests were performed according to protocols provided by New England BioLabs. Briefly, the restriction digest was made up of 2-3 µg DNA, the appropriate NEbuffer (1X) (New England BioLabs), BSA (1X) (New England BioLabs), 0.5 µl restriction enzyme (New England BioLabs) per 1 µg DNA and made up to 50 µl with deionised water. For double digest both enzymes were added at the same time, or if sequential the second restriction enzyme was added after digest with the first restriction enzyme. Loading buffer was added to each digest and they were run on a 1% agarose gel containing 1:50 (1% stock, 0.02% final) ethidium bromide.

2.3.1.5. Gel extraction

DNA was extracted using the QIAquick gel extraction kit according to the protocol provided by QIAGEN. Briefly, the DNA fragment was removed from the agarose gel and 3 volumes of Buffer QG were added to 1 volume of gel. The sample was placed in a QIAquick spin column and was centrifuged for 1 min. The sample was washed with 500 µl of Buffer QG and centrifuged for a further 1 min, and also washed with

750 µl of Buffer PE and centrifuged for a further 1 min. The column was centrifuged for a further 1 min and placed in a clean 1.5 ml microcentrifuge tube, 30 µl elution buffer was added to the column and left to stand for 1 min. Then the column was centrifuged for 1 min to elute the DNA. A Nanodrop Spectrophotometer (Labtech International) was used to quantify the concentration and purity of the DNA.

2.3.1.6. Minipreps

1 ml of bacterial overnight culture with the appropriate selection antibiotic was centrifuged at 13,000 rpm for 5 min. The supernatant was discarded and the pelleted bacterial cells were resuspended in 250 µl of Buffer P1. Before using Buffer P1, LyseBlue reagent was added to Buffer P1 at a ratio of 1 to 1000, RNase was also added and mixed in. 250 µl of Buffer P2 was then added and mixed thoroughly by inverting the tube 4–6 times until the solution became clear. The solution turned blue due to the addition of LyseBlue reagent. 350 µl of Buffer N3 was added and mixed immediately and thoroughly by inverting the tube 4–6 times or until the solution became colourless. The solution was centrifuged for 10 min at 13,000 rpm (~17,900 x *g*) in a table-top microcentrifuge at room temperature. The supernatant was transferred to the QIAprep spin column and centrifuged for 1 min and the flow-through was discarded. To wash the QIAprep spin column, 0.75 ml Buffer PE was added and centrifuged for 1 min and the flow-through was discarded. The QIAprep spin column was centrifuged again for 1 min to remove residual wash buffer. To elute DNA, 50 µl of deionised water was added to the centre of the QIAprep spin column, and allowed to stand for 1 min at room temperature and finally centrifuge for 1 min. The flow-through contained the DNA which was measured using a Nanodrop Spectrophotometer.

2.3.1.7. Midipreps

25-50 ml of bacterial culture was grown up overnight with the appropriate antibiotic and pelleted by centrifugation at 13000 rpm for 15 min. The pellet was resuspended by pipetting in 2 ml of Buffer P1. 2 ml of Buffer P2 was added and gently mixed by inverting and incubated at room temperature for 3 min. LyseBlue reagent was added to Buffer P2 and the cell suspension turned blue as a control of cell lysis and DNA denaturation. Then a further 2 ml of Buffer S3 was added to the lysate and mixed immediately by inverting 4–6 times. Addition of Buffer S3 caused rapid pH neutralisation and a fluffy white precipitate to form containing genomic DNA, proteins, cell debris, and SDS. The suspension was mixed until all trace of blue was gone and the suspension was colourless. The mixture was transferred into the QIAfilter cartridge and incubated at room temperature for 10 min. A plunger was inserted into the QIAfilter cartridge and the cell lysate was filtered the into a new tube, to which 2 ml of Buffer BB was added and mixed by inverting 4–6 times. The lysate was then transferred to a QIAGEN Plasmid Plus Midi spin column with a tube extender attached on the QIAvac 24 Plus. Using vacuum, the solution was drawn through the column. DNA bound to the column was washed with 0.75 ml of Buffer and again washed with 0.7 ml of Buffer PE. To completely remove the residual wash buffer, the column was centrifuged for 1 min at 10,000 x g in a microcentrifuge. The column was then placed into a clean 1.5 ml microcentrifuge tube and to elute the DNA, 200 µl of deionised water was added to the centre of the column, with 1 min incubation at room temperature, and then finally centrifuged for 1 min. The DNA concentration and quality was measured using a Nanodrop Spectrophotometer.

2.3.2. Cell culture

2.3.2.1. Cell lines

MDA-MB-231 human breast carcinoma, 293T and HeLa cervical cancer cells were maintained at 37 °C in Dulbecco's Modified Eagle's Medium (DMEM) with 4500 mg/L glucose supplemented with 10% fetal bovine serum (FBS), 1% L-Glutamine, 1:100 dilution of 10000 penicillin units and 10 mg/ml of streptomycin. To passage, cells were washed once with PBS (without Ca and Mg, PAA) and trypsinised (Trypsin in EDTA at 0.05% concentration). After detachment the cells were centrifuged for 3 min at 1200 rpm and resuspended in 6 ml of media, which were divided in T75cm^2 flasks. To freeze the cells down, they were resuspended in 3 ml of media with 10% DMSO and divided in three vials. Stocks of all cell lines were retained in liquid nitrogen.

2.3.2.2. Producing lentiviral particles and infecting cells

To generate stable cell lines of MDA-MB-231 cells expressing the shRNA targeting fascin, this was cloned into the pLentiLox 3.7 (LL3.7) or pLKO lentiviral vector. A scrambled sequence of the shRNA was also cloned and used as a control. For each plasmid to be transfected, a flask of T25 cm^2 of HEK293T was plated. The transfection mix was prepared with a total of 11.4 μg of DNA (5.7 μg target plasmid i.e. LL3.7 transfer vector containing the scrambled or the shRNA sequence, 4.3 μg of packaging plasmid Δ8.91 and 1.4 μg of envelope plasmid pMD2.G) in 600 μl of OPTI-MEM. A mastermix of PEI transfection reagent in serum-free OPTI-MEM was also created. This consisted of 5 μl of PEI (30 μM, diluted from an original stock of 10

mM) in 600 µl of OPTI-MEM for every reaction. These were left to incubate for 5 min at room temperature. The PEI mastermix was then added to the DNA transfection mix and incubated for a further 20 min at room temperature. The DNA:PEI mix was added to the HEK293T cells, the media in these cells were changed to OPTI-MEM beforehand to remove the presence of antibiotics. The cells were incubated for 4-5 hours at 37 °C. The media was then changed to remove the transfection reagent and replaced with DMEM plus 10% FBS and penicillin/streptomycin and again left to incubate for 24 h at 37 °C. At this point the virus was harvested by removing the media, which contained the virus particles and centrifuging at 1200 rpm for 3 min as well as filtering through a 0.45 µm filter to remove cells. The cells were replaced with fresh media and the virus was collected again after 24 h. The virus was used immediately for infecting cells or was stored at -80 °C.

For infection of the target cells, MDA-MB-231 or HeLa cells were plated on 6 well plates and grown to 70% confluency. The media was replaced but with the addition of polybrene at a concentration of 8 µg/ml to increase efficiency of viral infection. 1 ml of lentiviral particle solution was added to the cells and left to incubate at 37 °C. The media was changed after 24 h to remove the virus and cells were grown and passaged. Cells infected with the LL3.7 lentiviral vector were put through fluorescence activated cell sorting (FACS) and selected for GFP expression. The divided cell populations were trypsinised and centrifuged at 1200 rpm for 3 min. They were then resuspended in 5 ml of 10% DMEM media, plated on T25 cm^2 flasks and used for further experiments. Cells infected with the pLKO vector were selected with Puromycin 0.5 µg/mL. Expression levels of GFP-fascin/fascin were regularly checked by immunofluorescence and western blotting.

For transient re-expression of GFP-tagged wild type and mutant forms, shRNA-resistant hFascin cDNA wild type and mutant fascin were tagged in the N terminal site with EGFP (pEGFP vector, Takara Bio Inc). To generate MDA-MB-231 fasKD cells

transiently expressing the shRNA-resistant fascin (rescued or res cells), cells were grown to 50% confluence the day before transfection. Each DNA mix was prepared with 1 µg of DNA in 50 µl of OPTI-MEM. 2 µl of lipofectamine in 50 µl of OPTI-MEM was also prepared for every reaction. These were left to incubate for 5 min at room temperature. The lipofectamine mixture was then added to the DNA and incubated for a further 20 min at room temperature. The DNA:lipofectamine mix was added to the MDA-MB-231 fasKD cells, the media in these cells were changed to OPTI-MEM beforehand to remove the presence of antibiotics. The cells were incubated for 4-5 hours at 37 °C. The media was then changed to remove the transfection reagent and replaced with DMEM plus 10% FBS and penicillin/streptomycin and again left to incubate for 24 h at 37 °C to allow cells to recover and express the GFP tagged proteins. An epifluorescence microscope was used to check the efficiency of GFP tagged wild type and mutant fascin epression. Note that GFP expression in rescued cells was much stronger than in fasKD stable cells (example images are shown in the Result sections).

2.3.2.3. Nocodazole treatment and washout assay

For the nocodazole treatment and washout assay, MDA-MB-231 and HeLa control and fascin knockdown or rescued cells were seeded on 24 well plates on different ECM proteins. The day after, the cells were treated with nocodazole (Sigma) used at 10 µM diluted in 10% FBS DMEM media for 15 min to completely inhibit MT polymerisation. Dimethyl sulfoxide (DMSO) was diluted in 10% DMEM media and used as control. After the treatment, the cells were either fixed with 4% para-formaldehyde (PFA) in PBS and stained for immunofluorescence or the nocodazole was washed out and replaced with fresh 10% FBS DMEM media for 30 or 60 min to allow MT re-growth followed by fixation with PFA. The cells were stained with antibodies for total tubulin or phospho-tyrosine and imaged with confocal

microscopy. Imaged cells were scored for microtubule assembly or adhesion size and number (see Image Analysis section).

2.3.2.4. Cell binding assay

For the adhesion assay, MDA-MB-231 control, fascin knockdown or WT and mutant fascin rescued cells were plated in a 24-well plate onto coverslips, previously coated with fibronectin (see Microscopy section). The cells were left overnight in 10% FBS DMEM. The day after, the media was changed and the cells adhering to the substrate were counted. Multiple fields of view were analysed in each experiment, which was repeated at least three times.

2.3.3. Protein production, purification and MT/actin polymerisation/co-sedimentation analysis

2.3.3.1. His_6 tagged WT and mutant fascin purification

BL21 cells containing DNA of interest were grown overnight at 37°C overnight. The culture was diluted (1:100) with fresh broth and cells grown at 37°C in a shaking incubator for 3-4 h. Protein production was induced with Isopropyl β-D-1-thiogalactopyranoside (IPTG, 0.2 mM) and incubated for a further 5 h at 37°C. The bacterial culture was pelleted by centrifuging at 3900 rpm for 15 min, 4°C. The pellet was then resuspended in 50 µl ice cold PBS per ml of original culture volume, containing protease inhibitors (Calbiochem) and disrupted by sonication for 2 minutes, using 10 second pulses at 10 A on ice. The solution was centrifuged at 3900 rpm for 30 min at 4°C and the supernatant collected. Ni-NTA agarose beads (Qiagen) were equilibrated with Lysis Buffer and subsequently added to the supernatant to 5 µl beads/1 ml original culture and left to mix overnight at 4°C. The beads were

centrifuged and washed with buffers containing increasing concentration of imidazole. A high concentration of imidazole (250 mM) was used to elute the proteins. The eluted was dialysed against Storage Buffer three times for at least 2 hours at 4 °C. Proteins were recovered and used for further experiments. Stocks of protein were kept at -80 °C and SDS-PAGE was run to check protein purification.

2.3.3.2. GST Focal Adhesion Kinase domain purification

The cDNAs encoding the GST tagged FERM domain, Kinase domain and C terminal domain of Focal Adhesion Kinase were kindly donated by Dr Margaret Frame (University of Edinburgh, UK). 5 ml of LB broth and ampicillin (1:1000) were seeded with BL21 cells containing DNA of interest and grown overnight at 37°C overnight. The culture was diluted (1:100) with fresh broth and cells grown at 37°C in a shaking incubator for 3-4 h. Protein production was induced with Isopropyl β-D-1-thiogalactopyranoside (IPTG, 0.2 mM) and incubated for a further 5 h at 37°C. The bacterial culture was pelleted by centrifuging at 3900 rpm for 15 min, 4°C. The pellet was then resuspended in 50 µl ice cold PBS per ml of original culture volume, containing protease inhibitors (Calbiochem) and disrupted by sonication for 2 minutes, using 10 second pulses at 10 A on ice. The solution was centrifuged at 3900 rpm for 10 min at 4°C and the supernatant collected. Pre-washed glutathione Sepharose 4B beads (GE Healthcare) were added to the supernatant to 1 µl beads/1 ml original culture and left to mix overnight at 4°C. The beads were spin down, washed and resuspended in 1 ml buffer with protease inhibitor. SDS-PAGE was run to check protein purification. Regardless different purification experiments, it was impossible to purify the GST-FAK Kinase domain, probably because of its toxicity to bacteria.

2.3.3.3. Microtubule polymerisation and co-sedimentation assays

The microtubule polymerisation and co-sedimentation assays were performed as previously described (Beraud-Dufour et al 2007). Briefly, bovine brain tubulin powder (Cytoskeleton) was diluted in General Tubulin Buffer (GTB) in a final concentration of 10 μg/μl. Tubulin stocks were kept at -80 °C for further experiments. 5 μg of purified tubulin were polymerised for 15 min at 37 °C in Tubulin Polymerisation Buffer (TB1). Increasing concentrations of paclitaxel (taxol) were added every 10 min. The turbidity of the reaction was measured as index of tubulin polymerisation and microtubule structure was analysed using electron microscopy (EM facility, Guy's campus, King's College London) (see Section 5.2 in Result Chapter 3). The mixture (approximately 90 μl) was then layered onto 60 μl of Tubulin Pelleting Buffer (TB2) and centrifuged at 13,000 rpm for 20 min at 25 °C. TB2 was prepared in 50% glycerol, which allows polymerised tubulin (MT) sedimentation. The MT pellet was resuspended in 60 μl of Tubulin resuspension buffer (TB3) and used for 5-6 co-sedimentation reactions. Polymerised tubulin corresponding to approximately 5 μg (1 μmol) was incubated with His_6 tagged WT or mutant fascin protein (1:1 ratio) in GTB for 30 min at 25 °C. Each reaction mixture (approximately 30 μl) was then layered onto 20 μl of GTB (2 μM taxol and 30% glycerol were added to GTB to preserve tubulin polymerisation and protein co-sedimentation). Reactions were finally centrifuged at 13,000 rpm for 30 min at 25 °C. As a control, MT, WT and mutant fascin proteins were subjected to centrifugation alone in every co-sedimentation experiment. 5x Loading Buffer was added to supernatants (unbound fraction), while each pellet was resuspended in 40 μl of GTB (15% Glycerol was added to GTB) and 2x Loading Buffer was added. The supernatant (s) and pellet (p) fractions were recovered by SDS-PAGE and stained by silver staining. Protein bands were quantified by densitometry.

2.3.3.4. Actin polymerisation and co-sedimentation assays

The actin polymerisation and co-sedimentation assays were repeated as in (J. Zanet et al. 2012). Briefly, G-actin powder (Sigma Aldrich) was resuspended in KME buffer 1x in a final concentration of 1.35 µg/µl. G-actin stocks were kept at -80 °C for further experiments. 67.5 µg of G-actin were polymerised in F-actin Polymerisation Buffer for 1 hour at 25 °C. Fresh buffer was prepared for every experiment. The mixture reaction was centrifuged at 80,000 rpm (Beckman TLA 100 rotor) for 1 hour at 25 °C. The pellet was resuspended in 50 µl of KME buffer 1x. 2 µl of this reaction correspond approximately to 3 µg of F-actin was added to fascin proteins or polymerised MT or to the two together after their co-sedimentation for 15 min at 25 °C. Reactions were finally centrifuged at 13,000 rpm for 30 min at 25 °C. As a control, F-actin was subjected to centrifugation alone in every co-sedimentation experiment. 5x Loading Buffer was added to supernatants (unbound fraction), while each pellet was resuspended in 40 µl of either KME 1x buffer (if incubated with fascin) or 15% glycerol GTB (if incubated with MT) and then 2x Loading Buffer was added. The supernatant (s) and pellet (p) fractions were recovered by SDS-PAGE and stained with silver staining. Protein bands were quantified by densitometry.

2.3.3.5. GST pulldowns

Control or fascin knockdown MDA-MB-231 cells rescued for GFP tagged WT fascin were washed twice with ice-cold PBS. The cells were scraped into cold lysis buffer (50 mM Tris (pH7.2), 500 mM NaCl, 10 mM MgCl, 0.5% sodium deoxycholate, 1% Triton X-100), containing protease inhibitor cocktail (see Table 2.1) and phosphatase inhibitors (50 mM sodium fluoride and 1 µM calyculin A. 500 µl of the lysis buffer were used for ~80% confluent T75 cm^2 flask. Cells were then transferred into 1.5 ml tubes. These were left on a rotator at 4 °C for 30 min to ensure complete lysis and then centrifuged at 13,000 rpm for 1 min at 4 °C to pellet insoluble material. 20 µl of

the sample of cell lysate was removed before adding lysate to beads to allow analysis of total protein on the same gel as the pulldown samples. The cleared lysates were transferred into tubes with 50 µl GST-tagged protein and placed on a rotator at 4 °C for 60 min. The beads were washed 4 times with ice-cold lysis buffer. After the final wash, the wash buffer was removed and SDS sample buffer was added. The sample was boiled for 10 min and run on a 10% acrylamide gel. The western blotting protocol was then followed. Each pulldown was performed at least 3 times.

2.3.3.6. Immunoprecipitation (IP)

Control or fascin knockdown MDA-MB-231 cells rescued for GFP tagged WT or mutant fascin expression were cultured until 80% confluent in 6-well plate and lysed in 250 µl lysis buffer on ice. A/G agarose affinity matrix suspension was washed 3 times with PBS prior to use. Lysates were pre-cleared with 100 µl washed A/G agarose affinity matrix suspension rotating at 4 °C for 30 min, and 50 µl lysate was kept (1:1 IP buffer: sample buffer) prior to pre-clearing at -20 °C for an input sample. Pre-cleared lysates were centrifuged and the supernatants were collected. Each IP experiment had a duplicate of primary antibody and control IgG. Antibody or control IgG was incubated with 200 µl pre-cleared lysate tumbling at 4 °C overnight. Then 50 µl of washed A/G agarose affinity matrix suspension was added to the antibody lysate mix for 2 h tumbling at 4 °C. Alternatively, antibody was pre-incubated with beads overnight tumbling at 4 °C. Then, excess antibody was removed by washing 3 times with PBS, and pre-cleared lysate was added to each antibody A/G agarose affinity matrix suspension mix for 2 h tumbling at 4 °C. After antibody, lysate and A/G agarose affinity matrix suspension incubation, the mixtures were centrifuged and 25 µl supernatant (1:1 supernatant: sample buffer) was kept for an unbound sample and was stored at -20 °C. The rest of the supernatant was removed and the A/G agarose affinity matrix suspension was washed three times for 10 min in IP buffer.

Samples were either used immediately or stored at -20°C. Lysates were boiled at 95 °C and centrifuged to clear cell debris before use. 40 µl of each sample was loaded in each well of 8 or 10% SDS-PAGE gels in 1.5 mm cassettes and subjected to SDS-PAGE, and then the western blotting protocol was followed. Each IP was performed at least 3 times.

2.3.3.7. SDS PAGE analysis

Sodium dodecyl sulphate-polyacrylamide gel electrophoresis (SDS-PAGE) separates protein based on molecular weights. SDS loading buffer, containing β-mercaptoethanol, was added to the samples, which denatured the protein from its tertiary structure to the basic amino acid primary structure. The SDS also induced a negative charge to proteins so that when an electrical charge was applied the protein would migrate towards the cathode pole. Gels of 8% or 10 % were made in 1.5 mm cassettes with stacking gel on top and resolving gel beneath. Along with the samples, a marker was run which includes molecular weight standards of known sizes. The gel was run for 1.5 h at 100 V.

2.3.3.8. Silver staining

The silver staining was used to detect binding in MT/actin co-sedimentation experiments. The polyacrylamide gels were silver-stained using the Plusone silver staining kit (GE Healthcare) to provide higher sensitivity for band detection. After SDS PAGE, the gel was first left in fixing solution for 30 min (40% ethanol and 10% glacial acetic acid in deionised water) and then left in sensitising solution for 30 min (30% ethanol, 25% sodium thiosulphate (5% w/v) and 0.07 g/ml sodium acetate). The gel was washed with deionised water 3 times for 5 min and silver solution was

added (10% silver nitrate solution (2.5 % w/v) in deionised water). After 20 min, the gel was washed 2 times for 1 min and then developing solution was added (0.025 g/ml sodium carbonate and 0.08% formaldehyde (37 % w/v) in deionised water), the gel was transferred to stopping solution when bands reached the desired intensity (0.015 g/ml EDTA-$Na_2 \cdot 2H_2O$ in deionised water). After washing for a further 3 times for 5 min the gel was left in preserving solution (30% ethanol and 22% glycerol in deionised water) for 30 min, twice.

2.3.3.9. Western Blotting

Western blotting was used for specific protein detection following SDS-PAGE. The proteins were transferred onto nitrocellulose membranes (Amersham Biosciences) for 1 h at 100 V using a transfer kit (Biorad) in Transfer Buffer (see Table 2.4). The membranes were blocked using 3% Milk/TBS Tween-20 (TBST, 0.1% Tween in TBS) or 3% BSA/TBST for 1 h at room temperature. The membranes were then probed with the primary antibody overnight at 4 °C or for 3 h at room temperature. The membranes were then washed 3 times for 10 min each with TBST prior to incubation with horseradish peroxidase-conjugated secondary antibodies for 1 h at room temperature. Membranes were then washed a further 3 times and proteins were detected by ECL chemiluminescence kit (Thermo Scientific) and either exposed on Medical X-ray film (Fuji) and developed using a Xograph compact X4 developer (Imaging Systems) or directly imaged using the BioRad imager. For reprobing, blots were stripped with Re-blot strong (10X) (Chemicon) diluted to 1X in distilled water for 10 min at room temperature, and then treated as before.

2.3.4. Microscopy

2.3.4.1. Immunofluorescence

The cells were plated onto 24-well plates containing acid washed circular coverslips (diameter = 13 mm, VWR). Briefly, coverslips were incubated in 1M HCl overnight, washed 2-3 times with distilled water and then in 70% ethanol one time. Coverslips were dried in a laminar-flow hood overnight. Before plating cells, coverslips were coated with extracellular matrix (ECM) proteins: human plasma fibronectin (FN, 10 μg/ml) (Millipore), bovine collagen type I (COL, 50 μg/ml) (BD Biosciences) or rat plasma vitronectin (VN, 10 μg/ml) (Sigma Aldrich). Fibronectin and vitronectin matrices were diluted in PBS 1x for a minimum of 30 min, while collagen I in acetic acid (0.02 N). Coated coverslips were then washed 3 times with PBS. The cells were plated in media and left overnight at 37 °C. At this point, cells were fixed using 4% para-formaldehyde (PFA/PBS) for 10 min, washed twice with PBS and then permeabilised with 0.2% Triton-X/PBS for 10 min. Coverslips were again washed with PBS and blocked with 3% BSA/PBS for 20 min. The selected primary and secondary antibodies were diluted in 3% BSA/PBS for 3 h and then 2 h at room temperature successively. Coverslips were washed three times with PBS and once with distilled water and finally mounted on slides using mounting media (FluorSave reagent, Calbiochem). Images of fixed cells were acquired on a confocal microscope with a 40 or 60x oil immersion objective.

2.3.4.2. Fluorescence assay for analysis of F-actin and MT

The fluorescence assay for F-actin-MT cross-linking was performed as previously published (Miller 2004). Rhodamine-labelled tubulin (Cytoskeleton) was polymerised and stabilised by Paclitaxel as described in section 2.3.3.3. Rhodamine-labelled polymerised MT were mixed with WT or mutant fascin for 30 min at 25 °C, as

previously described. Similarly, G-actin was also polymerised as described in section 2.3.3.4 and then incubated with Alexa 488-phallodin (1:10) for 15 min at 25 °C to stabilise and label F-actin. After MT binding reaction with fascin proteins, 488-labelled F-actin was added to the mixture for an additional 15 min at 25 °C. The mixture was then diluted fivefold, dropped onto a microscope slide, covered with a coverslip and visualised by fluorescence microscopy with a 100x oil immersion objective.

2.3.4.3. Confocal microscopy

Images of fixed cells were acquired on a Nikon A1R inverted confocal microscope (Nikon Instruments UK) equipped with an environmental chamber heated to 37 °C. Excitation wavelengths of 488 nm (Argon laser), 568 nm (Diode laser), or 633 nm (diode laser) were used. Images were taken using a 63x oil Plan Fluor immersion objective (numerical aperture 1.4) or 100x oil objective (NA1.49). Images were exported in .nd2 file format and analysed in NIS-Elements Imaging software and saved into TIFF files for further analysis. For live imaging of HeLa control and fascin knockdown cells expressing mCherry-α-tubulin, the cells were plated with 10% FBS DMEM medium in a 15 μm-slide-8-well chamber (Ibidi), pre-coated with fibronectin (10μg/ml). The cells were imaged using the Nikon A1R confocal microscope (as above). One image was acquired every three seconds for 5 minutes. For the Interference Reflection Microscopy (IRM) experiments, MDA-MB-231 control, fascin knockdown and rescued cells were plated in the same chamber as above and imaged with 488nm Argon-Ion laser (reflection signal recovered at 457-514 nm and GFP fluorescence emitted at 520-560 nm). The cells were imaged throughout the nocodazole assay acquiring one image every 30 seconds. All files were saved as AVI for export into ImageJ.

2.3.4.4. Image analysis

The Microtubule score (MT score) was calculated from images of cells stained for total tubulin and acquired on confocal microscope as the percentage of cells with normal MT network. Polymerised MT bundles, distributed throughout the cell body with a visible MT organising centre (MTOC) were scored with a high MT score (≈ 100%), while cells exhibiting small rounded area and depolymerised MT network with some residual MT present were given score close to zero (≈ 5%). Re-spreading cells exhibiting an incomplete development of MT network or lacking a clear MTOC were scored ≈ 50%). Figure 2.3 shows example images of cells for each MT score given. Left panel shows untreated cell stained for total tubulin and scored with high MT score, centre panel shows tubulin staining in nocodazole treated cell scored with low score and right panel shows 60 minute washed cell with delayed MT recovery and scored with MT score ≈ 50%.

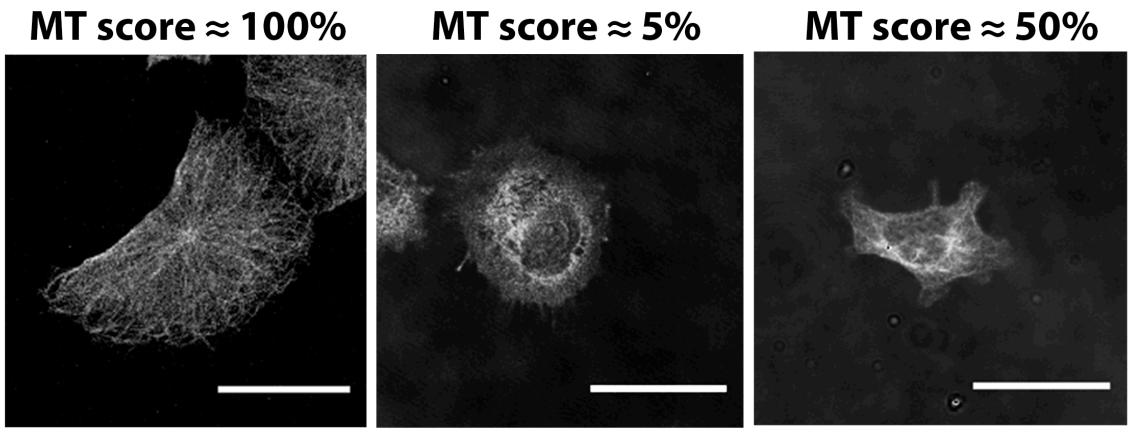

Figure 2.3. Example images of assignment of MT score

Quantification of cell size and focal adhesion (FA) size and number was performed by manual threshold of phospho-tyrosine stained images in ImageJ software. The Analyze Particle plug-in was used to measure adhesion sites between 1 and 3 μm in size. The threshold included adhesion sites sized between 1 and 3 μm. FA size data

were corrected per cell area and calculated as % of cell occupied by FA. In all the analysis, at least 20 cells were evaluated in three different experiments.

2.3.4.5. Statistical analysis

All statistical tests were performed using Student T-tests (Excel) and confirmed using Prism software. Data are expressed as means ± s.e.m. Significance was taken as $p<0.001$, 0.005 and 0.05 and significance values were assigned in specific figures/experiments as shown.

3 Fascin-dependent control of microtubule and adhesion dynamics.

INTRODUCTION

Previous studies have shown a role for fascin in promoting cancer cell migration and invasion by regulating assembly of actin bundles and stability of adhesion structures (Adams 2004). Fascin has not been found to localise in focal adhesions (FA) and the mechanisms by which fascin contributes to adhesion dynamics and assembly remain unknown. Moreover, it remains unclear whether fascin-actin binding is required for fascin-dependent control of FA assembly. Both actin and microtubule cytoskeletons are known to be essential for normal FA formation, and a number of proteins that stabilize actin filaments have been shown to co-ordinately control MT stability (Etienne-Manneville 2004; Palazzo et al. 2004; Gaillard et al. 2011). I hypothesised that fascin may play a dual role in co-ordination of actin and MT cytoskeletons to regulate FA assembly/disassembly and cell invasion.

The aim of the experiments in this chapter is to analyse the role of fascin in regulating MT and FA assembly using previously described nocodazole treatment and washout assays. Nocodazole (NOC) is a MT-depolymerising drug that has been used previously to study MT-dependent FA regulation. It has been shown that MT depolymerisation following NOC treatment results in increased FA assembly, and that subsequent drug washout leads to FA disassembly (Stehbens & Wittmann 2012). Previous studies in fibroblasts have shown that this mechanism depends on dynamin and FAK (Ezratty et al. 2005), but the role of cytoskeletal associated proteins in this process has not been tested. This assay therefore provides a robust model system in which to test the involvement of fascin in both FA assembly/disassembly and also MT re-growth.

3.1. Characterisation of fascin knockdown in human MDA-MB-231 breast carcinoma and HeLa cells

Fascin is known to be upregulated in many different types of human cancers and its overexpression is associated with poor prognosis (Hashimoto et al. 2005; Tan et al. 2013). Therefore, I chose to analyse the role of fascin in adhesion formation using two different human cancer cell lines: MDA-MB-231 breast carcinoma cells and HeLa cervical cancer cells.

Both MDA-MB-231 and HeLa cell lines were infected with a lentivirus containing a shRNA sequence to specifically knockdown fascin. A lentivirus carrying a shRNA scrambled sequence was used to infect the same cells as a control. The efficiency of the fascin knockdown was assessed by western blotting (Figure 3.1a). Western blots demonstrated >90% reduction in fascin protein levels in both fascin knockdown MDA-MB-231 and HeLa cells (fasKD) compared to the respective control cells (ctrl). The reduction in fascin levels in both knockdown cell lines was quantified by densitometry analysis of multiple western blots ($p =< 0.001$, Figure 3.1b). Fascin knockdown was stably maintained in cells throughout passaging and monitored regularly.

Fascin localisation and knockdown was also assessed by immunofluorescence (Figure 3.1c). The top panel in Fig 3.1c shows MDA-MB-231 control cells stained for fascin. Endogenous fascin localisation in MDA-MB-231 control cells was cytosolic and also localised in actin-based structures such as filopodia and stress fibres (shown in top left panel in Figure 3.1c). Staining for fascin in HeLa control cells (shown in bottom left panel in Figure 3.1c) also showed partial cytosolic localisation and a population of fascin localised in filopodia and stress fibres. The significant reduction of fascin protein levels in both knockdown cell lines was confirmed by immunofluorescence analysis (centre panels in Figure 3.1c). MDA-MB-231 and HeLa fasKD cells were transiently transfected with a plasmid encoding a shRNA resistant

WT fascin-GFP to rescue fascin expression levels (resWT). The efficiency of expression was assessed in immunofluorescence (right panels in Figure 3.1c). Around 90% of both rescue cell lines showed efficient expression of GFP-fascin level. WT fascin-GFP in MDA-MB-231 cells (top right panel in 3.1c) was localised at the cell periphery, and was clearly localised in filopodia and stress fibers in Hela cells (bottom right panel).

These results demonstrate that MDA-MB-231 and HeLa control, fasKD and resWT cells are suitable tools to study the role of fascin in adhesion formation.

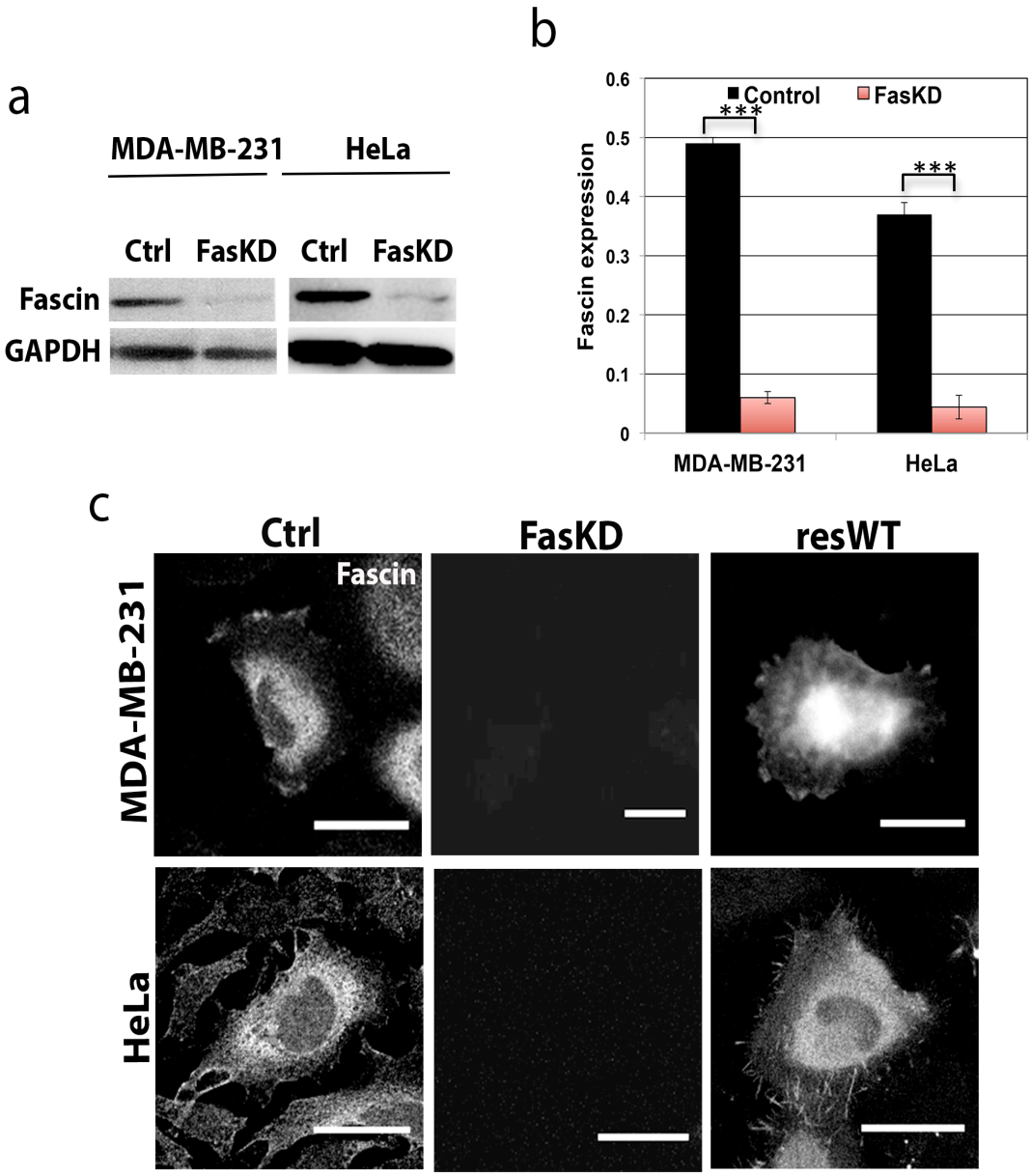

Figure 3.1. Characterisation of fascin knockdown in human breast carcinoma MDA-MB-231 and HeLa cells

(a) Western blots of lysates from MDA-MB-231 or HeLa cells expressing control shRNA or shRNA specifically targeting fascin. (b) Statistical analysis of fascin levels was performed by densitometry analysis of at least three western blots. P-value =< 0.001 (***) was considered as significant. Data are expressed as mean± sem and corrected on GAPDH loading as control. (c) Confocal microscope images of cells stained for fascin in both MDA-MB-231 (top panels) and HeLa (bottom panels). Left panels show control cells, centre panels show fasKD cells and right panels show cells expressing fascin shRNA re-expressing shRNA resistant WT fascin-GFP. Scale bar= 10 um.

3.2. Silencing fascin expression results in increased focal adhesion assembly

Fascin is known to play a role in regulating cell adhesion (Adams 2004) but the mechanisms are unknown. Fascin associates with the actin cytoskeleton and is known to regulate actin stability in filopodia. However, microtubule (MT) assembly and dynamics are known to be more directly involved in focal adhesion (FA) turnover (Wehrle-Haller & Imhof 2003). It was therefore important to analyse the MT network integrity in conjunction with FA number and size under basal conditions in fascin knockdown (fasKD) cells.

MDA-MB-231 control (ctrl), fascin knockdown (fasKD) and fasKD cells re-expressing WT fascin-GFP (resWT) were plated on coverslips, fixed and stained with tubulin antibodies to define the MT network and imaged by confocal microscopy. Figure 3.2a shows example images of total tubulin staining in control (left), fasKD (centre) and resWT cells (right). Fascin knockdown cells showed no clear difference in total tubulin staining compared to control or resWT cells. MT in control, fasKD and resWT cells were polymerised and distributed throughout the cell body. The MT organising centre (MTOC) was visible and clear in all cells adjacent to the nucleus (stained for total tubulin). These data suggest that depleting fascin does not grossly disrupt the MT cytoskeleton under basal conditions.

As fascin depletion results in decreased FA turnover (Hashimoto et al. 2007), I analysed whether FA assembly was altered in control, fasKD and fasKD cells re-expressing WT fascin (resWT). MDA-MB-231 control, fasKD and resWT were stained for phospho-tyrosine (p-Tyr) as a marker of focal adhesions (Maher et al. 1985) and imaged by confocal microscopy to observe and quantify changes in % of cell occupied by FA (FA size) and FA number. Figures in 3.2b show example images of p-Tyr staining in control (left), fasKD (centre) and resWT cells (right). P-Tyr staining in control cells showed peripheral FA with some smaller punctate FA underneath the

nucleus/cell body. FasKD cells showed a similar FA distribution but with more FA at the periphery compared to control cells. Rescuing WT fascin expression in fasKD cells (right panel in 3.2b), FA distribution was restored to levels seen in control cells. Analysis of p-Tyr staining in control, fasKD and resWT cells from three different experiments was performed in ImageJ and corrected for cell area (at least 20 cells were analysed in each experiment). Quantification of % of cell occupied by FAs (FA size) and FA number per cell in control (black bars), fasKD (white bars) and resWT (red bars) is shown in Figure 3.2c,d. Data showed a significant increase in both % of cell occupied by FAs and FA number in fasKD cells compared to controls.

To confirm that fascin depletion does not grossly affect normal MT growth, I performed live imaging experiments in control and fasKD Hela cells expressing mCherry-α-tubulin (Movie 1 and 2). Figure 3.2e left panel shows a still image from Movie 1 (mCherry-α-tubulin control Hela cell) and right panel shows a still image from Movie 2 (mCherry-α-tubulin fasKD Hela cell). Control and fasKD cells did not show any major difference in total tubulin arrangement and distribution in basal conditions.

Taken together, these results show that fascin depletion in MDA-MB-231 cells does not have an obvious effect on the basal MT network integrity but results in increased FA assembly.

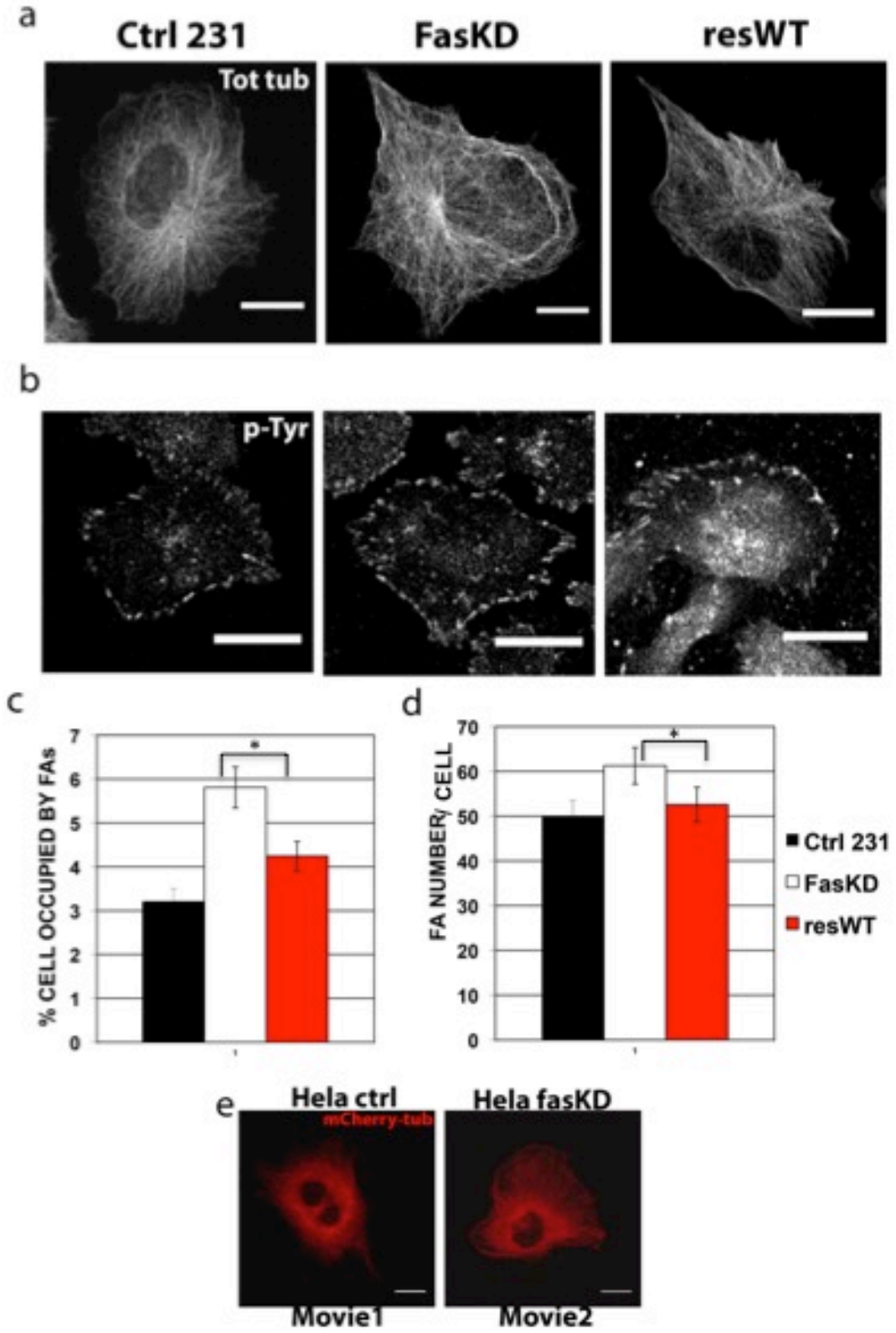
a
Ctrl 231
FasKD
resWT
Tot tub
b
p-Tyr
c
% CELL OCCUPIED BY FAs
0
1
2
3
4
5
6
7
*
d
FA NUMBER/ CELL
0
10
20
30
40
50
60
70
*
Ctrl 231
FasKD
resWT
e
Hela ctrl
mCherry-tub
Hela fasKD
Movie1
Movie2

Figure 3.2. Silencing fascin expression results in increased focal adhesion assembly
Confocal microscope images of MDA-MB-231 cells stained for total tubulin (a) and phospho-tyrosine (p-Tyr) (b). Left panels show MDA-MB-231 control cells, centre panels show MDA-MB-231 fascin knockdown cells and right panels show fascin knockdown cells re-expressing WT fascin-GFP. Scale bar= 10 um. (c, d) Quantification of % of cell occupied by FAs (c) and FA number per cell (d) in control cells (in black), fasKD cells (in white) and fasKD cells re-expressing WT fascin-GFP (in red). Statistical analysis of p-Tyr staining was performed in ImageJ. At least 20 cells were evaluated in three different experiments. P-value =< 0.05 (*) was considered as significant. Data are expressed as mean± sem and corrected on cell area. (e) Still images from Movies 1 and 2. Scale bar = 20 um.

3.3. Endogenous and GFP-fascin localises with microtubules at the cell-periphery in MDA-MB-231 cells

As data in Figure 3.2 demonstrated a role for fascin in regulating FA size, it was important to determine whether fascin localised to or near sites of FA assembly in these cells. As MTs are known to target FA and be involved in regulating FA dynamics, I hypothesised a possible co-ordination between fascin and MTs at sites of adhesion formation to regulate FA dynamics.

To test this hypothesis, MDA-MB-231 control (ctrl) cells were stained for fascin and total tubulin and imaged by confocal microscopy. Top panels in Figure 3.3 show example images of fascin and total tubulin staining in cells. Fascin localised at the cell periphery co-localising with the distal ends of MTs, suggesting fascin-MT interplay may occur at the cell edge. To confirm this, total tubulin staining was repeated in resWT-GFP cells and observed by confocal microscopy together with GFP-WT fascin. Bottom panels in Figure 3.3 show example images of total tubulin staining in resWT-GFP cells. WT fascin-GFP also localised at the cell periphery similar to that seen with endogenous fascin, showing co-localisation with MTs. GFP alone did not localise at the cell periphery (data not shown).

These data together suggest that fascin and MT may co-operate at the cell periphery in the regulation of FA turnover.

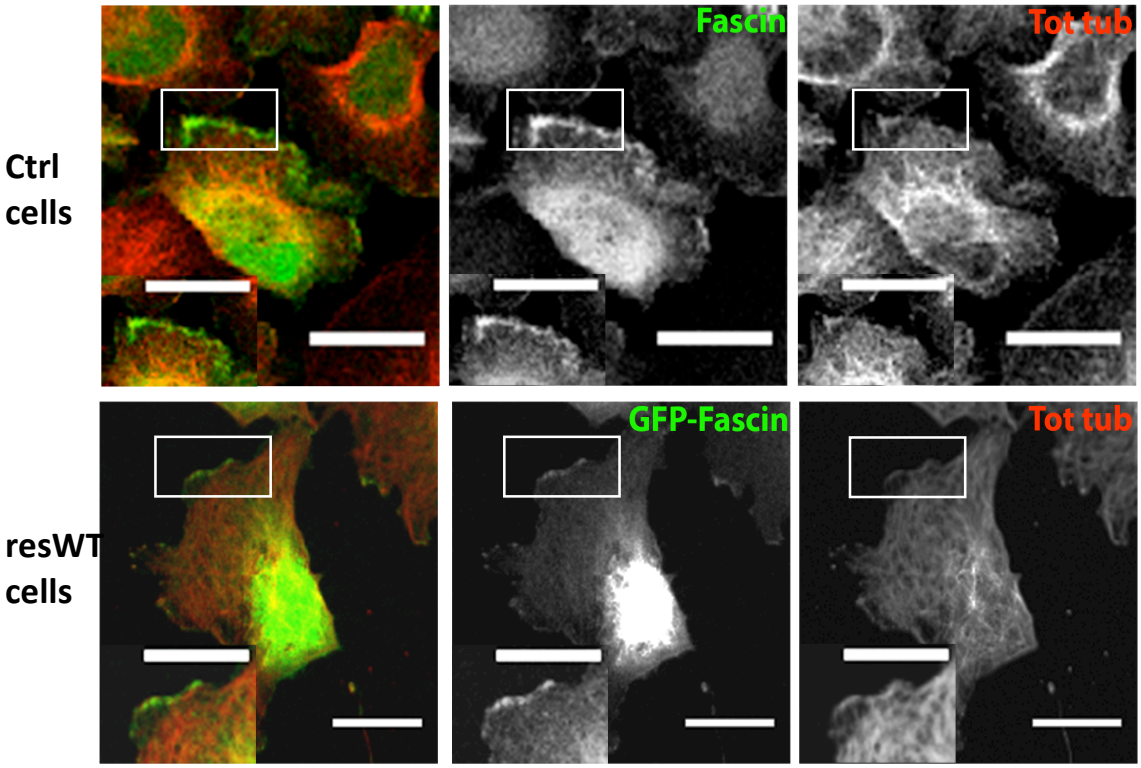

Figure 3.3. Endogenous and rescue GFP-fascin localisation with microtubules at the cell periphery in MDA-MB-231 cells

Confocal microscope images of cell co-stained for fascin and total tubulin in MDA-MB-231 control cells (top panels) and fasKD cells re-expressing WT fascin-GFP stained for total tubulin (bottom panel). Left panel top row shows co-staining of fascin and total tubulin in control cells, whereas centre and right panels show single staining of fascin and total tubulin, respectively. Left panel bottom row shows staining of total tubulin in fasKD cells re-expressing WT fascin-GFP, whereas centre and right panels show GFP-fascin and staining of total tubulin, respectively. Scale bar= 10 um.
Zoom of the highlighted area is shown to show fascin co-localisation with end of MTs at the cell periphery. Scale bar= 3 um.

3.4. Fascin depletion leads to higher levels of acetylated tubulin

Data in Fig 3.3 showed fascin co-localising with the ends of MTs at the cell periphery, suggesting a co-operation and potential involvement in regulating FA dynamics. However, Figure 3.2 showed that fascin depletion had no obvious effect on MT network assembly in cells under basal conditions. Therefore, it was important to investigate whether fascin knockdown affects any other aspect of MT integrity. MT stability has been previously shown to correlate directly with post-translational acetylation of α-tubulin and to be important in regulating cell function and MT targeting (Ikegami & Setou, 2010). In addition, it has been reported that an increased MT stability leads to a decrease in cell spreading and motility (Tran et al. 2007).
To investigate a possible role for fascin in regulating MT stability, total and acetylated tubulin levels were analysed by western blotting in MDA-MB-231 control (ctrl) and fascin knockdown (fasKD) cells (Figure 3.4a). Western blots demonstrated a 2-fold increase in acetylated tubulin levels in fasKD cells compared to control cells, whereas total tubulin levels remained unchanged. Total and acetylated tubulin levels in control and fasKD cells were quantified by densitometry analysis of multiple western blots ($p = < 0.001$, Figure 3.4b).

To confirm increased levels of acetylated tubulin in fasKD cells compared to controls were dependent upon fascin, WT fascin-GFP was expressed in fasKD cells and acetylated tubulin levels analysed in fasKD and resWT cells on the same coverslip by confocal microscopy. As explained in the Material and Method section, the GFP expression in rescued cells was much stronger than in fasKD stable cells. Figure 3.4c shows example images of acetylated tubulin staining in fasKD cells (really low GFP levels) together with resWT fascin cells (green cells). Merge channel of GFP-fascin and acetylated tubulin and respective channels alone are shown. Figure 3.4c shows a strong increase in tubulin acetylation in fasKD cells compared to cells expressing WT

fascin-GFP. Taken together, these data show a role for fascin in regulating MT stability.

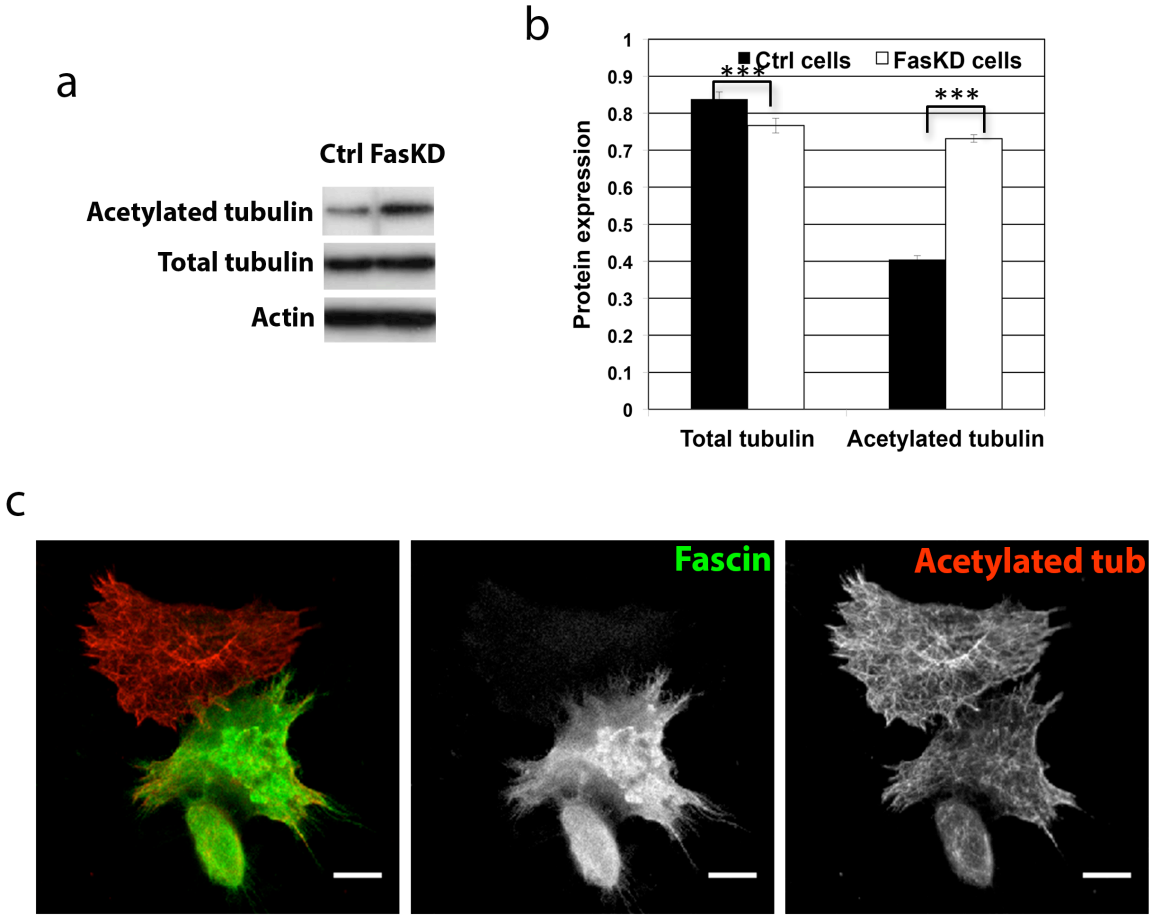

Figure 3.4. Fascin depletion leads to higher levels of acetylated tubulin

(a) Western blots of lysates from MDA-MB-231 control and fasKD cells. (b) Statistical analysis of total and acetylated levels was performed by densitometry analysis of at least three western blots. P-value =< 0.001 (***) was considered as significant. Data are expressed as mean± sem and corrected on actin loading as control. (c) Confocal microscope images of fasKD cells re-expressing GFP-WT fascin stained for acetylated tubulin. Left panel shows staining of acetylated tubulin in cells re-expressing WT fascin-GFP, whereas centre panel shows cells re-expressing WT fascin-GFP and right panel shows staining of acetylated tubulin in either a fasKD cell or a fasKD cell re-expressing WT fascin-GFP. Scale bar= 20 um.

3.5. Fascin knockdown does not alter total levels of focal adhesion proteins

Having demonstrated fascin translocation to the cell periphery and shown a role for fascin in regulating FA assembly, it was important to clarify whether levels of FA components were affected by fascin knockdown. FA proteins such as vinculin and Focal Adhesion Kinase (FAK) are key components in the regulation of cell adhesion and FA turnover (Carisey & Ballestrem, 2010; Hamadi et al., 2005). Therefore, levels of these proteins were analysed in control and fascin depleted cells.

Vinculin staining was performed in MDA-MB-231 control (ctrl), fascin knockdown (fasKD) and fasKD cells re-expressing WT fascin (resWT). Figure 3.5a shows examples of confocal images of vinculin staining in ctrl cells (left panel), fasKD cells (centre panel) and resWT cells (right panel). Vinculin was present in large peripheral FA in control cells and in the larger more densely packed FA previously seen in fasKD cells. ResWT cells did not show differences in FA size and number compared to control cells.

To further determine whether vinculin levels were altered in the absence of fascin, FA protein levels were analysed by western blotting. Figure 3.5b shows total FAK and vinculin levels in control (ctrl), fascin knockdown (fasKD) and fasKD cells re-expressing WT fascin-GFP (resWT) MDA-MB-231. Endogenous and GFP-fascin levels were also assessed in the same samples. Total tubulin and GAPDH were used as loading controls. FAK and vinculin levels were quantified by densitometry analysis of multiple western blots (Figure 3.5c) together with endogenous or GFP-fascin and total tubulin levels in control, fasKD and resWT cells. Data confirmed the efficiency of both fascin knockdown and re-expression in cells and similar total tubulin levels between control and fasKD cells. No differences in total levels of FAK or vinculin were detected between the different conditions. Thus, fascin knockdown does not

result in change of total level of FA proteins. This data suggest that fascin does not regulate FA size through control of total FA protein levels.

To further investigate the role of fascin in FA dynamics, cell adhesion assays were performed on fibronectin-coated coverslips. Control (ctrl), fascin knockdown (fasKD) and fasKD re-expressing WT fascin-GFP (resWT) MDA-MB-231 cells were plated on fibronectin and the number of adhered cells were counted. Figure 3.5d shows quantification of the number of control, fasKD and resWT cells. FasKD cells showed higher adhesion to fibronectin compared to control and resWT cells, correlating with the previous observation of increase FA size in fasKD cells.

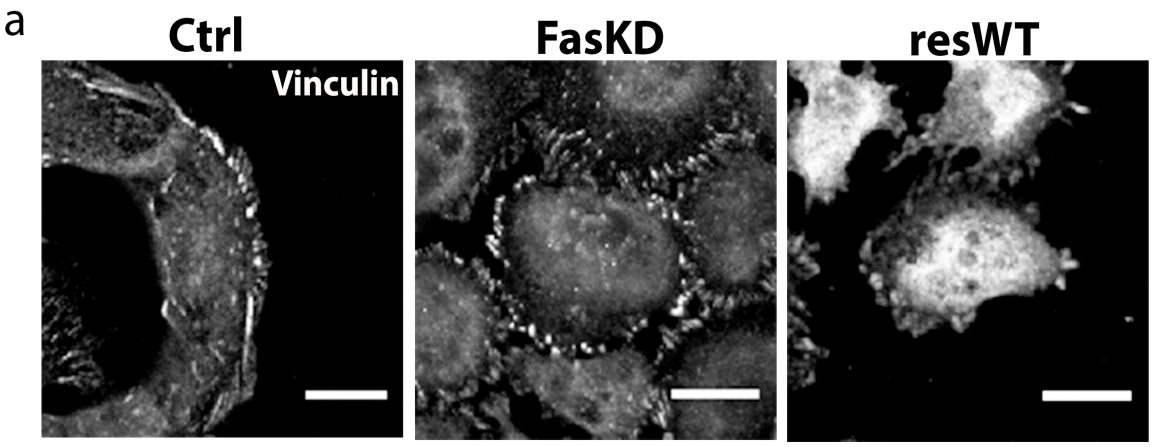
a
Ctrl
FasKD
resWT
Vinculin

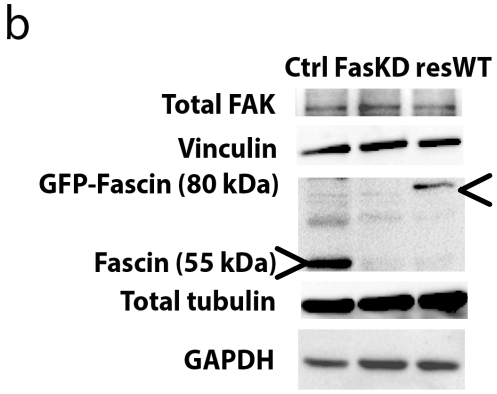
b
Ctrl FasKD resWT
Total FAK
Vinculin
GFP-Fascin (80 kDa)
Fascin (55 kDa)
Total tubulin
GAPDH

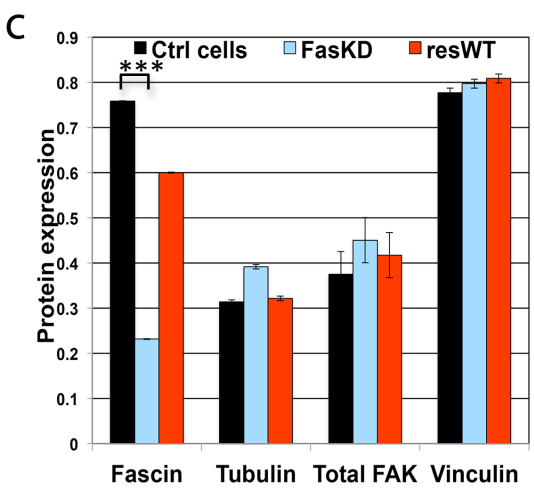
c
Ctrl cells
FasKD
resWT
***
Protein expression
0.9
0.8
0.7
0.6
0.5
0.4
0.3
0.2
0.1
0
Fascin
Tubulin
Total FAK
Vinculin

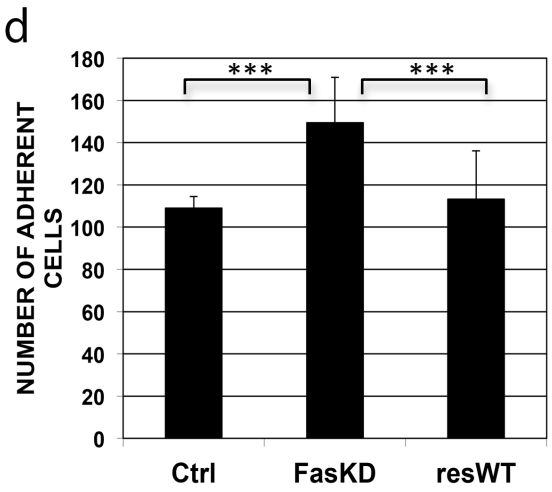
d
***
***
NUMBER OF ADHERENT CELLS
180
160
140
120
100
80
60
40
20
0
Ctrl
FasKD
resWT

Figure 3.5. Fascin knockdown does not alter total levels of focal adhesion proteins (a) Confocal images of cells stained for vinculin in MDA-MB-231 control cells (left panel), fasKD cells (centre panel) and fasKD cells re-expressing WT fascin-GFP (resWT). Scale bar= 10 um. (b) Western blots of lysates from MDA-MB-231 control cells, fasKD and resWT cells. (c) Statistical analysis of fascin, total tubulin, total Focal Adhesion Kinase (FAK) and vinculin levels was performed by densitometry analysis of at least three western blots. P-value =< 0.001 (***) was considered as significant. Data are expressed as mean± sem and corrected on GAPDH loading as control. (d) Count of control, fasKD and resWT adhering on fibronectin. Statistical analysis was performed using T-Test. P-value =< 0.001 (***) was considered as significant. Data are expressed as mean± sem. At least 20 cells were evaluated in three separate experiments.

3.6. β1 integrin ligation is required for MT re-growth following nocodazole washout

Having identified a potential role for fascin in regulating MT stability and FA assembly, it was therefore important to study whether fascin plays a role in the MT-dependent regulation of FA dynamics. It has been shown that treatment with the MT-depolymerising drug nocodazole leads to increased FA assembly in fibroblasts. Conversely, MT re-growth after nocodazole washout drives FA disassembly (Ezratty et al. 2005). To characterise the relationship between MT and FA, nocodazole (NOC) treatment and washout assays were performed on both MDA-MB-231 and HeLa cells. Control cells were either left untreated, treated with NOC for 15 minutes, followed by washout of the drug for 30 or 60 minutes. Cells were then fixed and stained for total tubulin and phospho-tyrosine (p-Tyr) and imaged by confocal microscopy.

Firstly, the adhesion receptor requirements for FA disassembly during MT re-growth were characterised. To analyse this, control MDA-MB-231 cells were plated on different extracellular matrix (ECM) proteins and subjected to treatment with nocodazole followed by washout of the drug. Cells were stained for total tubulin, imaged by confocal microscopy (Figure 3.6a) and scored for percentage of cells with normal MT network (MT score in Figure 3.6b). Polymerised MT bundles, distributed throughout the cell body with a visible MT organising centre (MTOC) were scored with a high MT score (≈ 100%), while cells exhibiting small rounded area and depolymerised MT network were given score close to zero (≈ 5%). I decided to give 5% score rather than 0% because I did not use a direct measurement of MT depolymerisation. Lastly, re-spreading cells exhibiting an incomplete development of MT network or without a clear MTOC were given score ≈ 50%). Example images of cells scored for MT are shown in Matherial and Method section (Figure 2.3).

Cells were plated on three different ECM proteins: fibronectin (FN), collagen I (COL) or vitronectin (VN). These ECM proteins are ligands for different types of β integrins. Fibronectin binds to both β1 and β3 integrins, collagen I binds only to β1 whereas vitronectin binds only to β3. Thus this choice of ligands would enable any specific requirements for integrin subunits to be defined.

Figure 3.6a shows examples of confocal images of total tubulin staining in control cells plated on FN (first row), COL (second row) or VN (third row). The first column shows untreated cells (UT), second shows nocodazole treated cells (NOC) and third and fourth show cells 30 and 60 minutes post-NOC washout respectively. MT bundles in untreated cells plated on all the ECM proteins appeared normal. The MTOC was visible in all cells (stained for total tubulin) and was particularly evident in cells plated on FN (first panel, first row in 3.6a) and COL (first panel, second row in 3.6a) compared to that seen in cells on VN (first panel, third row in 3.6a). Nocodazole treatment led to some cell rounding and MT organisation and polymerisation were completely lost in NOC treated cells on all ECM proteins (second column panels in 3.6a). 30 minutes after NOC washout (30'W, third column in 3.6a), only control cells plated on FN (third panel, first row in 3.6a) and COL (third panel, second row in 3.6a) recovered the MT network back to that seen in untreated cells, while no MT recovery was seen in cells plated on VN (third panel, third row in 3.6a). 30 minutes post-washout, cells on VN appeared rounded with no MT polymerisation, suggesting that β1 integrin ligation is essential in allowing MT recovery after nocodazole washout. Additionally, MT recovery after 30 minutes NOC washout was more efficient in cells plated on COL than on FN, further suggesting a preferential role for β1 in the MT re-growth. MTs in cells plated on VN did not recover, even following washout periods of up to 6 hours (data not shown).

The graph shown in Figure 3.6b demonstrates quantification of the percentage of control cells plated on FN (green bars), COL (blue bars) and VN (red bars) with

normal MT networks during the time course of the nocodazole washout assay. Data confirms that NOC leads to total MT disassembly in cells on all ECM proteins. 30 minutes after NOC washout, a normal MT score was seen in ~50% of cells plated on FN and in ~70% of cells plated on COL, whereas no cells with normal MT network were found on VN. Moreover, quantification confirmed a more efficient MT recovery in cells on COL than on FN at 30 minutes post-NOC washout. 60 minutes post-washout, cells on FN showed a significant 2-fold increase in MT recovery, similar to levels achieve in cells on COL. The MT score in 60 minute washed cells plated on VN was still negligible (p-value in 60 minute washout on VN compared to control cells =< 0.001).

This data demonstrates that MT recovery is dependent on β1 integrins. Moreover, data show that MT re-growth occurs faster on COL than on FN, further suggesting the preferential role of β1 integrin engagement and activation in MT re-growth after NOC washout.

a

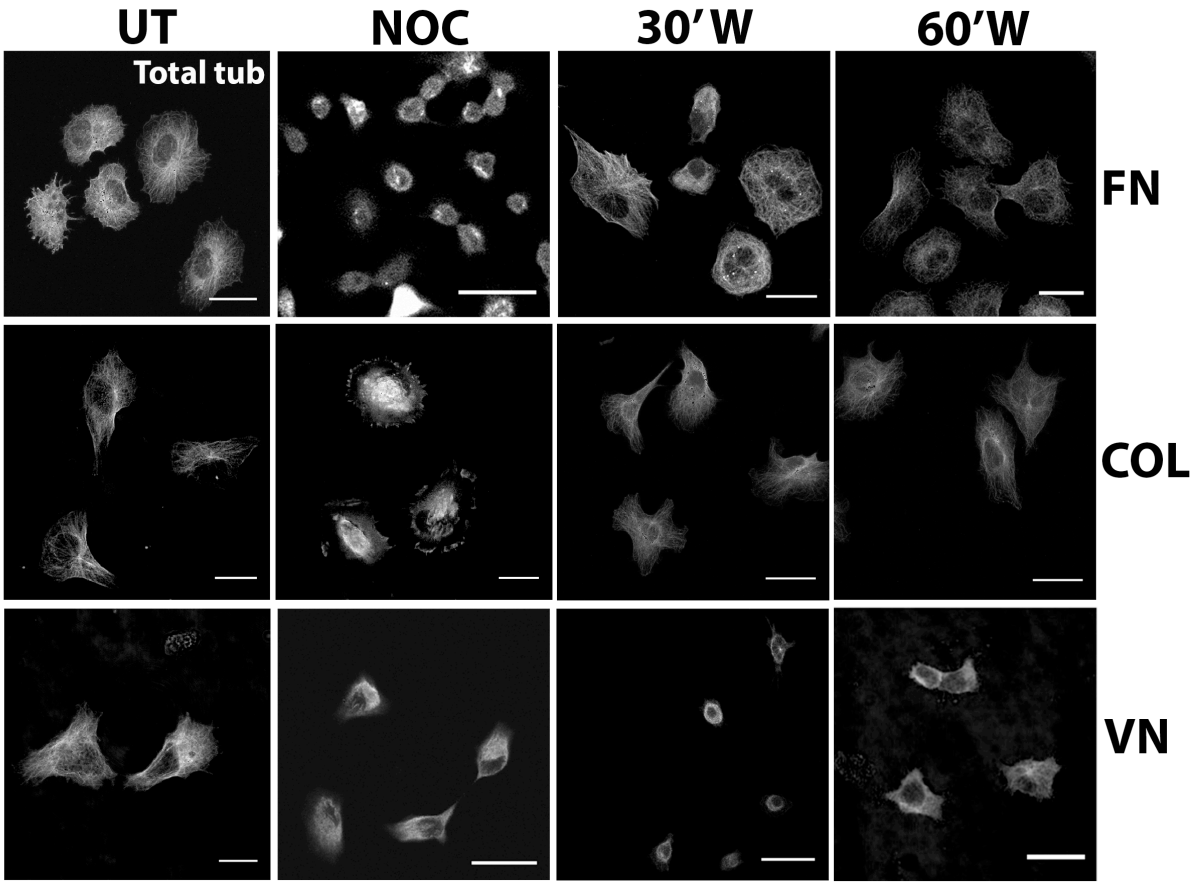
UT
NOC
30'W
60'W
Total tub
FN
COL
VN

b

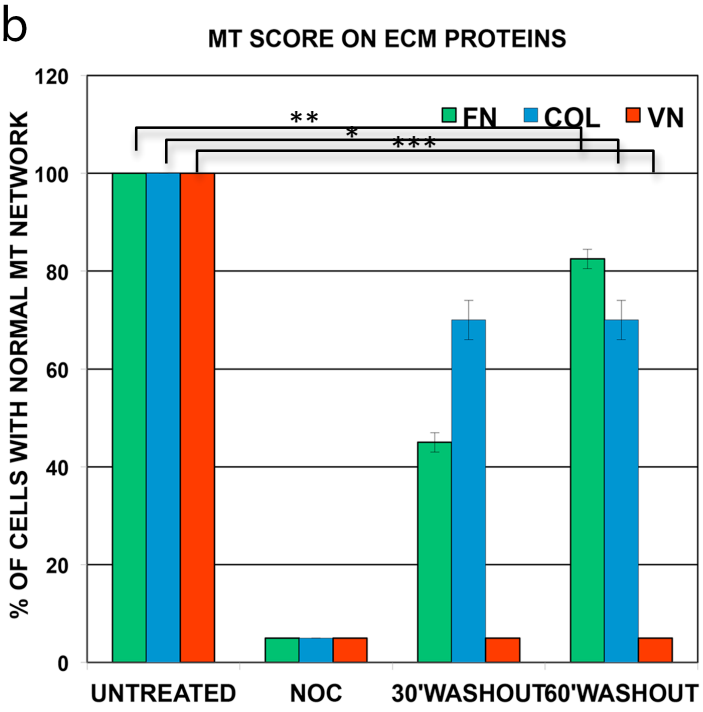
MT SCORE ON ECM PROTEINS
% OF CELLS WITH NORMAL MT NETWORK
120
100
80
60
40
20
0
FN
COL
VN
**
*
***
UNTREATED
NOC
30'WASHOUT
60'WASHOUT

Figure 3.6. β1 integrin ligation is required for MT re-growth following nocodazole washout

(a) Confocal microscope images of cells stained for total tubulin in MDA-MB-231 control cells untreated (UT, first column), nocodazole treated (NOC, second column), 30 minute washed (30'W, third column) and 60 minute washed (60'W, fourth column) plated on fibronectin (FN, first row), collagen (COL, second row) and vitronectin (VN, third row). Scale bar= 20 um. (b) Statistical analysis of % of cells with normal MT network (MT score) in the same conditions as above. P-value =< 0.001 (***), =< 0.005 (**) and =< 0.05 (*) were considered as significant. Data are expressed as mean± sem. At least 20 cells were evaluated in three separate experiments.

3.7. Fascin knockdown cells show delayed microtubule re-growth following nocodazole washout

Having tested MDA-MB-231 control cells and identified specific adhesion requirements in the nocodazole assay, the next step was to analyse whether fascin was involved in MT and FA dynamics as measured in the assay. To do so, nocodazole treatment and washout assays were performed in control, fascin knockdown (fasKD) or fasKD cells re-expressing WT fascin (resWT) plated on fibronectin (FN). FN was chosen as a suitable ligand because this enabled the study of both β1 and β 3 integrin engagement and because the slower MT recovery speed observed in cells on FN allowed more careful analysis of any potential temporal differences in MT recovery between cell types.

Figure 3.7a shows example confocal images of total tubulin staining in MDA-MB-231 control (first row), fasKD (second row) and resWT cells (third row) during Nocodazole treatment and washout assay. First column shows untreated cells (UT), second column shows nocodazole treated cells (NOC), third column shows 30 minute washed cells (30'W) and fourth column shows 60 minute washed cells (60'W). As previously observed, there were no differences in basal MT network formation between control, fasKD and resWT cells (figure 3.7a). Nocodazole treatment led to rounding in all cells and a complete loss of the MT network (second column panels in 3.7a). 30 minutes after NOC washout, the majority of control cells recovered their MT network (third panel, first row in Figure 3.7a), whereas fasKD cells showed delayed MT re-growth (third panel, second row in Figure 3.7a). Indeed, after the 30 minute NOC washout, fasKD cells did not show a clear MT network, despite showing an increase in spread area. Fascin re-expression in fasKD cells resulted in MT polymerization and recovery as seen in control cells, with visible MTOC in the majority of cells (third panel, third row in 3.7a). After the 60 minute NOC washout, control cells re-spread and fully restored the MT network (fourth panel, first row in

3.7a), whereas only few fasKD cells showed recovered MT networks (fourth panel, second row in 3.7a). A complete MT recovery was seen after the 60 minute NOC washout in fasKD cell re-expressing WT fascin-GFP (fourth panel, third row in 3.7a).

Cells were scored for MT recovery (Figure 3.7b) to quantify the percentage of cells with normal MT network at all time points. Control (black bars), fasKD (white bars) and resWT (grey bars) cells all showed complete MT disassembly after nocodazole treatment. 30 minutes following NOC washout, 50% of control and resWT cells recovered their MT network, while fasKD cells showed a significant delay in the recovery. 60 minutes post-NOC washout, both control and resWT cells showed ~80 % of cells with normal MT network, confirming the observed gradual MT recovery on FN seen previously (Fig 3.6.). However, fasKD cells were delayed in MT recovery after 60 minute NOC washout, showing ~40% of cells with normal MTs.
This data demonstrates that fascin is required for efficient MT recovery after nocodazole washout.

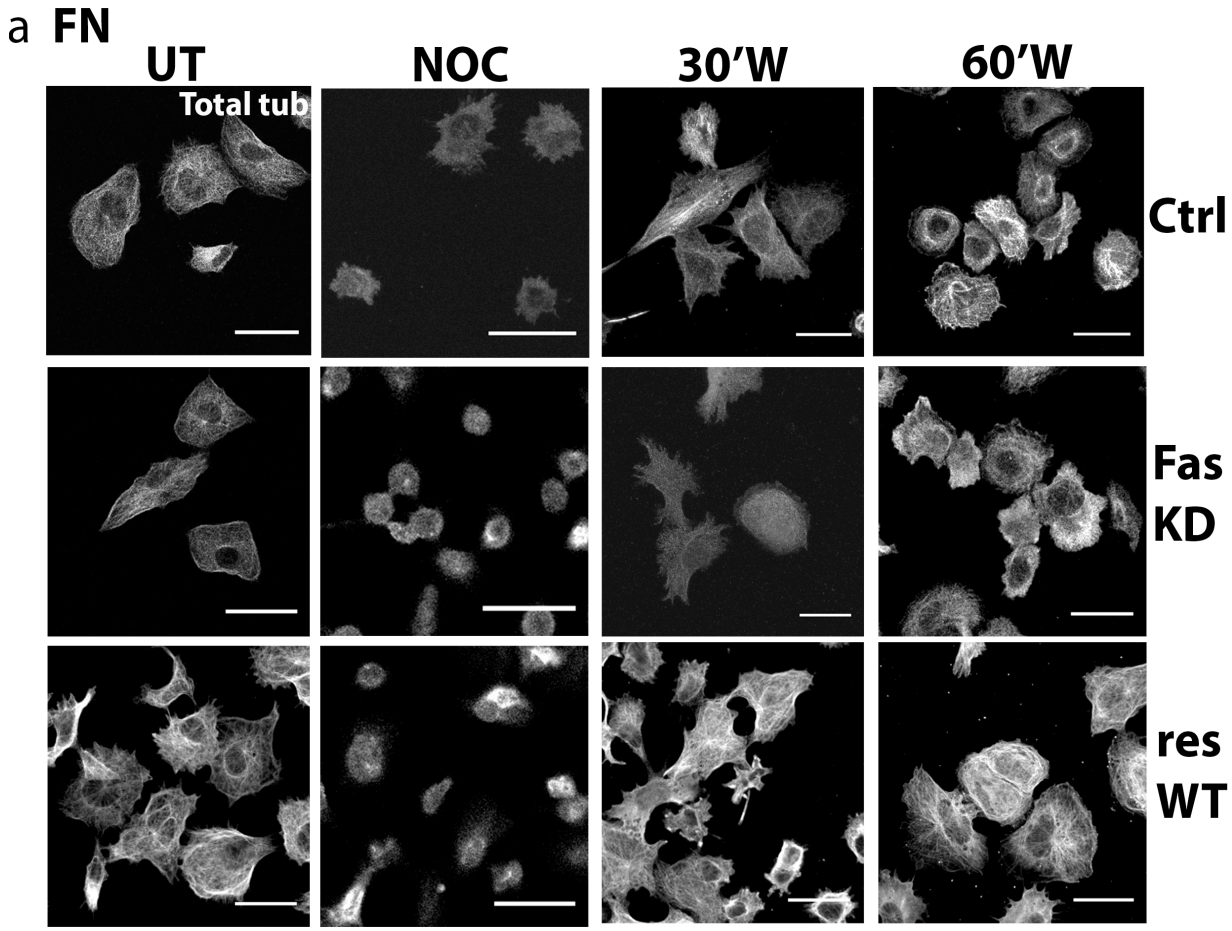
a FN
UT
NOC
30'W
60'W
Total tub
Ctrl
Fas KD
res WT

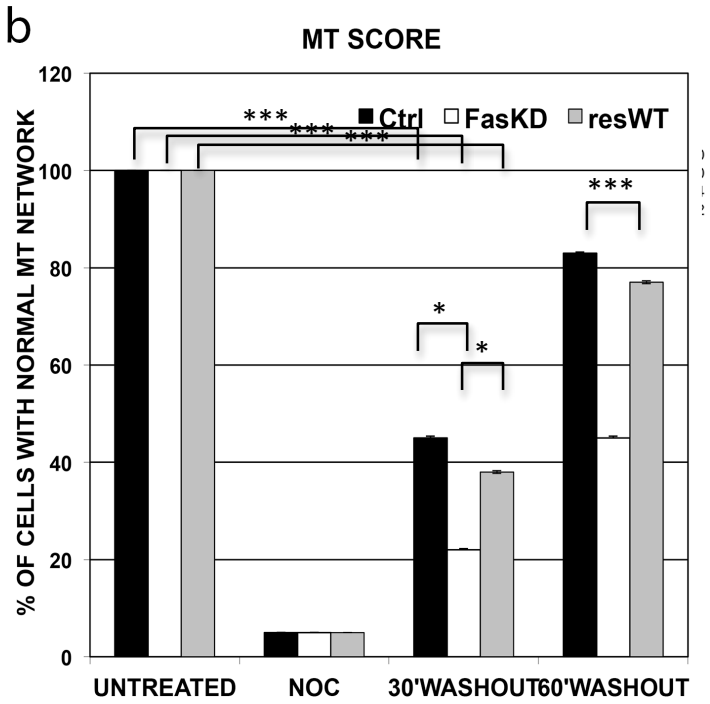
b
MT SCORE
% OF CELLS WITH NORMAL MT NETWORK
120
100
80
60
40
20
0
Ctrl
FasKD
resWT
***
***
***
***
*
*
UNTREATED
NOC
30'WASHOUT
60'WASHOUT

Figure 3.7. Fascin knockdown cells show delayed microtubule re-growth following nocodazole washout

(a) Confocal microscope images of cells stained for total tubulin in MDA-MB-231 control cells (first row), fasKD cells (second row) and fasKD cells re-expressing WT fascin-GFP (third row). First column shows untreated cells (UT), second shows nocodazole treated cells (NOC), third shows 30 minute washed cells (30'W) and fourth shows 60 minute washed cells (60'W). Scale bar= 20 um. (b) Statistical analysis of % of cells with normal MT network (MT score) in the same conditions as above. P-values =< 0.001 (***) and =<0.05 (*) were considered as significant. Data are expressed as mean± sem. At least 20 cells were evaluated in three separate experiments.

3.8. Characterisation of nocodazole treatment and washout assay in HeLa cells

After studying MT and FA dynamics in MDA-MB-231 cells, we wanted to characterise the relationship between MT and FA in HeLa cells. I included this cell line in our study because it is a suitable model to study cell spreading and cytoskeletal dynamics. The nocodazole treatment and washout assay was therefore repeated in HeLa cells plated on fibronectin. Cells were then stained for total tubulin and phospho-Tyrosine (p-Tyr) and imaged by confocal microscopy.

Figure 3.8 shows example images of merge and total tubulin and p-Tyr respective staining in HeLa cells. Untreated cells (Figure 3.8, first row) were well spread with polymerised MTs and peripheral regular FAs. As previously reported, NOC treatment lead to MT depolymerisation (second row, centre panel) and an increase in FA size (second row, right panel). MTs were still depolymerised following the 30 minute NOC washout (third row, centre panel) and therefore FA remained larger than in untreated cells at this time point (third row, right panel). 60 minutes post- NOC washout led to MT re-growth (fourth row, centre panel) and FA appeared smaller, similar to untreated cells (fourth row, right panel).

These data show that MT regulate FA turnover after NOC washout in HeLa cells. This characterization is important for future experiments to analyse fascin dependent FA and MT assembly in these cells.

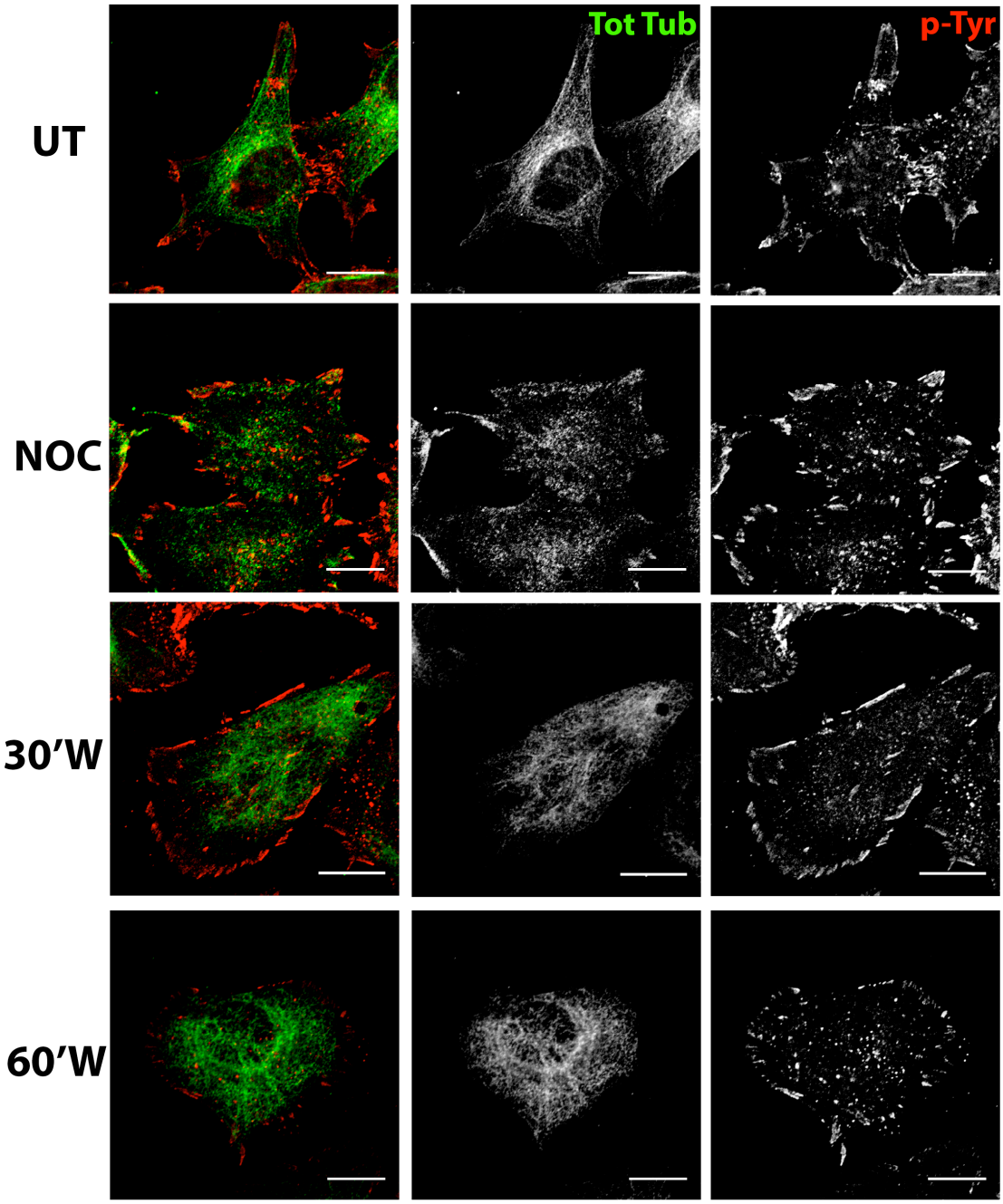

Figure 3.8. Characterisation of Nocodazole treatment and washout assay in HeLa cells

Confocal microscope image of cells stained for total tubulin and phospho-tyrosine (p-Tyr) in Hela cells untreated (UT, first row), nocodazole treated (NOC, second row), 30 minute washed (30'W, third row) and 60 minute washed (60'W) plated on fibronectin. First column shows total tubulin and p-Tyr staining together, whereas second and third columns show total tubulin and p-Tyr staining, respectively. Scale bar= 10 um.

3.9. Fascin knockdown cells do not disassemble focal adhesions following nocodazole washout

Having identified a role for fascin in MT recovery after NOC washout, the next step was to investigate whether fascin also plays a role in MT-dependent FA disassembly in the NOC assay. To assess this, the nocodazole treatment and washout assay was repeated in MDA-MB-231 control, fascin knockdown (fasKD) and fasKD re-expressing WT fascin (resWT) cells and cells were stained for phospho-Tyr (p-Tyr) to analyse FA.

Figure 3.9a shows example images of p-Tyr staining in control (first row), fasKD (second row) and resWT cells (third row) during nocodazole assay. First column shows untreated cells (UT), second column shows nocodazole treated cells (NOC) and third column shows 60 minute post-NOC washout cells (60'W). Only 60 minute washout cells were analysed as the delayed MT recovery observed in fasKD cells was greater at this time point rather than at 30 minutes. As shown previously in Figure 3.2, fasKD cells had a higher FA coverage per cell compared to either control or resWT cells in untreated conditions (first column in 3.9a). Nocodazole treatment resulted in increased FA area per cell in control, fasKD and resWT cells (second column in 3.9a). Control cells showed fewer and smaller FA 60 minutes post-NOC washout (third panel, first row in 3.9a), confirming FA disassembly occurred as has been previously reported in other cell types. Conversely, fasKD cells did not disassemble FA after nocodazole washout, showing strong p-Tyr localisation after drug washout (third panel, second row in 3.9a). This data suggests a role for fascin in MT-dependent FA disassembly. In addition, FAs did disassemble after NOC washout by rescuing WT fascin expression in fasKD cells (third panel, third row in 3.9a).

Quantification of p-Tyr staining in control, fasKD and resWT cells was performed in ImageJ. The percentage of cell occupied by FA (FA size) and FA number per cell in

control (black bars), fasKD (white bars) and resWT (red bars) was calculated and is shown in Figure 3.9b, c. All data was normalised against cell area. Quantification (figure 3.9b) confirmed the increased FA assembly in untreated fasKD cells compared to both control or resWT cells. Data showed a significant increase in percentage of cell occupied by FAs in all NOC treated cells (Figure 3.9b, p-value between untreated and treated fasKD or resWT cells =< 0.001). Statistical analysis confirmed a decrease in FA size to untreated levels in control and resWT cells, while fasKD showed no recovery in FA size following NOC washout. Figure 3.9c shows quantification of FA number per cell during the nocodazole treatment and washout assay. Both control and resWT cells showed increased FA number after NOC treatment, while fasKD cells showed a decrease in FA number. In addition, 60 minute NOC washout results in a decrease of FA number per cell in control and resWT cells, while fasKD cells did not show a regulation of FA number after NOC washout. Taken together, these data suggest that fascin is required for control of FA dynamics following MT re-growth.

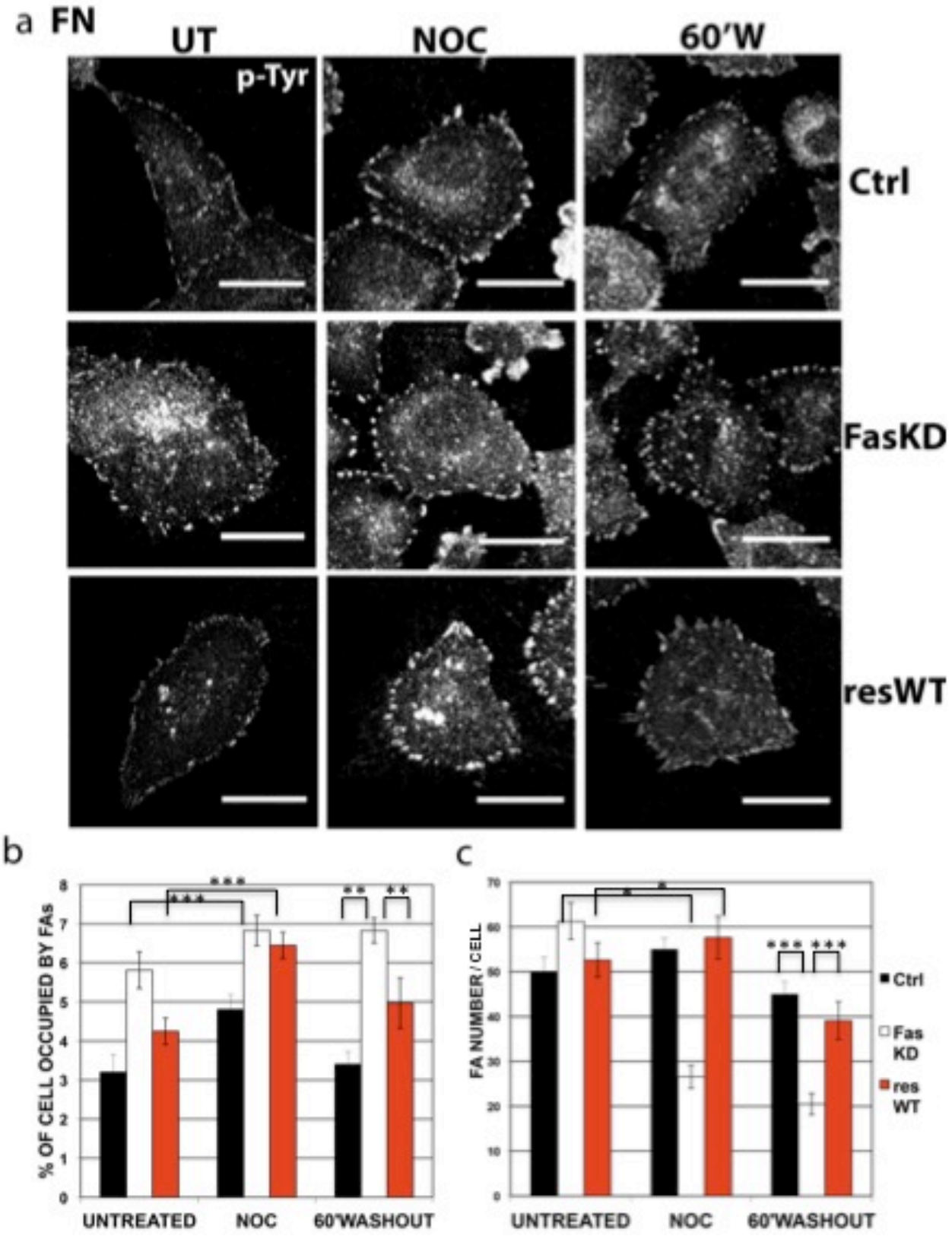
a FN
UT
NOC
60'W
p-Tyr
Ctrl
FasKD
resWT
b
% OF CELL OCCUPIED BY FAs
UNTREATED
NOC
60'WASHOUT
c
FA NUMBER / CELL
UNTREATED
NOC
60'WASHOUT
Ctrl
Fas KD
res WT

Figure 3.9. Fascin knockdown cells do not disassemble focal adhesions following nocodazole washout

(a) Confocal microscope images of MDA-MB-231 cells stained for phospho-tyrosine (p-Tyr) in control cells (first row), fasKD cells (second row) and fasKD cells re-expressing WT fascin-GFP (third row). Left column shows untreated cells (UT), centre column shows nocodazole treated cells (NOC) and right column shows 60 minute washed cells (60'W). Scale bar= 5 um. (b, c) Quantification of % of cell occupied by FAs (b) and FA number per cell (c) in control cells (in black), fasKD cells (in white) and fasKD cells re-expressing WT fascin-GFP (in red). Statistical analysis of p-Tyr staining was performed in ImageJ. At least 20 cells were evaluated in three different experiments. P-value =< 0.001 (***), =< 0.005 (**) and =< 0.05 (*) were considered as significant. Data are expressed as mean± sem and corrected on cell area.

3.10. Fascin is required for control of FA dynamics following MT re-growth in IRM live imaging experiments

Data showed in section 3.9 showed fascin to play a role in driving FA disassembly following MT re-growth. To confirm this further, I performed live imaging experiments in MDA-MB-231 control, fasKD and fasKD rescued for GFP-WT fascin expression during nocodazole treatment and washout assay. Cells were plated in chambers pre-coated with fibronectin and imaged by Interference Reflection Microscopy (IRM) throughout the nocodazole assay. Note that IRM shows in black the area of the cell in contact with the ECM.

Figure 3.10 shows still images taken from IRM Movies 3,4 and 5. As expected, control cells showed increased FA assembly after NOC treatment and subsequent decrease following drug washout (top row). On the other hand, fasKD cells after NOC washout were delayed in disassembling FA, whose assembly was induced by NOC treatment (centre row). FA dynamics observed in control cells during the NOC assay were also observed in fasKD cells rescued for GFP-WT fascin expression (bottom row). This data confirms that fascin specifically regulates FA disassembly following MT re-growth.

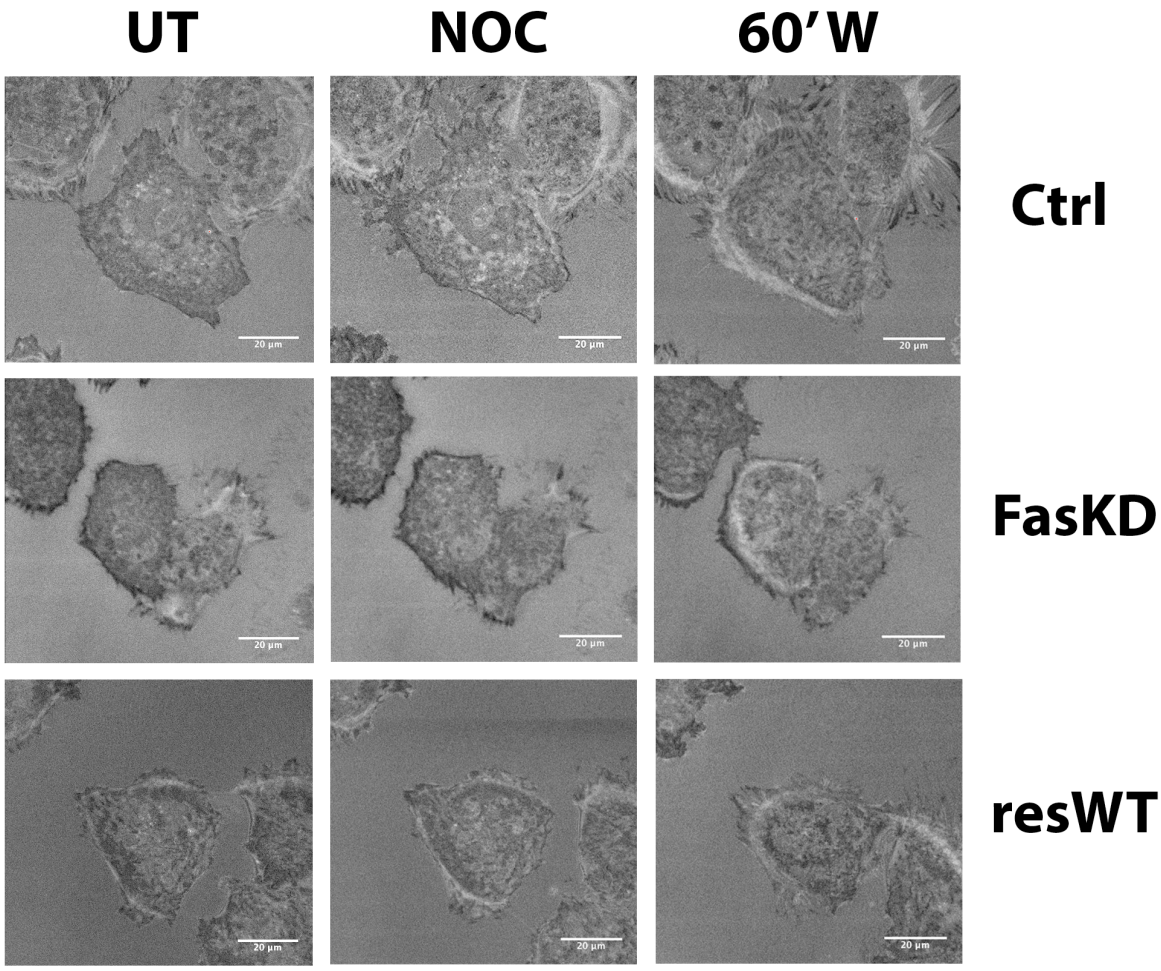

Figure 3.10. **Fascin is required for control of FA dynamics following MT re-growth in IRM live imaging experiments**

Still images from IRM movies 3,4,5 of MDA-MB-231 control (top row), fasKD (centre row) and fasKD rescued for GFP-WT fascin (resWT, bottom row) during nocodazole treatment and washout assay. First column shows untreated cells (UT), second column shows nocodazole treated cells (NOC) and third column shows 60 minute washed cells (60'W). Scale bar= 20 um.

3.11. Fascin localises to the cell periphery following Nocodazole washout

As shown in Figure 3.3, fascin is recruited to the cell periphery where it shows co-localisation with the tips of MTs. After identifying a role for fascin in regulating both MT and FA dynamics, it was important to more carefully define fascin localisation during the Nocodazole treatment and washout assay in control and resWT MDA-MB-231 cells.

Figure 3.11 shows example images of fascin staining in untreated control cells (UT), Nocodazole treated cells (NOC), 30 minute washed cells (30'W) and 60 minute washed cells (60'W). Endogenous fascin and rescued WTfascin-GFP in fasKD cells was seen at the cell periphery in untreated cells (first panels). Nocodazole treatment led to decreased levels of fascin at the cell periphery in both endogenous and rescued fasWT cells (second panels, Figure 3.11). Interestingly, 30 minutes after NOC washout (third panel, top row in 3.11) fascin was clearly recruited to the cell edge within dot-like structures and this was also evident at 60 minutes washout in both cell types. These data suggest that fascin translocation to the cell periphery could provide a mechanism for fascin to regulate MT stability and FA dynamics.

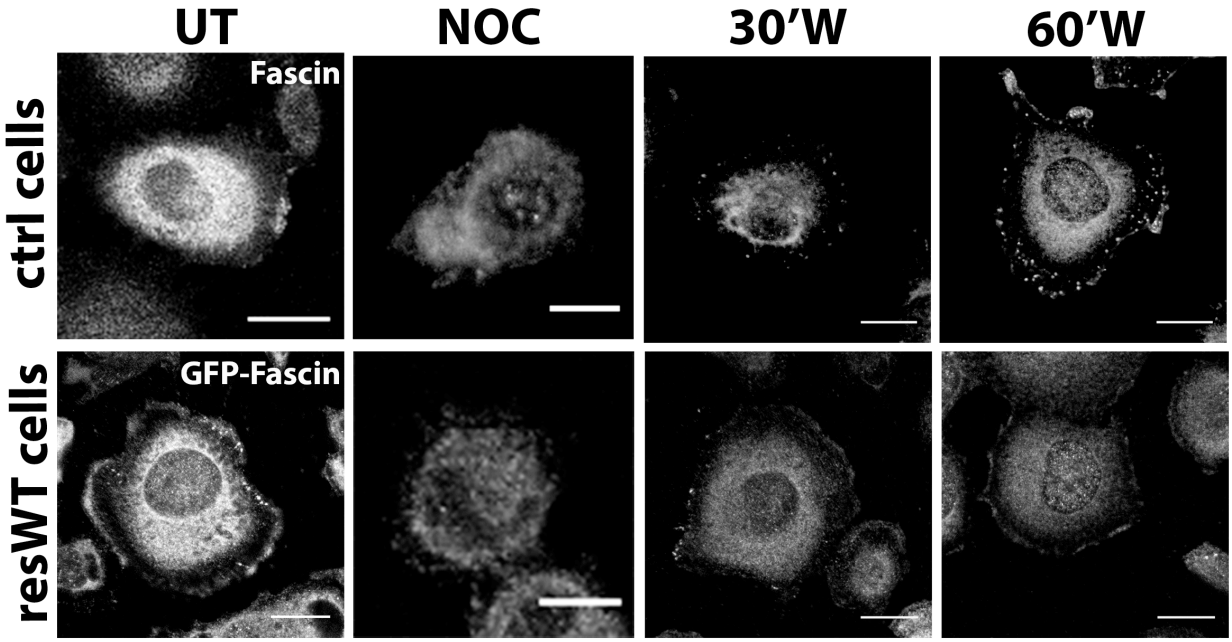

Figure 3.11. **Fascin localises to the cell periphery following nocodazole washout**
Confocal microscope image of cells stained for endogenous fascin in control cells (above) and WT fascin-GFP rescue in MDA-MB-231 fasKD cells re-expressing WT fascin-GFP (below). First column shows untreated cells (UT), second column shows nocodazole treated cells (NOC), third column shows 30 minute washed cells (30'W) and fourth column shows 60 minute washed cells (60'W). Scale bar= 10 um.

DISCUSSION

Data presented in this chapter demonstrates a role for fascin in regulating MT and FA dynamics after Nocodazole washout. This could potentially happen through transient localization of fascin to the periphery of the cell, adjacent to FA, during dynamic membrane MT targeting. It has been previously demonstrated that MT play a role in the regulation of FA stability (Ballestrem et al. 2000; Wehrle-Haller & Imhof 2003) and studies using Nocodazole (NOC) have shown MT depolymerisation drives adhesion growth, and MT recovery induces FA disassembly (Ezratty et al. 2005). Although molecular mediators of the MT-FA crosstalk have been proposed, the details of how MT regulate adhesion dynamics remain unclear (Rodriguez et al. 2003). In addition, role for fascin in stabilising F-actin structures has been well documented by our lab and others (Anilkumar et al. 2003; Hashimoto et al. 2007; Parsons & Adams 2008). However, the role of fascin in controlling adhesion dynamics has not been yet addressed. Here I show fascin regulation of MT re-growth and FA disassembly after NOC washout, suggesting fascin regulates adhesions dynamics potentially through control of MT.

Data shown in this chapter demonstrates that fascin has a role in regulating MT re-growth after NOC washout on fibronectin (FN, ligand for both β1 and β3 integrins) and collagen I (COL, ligand for β1 integrin only). The complete lack of MT recovery in cells plated on vitronectin (ligand for β3 integrin only) suggests that the engagement of β1 integrin is an essential requirement for MT re-growth in cells. Moreover, the delayed MT assembly following NOC washout on FN compared to that seen on COL suggests that the activation of β3 integrin may act as a negative modulator of MT re-growth. Accordingly, the faster MT recovery in cells plated on COL compared to FN confirms a major role for β1 integrin in fascin regulation of MT dynamics.

Both β1 and β3 integrins have been associated with increased cancer cell invasion and metastasis (Felding-Habermann et al. 2001) and they have been proposed to be involved in different types of migration (Brockbank et al. 2005). β1 integrin has been shown to be required for the invasive behavior of squamous carcinoma cells, while β3 integrin up-regulation drives cell proliferation. It is therefore possible a preferential requirement of β1 integrin in the regulation of cancer cell adhesion. Furthermore, β3 integrin has been already proposed as a negative modulator of adhesion dynamics and migration (Worth & Parsons 2010). Interestingly, molecules such as the MT plus-end tracking protein (+TIP) EB3 has been demonstrated to be recruted specifically in β1, but not β3 integrin-adhesion complexes in mass spectrometry analysis (Byron et al. 2012).

Fascin knockdown expression in human carcinoma cell lines has been previously shown by our lab to decrease FA dynamics, suggesting it may play a role in adhesion site stability (Hashimoto et al. 2007). Fascin localises in structures such as podosomes and invadopodia, promoting their stability and regulating PKC-dependent invasiveness of the filopodia (Quintavalle et al. 2003; Li et al. 2010; Vignjevic et al. 2006). However, previous studies had not found fascin to be localised in FA. Data presented here proposes fascin localisation at the cell periphery through co-operation with MT as a mechanism regulating FA dynamics. Therefore, peripheral localisation enables fascin to regulate basal MT and FA stability and turnover. Fascin localisation in FA is not as stable and clear in these membrane punctate structures as in filopodia structures. Peripheral fascin may be transiently localised in regions near or within FA contributing to their turnover. In addition, the role of fascin at adhesion sites might be dynamically regulated by other FA components and by fascin-actin binding. These issues will be addressed experimentally in the following chapters.

Fascin depleted cells showed increased MT stability, without any major effect on MT polymerisation. Peripheral fascin co-localises with ends of MT, potentially promoting

the dynamic instability of MT as they target the membrane. Fascin depletion (Jayo & Parsons, 2010) and decreased MT dynamics due to higher acetylated tubulin levels (Ikegami & Setou, 2010; Perdiz et al. 2010) have been shown to decrease cell migration. In addition, the data presented in this chapter shows increased tubulin acetylation in fasKD cells and delayed MT recovery after NOC washout suggesting that fascin control of MT dynamics may be required for MT re-growth and network assembly. MT dynamics and stability are controlled by MT +TIP proteins. Proteins such as EB1 and EB3 are master regulators of the MT + end network, mediating the interaction between MT and other proteins (Matov et al., 2010). Other capping proteins are involved in the regulation of MT stability. Molecules involved in tubulin acetylation, such as histone deacetylase 6 (HDAC6), have been shown to play a role in regulating tubulin post-translational modifications and cell motility (Tran et al. 2007). Therefore, I speculated about a possible role for peripheral fascin in displacing MT +TIP proteins or in controlling enzymes regulating tubulin acetylation. Experiments in following chapters will address how fascin binding to actin may contribute to this, and whether fascin may associate directly with the MT cytoskeleton.

Fascin regulation of MT may also promote a feedback loop control of MT on fascin localisation at the cell edge. MT are known to target FA and this is thought to deliver FA components at adhesion sites (Morrison 2007; Stehbens & Wittmann 2012). Our hypothesis is that highly dynamic MT may transiently interact with fascin, promoting its localisation at the periphery near FA and therefore enabling fascin-dependent control of FA turnover. Fascin depleted cells also showed increased FA assembly under basal conditions. This might be due to the more stable MT observed in fasKD cells, which in turn slows down FA turnover, causing accumulation of molecules at adhesion sites. Data presented in this chapter demonstrates that levels of total FAK or vinculin (characterized classical components of FA) are not affected by fascin depletion. Therefore, fascin likely controls dynamics of FA proteins rather than levels

through transcriptional mechanisms. This would also agree with a role for fascin in control of MT stability.

Given the observed role for fascin in both MT and FA dynamics in this chapter, the next important step therefore was to study the mechanism explaining this new role for fascin in regulating the MT network.

4 The role of fascin-actin binding in controlling MT-dependent adhesion dynamics.

INTRODUCTION

Fascin is most well-known for its ability to cross-link parallel actin filaments and form finger-like structures called filopodia (Vignjevic et al. 2006). Fascin actin bundling activity is directed by the two major actin binding sites, situated at the N- and C-terminal β-trefoil domain, respectively (Ono 1996). The best-characterised actin-binding site resides on the N-terminus at Serine 39 (Ser39) within the first β-trefoil domain. PKC-dependent phosphorylation of Ser39 results in the loss of the actin binding and greatly reduced filopodia formation (Anilkumar et al. 2003; J. Adams 2004). In addition, a second actin-binding site at the C terminus of the protein has been recently characterised (Zanet et al. 2012). The molecular mechanism regulating this novel actin-binding site is not yet understood, but evidence suggests that it involves phosphorylation changes on serine 274 (Ser274). Mutations of Ser274 to a non-phosphorylatable residue (alanine, A) or to a phospho-mimic aspartic acid (D) result in the disruption of fascin actin binding activity. In cells, it has been shown that S274A fascin expression can still promote filopodia formation even in the absence of normal actin binding activity, whereas S274D fascin cannot. This serine is known to reside in a non-exposed fold between the second and the third β-trefoil domains of fascin, which does not allow an efficient binding to actin. Its binding mechanism is, therefore, under investigation (Jansen et al., 2011). Since both mutations that change S274 phosphorylation status (A/D) affect fascin-actin binding and show different effects on filopodia formation, an actin-independent mechanism or role for fascin has been suggested.

Experiments in this chapter aim to analyse the potential co-operation between fascin, actin binding and MT dynamics in controlling FA assembly. This will make use of these previously published mutants of fascin within S39 and S274 to determine whether uncoupling of fascin-actin binding can lead to changes in MT dynamics.

4.1. Fascin-actin binding is required for Focal Adhesion stability

Data in the previous chapter demonstrated a role for fascin in controlling MT stability and focal adhesion assembly. To determine whether this novel role of fascin depended upon fascin binding to actin, fascin expression was rescued in fascin knockdown MDA-MB-231 cells (fasKD) by re-expression of GFP tagged sh-resistant fascin constructs. Cells were transfected with either GFP-tagged WT fascin, fascin S39A (known to bind and bundle actin), fascin S39D (does not bundle actin), S274A or S274D (neither bundle actin, but are not well characterized in other functions) (Zanet et al. 2012).

Cells were plated on fibronectin and stained for phospho-tyrosine (p-Tyr) levels as a marker of FA. Cells were imaged by confocal microscopy to observe and quantify changes in percentage of cell occupied by FA (FA size) and FA number. Figure 4.1a shows example images of p-Tyr staining in fasKD cells rescued with WT fascin or mutant fascin-GFP. As previously described in section 3.2 (Results Chapter 1), p-Tyr staining in fasKD cells rescued for WT fascin (resWT) showed peripheral FA with some smaller punctate FA beneath the cell body. S39A fascin expression in fasKD cells resulted in increased FA number and more peripherally localized FA (left top panel in Figure 4.1a). P-Tyr staining in resS39A fascin cells showed larger FA compared to those seen in resWT cells, suggesting that fascin-actin binding can promote FA stability. Conversely, S39D fascin rescue cells (right top panel in Figure 4.1a) showed significantly fewer and smaller FA compared to resS39A expressing cells, with localisation of small FA underneath the cell body. This further supports the concept of fascin-actin binding being required for regulation of FA stability. Cells expressing S274A fascin (left bottom panel in Figure 4.1a) had numerous membrane spikes with FA localised at the ends of these spikes. P-Tyr staining in cells expressing S274D fascin (right bottom panel in Figure 4.1a) showed large and densely packed FA

decorating the cell edge, similar to p-Tyr staining observed in S39A fascin expressing cells.

P-Tyr staining was quantified in fasKD cells re-expressing WT and mutant fascin from three different experiments. FA size and number quantification was performed using in ImageJ and data was corrected for cell area (at least 20 cells were analysed in each experiment). Quantification of the percentage of cell occupied by FAs (FA size) and FA number per cell in fasKD cells rescue for WT (black bars), S39A (green bars), S39D (orange bars), S274A (blue bars) and S274D (purple bars) is shown in Figure 4.1b,c. Quantification showed an increase in both % of cell occupied by FAs and FA number in cells expressing S39A fascin compared to resWT cells. A significant decrease in both FA occupied cell area and FA number was observed in cells re-expressing S39D fascin, confirming the smaller FA observed in these images. Furthermore, a significant increase in FA size and FA number in cells expressing S274A fascin was observed. Indeed, FA in S274A fascin cells were larger and more numerous than in S39A fascin cells (p-value S274A compared to S39A cells: $p =< 0.05$). S274A fascin re-expression had a greater effect on FA size than FA number. FA in S274D fascin cells were larger and more numerous compared to WT. Interestingly, similar FA size and number was observed between S274D fascin rescue cells (purple bars) and cells re-expressing S39A fascin (green bars), implying two different mechanisms regulating fascin role in FA stability, one actin-binding dependent and one independent. Taken together, this data shows that fascin-actin binding is required for FA stability and also proposes that a second actin-binding independent mechanism may exist for fascin-dependent FA assembly.

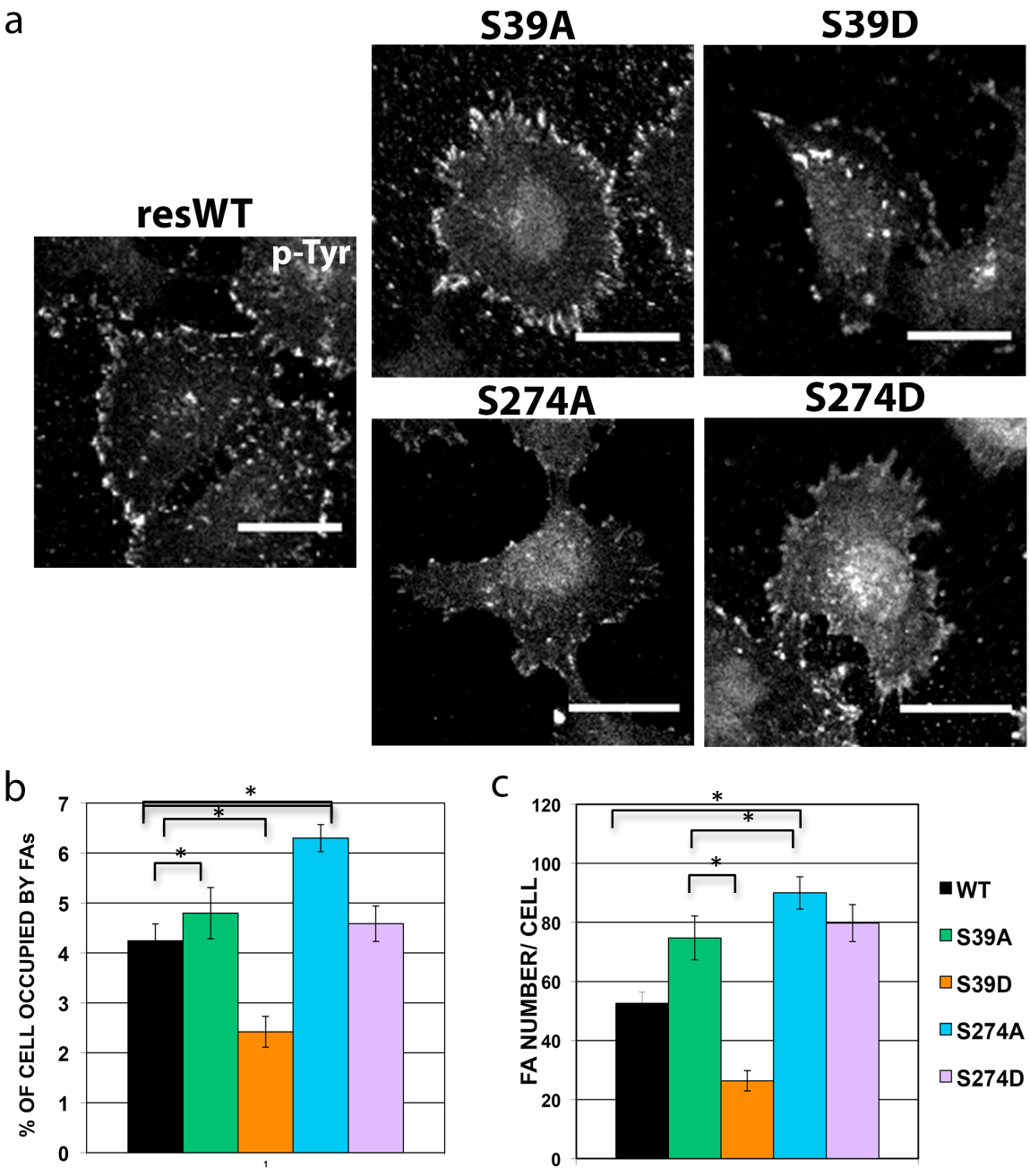

Figure 4.1. Fascin-actin binding is required for focal adhesion stability

(a) Confocal microscope images of phospho-tyrosine (p-Tyr) staining in MDA-MB-231 fasKD cells expressing fascin shRNA re-expressing shRNA resistant WT or mutant fascin-GFP. Scale bar= 10 um. (b, c) Quantification of % of cell occupied by FAs (b) and FA number per cell (c) in fasKD cells re-expressing WT and mutant fascin. Statistical analysis of p-Tyr staining was performed in ImageJ. At least 20 cells were evaluated in three different experiments. P-value =< 0.05 (*) was considered as significant. Data are expressed as mean± sem and corrected on cell area.

4.2. Expression of fascin mutants does not alter total levels of focal adhesion proteins

Having identified changes in FA size and number in cells expressing fascin mutants with different actin bundling capabilities, it was next important to determine whether these changes were due to altered total levels of FA components. Therefore, levels of FAK and vinculin were analysed in fascin knockdown MDA-MB-231 (fasKD) cells rescued with WT and mutant fascin by western blotting as previously also performed in Results Chapter 1(3.5).

Figure 4.2a shows western blots for total FAK and vinculin levels in lysates from fasKD cells re-expressing GFP-tagged WT (resWT), S39A, S39D, S274A, or S274D fascin. GFP-fascin levels are also shown and GAPDH was used as loading control. FAK and vinculin levels were quantified by densitometry analysis of multiple western blots, together with GFP-fascin levels in fasKD cells rescue for WT and mutant fascin (Figure 4.2b). Data showed similar efficiency of fascin re-expression in all cases. No differences in total levels of FAK or vinculin were detected between mutant fascin expressing cells. Thus, expression of fascin mutants does not result in change of total level of these FA proteins.

To investigate whether the observed dependence of fascin-actin bundling on FA dynamics played a functional role in cell adhesion, cell-binding assays were performed on fibronectin-coated coverslips. FasKD cells re-expressing WT or mutant fascin-GFP were plated on fibronectin and cells were counted after 24 hours. Figure 4.2c shows quantification of the number of adhered cells re-expressing WT, S39A, S39D, S274A or S274D fascin. S39A fascin expressing cells showed significantly higher adhesion to fibronectin compared to resWT cells (p-value S39A rescue cells compared to WT =< 0.001), whereas S39D fascin cells showed lower adhesion to fibronectin (p-value S39D rescue cells compared to WT =< 0.001). Adhesion to

fibronectin in S274A rescue cells was as efficient as that seen in resWT cells (p-value S274A rescue cells compared to WT =< 0.001). Conversely, S274D fascin re-expressing cells showed lower adhesion compared to WT fascin rescue cells (p-value S274D rescue cells compared to WT =< 0.001). Interestingly, S274D rescue cells showed similarly sized FA to those seen in S39A fascin rescue cells (Figure 4.1), but significantly lower adhesion to fibronectin.

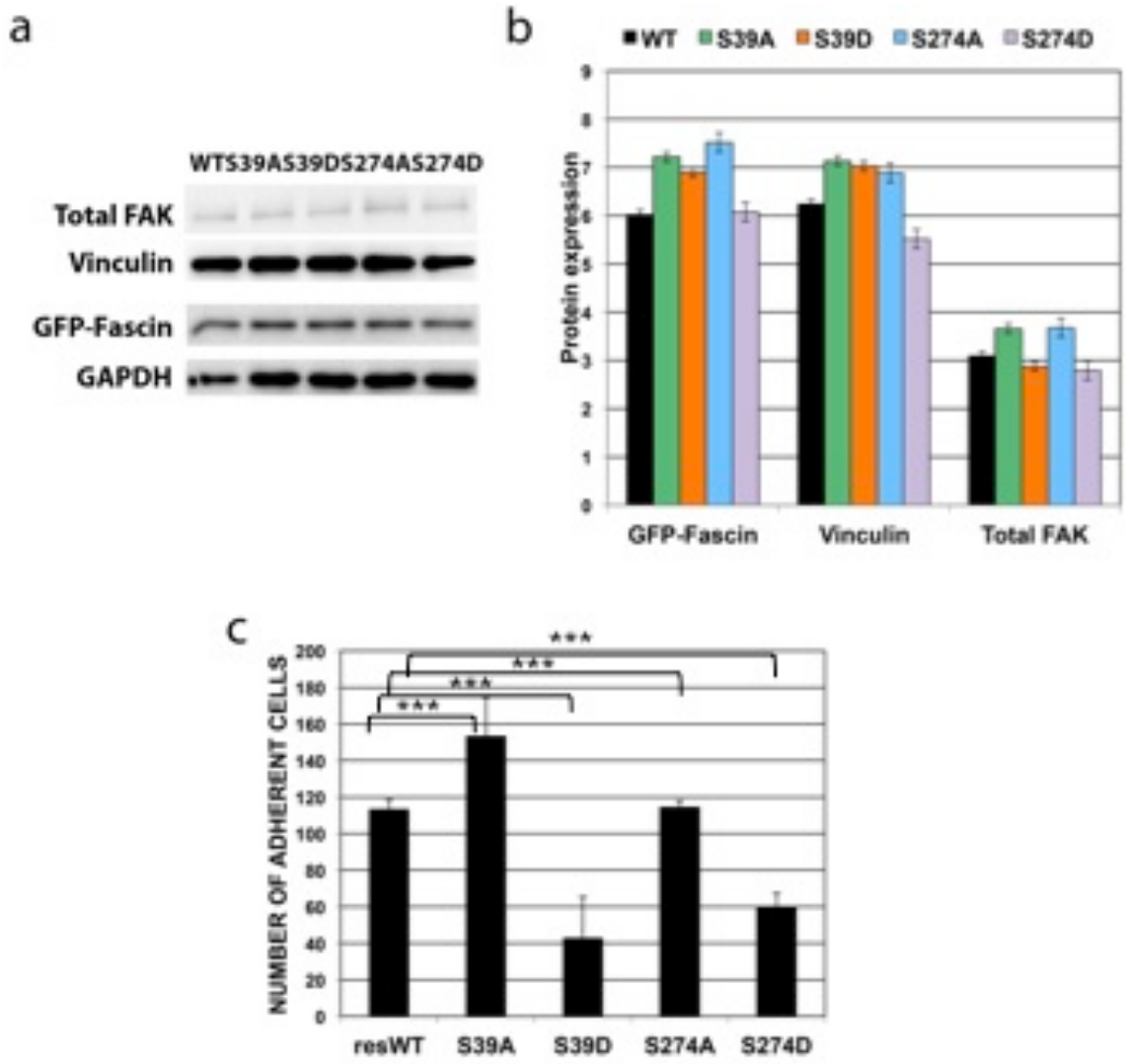

Figure 4.2. Expression of fascin mutants does not alter total levels of focal adhesion proteins

(a) Western blots of lysates from MDA-MB-231 fasKD cells re-expressing WT or mutant fascin-GFP. (b) Statistical analysis of GFP-fascin WT and mutants, total Focal Adhesion Kinase (FAK) and vinculin levels was performed by densitometry analysis of at least three western blots. Data are expressed as mean± sem and corrected on GAPDH loading as control. (c) Count of cells re-expressing WT or mutant fascin-GFP adhering on fibronectin. Statistical analysis was performed using T-Test. P-value =< 0.001 (***) was considered as significant. Data are expressed as mean± sem. At least 20 cells were evaluated in three separate experiments.

4.3. Fascin-actin binding promotes increased cell spreading

Data shown in Chapter 1 showed WT fascin localisation at the cell periphery in small punctate structures, that potentially represent transient sites for fascin to regulate MT and FA dynamics. As data in Figure 4.2 also showed fascin-actin binding to regulate FA stability, it was important to also determine localization of mutant fascin-GFP expressed in fasKD cells.

To test this, WT and mutant fascin-GFP constructs were expressed in MDA-MB-231 fasKD cells and localisation analysed by confocal microscopy. Example representative images are shown in Figure 4.3a. Zoom of cell periphery area is shown in each panel to show fascin localisation. WT fascin-GFP (first panel) localised at the cell periphery in the same way as endogenous fascin (see Figure 3.3 in Results chapter 1). Zoomed area in resWT fascin panel shows fascin localisation to filopodia and larger peripheral structures. As previously reported, S39A fascin (left top panel in Figure 4.3a) localised to actin-based structures such as filopodia and stress fibres, without showing localisation in punctuate FA (zoomed area in left top panel). S39D fascin (right top panel in Figure 4.3a) was localized diffusely in the cytoplasm and not seen in any peripheral actin-based structures (zoomed area in the right top panel). S274A fascin (left bottom panel in Figure 4.3a) localised at the cell periphery, particularly at the end of the spikes formed in these cells (Figure 4.1 and zoomed area in left bottom panel). S274D fascin (right bottom panel in Figure 4.3a) also localised to the cell periphery and also within intracellular punctate or striped structures (Figures 4.1 and 4.2c and zoomed area in right bottom panel in 4.3a). Dynamic turnover of focal adhesions is required to drive changes in cell spreading. Therefore, the spread area was analysed in cells expressing WT or mutant fascin to compare with the FA characterization data. Cells were stained for phospho-Tyr (p-Tyr) as before, and images were quantified using ImageJ in three different experiments (at least 20 cells were evaluated in each experiment). P-Tyr was used as a marker of cell area as this

faithfully reported on cell area changes induced by nocodazole treatment (Figures 3.7 and 3.8, Results Chapter 1). Figure 4.3b shows analysis of cell area in fasKD MDA-MB-231 cells re-expressing GFP-fascinWT (black bar), S39A (green bar), S39D (orange bar), S274A (blue bar) or S274D (violet bar) fascin. Cells expressing S39A fascin were significantly more spread than WT fascin rescue cells (p-value S39A expressing cells compared to WT =< 0.001), correlating with large FA observed in these cells (Figure 4.1). S39D expressing cells showed smaller cell area than WT fascin rescue cells. Cells expressing S274A and S39D fascin rescue cells showed a similar significant reduction in cell area when compared to WT fascin. Conversely, S274D fascin expressing cells had a larger cell area than WT fascin rescue cells (p-value in S274D expressing cells compared to WT =< 0.001), but smaller than S39A fascin rescue cells. This data suggests that fascin-actin binding can control both FA size/number and location and this also correlates with changes in spread cell area.

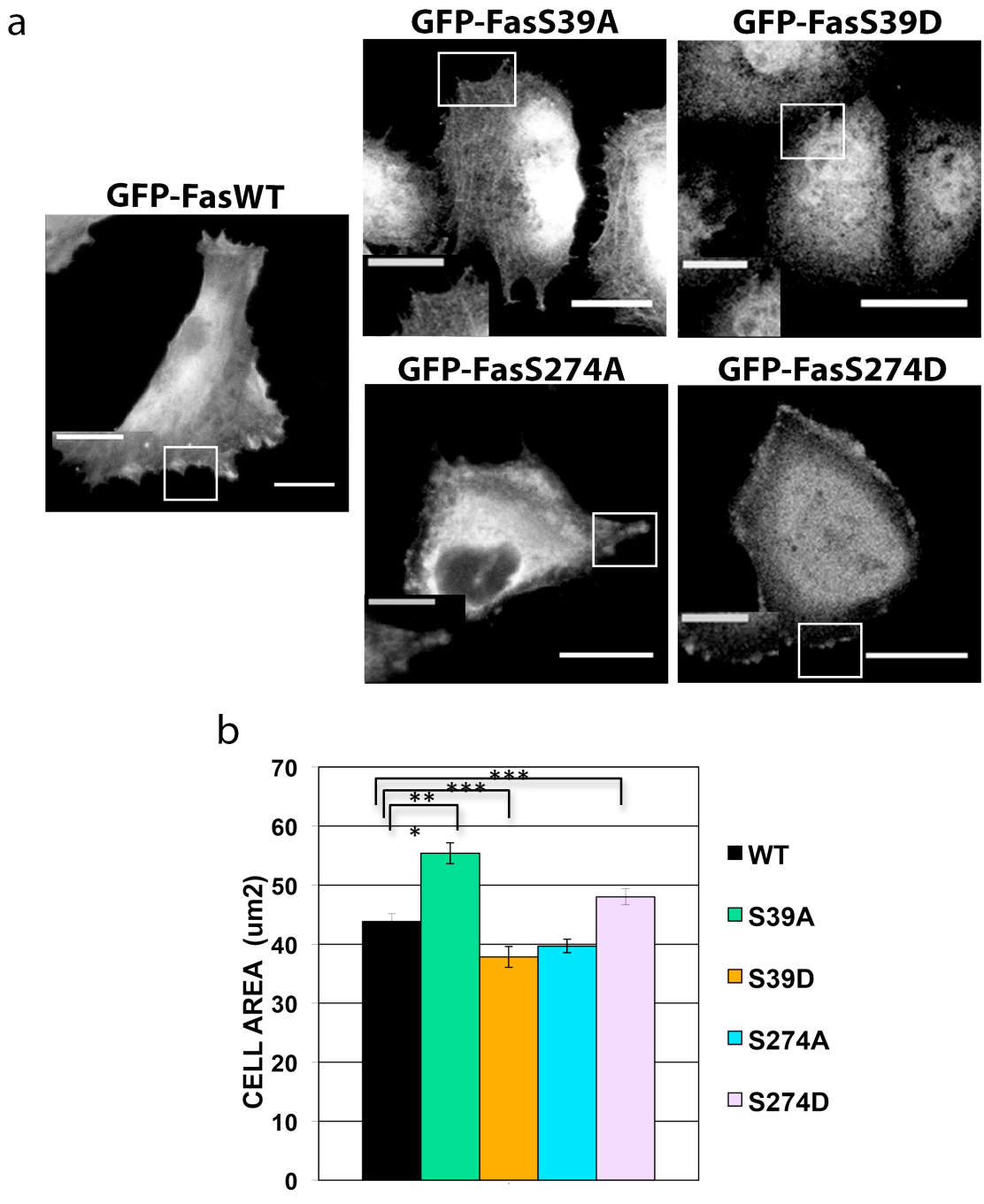

Figure 4.3. Fascin-actin binding promotes increased cell spreading

(a) Confocal microscope images of WT and mutant fascin-GFP in MDA-MB-231 fascin knockdown cells re-expressing WT or mutant fascin-GFP. Scale bar= 10 um. Zoom of the highlighted area is shown in each panel to show WT or mutant fascin-GFP localisation. Scale bar = 3 um. (b) Quantification of cell size in fasKD cells re-expressing WT and mutant fascin. Statistical analysis of p-Tyr staining was performed in ImageJ. At least 20 cells were evaluated in three different experiments. P-value =< 0.001 (***) was considered as significant. Data are expressed as mean± sem.

4.4. Rescue of fascin knockdown cells with S274D fascin restores microtubule re-growth following nocodazole washout

Data shown in Figures 3.7 and 3.8 in Results Chapter 1 showed fascin plays a role in control of MT-dependent regulation of FA disassembly. After characterising FA in cells expressing mutant fascin and observing S274D fascin localisation at the cell periphery, the next step was to investigate whether fascin-actin binding also affected basal MT integrity and MT recovery in nocodazole treatment and washout assays.

To test this, fascin knockdown MDA-MB-231 (fasKD) cells expressing WT or mutant fascin-GFP were left untreated or treated with nocodazole for 15 minutes or following washout of the drug for 60 minutes. Total tubulin staining was performed and cells were scored for percentage of normal MT network (MT score) as in Results Chapter 1. Figure 4.4a shows example images of tubulin staining in untreated cells (UT, first row), nocodazole treated cells (NOC, second row) and 60 minute washed cells (60'W, third row). First column in Figure 4.4a shows staining of the MT network during the NOC assay in fasKD cells expressing WT fascin, S39A fascin (second column), S39D (third column), S274A fascin (fourth column) or S274D fascin (fifth column). No obvious effects were seen on basal MT polymerization or network formation in any of the cells expressing WT or mutant forms of fascin. All cells showed polymerised MT bundles with clear MT organising centre (MTOC). As reported in Chapter 1, NOC treatment led to rounded cells with complete MT depolymerisation in all the cell lines (second row in Figure 4.4a). As observed in Figure 3.7 in Result Chapter 1, WT fascin expressing cells showed a fully restored MT network after 60 minute NOC washout, showing clear MT bundles and MTOC localisation adjacent to the nucleus (first panel, third row in Figure 4.4a). Conversely, S39A and S39D expressing cells were delayed in MT recovery following NOC

washout, showing depolymerised MT and no clear MTOC (third row in Figure 4.4a). S274A expressing cells showed more organized MT than S39 mutant expressing cells following NOC washout, but not to levels seen in WT fascin cells. However, S274D fascin expressing cells demonstrated a complete MT recovery post-NOC washout with normal MT bundles and visible MTOC next to the nucleus, similar to that seen in WT fascin cells.

Cells were scored for MT recovery (as in Results Chapter 1) to quantify the percentage of cells with normal MT network in the nocodazole assay time points (Figure 4.4b). FasKD cells were rescued for WT fascin (black bars), S39A (green bars), S39D (orange bars), S274A (blue bars) and S274D (purple bars). Over 80% of untreated cells in all conditions showed normal MT network while <5% had polymerised MT bundles after NOC treatment. WT fascin expressing cells showed efficient MT recovery post-NOC washout to ~80% of that seen in pre-NOC treated cells. Statistical analysis on both S39 mutants confirmed a delay in MT recovery following NOC washout (MT score ≈ 50-60%), whereas both S274 fascin mutant rescue cells showed more efficient MT recovery after drug washout (Figure 4.4b). Around 70% of S274A fascin expressing cells showed a normal MT network, but more than 80% of S274D fascin rescue cells restored their MT network completely. S274D fascin expressing cells showed an efficient MT recovery as seen in WT fascin expressing cells (p-value in 60 minute washed cells compared to untreated =< 0.001).

a

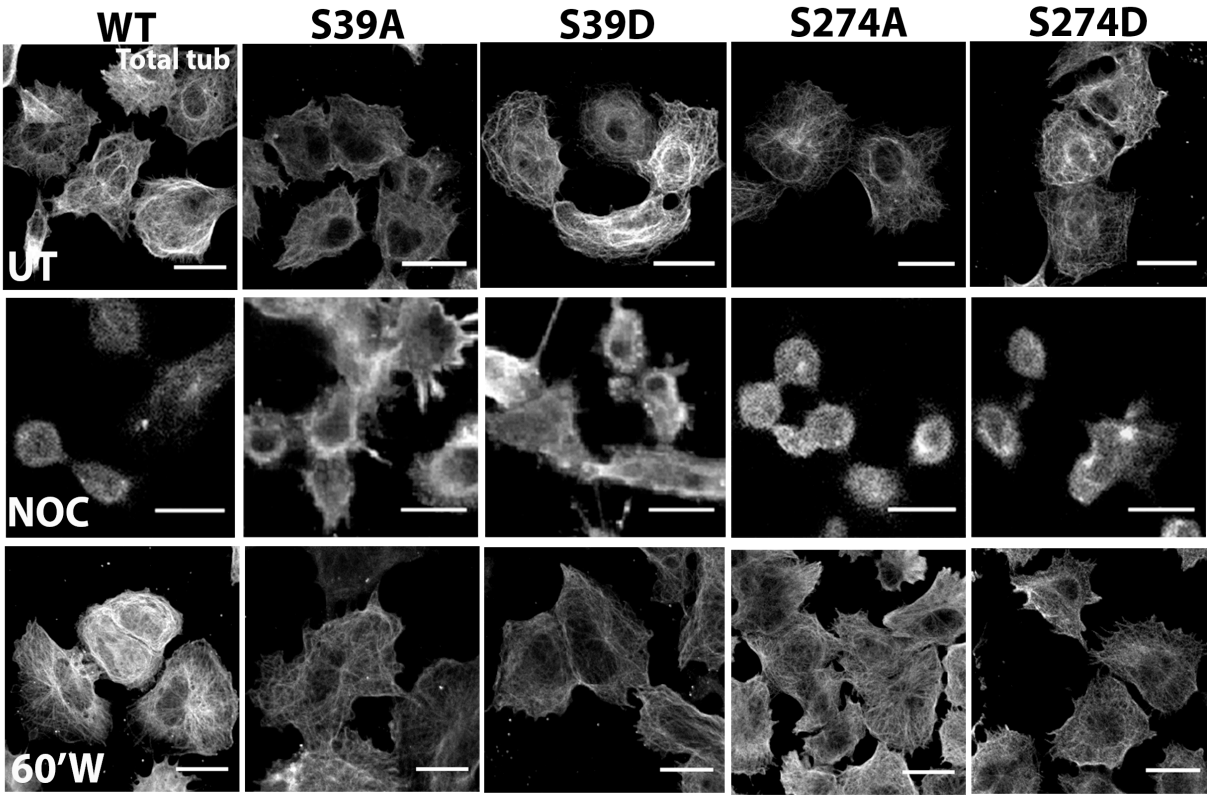
WT
S39A
S39D
S274A
S274D
Total tub
UT
NOC
60'W

b

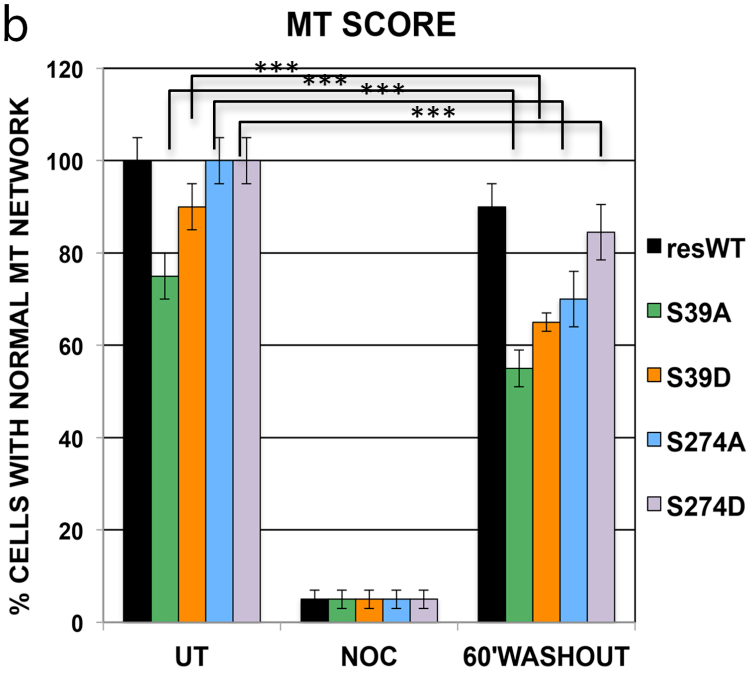
MT SCORE
% CELLS WITH NORMAL MT NETWORK
120
100
80
60
40
20
0
***
***
***
***
UT
NOC
60'WASHOUT
resWT
S39A
S39D
S274A
S274D

Figure 4.4. Rescue of fascin knockdown cells with S274D fascin restores microtubule re-growth following nocodazole washout

(a) Confocal microscope images of cells stained for total tubulin in MDA-MB-231 fasKD cells re-expressing WT fascin-GFP (first column), S39A-GFP (second column), S39D-GFP (third column), S274A-GFP (fourth column) and S274D-GFP (fifth column). First row shows untreated cells (UT), centre shows nocodazole treated cells (NOC) and bottom shows 60 minute washed cells (60'W). Scale bar= 20 um. (b) Statistical analysis of % of cells with normal MT network (MT score) in same conditions as above. P-values =< 0.001 (***) was considered as significant. Data are expressed as mean± sem. At least 20 cells were evaluated in three separate experiments.

4.5. Cells expressing fascin S39 and S274 mutants exhibit distinct responses to nocodazole

Data in Figure 4.4 demonstrated that S274D was the only mutant form of fascin able to full restore the MT network to levels seen in WT cells following NOC washout. In Chapter 1, data demonstrated that fascin was required for MT-dependent FA disassembly following NOC washout. The next question was therefore whether mutant fascin also regulated FA size or number following NOC treatment or washout.

To test this, MDA-MB-231 fascin knockdown (fasKD) cells expressing WT or the four mutant fascin were subjected to the nocodazole treatment and washout assay as described in paragraph 4.4. Cells were stained for phospho-Tyrosine (p-Tyr) at each time point. Figure 4.5a shows example images of p-Tyr staining in untreated cells (UT, first row), nocodazole treated cells (NOC, second row) and 60 minute washed cells (60'W, third row). Columns 1-5 in Figure 4.5a shows FA during NOC assay in fasKD cells re-expressing WT fascin, S39A fascin, S39D fascin, S274A fascin and S274D fascin respectively. Basal changes in FA assembly previously reported in paragraph 4.1 were observed also in these experiments. Figure 4.4 showed the MT network was completely disrupted by nocodazole treatment in cells expressing all fascin constructs. Conversely, FA responses to nocodazole were different depending on the fascin mutant expressed. WT fascin expressing cells showed an increase in FA assembly following NOC treatment (first column, first two images in Figure 4.5a) and a similar response was observed in S39A and S39D fascin expressing cells (second and third column, respectively, first two images in Figure 4.5a). Interestingly, S274A expressing cells showed no change in FA size compared to untreated cells (fourth column, first two images in Figure 5.4a). Conversely, S274D fascin rescue cells showed reduced FA size compared with untreated cells (fifth column, first two images in Figure 4.5a).

As shown in Figure 3.8 in Results Chapter 1, WT fascin expression promoted FA disassembly following NOC washout (first column in Figure 4.5a). Similar levels of FA disassembly were observed in S39A and S39D fascin expressing cells 60 minute after NOC washout (second and third column, respectively, in Figure 4.5a). S274A fascin expressing cells did not show any response to NOC treatment in terms of FA assembly, but these cells showed decreased FA assembly after NOC washout (fourth column in Figure 4.5a). Conversely, the S274D expressing cells had significantly smaller FA after NOC treatment and instead showed a significant increase in FA size after NOC washout.

Quantification of p-Tyr staining in fasKD cells rescued for WT and mutant fascin was performed in ImageJ. The percentage of cell area occupied by FA (FA size) and FA number per cell in fasKD expressing WT fascin (black bars), S39A fascin (green bars), S39D (orange bars), S274A fascin (blue bars) and S274D fascin (purple bars) was calculated and data is shown in Figure 4.5b, c. All data was normalised to control for differences in cell area. Quantification confirmed basal differences in FA size and number previously shown in cells expressing WT or mutant fascin. Figure 4.5b shows the FA assembly/disassembly in response to both nocodazole treatment and 60 minute washout was similar in cells expressing WT, S39A and S39D fascin. S39A and S39D rescue NOC treated cells significantly increased FA size and decreased the percentage of cell area occupied by FA following NOC washout. This data confirms that the phosphorylation state of the well-characterised fascin-actin S39 binding site is not principally involved in regulating FA dynamics following NOC washout. Analysis of percentage of cell occupied by FA confirmed S274A rescue cells did not respond to NOC treatment in terms of FA growth. 274D fascin expressing cells demonstrated opposite responses to both NOC treatment and washout compared to other mutants. Indeed, 274D fascin expressing cells showed a significant decrease in FA

size compared to WT and S39 mutants when treated with NOC and an increased FA size following NOC washout.

Figure 4.5c shows FA number quantification in the same conditions as described above. WT, S39A and S39D fascin rescue cells showed more FA than untreated cells after NOC treatment, although the effect in S39A rescue cells was not as dramatic as in WT fascin rescue cells. Moreover, WT, S39A and S274A fascin expressing cells showed a decrease in FA number post-NOC washout, similar to the data shown in Figure 4.5b. However, S39D expressing cells showed a small increase in FA number after NOC washout, and S274D fascin cells showed a significant decrease in FA number following NOC treatment and, conversely, increased FA number after drug washout again confirming opposing responses to NOC in cells expressing this mutant. Taken together this data demonstrates that the S274D non-actin binding fascin mutant can fully restore the MT re-growth defects in fasKD cells following NOC washout but not promote MT-induced FA disassembly.

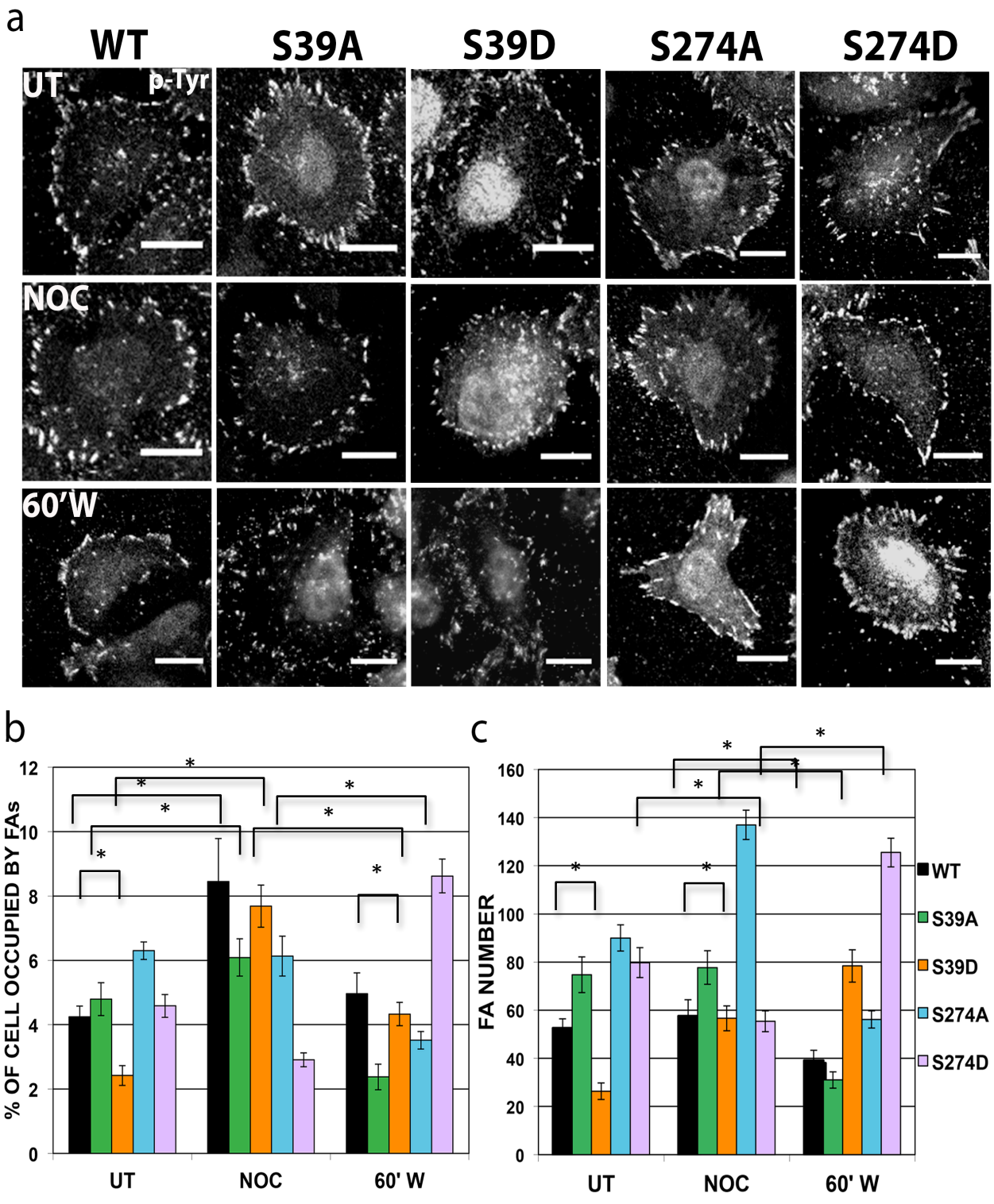
a
WT
S39A
S39D
S274A
S274D
UT
p-Tyr
NOC
60'W
b
% OF CELL OCCUPIED BY FAs
0
2
4
6
8
10
12
UT
NOC
60' W
c
FA NUMBER
0
20
40
60
80
100
120
140
160
UT
NOC
60' W
WT
S39A
S39D
S274A
S274D

Figure 4.5. Cells expressing fascin S39 and S274 mutants exhibit distinct responses to nocodazole

(a) Confocal microscope images of phospho-tyrosine (p-Tyr) staining in MDA-MB-231 fasKD cells re-expressing WT or mutant fascin-GFP. Scale bar= 10 um. (b, c) Quantification of % of cell occupied by FAs (b) and FA number per cell (c) in fasKD cells re-expressing WT and mutant fascin. Statistical analysis of p-Tyr staining was performed in ImageJ. At least 20 cells were evaluated in three different experiments. P-value =< 0.05 (*) was considered as significant. Data are expressed as mean± sem and corrected on cell area.

4.6. S274D fascin is localised to the cell periphery and colocalises with MT following nocodazole washout

Data in Figure 4.3 demonstrated that WT and S274D fascin could translocate to the cell periphery and that this correlated with increased FA disassembly. In Results Chapter 1, both endogenous and WT fascin-GFP expressed in fasKD cells showed partial colocalisation with MT at the cell periphery and this co-localisation increased after nocodazole washout. It was, therefore, important to study mutant fascin localisation with respect to MT and the response to NOC washout to define whether these observations were dependent upon fascin-actin binding.

To test this, MDA-MB-231 fascin knockdown (fasKD) cells expressing WT or mutant fascin-GFP were subjected to the nocodazole (NOC) treatment and washout assay and fascin localisation with MT was analysed before and after NOC washout. Figure 4.6 first row shows example images of total tubulin staining together with GFP fascin in untreated WT and mutant fascin rescued cells. As observed in Figure 4.3, WT and S274D fascin localised in peripheral punctuate adhesion-like structures in basal conditions. Total tubulin co-staining confirmed partial WT fascin co-localisation with MT at the cell periphery as also observed in Figure 3.3 in Result Chapter 1 (first panel, first row in Figure 4.6). S39A fascin localised in filopodia (second panel, first row in Figure 4.6), while S39D fascin did not translocate to the cell periphery, remaining mainly cytosolic (third panel, first row in Figure 4.6). In addition, neither of the S39 mutants showed colocalisation with MT at the cell periphery. S274A fascin did not localise in FA or show any overlap with MT (fourth panel, first row in Figure 4.6). Interestingly, S274D fascin, which localised at the cell periphery also showed co-localisation with MT bundles (fifth panel, first row in Figure 4.6).

Images in Figure 4.6 second row show total tubulin staining in fasKD cells expressing WT or mutant fascin-GFP after NOC treatment and 60 minute washout. The zoomed

panel of the highlighted area is shown to more clearly demonstrate fascin co-localisation with the ends of MT after nocodazole washout. As described in Figure 3.9 in Results Chapter 1, WT fascin translocation to the cell periphery increased after NOC washout (first panel, second row in Figure 4.6), increasing its colocalisation with the ends of MT (zoomed area in the first panel). S39A and S39D fascin localisation post-NOC was less peripheral than WT fascin (second and third panel, respectively, second row in Figure 4.6) and these mutants did not show a clear colocalisation with MT (zoomed area in second and third panel). S274A fascin translocation to the cell periphery following NOC washout was more prominent than in S39 mutant rescued cells (fourth panel, second row in Figure 4.6) and showed some colocalisation with MT ends (zoomed area in fourth panel). However, fascin translocation induced by NOC washout effect in S274A rescue cells was not as notable as in WT fascin rescued cells. S274D fascin showed strong translocation to the cell periphery after NOC washout (fifth panel, second row in Figure 4.6) and clear colocalisation with the ends of MT (zoomed area in fifth panel). Indeed, S274D fascin was localised at the cell periphery after NOC washout as seen in WT fascin.

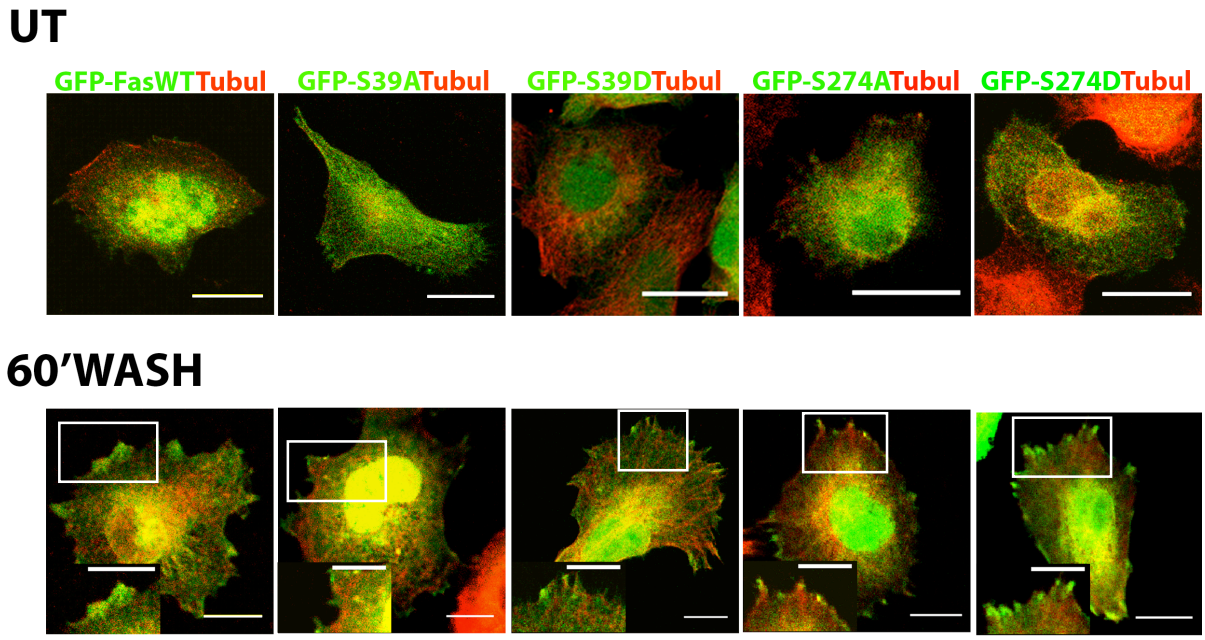

Figure 4.6. S274D fascin is localised to the cell periphery and colocalises with MT following nocodazole washout

Confocal microscope images of fascin WT and mutant-GFP in MDA-MB-231 fasKD cells re-expressing WT or mutant fascin-GFP stained for total tubulin. First line shows untreated cells (UT), whereas second line shows 60 minute-nocodazole washed cells (60'W). Scale bar= 10 um. Zoom of the highlighted area is shown to show fascin co-localisation with end of MTs at the cell periphery after nocodazole washout. Scale bar= 3 um.

4.7. S274D fascin colocalises with acetylated tubulin at the cell periphery

In Figure 3.4 in Result Chapter 1, data demonstrated that fascin knockdown cells showed higher acetylated tubulin levels compared to fascin expressing cells. This suggests a fascin-dependent regulation of MT stability. I therefore analysed acetylated tubulin staining in WT and mutant fascin rescue cells to determine whether MT stability correlates with the different roles of fascin mutants in regulating FA dynamics.

Figure 4.7 show example images of acetylated tubulin staining in MDA-MB-231 fascin knockdown (fasKD) cells rescued for WT and mutant fascin-GFP expression. First column in Figure 4.7 shows merge images of cells re-expressing WT and mutant fascin-GFP (green) stained for acetylated tubulin (red), respectively, whereas second column show acetylated tubulin staining alone.

Figure 4.7 shows acetylated tubulin staining in fasKD cells rescue for WT and mutant fascin-GFP. S39A fascin expressing cells (second row images in Figure 4.7) showed similar acetylated tubulin levels as in WT fascin expressing cells (first row images in Figure 4.7). Cells showed a clear MT organising centre (MTOC) with stable MT bundles. However, S39D fascin and S274A fascin expressing cells (third and fourth row respectively in Figure 4.7) showed lower acetylated tubulin levels compared to WT. Interestingly, S274D fascin expressing cells (fifth row Figure 4.7) showed similar acetylated tubulin staining to that seen in WT and S39A cells, with clear MTOC localisation and acetylated MT bundles. S274D fascin, but not S39A fascin showed partial colocalisation with acetylated MT bundles.

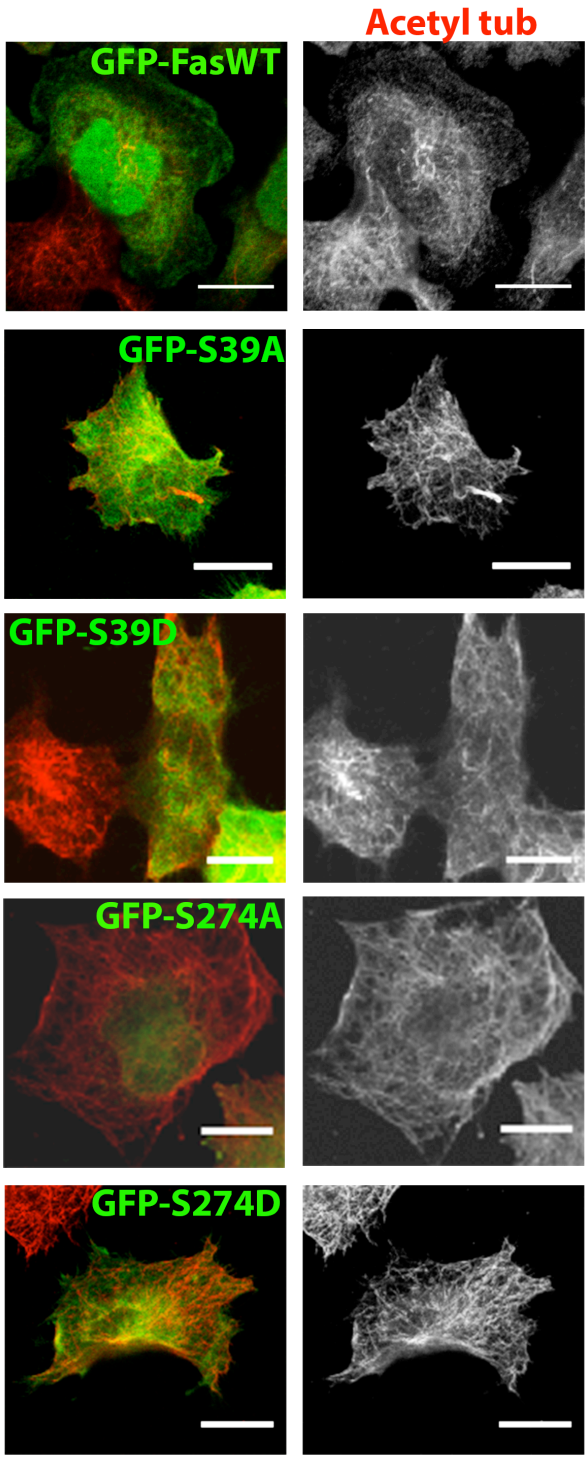

Figure 4.7. **S274D fascin colocalises with acetylated tubulin at the cell periphery**
Confocal microscope images of acetylated tubulin staining in MDA-MB-231 fasKD re-expressing WT and mutant fascin-GFP. First column shows cells re-expressing WT and mutant fascin-GFP stained for acetylated tubulin, whereas second column shows acetylated tubulin staining alone. Scale bar= 10 um.

DISCUSSION

Data presented in this chapter suggested a potential mechanism by which fascin co-operate with MT to regulate FA disassembly. The molecular mechanisms driving FA assembly have been well characterised and they are known to be dependent on integrin engagement and Rho family GTPases (Small et al. 2002). On the other hand, mechanisms regulating FA disassembly are still poorly understood. However, it has been reported that FA disassembly is not simply a passive response to losing FA maturation or stability signals (Ezratty et al. 2005). Rather data has demonstrated that FA disassembly is an active process involving crosstalk between MT, dynamin and Focal Adhesion Kinase (FAK). The suggested mechanism proposes FAK-dependent recruitment of dynamin at FA and this in turn promotes dynamin co-operation with MT in inducing FA disassembly (Ezratty et al. 2005). FAK accumulation at FA has been previously suggested to be involved in the release or delivery of 'relaxing factors' which may drive FA disassembly (Tomar & Schlaepfer 2009).

The regulation and function of the actin-binding site within the C terminus of fascin is not fully understood, although mutation of residues within this domain has been suggested to reveal functions for fascin that are independent of actin binding (Jansen et al., 2011; Zanet et al., 2012). Data shown here demonstrates that S274A fascin expressing cells assemble peripheral actin spikes with large FA situated at the base of these protrusions. The phenotype observed in these cells was specific to this mutant and offers a potential explanation for the larger FA size and the decreased cell area observed in these cells (Figures 4.1 and 4.3). Unexpectedly, S274A rescue cells showed normal adhesion to fibronectin without fascin localisation to punctate adhesion-like structures at the cell periphery. We have previously shown S274A fascin localises in the distal end of actin-rich filopodia, promoting their stability. This suggests this mutant may play a non-actin binding dependent role or associating with filopodial tip complex proteins via an yet unknown mechanism (Zanet et al.

2012). This might also go some way to explaining the changes to FA size and number seen in these cells.

S274D fascin expressing cells showed the same size and number of FA as S39A fascin cells. Surprisingly, despite not being able to efficiently bundle actin, 274D fascin was also found to localise at the cell periphery as seen for WT fascin, suggesting this localization may contribute to the decreased FA disassembly seen in cells expressing this mutant. In addition, S274D expressing cells showed lower adhesion and smaller cell area compared to S39A expressing cells. These observations suggest that the large FA in S274D fascin expressing cells may potentially support faster spreading through control of cell membrane contact area with the substrate. Moreover, It suggests that peripherally localized S274D fascin may have a role in regulating FA disassembly, in an actin-binding independent manner.

MT are known to regulate FA disassembly in the nocodazole washout assay employed here (Ezratty et al. 2005) and in Chapter 1, data showed that fascin plays a role in regulating MT re-growth and FA disassembly following NOC washout. In this chapter, the data additionally shows that S274D fascin prevents MT-dependent FA disassembly after NOC washout. However, S274D fascin expressing cells recovered their MT as efficiently as cells rescued with WT fascin. All the other three mutant cells were delayed in MT reassembly following drug washout. Furthermore, only S274D fascin localised at ends of MT at the cell periphery, suggesting S274D fascin may control MT stability or turnover at these sites to regulate FA disassembly. S274D fascin expression in cells also led to increased tubulin acetylation compared to WT. Figure 4.7 showed only S274D fascin to localise with acetylated tubulin at the cell periphery. The co-operation between S274D fascin and tips of MT at the cell periphery may, therefore, stabilise MT preventing them from inducing FA disassembly. Therefore the putative MT-associated S274D fascin does not promote

FA disassembly, but instead may act to decrease MT dynamic instability post-NOC washout and enhance MT re-growth.

S39A and S39D fascin expressing cells did not show any significant difference in FA disassembly after nocodazole washout, compared to fascin KD cells rescued with WT fascin, or control/parental cells. This suggests that the N-terminal, S39-dependent actin binding site of fascin is not directly involved in MT-dependent FA disassembly. However, interestingly the S39A cells had larger FA and increased adhesion vs. the opposite phenotype in S39D cells under basal conditions. MT-dependent FA turnover might not require the N-terminal actin-binding site as FA after NOC treatment and washout are particularly unstable and artificially forced to turnover in an MT-dependent manner. The delayed MT re-growth in cells expressing both S39 mutants cells confirms this site of fascin is not principally involved in driving consequent FA disassembly. Indeed, only the S274D mutant fascin fully restored MT re-growth, but this potential co-operation with MT is not sufficient to promote FA disassembly. Indeed, I observed that S274D fascin localisation at the cell periphery and its efficient MT recovery did not permit FA disassembly following NOC washout. This leads to a possible model whereby fascin has a dual role regulated by phosphorylation cycles at these two sites on fascin to efficiently regulate MT re-growth and FA disassembly. It is not yet known how, or if, mutation of S274 impacts on the phosphorylation status of S39, but this data would strongly suggest that S274 plays the key role in mediating MT dynamic instability and targeting to FA, but another mechanism is required to drive the subsequent FA disassembly.

Data shown in this chapter also shows that fascin-actin-binding is not directly involved in the mechanism by which fascin controls FA disassembly in the NOC assay, but both S39 mutant forms of fascin are able to drive FA assembly. It is possible therefore that S274 controls MT and the consequent S39 site dependent FA disassembly in this context. We have no data concerning the phosphorylation status

of Ser39 when Ser274 is phosphorylated (and potentially MT-associated), but considering basal differences in FA size/number in S39D and S274D fascin expressing cells, we speculate that S39 is likely to be de-phosphorylated (and therefore actin bound) when fascin drives MT re-assembly. Moreover, non-phosphorylated fascin, bound to actin at the cell periphery, could readily be switched by phosphorylation of S274. Preliminary data in the lab, along with *in silico* analysis of the S274 site and mass spec phospho-mapping strongly suggests that this site may be a substrate for protein kinase A (PKA). PKA is known to act primarily at the membrane and has been previously shown to be localized to new sites of actin protrusion in migrating cells (Bachmann et al. 2013). This phosphorylation switch might promote S274D fascin-MT co-operation and reduce actin binding which subsequently necessary for FA disassembly in S274D fascin expressing cells. Although all this has to be further investigated, locking S274 fascin in a constitutive phosphorylated state and S39 in a dephosphorylated state could potentially drive efficient MT re-growth and FA disassembly in NOC-induced cytoskeleton dynamics.

Phosphorylation cycles on the two serines of fascin studied in this thesis may therefore be critical in driving fascin-dependent MT and FA dynamics. Our model proposes the phosphorylation on the two sites to be regulated by two different signalling cascades. The potential involvement of both PKC and PKA in fascin phosphorylation may explain the dual role of fascin in driving MT assembly and FA disassembly. Although PKA phosphorylation of S274 requires further analysis, its reciprocal regulation with Rac signaling (Bachmann et al. 2013) and association with actin-MT cross-linkers (Lee et al. 2012) suggest a key role for this kinase in regulating the actin-MT crosstalk. Other examples of proteins target of different kinases exist among molecules involved in the actin-MT crosstalk (Rodriguez et al. 2003). It is therefore realistic to consider fascin as a novel switch molecule in the actin and MT interplay.

In conclusion, this chapter proposes fascin phosphorylation at two different serine residues acts to regulate MT stability and FA assembly/disassembly cycles under both basal conditions and those where FA dynamics are induced by NOC. The next chapter will focus on determining whether fascin can control this process through direct interaction with tubulin/MT and/or other known molecular players in the process, such as FAK.

5 The mechanism of fascin-dependent control of actin-MT crosstalk.

INTRODUCTION

The crosstalk between actin and MT is known to be central in a number of processes such as neuronal cone development (Zhou et al. 2002) and metastasis dissemination in cancer progression (Hall 2009). A handful of molecules have been demonstrated to directly interact with actin and MT in these processes (Efimov & Kaverina 2009); however, the way in which these pathways integrate is still poorly understood (Morrison 2007). This chapter will analyse a potential role for fascin as a linking molecule between actin and MT.

Data shown in Chapter 4 showed a role for S274D fascin in promoting MT stability. Moreover, a dual role for fascin in regulating FA assembly and MT-dependent FA disassembly was proposed based on the lack of FA disassembly in the S274D cells following NOC washout. This chapter will analyse whether fascin can associate directly with tubulin to try and explain this role in regulating MT stability.

It is well established that FAK mediates FA formation through tyrosine phosphorylation during cell adhesion (Hamadi et al. 2005) and FAK phosphorylation on Tyrosine 397 (p-FAK) is widely known to promote the formation of a FAK-Src complex and increase FA turnover (Tomar & Schlaepfer 2009). The way in which MT co-operate with FAK to promote the full assembly/disassembly cycle remains unclear. Moreover, the role of actin binding proteins in this phenomenon has not been explored previously.

Experiments in this chapter aim to analyse whether fascin can bind directly to MT as a mechanism driving MT stability. Moreover, experiments will aim to further test the hypothesis that fascin acts as a novel switch mechanism regulating F-actin and MT in the context of FAK-regulated FA dynamics.

5.1. *In vitro* analysis of F-actin bundling by fascin mutants

Fascin-actin binding and bundling activity is crucial in the formation of parallel actin bundles. Published data showed that WT and S39A fascin can efficiently bind and bundle actin, while S39D fascin can not bind or bundle actin (Anilkumar et al. 2003; Hashimoto et al. 2007). Moreover, it has been shown that S274A fascin is able to bundle actin without showing binding activity, while S274D fascin does not bind or bundle actin (Zanet et al. 2012). To confirm this data, fluorescence *in vitro* actin-binding assays were performed using purified His_6-tagged fascin mutant proteins. This assay was performed as in (Zanet et al. 2012) with an additional step; F-actin was stabilised with 488-phalloidin before incubation with purified fascin mutants in order to analyse bundle formation by confocal microscopy (see Material and Methods and also (Miller 2004).

Figure 5.1 shows example images of the formation of F-actin bundles in the presence of F-actin alone stabilized with 488-phalloidin (left panel, top row) or incubated with WT (centre panel, top row), S39A (right panel, top row), S39D (left panel, bottom row), S274A (centre panel, top row) and S274D (right panel, bottom row) fascin. As expected, F-actin did not bundle on its own (left panel, top row), but was efficiently bundled in the presence of WT fascin binding (centre panel, top row). Incubation of F-actin with S39A fascin showed a striking effect on actin bundling (right panel, top row), while S39D fascin incubation showed no visible bundled F-actin (right panel, bottom row). Interestingly, the incubation of F-actin with S274A fascin resulted in shorter F-actin filaments than in presence of WT fascin (centre panel, bottom row). S274A fascin is known to not bind to actin; therefore, this data supports previous evidence of S274A actin binding activity (Zanet et al, 2012). Furthermore, S274D fascin, which is also known to not bind to actin, did not show any F-actin bundle formation as seen for F-actin alone or S39D fascin (right panel, bottom row).

This data confirmed the role of S39 and S274 fascin in bundling actin and validates the use of this assay to study the potential role of fascin-actin binding *in vitro*.

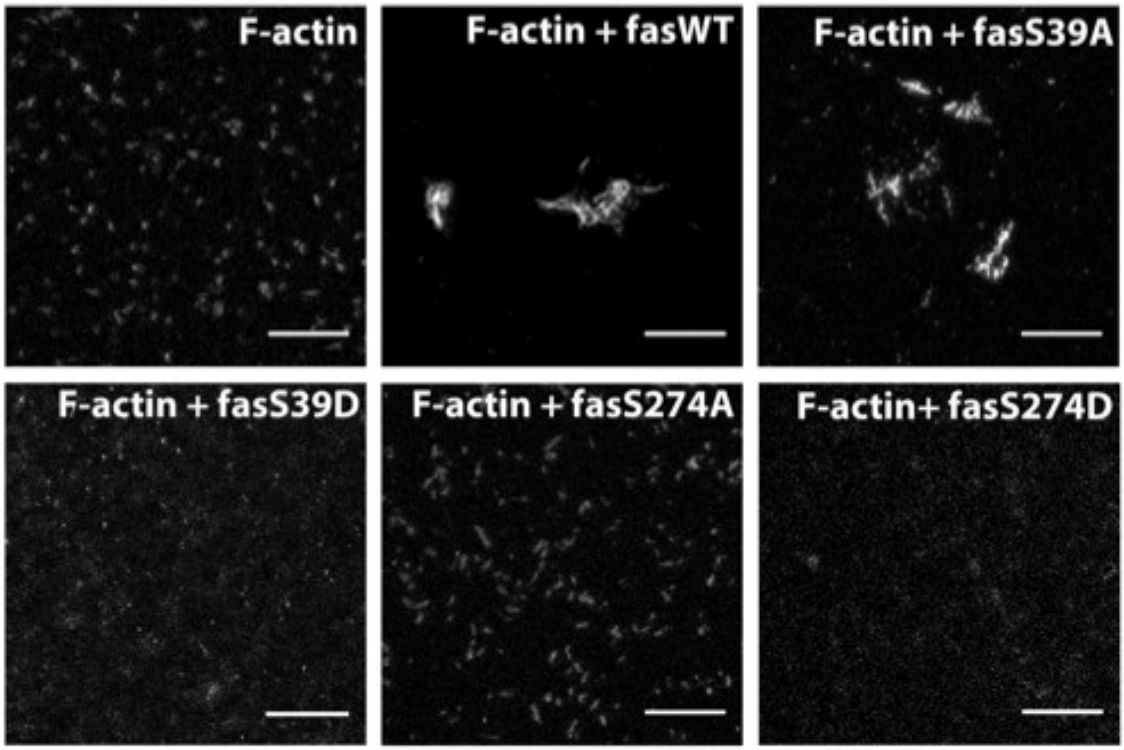

Figure 5.1. ***In vitro*** **analysis of F-actin bundling by fascin mutants**
Confocal microscope images of WT and mutant fascin co-incubated with F-actin. Actin was polymerised *in vitro* and stabilised with 488-phallodin (first panel) and then incubated with WT fascin (second panel), S39A fascin (third panel), S39D fascin (fourth panel), S274A fascin (fifth panel) or S274D fascin (sixth panel). Scale bar= 3 um.

5.2. Establishing and characterising *in vitro* microtubule binding assay

Chapter 2 showed a preferential role of S274D fascin in promoting MT stability and in MT-dependent FA disassembly. This raised an interesting possibility that fascin could directly bind to MT.

To test the direct binding of fascin to MT, an *in vitro* tubulin polymerisation assay was established and characterised in the lab (Figure 5.2). This assay was taken form (Béraud-Dufour et al. 2007) and steps were carefully explained in the Material and Methods Chapter. Briefly, bovine brain purified tubulin was polymerised at 37 °C in the presence of salts, GTP and glycerol, followed by stabilisation with increasing concentration of taxol (to stabilize the MT). At this step, the turbidity of the reaction was measured as index of the tubulin polymerisation. Figure 5.2a shows the turbidity measurement before polymerisation reaction (t0) and after stabilisation with taxol (tf) and is representative of at least three different polymerisation reactions. Figure 5.2a shows almost 100% tubulin polymerisation. Before using the *in vitro* polymerised tubulin in the co-sedimentation assay, the structure of the polymerised MT was analysed using electron microscopy. Figure 5.2b shows an example image of an *in vitro* polymerised MT. MT are polymerised with a reported outer diameter of 25 nm and lateral side of 6-7 protofilaments, formed by the αβ tubulin dimer polymerisation. MT are typically formed by 13-14 protofilaments, which gives the striated feature shown in Figure 5.2b. This data confirms that establishment of the MT polymerisation assay for experimental use.

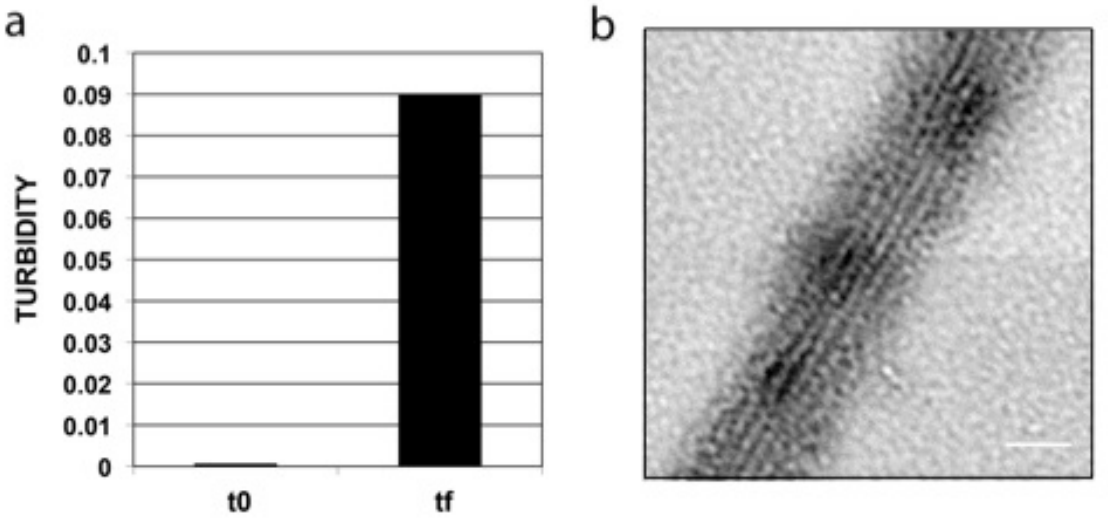

Figure 5.2. **Establishing and characterising *in vitro* microtubule binding assays**
(a) Turbidity measurement before (t0) and after (tf) bovine brain purified tubulin polymerisation and stabilisation with taxol. (b) Electron microscopy image of the microtubules polymerised *in vitro*. Scale bar= 12 nm.

5.3. Fascin associates with microtubules *in vitro*

Having characterised the tubulin polymerisation assay, the next aim was to investigate whether fascin directly binds to MT. To test this, a co-sedimentation assay was performed *in vitro* to incubate the polymerised MT with WT and mutant forms of purified fascin.

Polymerised MT corresponding to approximately 1 μmol of tubulin was incubated with WT or mutant fascin as described in Material and Methods. A 1:1 ratio was kept between MT and fascin throughout the experiments. The reaction mixture was centrifuged and the percentage of fascin co-sedimented with polymerised MT was determined by analysing samples by SDSPAGE, silver staining and densitometry analysis (Figure 5.3). Examples of silver-stained gels showing levels of fascin and/or MT in the respective fractions are shown in Figure 5.3a-d. Firstly, control experiments were performed with fascin alone to ensure the protein was not sedimented in the absence of MT. As shown in Figure 5.3a, none of the fascin proteins showed sedimentation on their own as no fascin was present in the pellet. The next step was to study ratio of MT alone and taxol-stabilised MT in the supernatant vs. pellet (s/p ratio). Figure 5.3b shows around 50% of the MT co-sedimented in the pellet fraction without taxol. Taxol addition resulted in a large increase in MT co-sedimentation, with almost 100% of the MT found in the pellet confirming *in vitro* MT stability to be dependent on taxol. Fascin and MT were then co-incubated and the experiment was repeated. Figure 5.3c shows a very small amount of WT fascin was co-sedimented with MT *in vitro* in the absence of taxol, suggesting WT fascin can directly bind to MT. Taxol was then added to the reaction mixture to promote maximal MT polymerisation. Figure 5.3d shows levels of WT, S39A, S39D, S274A and S274D fascin in the supernatant and pellet fractions in the presence of MT and taxol. WT fascin pellet increased by adding taxol (Figures 5.3c,d), suggesting the levels of fascin in the pellet was also dependent on MT stability.

Surprisingly, all fascin mutant proteins were found to varying degrees within the pellets containing taxol-stabilised MT.

Figure 5.3e shows statistical analysis of the percentage of the fascin in pellet with MTs performed by densitometry analysis of >4 silver-stained gels. Statistical analysis confirmed WT and mutant fascin co-sediment with MT but with differing efficiencies. WT fascin, S39A, S39D and S274A fascin all showed ~10% of the protein associating with MT. Interestingly, however, S274D fascin showed 25% of pelleted protein with MT - almost 3-times higher than WT and the other three mutants (P-value of S274D fascin co-sedimented with MT compared to WT: p-value =< 0.05). Taken together, this data shows that fascin associates with MT *in vitro* with a preferential association of S274D fascin in this complex.

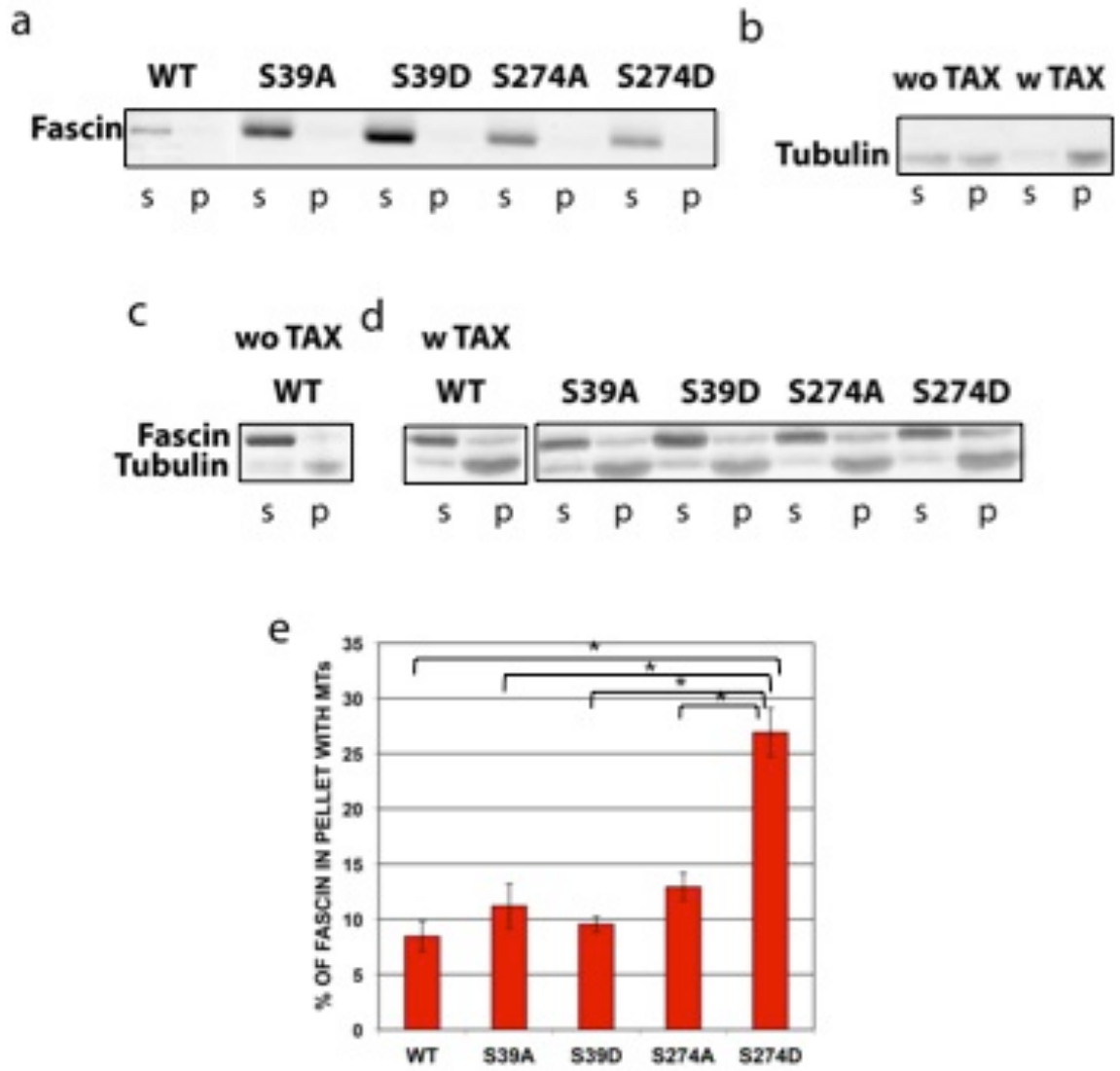

Figure 5.3. Fascin associates with microtubules *in vitro*

(a) Silver-stained gel of supernatant-pellet partitioning for WT and mutant fascin incubated on their own. Supernatant (s) and pellet (p) show the soluble and the insoluble fraction of the protein, respectively. (b) Silver-stained gel of supernatant-pellet partitioning for microtubules (MTs) on their own, with and without taxol (TAX). MTs were polymerised *in vitro* from bovine brain purified tubulin and stabilised with taxol. (c) Silver-stained gel of supernatant-pellet partitioning for WT fascin incubated with MTs in absence of taxol. (d) Silver-stained gel of supernatant-pellet partitioning for WT and mutant fascin incubated with MTs in presence of taxol. (e) Statistical analysis of the percentage of fascin in pellet with MTs was performed by densitometry analysis of at least three silver-stained gels. P-value =< 0.05 (*) was considered as significant. Data are expressed as mean± sem and corrected with fascin alone supernatant-pellet ratio.

5.4. Fascin S274D preferentially associates with microtubules *in vitro*

Data in Figure 5.3 showed WT and mutant fascin can associate with MT *in vitro*. The next step was to determine whether WT and mutant fascin binding to MT could occur in the presence of co-incubated actin. The assay was therefore repeated in the presence of F-actin to test relative sedimentation efficiencies of all fascin proteins under these conditions.

F-actin was polymerised *in vitro* as described in Material and Methods and in (J. Zanet et al. 2012) the MT-fascin co-sedimentation assay was repeated as previously described for Figure 5.3. F-actin was then added to the reaction following MT polymerisation. The reaction mixture was centrifuged and the percentage of fascin co-sedimented with MT and F-actin was determined by SDS-PAGE gels, silver staining and densitometry analysis (Figure 5.4). Example silver-stained gel analysis showed in Figure 5.4 shows supernatant/pellet (s/p) ratio in control gels (a) and experimental gels (b). Figure 5.4a shows a control gel of F-actin incubated with MT alone, with and without taxol. F-actin s/p ratio did not change in the presence of MT or taxol-stabilised MT. This suggests no interaction occurs between actin and MT alone in vitro. Figure 5.4b shows a silver-stained gel of s/p ratio of WT, S39A, S39D, S274A and S274D fascin incubated and co-sedimented together with MT and F-actin. F-actin was added to the reaction following fascin incubation with MT. F-actin addition lead to changes in the levels of fascin in the pellet in all cases. The presence of both MT and F-actin led to higher levels of fascin in the pellet in all cases except the reaction containing the S274D mutant compared to MT alone (Figure 5.3d). Addition of F-actin did not have any effect on S274D fascin co-sedimentation with MT.

Figure 5.4c shows densitometry analysis of the percentage of fascin co-sedimented with MTs (red bars) and with MT and F-actin (green bars) from >4 silver stained gels over independent experiments. Statistical analysis shown in Figure 5.4c confirmed a

2-fold increase of the percentage of WT, S39A, S39D and S274A fascin co-sedimented together with MT and F-actin (green bars) compared to that seen with MT alone (red bars). This data also confirmed that the addition of F-actin did not result in changes to the amount of S274D fascin co-sedimented with MT. This data demonstrates that the S274D mutant shows significantly higher association with MT compared to other fascin proteins also in presence of F-actin.

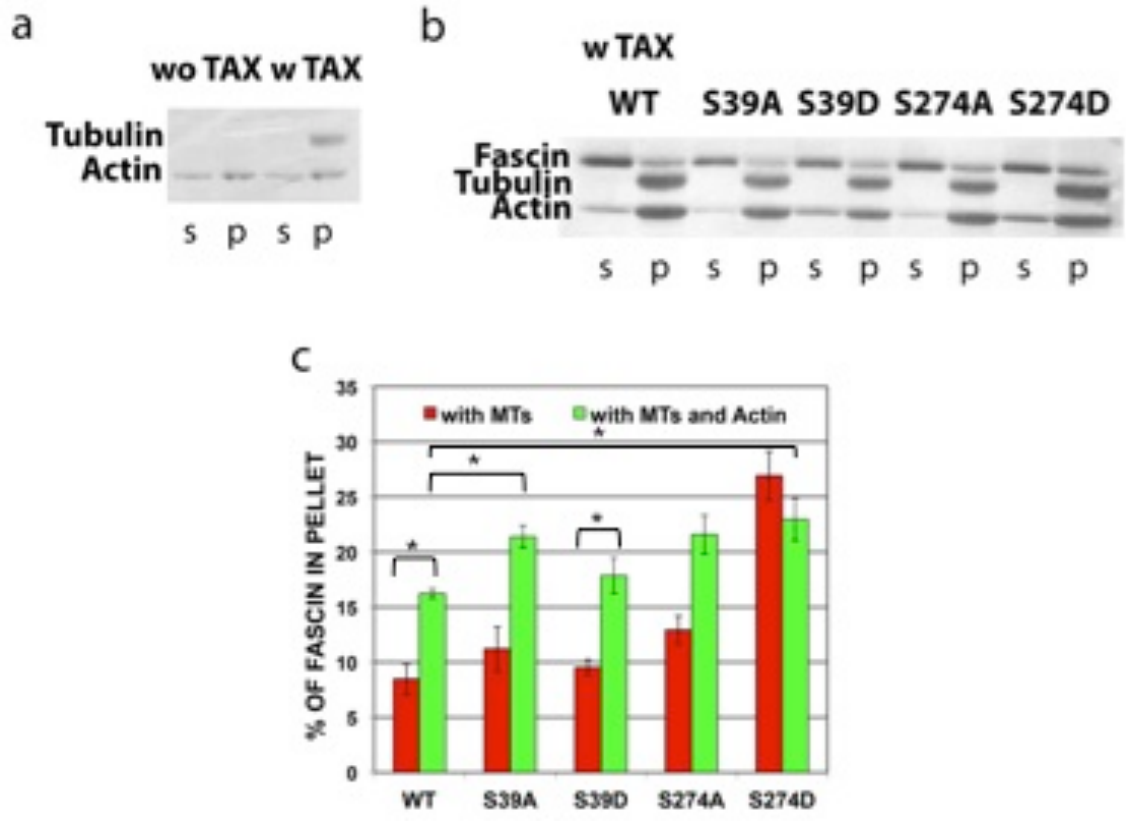

Figure 5.4. Fascin S274D preferentially associates with microtubules *in vitro*
(a) Silver-stained gel of supernatant-pellet partitioning for F-actin, incubated on its own with and without taxol (TAX). (b) Silver-stained gel of supernatant-pellet partitioning for WT and mutant fascin incubated with MTs and F-actin in presence of taxol. (e) Statistical analysis of the percentage of fascin in pellet with MTs and F-actin compared to the percentage of fascin in pellet with MTs (Figure 5.20) was performed by densitometry analysis of at least three silver-stained gels. P-value =< 0.05 (*) was considered as significant. Data are expressed as mean± sem and corrected on fascin alone supernatant-pellet ratio.

5.5. S274D fascin preferentially associates with MT in a fluorescence assay for analysis of F-actin and MT

After identifying a preferential association of S274D fascin with MT by biochemical analysis, the next step was to use microscopy analysis to study formation of tubulin and/or actin bundles in presence of WT and mutant fascin. Therefore, a fluorescent tubulin and F-actin polymerisation assay was performed in vitro as shown in 5.1 and 5.2. Rhodamine labeled tubulin from porcine brain was used in place of unlabeled tubulin, and 488-phallodin was used to stabilized F-actin and enable bundle formation to be observed by confocal microscopy. The combined binding assay was performed as described in 5.4 and in (Miller 2004). Polymerised rhodamine tubulin was first incubated with WT or mutant fascin followed by incubation with 488-F-actin.

Figure 5.5 shows example confocal images of MT and/or actin bundle formation in presence of tubulin alone (first panel, top row), tubulin and F-actin (second panel, top row), tubulin, F-actin and WT fascin (third panel, top row), and then tubulin, F-actin and S39A fascin (first panel, bottom row), S39D fascin (second panel, bottom row), S274A fascin (third panel, bottom row) or S274D fascin (fourth panel, bottom row). Tubulin alone did not show MT bundle formation *in vitro* at this magnification (first panel, top row). Addition of F-actin alone did not show any visible effect on MT bundling *in vitro* (second panel, top row). WT fascin incubation resulted in increased F-actin bundle formation and polymerised MT and interestingly, these bundles of actin and MT co-localised (third panel, top row). As shown in Chapter 3, fascin is not involved in basal tubulin polymerisation in cells but instead appears to regulate MT stability. Therefore, the observed co-localisation suggests that WT fascin may play a role in crosslinking bundled F-actin and stabilised MT. MT stability and co-localisation

with F-actin increased dramatically when S39A fascin was added (first panel, bottom row) and this was not seen in the presence of S39D fascin (second panel, bottom row). This data supports a potential feedback control of S39A fascin-actin binding on MT stability. Interestingly, S274A fascin incubation together with MT and F-actin showed no effect on tubulin polymerisation and/or stability, but confirmed its F-actin binding activity, as observed in Figure 5.1 and published previously in (J. Zanet et al. 2012). Conversely, S274D fascin incubation together with MT and F-actin showed increased MT bundling, without any effect on F-actin bundling. This data confirms the biochemical analysis of fascin, MT and F-actin co-sedimentation and further suggests that fascin can potentially crosslink MT and F-actin to form higher ordered cytoskeleton bundles.

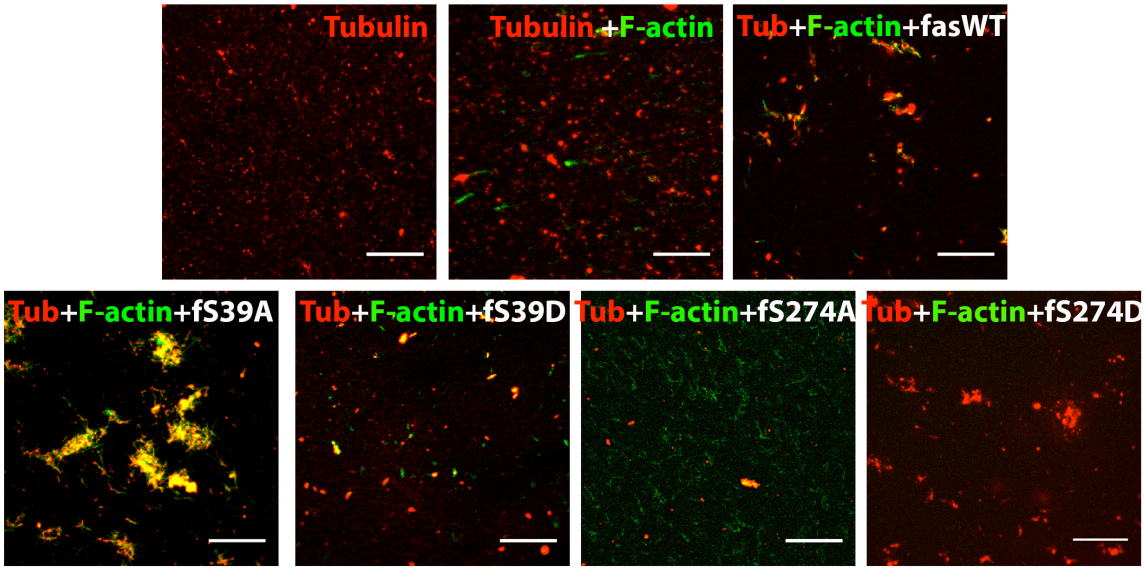

Figure 5.5. S274D fascin preferentially associates with MT in fluorescent binding assay

Confocal microscope images of WT and mutant fascin co-incubation with microtubules and F-actin. Rhodamine-labelled bovine brain purified tubulin was polymerised *in vitro* and stabilised with taxol (first panel) and then incubated with F-actin, previously stabilised with 488-labelled phalloidin (second panel). WT fascin (third panel), S39A fascin (fourth panel), S39D fascin (fifth panel), S274A fascin (sixth panel) or S274D fascin (seventh panel) was added together with tubulin and F-actin.

5.6. Fascin knockdown disrupts the balance of actin-MT crosstalk

In vitro data and results discussed in Chapter 4 and Figure 5.5 propose fascin as a possible molecular bridge between actin and MT cytoskeletons. To further analyse this hypothesis in intact cells, F-actin formation during nocodazole treatment and after 60 minute nocodazole washout was studied by confocal microscopy in control and fasKD cells. I also analysed F-actin formation in response to the MT-stabilising drug taxol in fasKD cells and in fasKD cells re-expressing GFP-WT fascin.

Figure 5.6 a,b show example images of control and fascin knockdown MDA-MB-231 (fasKD) cells stained for total tubulin and phalloidin (to visualise F-actin) during nocodazole assays. Top rows in Figure 5.6 a,b show untreated cells (UT), centre rows show nocodazole treated cells (NOC) and bottom rows show cells 60 minutes after nocodazole was washed out (60'NOC wash). The first column shows merged staining of total tubulin and F-actin staining, while the second and third columns show total tubulin and F-actin alone, respectively. Control cells showed normal MT network and F-actin fibre formation (top row in Figure 5.6a). MT depolymerisation induced by nocodazole treatment is known to increase F-actin fibre stability (Rooney et al. 2010). Consistently, NOC treated MDA-MB-231 control cells became rounded and increased stress fibres (centre row in Figure 5.6a). After 60 minute NOC washout, control cells spread again showing re-polymerised MT and decreased stress fibre formation compared to treated cells (bottom row in Figure 5.6a). Figure 5.6b shows the same experiment performed in MDA-MB-231 fasKD cells. As previously shown, fascin depletion did not affect total tubulin polymerisation, but did alter F-actin structural organisation. Indeed, fasKD cells showed loss of filopodial organisation and stress fibre formation (third panel, top row in Figure 5.6b). Fascin depleted cells rounded up after NOC treatment, but these cells showed fewer F-actin bundles

compared to control cells in the same condition (centre row in Figure 5.6b). Moreover, fasKD cells after 60 minute NOC washout did not show MT recovery, but a dramatic increase in cortical F-actin fibre formation was induced (third panel, bottom row in Figure 5.6b). Data shown in Figure 5.6 a,b suggests a role for fascin in regulating F-actin fibre formation in response to changes in MT integrity.

Finally, to investigate further the role of fascin in linking the actin and MT cytoskeletons, I studied F-actin formation in response to the MT-stabilising drug taxol. Figure 5.6c shows example images of MDA-MB-231 fasKD cells and fasKD cells re-expressing GFP-WT fascin stained for total tubulin and F-actin. The top row shows untreated cells (UT) and the bottom row shows taxol treated cells (TAX). The first column shows a merged image of total tubulin and F-actin staining, whereas the second and third columns show total tubulin and F-actin staining, respectively. FasKD cells (expressing low GFP levels) and fasKD resGFP-WT fascin (green cells) are shown in the same image to compare protein staining in the presence and absence of fascin. Data shown in Chapter 3 demonstrated that resWT cells behave as control cells. Data shown in Figure 5.6c confirmed that fascin depletion did not result in an obvious change in total tubulin organization (second panel, top row), but did affect F-actin structure organisation (third panel, top row). Moreover, taxol treatment resulted in a clear increase in stable bundled MT and also increased F-actin in GFP-WT fascin expressing cells (green cell in bottom row) but no increase was observed in fasKD cells (GFP-negative cell in bottom row).

Taken together, this data suggests that fascin plays a role in regulating F-actin-MT cytoskeleton responses to different types of MT-targeting drugs.

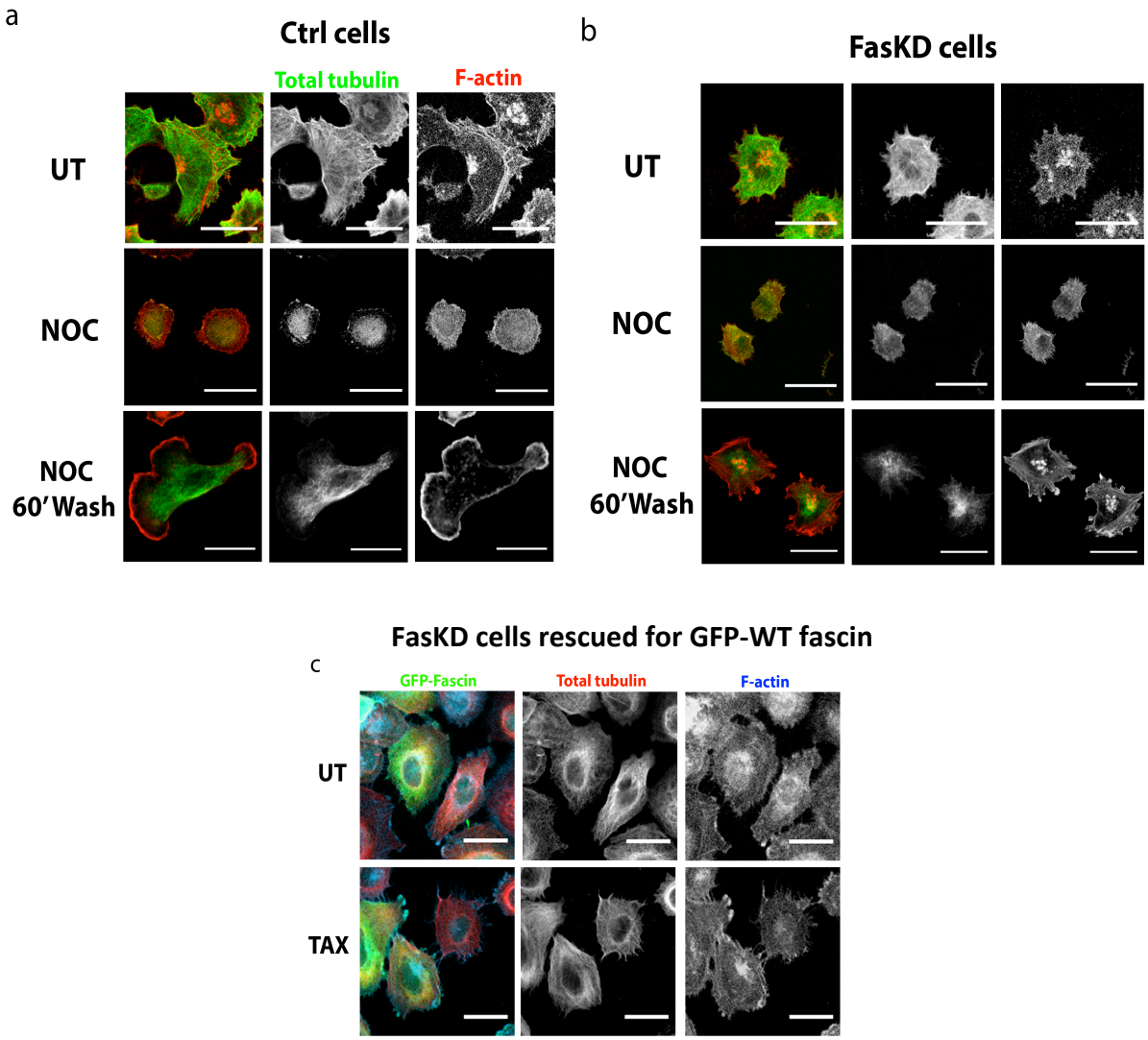

Figure 5.6. Fascin knockdown disrupts the balance of actin-MT crosstalk

(a) Confocal microscope images of MDA-MB-231 control cells stained for total tubulin and phallodin (to stain F-actin) during nocodazole treatment and after 60 minute washout. (b) Confocal microscope images of MDA-MB-231 fasKD cells stained for total tubulin and phallodin (F-actin) during nocodazole treatment and after 60 minute washout. First rows in a, b show untreated cells (UT), second rows show nocodazole treated cells (NOC) and third rows show 60 minute washed cells (NOC 60'Wash). First column in a, b shows control cells stained for total tubulin and phallodin (F-actin) together, whereas second and third rows show total tubulin or phallodin, respectively. (c) Confocal microscope images of tubulin and F-actin in fascin knockdown MDA-MB-231 cells re-expressing WT fascin-GFP. First row shows untreated cells (UT) and second row shows taxol treated cells (Tax). First column shows fasKD cells together with fasKD cells re-expressing WT fascin-GFP stained with total tubulin and phalloidin (used to stain F-actin), second column shows tubulin staining alone and the third column shows phalloidin staining alone. Scale bar= 10 um.

5.7. Fascin is required for cytoskeletal network remodeling

Data shown in Figure 5.6 showed fascin regulates F-actin changes in response to MT-targeting drugs. The next step was to investigate whether fascin also regulated the converse: ie: MT cytoskeleton changes in response to perturbation of the F-actin network. Therefore, control and fascin depleted cells were treated with the F-actin depolymerising drug cytochalasin D followed by fixation and staining for F-actin and MT by confocal microscopy. Cells were also analysed following drug washout to confirm specificity and reversibility of the response.

Figure 5.7 shows example images of MDA-MB-231 control (a) and fascin knockdown (b) cells stained for phalloidin (to visualize F-actin) and total tubulin. The top rows in 5.7a,b show untreated cells (UT), centre rows show cytochalasin D treated cells (cytoc D) and bottom rows show cytochalasin D 60 minute washout (cytoc D 60'wash). The first columns in 5.7a, b show merged staining of F-actin and total tubulin, while second and third columns show F-actin and total tubulin alone, respectively. Figure 5.7a top row shows normal F-actin assembly and polymerised MT in control cells. Cytochalasin D treatment completely depolymerised F-actin (second panel, centre row in Figure 5.7a) but cortical actin ruffles remained in these cells, and a striking increase in MT bundle formation was seen in the same cells (third panel, centre row, Figure 5.7a). Conversely, 60 minutes after cytochalasin D was washed out, F-actin appeared normal as in untreated cells (second panel, in Figure 5.7a) and subsequently MT network assembly was restored to normal organization as seen in UT cells (bottom row in Figure 5.7a). This data shows the balance between actin and MT cytoskeletons is tightly controlled in these cells. Figure 5.7b shows the same experiment performed in fasKD cells. Top row in Figure 5.7b confirms that fascin depleted cells to have increased stress fibres compared with control cells, but no differences in basal MT network assembly. FasKD cells showed a dramatic response to cytochalasin D, becoming rounded with strong

depolymerisation of both actin and MT (centre row in Figure 5.7). This is in contrast to control cells that showed a clear increase in MT bundles under the same conditions (middle panels, Figure 5.7a). Additionally, fasKD cells showed no recovery in F-actin structure and/or MT cytoskeleton following cytochalasin D washout, as observed in control cells. Indeed, fasKD cells showed complete disruption of both F-actin and MT networks after drug washout. This data supports a role for fascin in the control of cell responses to changes in cytoskeletal network assembly.

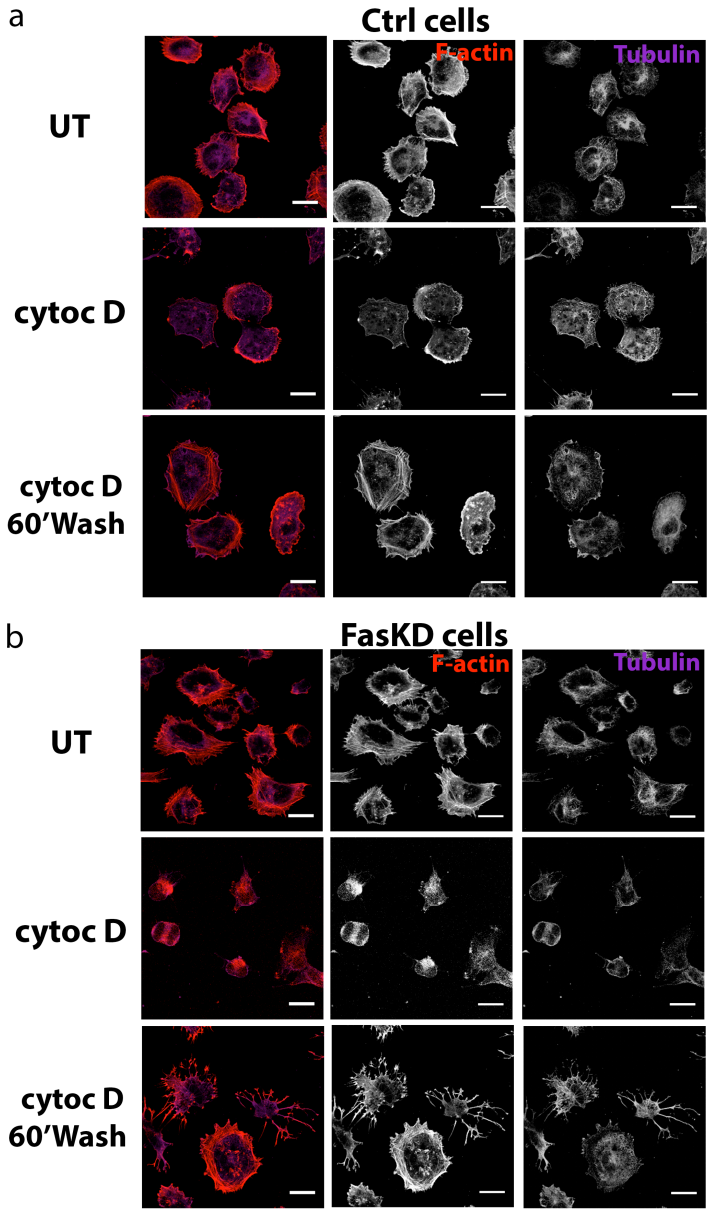

Figure 5.7. Fascin is required for cytoskeletal network remodelling (a) Confocal microscope images of MDA-MB-231 control cells stained for phallodin (to stain F-actin) and total tubulin during cytochalasin D treatment and 60 minutes washout. (b) Confocal microscope images of MDA-MB-231 fasKD cells stained for phallodin (F-actin) and total tubulin during cytochalasin D treatment and 60 minutes washout. First rows in both (a) and (b) show untreated cells (UT), second rows in both (a) and (b) show cytochalasin D treated cells (cytochD) and third rows in both (a) and (b) show 60 minute washed cells (cytochD 60'Wash). First column in both (a) and (b) shows control cells stained for phallodin (F-actin) and total tubulin together, whereas second and third rows show phallodin or total tubulin, respectively. Scale bar= 20 um.

5.8. Fascin knockdown cells show reduced levels of Focal adhesion kinase phosphorylation (p-FAK)

Data shown in Chapter 3 showed that fascin depletion did not alter total levels of Focal Adhesion Kinase (FAK) or vinculin protein but did lead to changes in FA size under basal conditions. Therefore the way in which fascin regulates FA assembly/disassembly remains unclear. Auto-phosphorylation of FAK on Tyrosine 397 is required for efficient FA dynamics (Hamadi et al. 2005) and active FAK has also been shown to be required for dynamin-dependent FA disassembly following NOC washout (Ezratty et al. 2005). FAK therefore presented an interesting potential protein as a molecular effector of fascin in regulating FA assembly/disassembly.

To test this, FAK phosphorylation on Tyrosine 397 (p-FAK) was analysed in cells expressing fascin and or silenced for fascin (fasKD) by confocal microscopy and western blotting (Figure 5.8). Figure 5.8a shows example images of p-FAK staining in MDA-MB-231 control (left panel), fascin knockdown (centre panel) and fasKD cells re-expressing WT fascin-GFP (right panel). Control cells showed clear peripheral p-FAK localisation in FA (left panel). Interestingly, fasKD cells showed smaller p-FAK-positive FA compared with the control cells, despite the fact that previous analysis has demonstrated larger FA assembly in these cells based on P-tyr staining (Figure 3.9). Similar localization of p-FAK was seen in fasKD re-expressing WT fascin as seen in control cells. This suggests that fascin depletion reduces levels of p-FAK at FA.

To further determine whether p-FAK levels were altered in the absence of fascin, FAK 397-phosphorlyation levels were analysed by western blotting. Figure 5.8b shows example western blots of total and p-FAK in control (ctrl) and fascin knockdown (fasKD) MDA-MB-231 or HeLa cell lysates. Endogenous fascin levels were also assessed in the same samples. GAPDH was used as a loading control. Total and p-FAK levels were quantified by densitometry analysis of multiple western blots

(Figure 5.8c) together with endogenous fascin levels. Data confirmed that fascin depletion resulted in a dramatic decrease of p-FAK without any change in total FAK levels (Figure 5.8b, c). To confirm that decreased p-FAK levels were specifically dependent on fascin depletion, western blotting and densitometry analysis was performed in MDA-MB-231 control (ctrl), fascin knockdown (fasKD) and fasKD rescued for WT fascin expression (resWT). Figure 5.8d shows total and p-FAK levels in a representative western blot. Endogenous and rescue WT fascin levels were also assessed in the same samples. Total FAK was used as a loading control. P-FAK levels were quantified by densitometry analysis of multiple western blots (Figure 5.8e), together with endogenous and rescue WT fascin levels in control, fasKD and resWT cells. Data confirmed that fascin depletion results in reduced p-FAK levels, and this was efficiently restored in cells re-expressing WT fascin (Figure 5.8d). The difference in FAK phosphorylation between control and fasKD cells in figure 5.8c and e may be due to the normalization done on total levels of different proteins (GAPDH in c and total FAK in e).

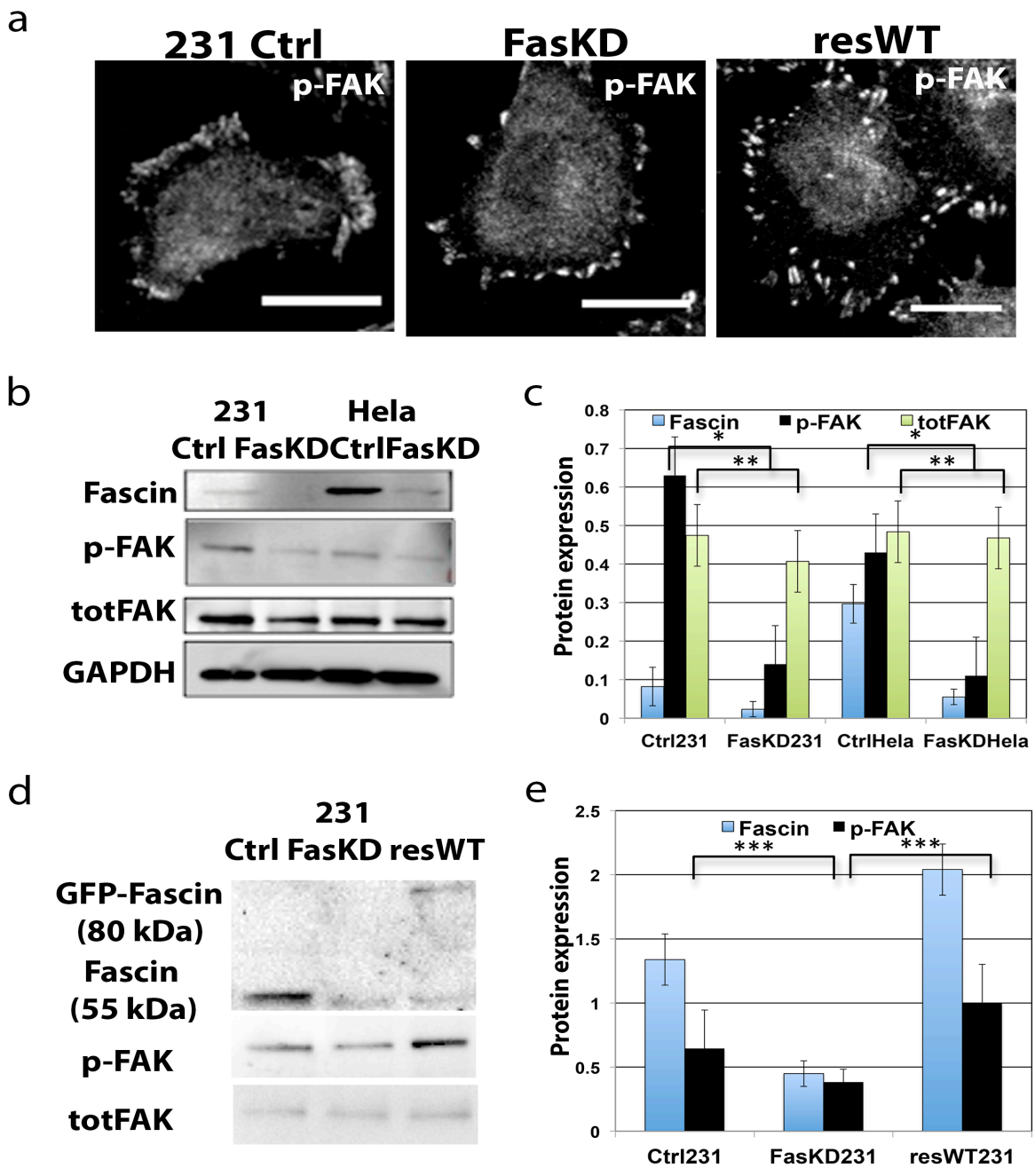
a
231 Ctrl
FasKD
resWT
p-FAK
p-FAK
p-FAK
b
231
Hela
Ctrl FasKD CtrlFasKD
Fascin
p-FAK
totFAK
GAPDH
c
Fascin
p-FAK
totFAK
Protein expression
0.8
0.7
0.6
0.5
0.4
0.3
0.2
0.1
0
*
**
*
**
Ctrl231
FasKD231
CtrlHela
FasKDHela
d
231
Ctrl FasKD resWT
GFP-Fascin
(80 kDa)
Fascin
(55 kDa)
p-FAK
totFAK
e
Fascin
p-FAK
Protein expression
2.5
2
1.5
1
0.5
0
***
***
Ctrl231
FasKD231
resWT231

Figure 5.8. Fascin knockdown cells show reduced levels of Focal adhesion kinase phosphorylation (p-FAK)

(a) Confocal microscope images of cells stained for phospho-FAK (p-FAK) in MDA-MB-231 control cells, fascin knockdown cells and fascin knockdown cells re-expressing WT fascin-GFP. Scale bar= 10 um. (b) Western blots of lysates from MDA-MB-231 and Hela control and fasKD cells. (c) Statistical analysis of fascin, total and p-FAK levels was performed by densitometry analysis of at least three western blots. P-value =< 0.005 (**) and =< 0.05 (*) was considered as significant. Data are expressed as mean± sem and corrected on GAPDH loading as control. (d) Western blots of lysates from MDA-MB-231 control, fasKD cells and fasKD cells re-expressing WT fascin-GFP. (e) Statistical analysis of fascin and p-FAK levels was performed by densitometry analysis of at least three western blots. P-value =< 0.001 (***) was considered as significant. Data are expressed as mean± sem and corrected on total FAK loading as control.

5.9. Fascin knockdown leads to lower p-397 FAK levels following nocodazole washout

Data presented in Figure 5.8 showed fascin dependent regulation of phospho-FAK under basal growing conditions. Given that previous data in this Chapter and Chapter 4 showed a role for fascin in driving MT-dependent FA disassembly following NOC washout, the next step was to investigate whether FAK phosphorylation was also differentially regulated by fascin under these conditions.

To test this, nocodazole treatment and washout assays were performed in MDA-MB-231 fascin knockdown (fasKD) cells and in fasKD cells rescued for GFP-WT fascin expression (resWT) and stained for p-FAK. Figure 5.9a shows example images of p-FAK staining before (UT, top row) and after NOC treatment and washout (60'W, bottom row). FasKD cells (expressing low levels of GFP) and fasKD resGFP-WT fascin (green cells) are shown in the same image to compare pFAK staining between conditions. The first and third columns show fascin, total tubulin and p-FAK staining alone, respectively. Additionally, the first panel in each row shows highlighted peripheral area of the cell to demonstrate co-localisation of proteins at FA. Images confirmed WT fascin peripheral co-localisation with MT ends, as also previously observed in Chapter 3. Moreover, partial co-localisation was seen between WT fascin with p-FAK in mature FA in cells rescued with GFP-WT fascin expression (left panel, top row). As also shown previously in Figure 5.8, fasKD cells showed reduced p-FAK localisation at the cell periphery than resWT cells. As expected no difference in MT polymerisation was observed between fasKD cells and fasKD/resWT fascin cells (centre panel, top row). The bottom row in Figure 5.9 shows WT fascin re-localisation at the cell periphery after NOC washout (left panel), re-assembling MT (centre panel) and p-FAK co-localisation with WT fascin at the ends of MT (right panel). On the other hand, the fasKD cell in the same image showed a lack in MT recovery and p-FAK localisation at the cell periphery.

To further analyse p-FAK involvement in fascin-dependent NOC washout responses, FAK p397-phosphorlyation levels were analysed during the NOC assay by western blotting. Figure 5.9b shows total and p-FAK in control (ctrl) and fascin knockdown (fasKD) MDA-MB-231 untreated, NOC treated and after 30 and 60 minute drug washout. Total FAK was used as a loading control. P-FAK levels were quantified by densitometry analysis of multiple western blots (Figure 5.9c) in control and fasKD cells. Figure 5.9b,c shows that pFAK levels in control cells increased following NOC washout as has been previously suggested (Ezratty et al, 2005). Conversely, fasKD cells did not show increased FAK phosphorylation after 60 minute NOC washout compared to control cells. This data suggests that fascin may co-operate with MT and FAK to promote efficient FA disassembly following NOC washout.

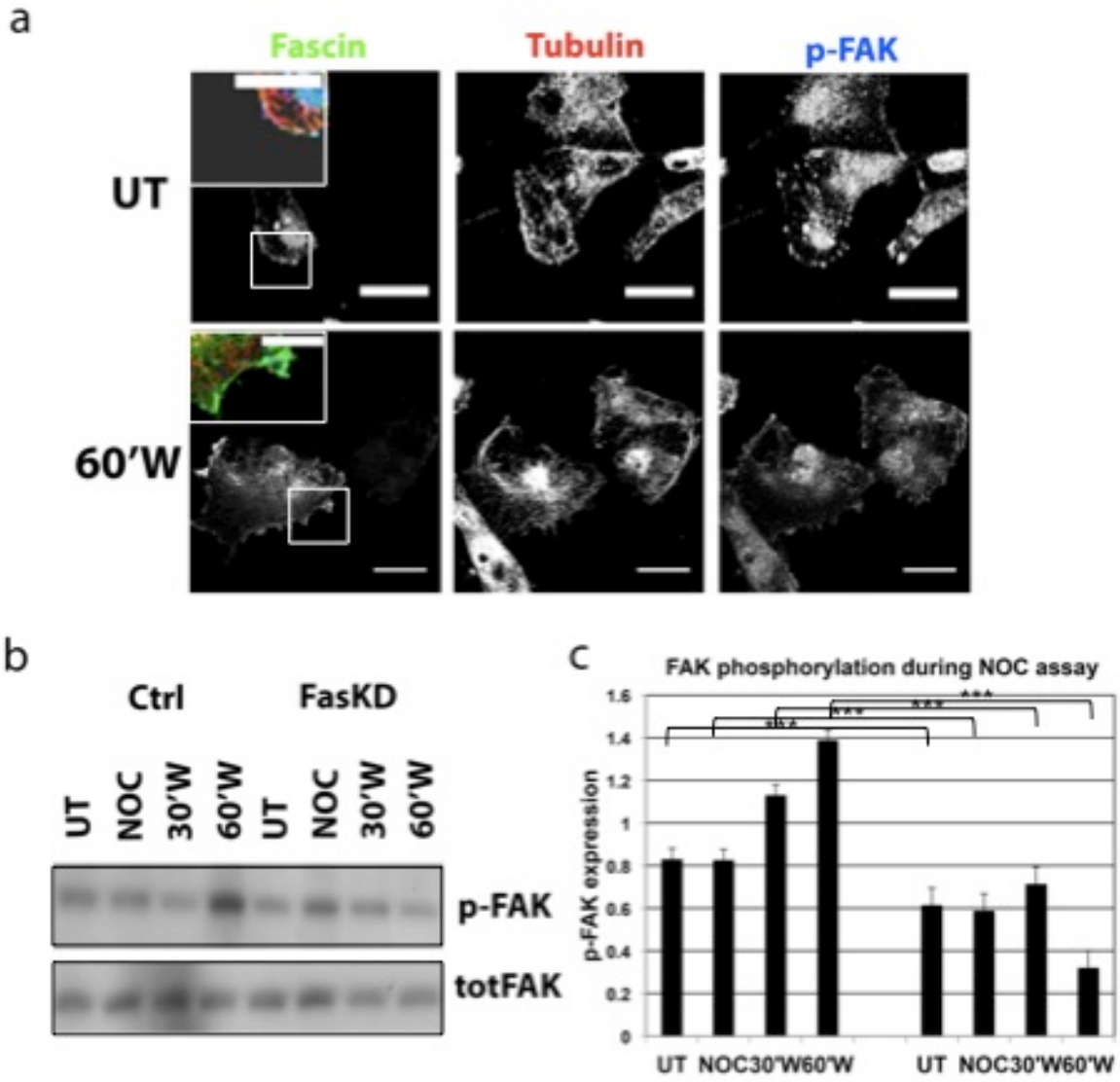
a
Fascin
Tubulin
p-FAK
UT
60'W
b
Ctrl
FasKD
UT
NOC
30'W
60'W
UT
NOC
30'W
60'W
p-FAK
totFAK
c
FAK phosphorylation during NOC assay
p-FAK expression
1.6
1.4
1.2
1
0.8
0.6
0.4
0.2
0
***
***
***
***
UT NOC30'W60'W UT NOC30'W60'W

Figure 5.9. Fascin knockdown leads to lower p-397 FAK levels following nocodazole washout

(a) Confocal microscope images of MDA-MB-231 cells expressing WT fascin-GFP stained for total tubulin and f-FAK before (UT) and after (60'W) nocodazole treatment and washout. Top row shows untreated cells (UT) and bottom row shows 60' minute washed cells (60'W). First column shows WT fascin-GFP, second column shows total tubulin staining and third column shows p-FAK staining. Scale bar= 20 um. Merged zoom of the highlighted area is shown to show fascin co-localisation with f-FAK. Scale bar= 3 um. (b) Western blots of lysates from MDA-MB-231 control and fasKD cells during nocodazole treatment and washout assay. (c) Statistical analysis of p-FAK levels was performed by densitometry analysis of at least three western blots. P-value =< 0.001 (***) was considered as significant. Data are expressed as mean± sem and corrected on total FAK loading as control.

5.10. S274D fascin shows increased colocalisation with p-397 FAK at the cell periphery

After observing changes in p-397 FAK levels and localisation in cells expressing WT fascin and in fascin depleted cells, the next step was to investigate whether expression of fascin mutants had any effect on p-FAK and whether this may correlate with the FA assembly/disassembly defects seen in these cells (Chapter 4).

To study this, fascin knockdown MDA-MB-231 cells (fasKD) were transfected wth GFP tagged sh-resistant fascin constructs. Cells re-expressing GFP-WT, S39A, S39D, S274A and S274D fascin were stained for p-FAK and levels and localisation with GFP-WT and mutant fascin were analysed by confocal microscopy (Figure 5.10a). Each panel in Figure 5.10a shows the highlighted peripheral area of the cell used to study co-localisation of fascin with p-FAK at FA. Western blotting was also performed on lysates from these cells to quantify basal p-FAK levels by densitometry analysis (Figure 5.10b,c). Figure 5.10a shows example images of GFP-WT and mutant expressing cells stained for p-397 FAK. As previously observed in Figure 5.9a, WT fascin localised at the cell periphery, co-localising with p-FAK in distinct FA (first panel in Figure 5.10a). The first panel top row shows larger FA containing high levels of p-FAK in cells expressing S39A fascin. However, S39A fascin was not found to clearly co-localise with p-FAK at the periphery. The second panel top row shows small immature FA with lower FAK-phosphorylation levels in S39D expressing cells, and no peripheral fascin localization, further suggesting fascin-actin binding is required to promote FA assembly/stability. The first panel in bottom row in Figure 5.10a shows large FA but no peripheral fascin localisation in cells expressing the S274A mutant. Finally, the second panel bottom row shows distinct co-localisation of p-FAK in S274D fascin within peripheral FA (Chapter 2) in cells re-expressing this mutant, as observed in WT fascin rescued cells.

FAK 397-phosphorlyation levels were analysed in mutant rescue cells under basal growing conditions by western blotting. Figure 5.10b shows total and p-FAK in MDA-MB-231 fasKD cells expressing GFP-WT, S39A, S39D, S274A and S274D fascin constructs. Total FAK was used as a loading control. P-FAK levels were quantified by densitometry analysis of at least three western blots (Figure 5.10c) in all cells. Figure 5.10c shows increased p-FAK levels in S39A fascin expressing cells compared to WT expressing cells. S39D fascin expressing cells showed lower p-FAK levels than in S39A or WT fascin expressing cells. S274A fascin expressing cells showed higher levels of p-FAK compared to any other fascin construct. S274D fascin rescue cells however showed a small but significant increase in p-FAK levels compared to WT fascin expressing cells, suggesting p-FAK was also involved in regulating basal FA in cells re-expressing this fascin mutant.

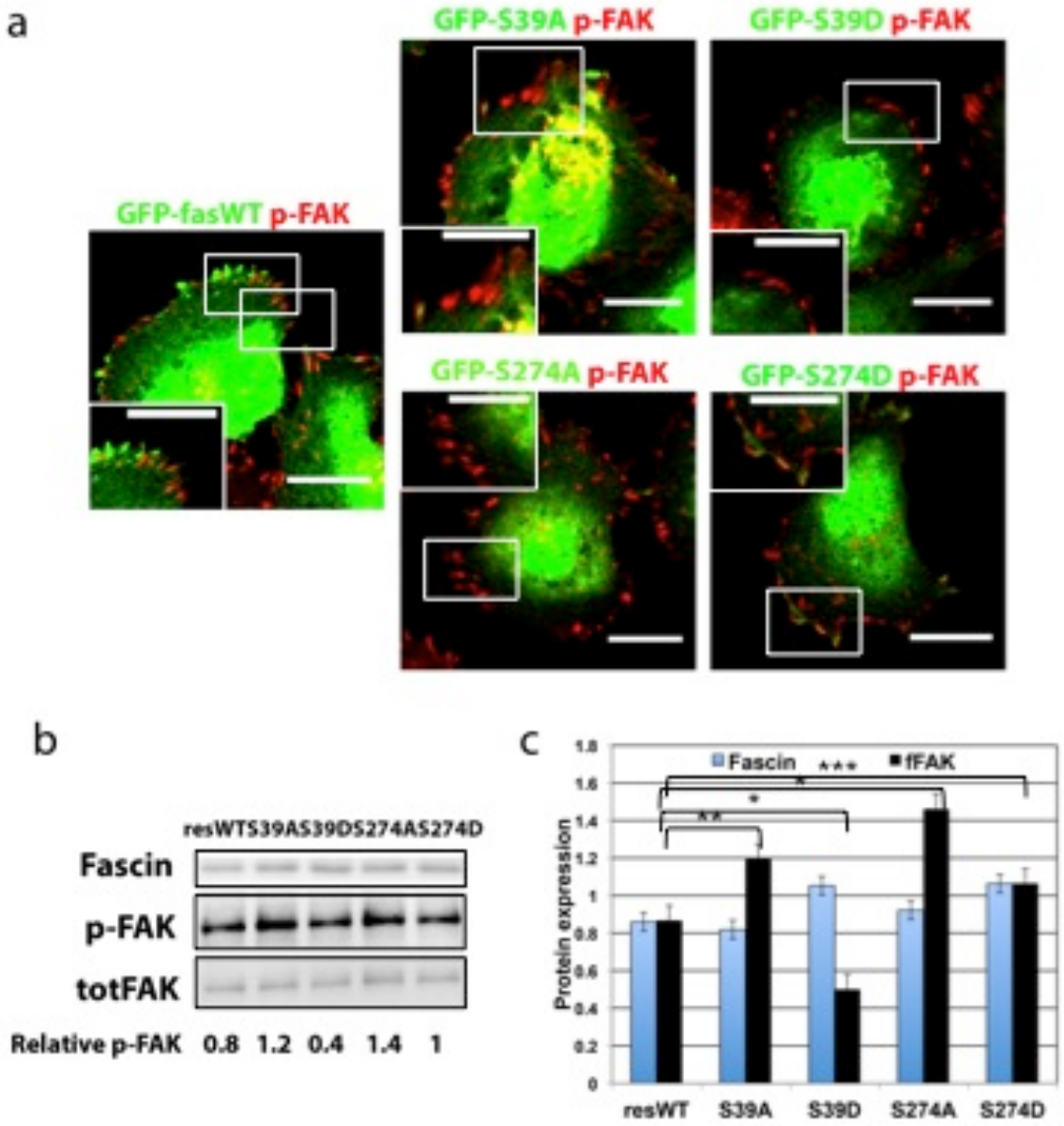

Figure 5.10. S274D fascin shows increased colocalisation with p-397 FAK at the cell periphery

(a) Confocal microscope images of cells stained for phospho-FAK (p-FAK) in MDA-MB-231 fascin knockdown cells re-expressing WT or mutant fascin-GFP. Scale bar= 10 um. Zoom of the highlighted area is shown to show fascin co-localisation with p-FAK. Scale bar= 3 um. (b) Western blots of lysates from MDA-MB-231 fasKD cells re-expressing WT and mutant fascin. (c) Statistical analysis of fascin and p-FAK levels was performed by densitometry analysis of at least three western blots. P-value =< 0.001 (***), =< 0.005 (**) and =< 0.05 (*) was considered as significant. Data are expressed as mean± sem and corrected on total FAK loading as control.

5.11. Fascin forms a complex with FAK

Data presented in Figures 5.8 and 5.9 supports a possible role for fascin in controlling levels of p-397 FAK in both basal and MT-induced FA disassembly conditions. Moreover, both WT and S274D fascin, but not other fascin mutants showed co-localisation with p-FAK at peripheral FA. The next step was therefore to investigate whether fascin may be able to form a complex with FAK in cells.

To test this, immuno-precipitations (IP) were performed using anti-total FAK antibody-coated beads incubated with lysates from control MDA-MB-231 cells (Figure 5.11a,b). GFP-WT fascin was overexpressed to permit analysis of potential fascin binding as opposed to endogenous fascin, as endogenous fascin runs at the same molecular weight as the IgG, whereas the GFP-tag allowed us to separate the GFP-fascin band (~80 kDa) from the control IgG band (~50 kDa). Experiments were performed under basal, untreated (UT) or in the presence of nocodazole (NOC) or taxol (TAX) treated cells to evaluate whether MT targeting drugs altered the putative fascin-FAK complex. Figure 5.11a shows example western blots of FAK IP assays in untreated, NOC and Tax treated cells. Non-specific IgG-coated beads were used as control for the non-specific binding in untreated cells (first lane in the IP blot shown in Figure 5.11a). Surprisingly, GFP-WT fascin was immuno-precipitated by FAK in untreated cells (second lane in the IP blot in Figure 5.11a). No fascin band was detected in the IgG negative control lane. Interestingly, GFP-fascin was readily detected in the UT cells in a complex with FAK, and this was significantly lower in cells treated with either NOC or taxol. Figure 5.11b shows densitometry analysis of multiple IP experiments. Data shows WT fascin forms a complex with FAK and its formation is dependent on MT integrity (p-value of WT fascin-GFP IPed by FAK in NOC or taxol cells compared to UT cells: p-value =< 0.005).

Figure 5.10 demonstrates that different fascin mutant expression results in different p-FAK levels and localisation. After observing WT fascin complex formation with FAK, the next step was to test the ability of the different fascin mutants to form a complex with FAK. FAK IP's were therefore performed as before in lysates from MDA-MB-231 fascin knockdown cells re-expressing GFP-WT, S39A, S39D, S274A or S274D fascin constructs (Figure 5.11c,d). IgG-coated beads were used as a control for non-specific binding as in Figure 5.11a. Figure 5.11c shows example western blots of these experiments. All fascin mutants were detected in a complex with FAK, but with differences in the level of co-association. Figure 5.11d shows densitometry analysis of multiple IP experiments. S39A fascin showed a modest but significant increase in binding to FAK compared to WT fascin. S39D fascin was also found in complex with FAK, at much higher levels than any of the other fascin constructs analysed. Similar levels of S274A fascin were immuno-precipitated with FAK to that seen for WT fascin. S274D fascin however formed similar levels in complex with FAK as S39D fascin. Data confirms that S39D fascin shows the highest association with total FAK in a complex, followed by S274D, S39A and WT/S274A fascin respectively.

Finally, to investigate whether fascin was able to directly bind to FAK, pull-down assays were performed using purified GST tagged domains of FAK. The diagram in Figure 5.11e shows the three main domains of the FAK protein: the N-terminal FERM domain, a central kinase domain and a C-terminal focal adhesion-targeting (FAT) region. The FERM domain at the N terminus of FAK is known to binding scaffolding proteins such as ezrin that indirectly link to the actin cytoskeleton (Frame et al. 2010). The kinase domain, which contains Y397, is essential for FAK phosphorylation activity (M. Schober et al. 2007) and the C terminus contains the Focal Adhesion Targeting (FAT) domain, which is critical to recruit FAK and other proteins such as Talin and Paxillin at FA (Hamadi et al. 2005). Figure 5.11e shows a Coomassie stained gel to show the presence of purified GST-FAK domains. Importantly, despite numerous attempts under different optimization conditions it emerged that the

Kinase domain of FAK was not suitable for protein production as it was toxic to bacteria (see Material and Methods). Thus only FERM and C-terminal domains could be considered in these assays. GST tagged FAK proteins or GST alone were incubated with lysates from MDA MB 231 cells expressing GFP-WT fascin and subjected to analysis of complexes by SDSPAGE gel and western blotting. Figure 5.11f shows an example of a western blot performed to detect WT fascin pulled down by FAK domains. Fascin was not pulled down by any of the FAK domains (Figure 5.11f), suggesting that direct binding did not occur between fascin and FAK in the complex formation.

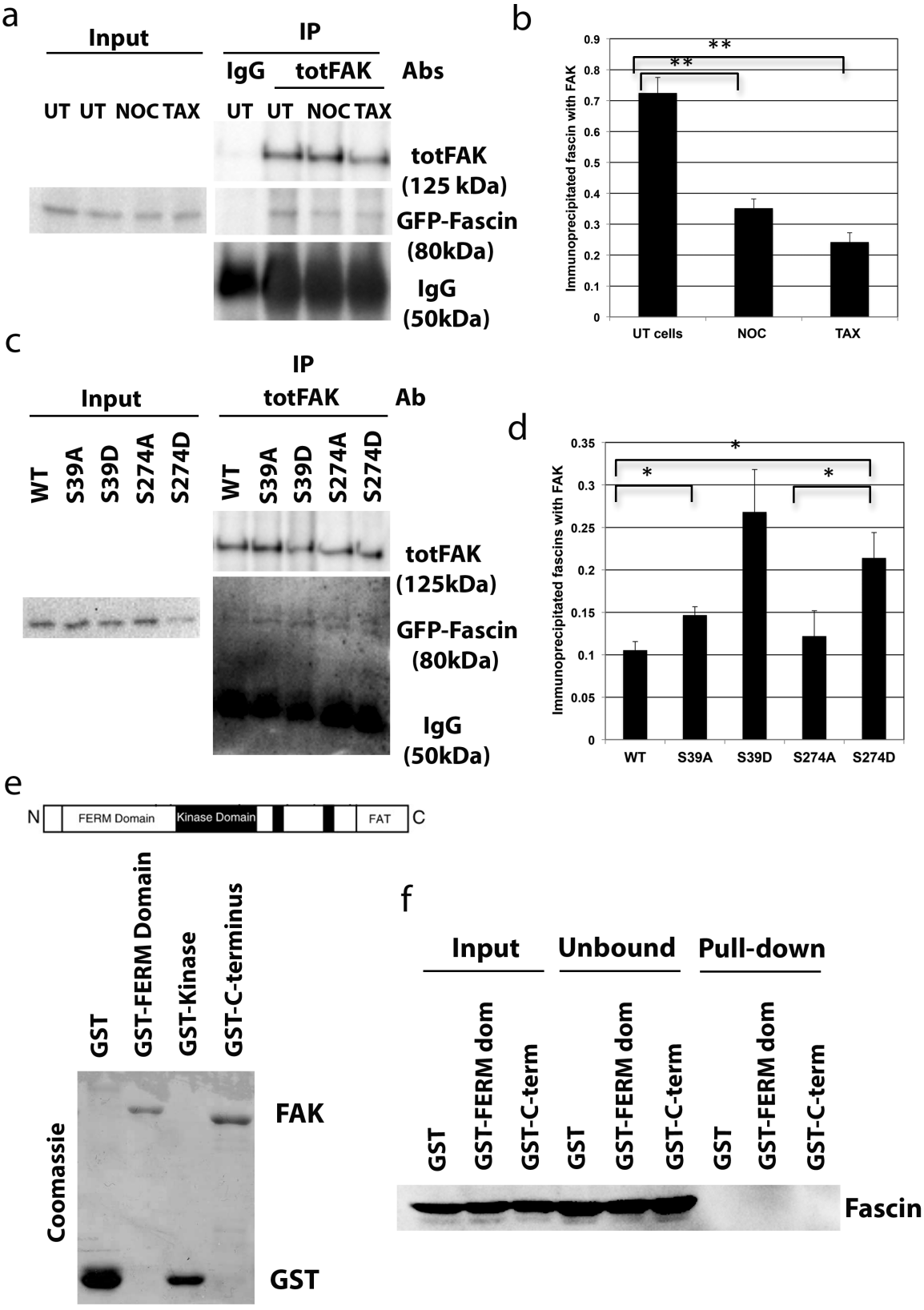
a
Input
IP
IgG
totFAK
Abs
UT UT NOC TAX
UT UT NOC TAX
totFAK
(125 kDa)
GFP-Fascin
(80kDa)
IgG
(50kDa)
b
Immunoprecipitated fascin with FAK
UT cells
NOC
TAX
c
Input
IP
totFAK
Ab
WT
S39A
S39D
S274A
S274D
totFAK
(125kDa)
GFP-Fascin
(80kDa)
IgG
(50kDa)
d
Immunoprecipitated fascins with FAK
WT
S39A
S39D
S274A
S274D
e
N
FERM Domain
Kinase Domain
FAT
C
GST
GST-FERM Domain
GST-Kinase
GST-C-terminus
Coomassie
FAK
GST
f
Input
Unbound
Pull-down
GST
GST-FERM dom
GST-C-term
Fascin

Figure 5.11. Fascin forms a complex with FAK

(a) Immunoprecipitation of WT fascin with total FAK (and IgG as control) in MDA-MB-231 rescue cells untreated (UT), nocodazole treated (NOC) and taxol treated (TAX). (b) Statistical analysis of immunoprecipitated fascin was performed by densitometry analysis of three experiments. P-value =< 0.005 (**) was considered as significant. Data are expressed as mean± sem and corrected on total FAK loading as control. (c) Immunoprecipitation of WT and mutant fascin with total FAK in MDA-MB-231 control cells rescued for WT and mutant fascin expression. (d) Statistical analysis of immunoprecipitated WT and mutant fascin was performed by densitometry analysis of three experiments. P-value =< 0.05 (*) was considered as significant. Data are expressed as mean± sem and corrected on total FAK loading as control. (e) Graphic panel and coomassie staining of GST-tagged FAK domain purification. (f) Pull-down assay between GST-tagged FAK domains and His6-tagged WT fascin. GST-Kinase domain of FAK is missing in (f) as the domain is not suitable for protein production.

DISCUSSION

Data presented in this chapter proposes fascin as a molecular mediator of the actin-MT crosstalk in human cancer cells. MT are known to play a role in regulating FA stability and turnover (Ezratty et al. 2005; Wehrle-Haller & Imhof 2003). Moreover, MT regulation on FA also involves a feedback control of MT dynamics by actin-based structures. For instance, stress fibers emanating from FA can act to stabilise the MT network (Kaverina et al. 1998). How this crosstalk is maintained remains poorly understood, although some molecules have been proposed as key regulators of this process. For example, +TIP MT binding protein family members have been demonstrated to co-operate with actin-dependent structures in different cellular contexts (Geraldo et al. 2008; Byron et al. 2012). For instance, the + TIP MT binding protein EB3 has been shown to localise to filopodia protrusions by direct binding to drebrin, a F-actin associated protein (Geraldo et al. 2008). Large scaffold proteins such as ACF7 have also been shown to act as linking molecules between actin and MT (Jefferson et al. 2004; Wu et al., 2011). However common signalling pathways involved in the regulation of both actin and MT-based structures are still poorly defined, particularly in the context of cancer cell invasion. Data presented in this Chapter showed that fascin plays a role in regulating both actin and MT in response to either MT or actin depolymerizing drugs. Thus, fascin may be a novel addition to the family of proteins that act at the interface between actin and MT cytoskeletons.

Data presented here showed that WT fascin is able to directly associate with MT *in vitro*. However, details of how fascin may bind to MT from a structural perspective remain untested. Indeed, fascin is not comprised of α-helices, which are characteristic of many of MT+ TIP protein structures (Akhmanova & Steinmetz 2008). Moreover, *in silico* or alignment analysis to identify putative MT binding domains within fascin have not revealed any sequence homology between fascin and MT-related proteins. However, MT binding domains are notoriously difficult to identify

using such means, meaning that a MT binding domain may exist within fascin but that extensive domain deletion or mutagenesis experiments would be required to identify this site. Potential MT-binding domains on MT associate proteins (MAPs) have been identified from the alignment of selected peptides to MAPs sequence (Cao & Mao 2009). Some of these MT-binding domains were found in Proline-rich regions or basic stretches and others in Ser/Thr/Val/Lys (S/T/V/K)-rich regions and repeats. Alignment analysis revealed two putative S/T/V/K rich regions within the second and the fourth β-trefoil domain of fascin. Although we could not find a potential MT-binding region in the third β-trefoil domain (containing the Ser274), the second β-trefoil domain of fascin resides in the same cleft of the protein structure. Indeed, the fascin polypeptide is known to fold into four β-trefoil domains with domain 1-2 and 3-4 forming two semi-independent units related by pseudo-2-fold symmetry (Jansen et al., 2011) Consequently, domains 2 and 3 (as domains 1 and 4) are parts of two independent units and they face each other forming a cleft in fascin structure. The cleft formed by domains 1 and 4 is critical in actin binding. On the other hand, a MT-binding cleft may be formed between domains 2 and 3. Indeed, the potential MT-binding regions within the second β-trefoil domain may co-operate with the Ser274 within the third β-trefoil domain in the MT-binding. Ongoing work in the lab aims to further investigate this hypothesis by studying different affinities to F-actin and/or MT of fascin mutants differentially mutated within the second β-trefoil domain.

It is not yet clear how the proposed phosphorylation cycles on the two major actin binding sites as discussed in the previous chapter might contribute to changes in fascin structure. In Chapter 4, a dual role of fascin in regulating actin and MT dynamics depending on both serines phosphorylation state was proposed. A recent study shows that both major actin binding sites on fascin are critical in bundling F-actin and that any impairment in one actin binding site leads to a concerted conformational change, which disables the other actin binding site (Yang et al. 2013).

In particular, their structural analysis showed fascin mutants in all actin-binding sites to display the same inactive configuration. They therefore concluded that the actin-binding sites are conformationally interconnected. Moreover, they proposed that individual fascin proteins are in constant motion, sampling active, inactive and possibly other conformations. It is therefore reasonable to propose a dynamic dual role of fascin in regulating actin and MT cytoskeletons. The *in vitro* co-sedimentation assay shown in this Chapter demonstrate that S274D fascin is the only mutant to preferentially bind to MT, and this binding level is unchanged in the presence of F-actin. Our model proposes a dual role for fascin that controls switching between F-actin and MT, depending on the serine phosphorylation state.

S274D fascin-MT binding may also promote a negative feedback control on assembly of fascin-dependent F-actin-based structures. Conversely, S39A-actin binding may promote MT stability. Data presented in Chapter 4 showed that S39A and S274D fascin expressing cells have similar increases in large bundles of acetylated tubulin, which further suggests that both mutants can contribute to MT dynamics under basal conditions, but that S39A fascin may be additionally preferentially phosphorylated at S274 in order to fulfill this task. Further experiments would be required to analyse this using either double S39A/S274D mutants, or antibodies specifically recognizing the phosphorylation at each Serine site individually.

Data presented here demonstrates that active p-Y397FAK may play a role in combination with fascin in regulating both basal FA turnover and FA disassembly following NOC washout. FAK phosphorylation on Tyrosine 397 (p-FAK) is known to promote the formation of a FAK-Src complex and increase basal FA turnover (Tomar & Schlaepfer 2009). Moreover, p-FAK has been shown to be involved in the co-ordination of dynamin-dependent endocytosis at FA and thus acts to promote FA disassembly after NOC washout (Ezratty et al. 2005). Data presented in this Chapter shows that levels of fascin can regulate levels of p-FAK and this potentially can in

turn explain differences in basal FA size and number seen in cells depleted of fascin or re-expressing fascin mutants. Low levels of p-FAK in fasKD cells correlated with increased numbers of FA observed in these cells in Chapter 3. Moreover, fasKD cells do not increase p-FAK levels after NOC washout as was seen in WT fascin expressing cells, suggesting fascin also plays a role in regulating activation of FAK to promote FA disassembly following MT re-growth. Further experiments demonstrated evidence of a fascin-FAK complex and that this was dependent on MT integrity. The formation of a fascin complex with FAK may explain the mechanisms driving both fascin roles in both basal and MT-dependent FA dynamics. Evidence presented here suggests fascin is not directly bound to FAK but instead may form part of a larger multimolecular complex with FAK bridged by another protein or proteins. Indeed, fascin localises at the cell periphery in basal conditions, where it is possible that fascin may act to form the complex with FAK and promoting FA turnover through its phosphorylation. NOC treatment leads to FA growth, but without a change in total p-FAK levels, which is indicative of FA stabilization. It is possible that under these conditions, fascin-FAK complexes are reduced or lost, and fascin is no longer present at the cell periphery, or in proximity to FA complexes or active FAK. Several FA components, such as Paxillin and/or Talin have already been shown to be associated with FAK (Schober et al. 2007), but their role in increasing FA assembly during MT de-polymerisation has not been investigated. Therefore, data presented here demonstrated fascin-FAK complex formation is involved in regulating basal and MT-dependent FA turnover but the accessory or scaffold molecules that form part of this complex have yet to be defined.

Fascin-complex formation with FAK provides a possible mechanism by which WT fascin is translocated to the cell periphery and then drives basal FA turnover. Experiments shown in this thesis did not investigate the phosphorylation status of FAK when in a complex with fascin. However, images showed WT fascin co-localisation with p-397 FAK at FA suggesting that the kinase may be phosphorylated

when in complex with fascin. Moreover, biochemical data presented in this chapter showed differences in fascin ability to form the complex with FAK depending on its actin binding ability. This also correlates with differences in basal FA numbers observed in the fascin mutant rescue cells (Chapter 4). S39A fascin, which is bound to actin at the periphery, is able to form a complex with FAK, albeit at lower levels than seen with S39D or S274D fascin. However, S39A fascin does not show clear co-localisation with p-397 FAK as was observed for WT or S274D fascin. This may explain why FA do not disassemble properly in the S39A fascin rescue cells, as the fascin-FAK complex is potentially less strong and thus fascin is unable to exert its effects over p-FAK dependent FA disassembly. This combined with the higher levels of acetylated, stable MT seen under basal conditions in the S39A fascin expressing cells would also slow down FA disassembly and lead to the larger FA seen in these cells, as well as the increased cell adhesion (Chapter 4). Interestingly, S39D fascin was seen at the highest levels in complex with FAK by co-IP, suggesting that fascin forms a tighter complex when it is not bound to actin. However, S39D fascin complex formation with FAK does not promote the FAK activation and/or S39D fascin localisation at the cell periphery. This may suggest that the complex is too stable to promote normal FA turnover. S274A fascin did not show a notable ability to form a complex with FAK and did not co-localise with p-FAK. However, S274A fascin can bundle F-actin in an actin-binding independent manner, and previous data has suggested a distinct filopodial tip localization of this mutant that suggests additional alternative binding partners (Zanet et al. 2012). Thus it is plausible that this mutant acts through an as yet unidentified alternative pathway that is largely independent of actin or MT binding capabilities. This will require more detailed analysis in future. 274D fascin showed higher binding in complex with FAK compared to WT, but lower than S39D mutant. However, S274D fascin co-localised with p-397 FAK at FA and S274D expressing cells showed higher levels of active FAK. It is therefore possible that S274D fascin, which shows preferential association with MT *in vitro* and

promotes MT stability is able to more readily form a complex with FAK and thereby co-ordinate MT and FAK within FA at the cell membrane.

Data presented in this chapter shows neither S39A nor S39D fascin expression promotes basal FA turnover. Indeed, S39A fascin expressing cells showed very large and stable FA and, conversely, S39D fascin expressing cells showed very small and immature FA. The S39A fascin complex formation with FAK and the protein localisation at the cell periphery (bound to actin) may promote the increased FA assembly in these cells, but another mechanism is involved in inducing FA disassembly and thus turnover. On the other hand, the increased level of S39D fascin in complex with FAK may disrupt FA growth. Indeed this complex does not correlate with fascin translocation to the cell periphery or the high levels of peripheral active FAK. The S274D fascin expressing cells showed the same size and number of FA as the S39A fascin cells. As previously discussed, despite not being able to efficiently bundle actin, 274D fascin was also found to localise at the cell periphery as seen for WT fascin. This localisation and co-localisation with the ends of MT and active FAK may contribute to the decreased FA disassembly seen in cells expressing this mutant. In addition, S274D expressing cells showed lower adhesion and smaller cell area compared to S39A expressing cells (Chapter 4). These observations suggest that the large FA in S274D fascin expressing cells may potentially support faster spreading through the control of cell membrane contact area with the substrate. I therefore concluded that peripherally localized S274D fascin has a role in regulating FA disassembly, in an actin-binding independent manner. Accordingly, the WT fascin-FAK complex was also shown to be dependent on MT integrity as decreased MT instability promoted fascin-FAK complex formation. MT instability decreases drastically after NOC washout and S274D fascin appears to play a primary role in this context. Therefore, S274D fascin-MT binding may control fascin-FAK complex formation and regulate FA turnover in both basal and NOC-induced conditions. However, data shown in Chapter 4 demonstrates that S274D cells do not

disassemble FA following NOC washout, but show an opposite FA response in the NOC assay compared with WT and S274A mutant. This suggests that the fascin-FAK complex seen in the case of this mutant is not active or viable in terms of the promoting FAK-dependent MT-induced FA disassembly. Chapter 4 showed fascin actin-binding at S39 is not required for MT-induced FA disassembly; therefore, the mechanism controlling S274-dependent FA crosstalk requires further investigation. It is possible that S274 needs to be de-phosphorylated to enable p-FAK to induce FA disassembly, and that the S274D fascin, locked in a phospho-mimetic state, is unable to undergo this transition.

In conclusion, data presented in this chapter proposes fascin phosphorylation status as a critical event to controlling fascin binding to MT and/or FAK and thereby basal and nocodazole-induced FA dynamics.

6 FINAL DISCUSSION.

6.1. Fascin regulates focal adhesion assembly and disassembly potentially through direct interactions with microtubules

A role for fascin in regulating Focal Adhesion (FA) turnover has previously been suggested, as colon carcinoma cells depleted of fascin showed more stable FA (Hashimoto et al. 2007). However, fascin has not been previously shown to localise in FA and therefore the mechanism(s) by which it regulates adhesion structure dynamics is still poorly understood. Microtubules (MT) have been widely shown to target FA components promoting their turnover (Ganguly et al. 2012; Stehbens & Wittmann 2012). The nocodazole (NOC) treatment and washout assay employed in this thesis is widely used to control FA assembly/disassembly and permit the role of MT and associated proteins in FA turnover to be dissected. MT re-growth following NOC washout has been shown to induce FA disassembly in fibroblasts (Ezratty et al. 2005) and data in this thesis demonstrates that this is also the case in breast and cervical cancer cells. Moreover, data presented in Chapter 3 (Results 1) showed that fascin is important in the control of both MT re-growth and FA disassembly in cells post-NOC washout.

The localization of WT fascin with MT at the cell periphery prompted us to further analyse the fascin-dependent mechanisms controlling both MT recovery and the subsequent FA turnover. Data demonstrated that fascin was able to directly interact with polymerised MT *in vitro*, and was also required to promote MT-dependent FA disassembly in cells. Furthermore, the S274 phospho-mimic mutant of fascin (S274D), which we have previously shown is unable to bind to actin or support filopodia formation (Zanet et al. 2012), demonstrated a higher affinity for MT compared to WT fascin and the other mutant fascin proteins tested. Moreover, the association between S274D fascin and MT *in vitro* was unchanged in presence of F-actin, suggesting phosphorylation at this residue may act to preferentially promote MT binding over actin bundling. Therefore, I propose fascin as a novel molecular

mediator of the actin-MT crosstalk and potentially an important molecular linker in the control of FA dynamics and cancer cell invasion. Table 6.1 provides an overview of data from this thesis to summarise WT and mutant fascin actin and MT binding activity.

	Actin binding	Actin bundling	MT binding
Fascin WT	+	+	+
Fascin S39A	++	++	+
Fascin S39D	-	-	+
Fascin S274A	-	+	+
Fascin S274D	-	-	++

Table 6.1. WT and mutant fascin actin and MT binding activity
In the table above, **+** stands for 'involved', **++** stands for 'essential' and **–** stands for 'not involved'.

The role of fascin in binding/bundling F-actin structures has been well documented by our lab and others (Anilkumar et al. 2003; Hashimoto et al. 2007; Parsons & Adams 2008; Vignjevic et al. 2006). However, data presented in this thesis proposes a dual role for fascin in regulating both actin and MT networks. Moreover, data presented in Chapter 4 (Results 2) showed fascin regulation to be dependent on the phosphorylation state of the two characterised actin-binding sites of the protein. Serine 39 (S39), which is phosphorylated by classical Protein Kinase C (PKC) isoforms, partly controls the actin-binding and filopodia formation, and data shown in this thesis demonstrates S39 can also promote larger, more stable FA under basal conditions, but does not appear to play a role in dynamic FA turnover. Conversely, the expression of the MT-associated S274D fascin regulated FA stability and also showed clear localisation within peripheral adhesion structures. Actin-MT binding proteins captured by MT at the plasma membrane have been previously shown to regulate cell spreading and migration (Zaoui et al. 2010). Therefore, S274D fascin may be delivered to the plasma membrane through its contact with MT and thus regulate FA turnover. Molecular details of how the Ser274 is phosphorylated are

poorly characterised but our unpublished *in silico* analysis has suggested this site is a consensus target sequence for Protein Kinase A (PKA). Interestingly, PKA phosphorylation has already been shown to regulate the MT binding affinity of other F-actin binding proteins (Lee et al. 2012). It therefore seems feasible that a phosphorylation-dependent switch in fascin may act to regulate its association with actin or MT and therefore control FA assembly/disassembly.

6.2. Phosphorylation cycling determine fascin association with actin and/or MT

FA assembly and disassembly have recently been proposed to be controlled through two distinct pathways. Several studies have shown adhesion disassembly is under the control of RhoA and MT in signaling pathways, which are not directly involved in FA assembly and stability (Chang et al. 2008; Goldyn et al. 2009; Rooney et al. 2010). Data presented in this thesis showed WT and S274D fascin associate with MT at the cell periphery following NOC washout and this may be one way to direct MT re-growth and FA targeting. Indeed, MT-S274D fascin expression restored MT network assembly following NOC washout as efficiently as WT fascin. However, the S274D mutant did not promote FA disassembly following NOC washout. This could be due to the known inability of the S274D fascin to bind F-actin and/or change its association with MT in presence of F-actin. An F-actin-MT cross-linking protein relies on its ability to re-organise and dynamically integrate both actin and MT cytoskeletons (Lee et al. 2012; Geraldo et al. 2008). Therefore, phosphorylation cycles regulating WT fascin ability to bind F-actin and MT may be crucial to coordinate their roles in FA assembly/disassembly. The phosphorylation status of S39 when fascin is bound to MT remains unknown, but our *in vitro* and *in vivo* analysis supports a potential role for a phosphorylation switch event at S39 that subsequently promotes FA disassembly, following 274D fascin-dependent MT targeting. The peripheral localisation of both S39A and S274D fascin mutants, albeit within different subdomains, would also support the notion of a local change in

phosphorylation status of each residue to control an on-off switch in MT/actin binding. Ongoing studies in the lab are evaluating this hypothesis by studying FA dynamics in cells expressing fascin mutated at both S39 and S274.

Several recent studies have identified molecules and signals that control crosstalk between actin and MT cytoskeletons. ACF7 is one example of a large scaffolding protein that has been shown to act as linking molecules between actin and MT (Jefferson et al. 2004; Wu et al. 2011). Data presented in this thesis showed that fascin plays a role in regulating both actin and MT in response to either MT or actin depolymerizing drugs. Common signalling pathways involved in the regulation of both actin and MT-based structures are still poorly defined, particularly in the context of cancer cell invasion.

6.3. Fascin control of MT stability

Fascin-dependent regulation of MT dynamics was not directly measured in this thesis. However, data demonstrated that fascin depletion did not alter MT network assembly on a gross scale under basal conditions, but did lead to increased levels of tubulin acetylation. Moreover, data demonstrated that S274D fascin co-localised with acetylated tubulin and thus contributing to their association at the cell membrane. MT +TIP proteins such as EB1 are known to promote MT assembly. Therefore, it is possible that peripherally localised fascin may regulate MT +TIP protein association with the MT network. Competition between fascin and +TIP proteins may provide a way in which fascin could capture and stabilize MT at the periphery in order to co-ordinate FA targeting. Similarly, enzymes involved in tubulin acetylation and stabilisation, such as HDAC6, have also been shown to alter adhesion dynamics (Tran et al. 2007; Gierke & Wittmann 2012). It is possible therefore that fascin may act to directly or indirectly control enzymes regulating tubulin acetylation providing one mechanism by which fascin can locally control MT dynamics.

As discussed in Chapter 5 (Results Chapter 3), the structural details of the MT-binding domain of fascin are still unknown. However, analysis of putative consensus MT binding domains within the fascin sequence revealed a possible MT-binding region within the second β-trefoil domain. The second β-trefoil domain lies within the tertiary pseudo-2-fold symmetric structure of the fascin protein and acts in concert with domain one to regulate the N-terminal actin-binding site. However, the fold between domains 2 and 3 is also tightly controlled, potentially to allow fascin to form the correct tertiary structure required to stabilize the correct conformation for F-actin bundling. Therefore, it is possible that the identified putative MT binding sequence within the second β-domain may undergo a conformational change following post-translational modification of S274 on the third β-trefoil domain to promote MT binding. There is currently no data in the literature that explores the potential for fascin to undergo conformational changes in response to actin binding or post-translational modification. However, ongoing work in the lab is evaluating MT binding affinity and functions in cells of fascin mutated in residues lying within the putative MT binding site in the second β-trefoil domain of fascin. Identifying mutant forms of fascin that bind specifically to MT or actin would permit important future dissection of the relative contributions of fascin to regulating each cytoskeletal network during cell migration and invasion.

6.4. Fascin complexes with adhesion signaling molecules

Focal Adhesion Kinase (FAK) has been shown to co-operate with dynamin and promote MT-induced FA dynamics following NOC washout in fibroblasts (Ezratty et al. 2005; Wang et al. 2011). Data shown in this thesis confirms that levels of autophosphorylation of 397-Tyrosine on FAK is also tightly regulated during cancer cell FA disassembly post-NOC washout and this is dependent on the presence of fascin. Moreover, co-immunoprecipitation shows the presence of a fascin-FAK

complex that is indirect, and may act as a regulatory mechanism for fascin-MT translocation to the cell membrane. The fascin-FAK complex was further shown to depend upon fascin association with actin or MT. Both S39D and S274D fascin were found at higher levels in complex with FAK, but only S274D fascin was seen to co-localise with p-FAK at the plasma membrane. This may suggest that the observed high levels of S274D fascin-MT association may activate FAK and thus indirectly co-ordinate FA turnover. Conversely, the S39D fascin may favour binding to inactive FAK and in doing so restrict delivery or localization of active FAK to FA. S39A fascin is known to be stably bound to F-actin and is located in peripheral filopodia, and this may explain the lower levels of FAK found in complex with this mutant. An overview of the proposed model for fascin-dependent regulation of MT and FA dynamics is shown in Figure 6.1.

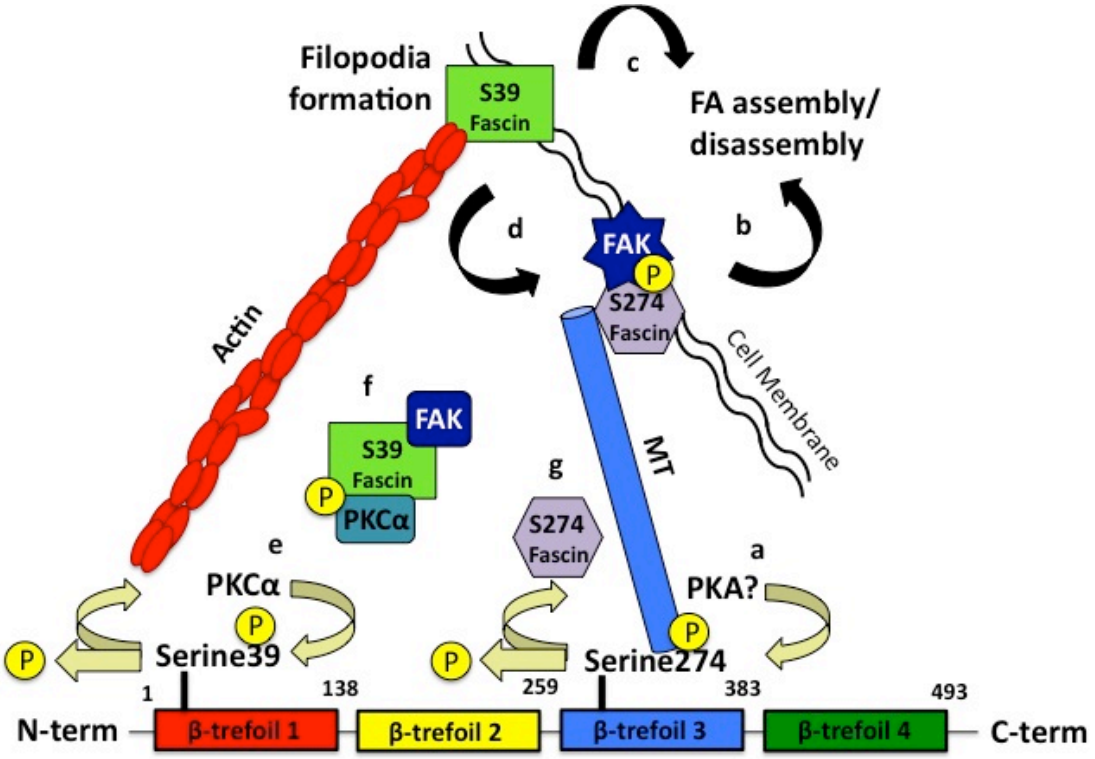

Figure 6.1. Proposed model of mutant fascin regulation of FA turnover through direct binding to MT

(a) Fascin phosphorylation on S274 (potentially PKA-dependent) results in more stable association between fascin and MT. (b) Fascin-MT binding occurs preferentially at the cell periphery. Phospho-S274 fascin forms a complex with phospho-FAK at the membrane and thus brings MT and FAK into close proximity and promotes FA turnover. (c) Fascin that is de-phosphorylated at S39 bundles F-actin at the cell periphery, promoting FA assembly. (d) S39 fascin also promotes MT stability contributing to MT-dependent FA turnover. (e) PKCα-dependent phosphorylation of the S39 results in loss of actin bundling by fascin. (f) The cytosolic phospho-S39 fascin forms a complex with inactive FAK. The potential function of this complex is still unknown. (g) Fascin that is de-phosphorylated at Ser274 does not bundle F-actin and therefore does not promote FA assembly or contribute to FA turnover. Yellow arrows show phosphorylation cycles on fascin and black arrows show the novel roles for fascin identified in this thesis.

6.5. Fascin as a F-actin-MT crosslinker: involvement in cancer cell adhesion and invasion

PKCα-dependent fascin phosphorylation is known to promote filopodia and invadopodia formation in invasive cancer cells. Indeed, high levels of fascin expression have been proposed to act as a marker for poor prognosis in disease. However, the precise changes in cytoskeletal network reorganisation associated with fascin up-regulation at the invasive tumour front have not been defined. Several studies have speculated about an unknown role for fascin role beyond the ability to control actin bundling (Machesky & Li 2010; Zanet et al. 2012). Data shown here provides novel evidence to suggest that fascin may also regulate cytoskeletal changes through direct associations with MT. Therefore, this thesis contributes to a better understanding of the role of fascin in driving cancer cell adhesion and invasion and proposes fascin protein as a central molecule regulating actin-MT crosstalk, as

switch that is controlled through action of PKC and potentially PKA. Such a cycle of phosphorylation would thereby control fascin-dependent filopodia stability as well as invadopodia or FA dynamics, and thus locally and dynamically regulate the cytoskeleton and cell invasion. It has been shown that altering or locking one or more phosphorylation sites on fascin alters cytoskeletal structure assembly/stability (Yang et al. 2013). Additionally, the concept that different forms of fascin, both active and inactive, exist in the cytosol has been proposed. It is therefore tempting to speculate that fascin can also act as a dynamic modulator of cell sensing of the EC environment and potentially respond to local changes in extracellular environment during tumour cell invasion. An important future direction of this study would be to study and correlate fascin association with MT and its regulation of FA with cell invasion in a more physiological 3D extracellular matrix environment.

In conclusion, work arising from this thesis has led us to propose a novel function for fascin in controlling MT-dependent FA turnover and thereby potentially offering an additional way in which fascin contributes to cancer cell adhesion and invasion.

FUTURE DIRECTIONS

- Analyse fascin phosphorylation-dependent roles in regulating MT-induced FA assembly and disassembly by performing fixed and live imaging experiments in cells expressing fascin mutated at both S39 and S274 (eg. S39A/S274D or S39D/S274D).

- Analyse the role of PKA in S274 phosphorylation *in vitro* and biochemical analysis and study PKA inhibition effects on fascin peripheral localisation and/or pFAK activation.

- Inhibiting FAK phosphorylation to determine whether this alters co-association with fascin and analyse the potential role of a fascin-inactive FAK complex.

- Characterise the MT-binding domain of fascin by performing *in vitro* MT co-sedimentation assay using fascin mutated within the putative identified MT binding region within the second β-trefoil domain of fascin.

- Elucidate the role of fascin in MT growth and stability by analysing MT dynamics in live imaging experiments in fascin knockdown and cells rescued for different fascin mutants.

- Inhibit enzymes involved in tubulin post-translational modification such as HDAC6 to identify signaling pathways involved in fascin-dependent MT stability.

- Analyse fascin-dependent regulation of MT growth and filopodia/invadopodia formation in cells in 3D collagen/fibronectin gels.

7 Bibliography

- Adams, J., 2004. Roles of fascin in cell adhesion and motility. *Current Opinion in Cell Biology*, 16(5), pp.590–596.
- Ahmed, S., Goh, W.I. & Bu, W., 2010. I-BAR domains, IRSp53 and filopodium formation. *Seminars in cell & developmental biology*, 21(4), pp.350–356.
- Akhmanova, A et al., 2001. Clasps are CLIP-115 and -170 associating proteins involved in the regional regulation of microtubule dynamics in motile fibroblasts. *Cell*, 104(6), pp.923–935.
- Akhmanova, A. & Steinmetz, M., 2008. Tracking the ends: a dynamic protein network controls the fate of microtubule tips. *Nature Reviews Molecular Cell Biology*, 9(4), pp.309–322.
- Anilkumar, N. et al., 2003. Interaction of fascin and protein kinase Calpha: a novel intersection in cell adhesion and motility. *The EMBO journal*, 22(20), pp.5390–5402.
- Anthis, N. et al., 2009. The structure of an integrin/talin complex reveals the basis of inside-out signal transduction. *The EMBO journal*, 28(22), pp.3623–3632.
- De Arcangelis, A., Georges-Labouesse, E. & Adams, J., 2004. Expression of fascin-1, the gene encoding the actin-bundling protein fascin-1, during mouse embryogenesis. *Gene expression patterns*, 4(6), pp.637–643.
- Askari, J.A. et al., 2010. Focal adhesions are sites of integrin extension. *The Journal of cell biology*, 188(6), pp.891–903.
- Bachmann, V. A. et al., 2013. Reciprocal regulation of PKA and Rac signaling. *Proceedings of the National Academy of Sciences of the United States of America*, 110(21), pp.8531–6.
- Baldassarre, M. et al., 2006. Actin dynamics at sites of extracellular matrix degradation. *European journal of cell biology*, 85(12), pp.1217–1231.
- Ballestrem, C et al., 2000. Actin-dependent lamellipodia formation and microtubule-dependent tail retraction control-directed cell migration. *Molecular biology of the cell*, 11(9), pp.2999–3012.
- Ballestrem, C et al., 2001. Marching at the front and dragging behind: differential alphaVbeta3-integrin turnover regulates focal adhesion behavior. *The Journal of cell biology*, 155(7), pp.1319–1332.
- Balzer, E.M. et al., 2010. c-Src differentially regulates the functions of microtentacles and invadopodia. *Oncogene*, 29(48), pp.6402–6408.
- Bamburg, J.R., McGough, a & Ono, S., 1999. Putting a new twist on actin: ADF/cofilins modulate actin dynamics. *Trends in cell biology*, 9(9), pp.364–370.

- Bannigan, A. & Baskin, T., 2005. Directional cell expansion -- turning toward actin. *Current Opinion in Plant Biology*, 8(6), pp.619–624.
- Bartolini, F., Ramalingam, N. & Gundersen, G.G., 2012. Actin Capping Protein Promotes Microtubule Stability By Antagonizing mDia1's Actin Activity. *Molecular biology of the cell*, (23)20, pp. 4032-4040.
- Bear, J.E. & Gertler, F.B., 2009. Ena/VASP: towards resolving a pointed controversy at the barbed end. *Journal of cell science*, 122(12), pp.1947–1953.
- Béraud-Dufour, S. et al., 2007. Krit 1 interactions with microtubules and membranes are regulated by Rap1 and integrin cytoplasmic domain associated protein-1. *FEBS Journal*, 274(21), pp.5518–5532.
- Breitsprecher, D. et al., 2011. Cofilin cooperates with fascin to disassemble filopodial actin filaments. *Journal of cell science*, 124(19), pp.3305–3318.
- Bretscher, M.S., 1996. Getting membrane flow and the cytoskeleton to cooperate in moving cells. *Cell*, 87(4), pp.601–606.
- Brockbank, E.C. et al., 2005. Integrin beta1 is required for the invasive behaviour but not proliferation of squamous cell carcinoma cells in vivo. *British journal of cancer*, 92(1), pp.102–112.
- Broussard, J., Webb, D. & Kaverina, I., 2008. Asymmetric focal adhesion disassembly in motile cells. *Current Opinion in Cell Biology*, 20(1), pp.85–90.
- Brown, E., 2002. Integrin-associated proteins. *Current Opinion in Cell Biology*, 14(5), pp.603–607.
- Brown, M. et al., 2005. Src and FAK kinases cooperate to phosphorylate paxillin kinase linker, stimulate its focal adhesion localization, and regulate cell spreading and protrusiveness. *Molecular biology of the cell*, 16(9), pp.4316–4328.
- Buccione, R., Caldieri, G. & Ayala, I., 2009. Invadopodia: specialized tumor cell structures for the focal degradation of the extracellular matrix. *Cancer metastasis reviews*, 28(1-2), pp.137–149.
- Byron, A. et al., 2012. Proteomic analysis of α4β1 integrin adhesion complexes reveals α-subunit-dependent protein recruitment. *Proteomics*, 12(13), pp.2107–2114.
- Caldieri, G. et al., 2009. Cell and molecular biology of invadopodia. *International review of cell and molecular biology*, 275, pp.1–34.
- Calvo, F. et al., 2011. RasGRF suppresses Cdc42-mediated tumour cell movement, cytoskeletal dynamics and transformation. *Nature cell biology*, 13(7), pp.819–826.
- Campellone, K.G. et al., 2008. WHAMM is an Arp2/3 complex activator that binds microtubules and functions in ER to Golgi transport. *Cell*, 134(1), pp.148–161.
- Cant, K. et al., 1994. Drosophila singed, a fascin homolog, is required for actin bundle formation during oogenesis and bristle extension. *The Journal of cell biology*, 125(2), pp.369–380.

- Cao, B. & Mao, C., 2009. Identification of microtubule-binding domains on microtubule-associated proteins by major coat phage display technique. *Biomacromolecules*, 10(3), pp.555–564.
- Carisey, A. & Ballestrem, C., 2011. Vinculin, an adapter protein in control of cell adhesion signalling. *European journal of cell biology*, 90(2-3), pp.157–163.
- Cau, J. & Hall, A., 2005. Cdc42 controls the polarity of the actin and microtubule cytoskeletons through two distinct signal transduction pathways. *Journal of cell science*, 118(12), pp.2579–2587.
- Chan, K., Cortesio, C. & Huttenlocher, A., 2009. FAK alters invadopodia and focal adhesion composition and dynamics to regulate breast cancer invasion. *The Journal of Cell Biology*, 185(2), pp.357–370.
- Chang, Y.-C. et al., 2008. GEF-H1 couples nocodazole-induced microtubule disassembly to cell contractility via RhoA. *Molecular biology of the cell*, 19(5), pp.2147–2153.
- Cho, K., Meyer, T. & Heo, W. D., 2012. Cooperative activation of PI3K by Ras and Rho Family Small GTPase. *Mol Cel*, 47(2), pp.281–290.
- Choi, C.K. et al., 2008. Actin and alpha-actinin orchestrate the assembly and maturation of nascent adhesions in a myosin II motor-independent manner. *Nature cell biology*, 10(9), pp.1039–1050.
- Costa, P. & Parsons, M., 2010. New insights into the dynamics of cell adhesions. *International review of cell and molecular biology*, 283, pp.57–91.
- Courson, D. & Rock, R., 2010. Actin cross-link assembly and disassembly mechanics for alpha-Actinin and fascin. *The Journal of biological chemistry*, 285(34), pp.26350–26357.
- Doherty, G. & McMahon, H., 2008. Mediation, Modulation, and Consequences of Membrane-Cytoskeleton Interactions. *Annual Review of Biophysics*, 37(1), pp.65–95.
- Drechsel, D.N. & Kirschner, M.W., 1994. The minimum GTP cap required to stabilize microtubules. *Current biology*, 4(12), pp.1053–1061.
- Dumbauld D.W. et al., 2010. Contractility Modulates Cell Adhesion Strentghening Through Focal Adhesion Kinase and Assmbly of Vinculin-Containing Focal Adhesions. *J Cell Physiol*, 223(3), pp.746–756.
- Efimov, A & Kaverina, I, 2009. Significance of microtubule catastrophes at focal adhesion sites. *Cell adhesion & migration*, 3(3), pp.285–287.
- Efimov, A. et al., 2008. Paxillin-dependent stimulation of microtubule catastrophes at focal adhesion sites. *Journal of cell science*, 121(2), pp.196–204.
- Egile, C. et al., 2005. Mechanism of filament nucleation and branch stability revealed by the structure of the Arp2/3 complex at actin branch junctions. *PLoS biology*, 3(11), pp.259-266.
- Etienne-Manneville, S & Hall, A., 2001. Integrin-mediated activation of Cdc42 controls cell polarity in migrating astrocytes through PKCzeta. *Cell*, 106(4), pp.489–98.

- Etienne-Manneville, S., 2004. Actin and microtubules in cell motility: which one is in control? *Traffic*, 5(7), pp.470–477.
- Etienne-Manneville, S. & Hall, A., 2002. Rho GTPases in cell biology. *Nature*, 420(6916), pp.629–635.
- Evans, J. & Matsudaira, P., 2006. Structure and dynamics of macrophage podosomes. *European journal of cell biology*, 85(3-4), pp.145–149.
- Ezratty, E., Partridge, M. & Gundersen, G.G., 2005. Microtubule-induced focal adhesion disassembly is mediated by dynamin and focal adhesion kinase. *Nature Cell Biology*, 7(6), pp.581–590.
- Felding-Habermann, B. et al., 2001. Integrin activation controls metastasis in human breast cancer. *Proceedings of the National Academy of Sciences of the United States of America*, 98(4), pp.1853–1858.
- Frame, M.C. et al., 2010. The FERM domain: organizing the structure and function of FAK. *Nature reviews. Molecular cell biology*, 11(11), pp.802–814.
- Friedl, P. et al., 2012. Classifying collective cancer cell invasion. *Nature cell biology*, 14(8), pp.777–783.
- Friedl, P., 2004. Prespecification and plasticity: shifting mechanisms of cell migration. *Current opinion in cell biology*, 16(1), pp.14–23.
- Friedl, P. & Wolf, K., 2010. Plasticity of cell migration: a multiscale tuning model. *The Journal of cell biology*, 188(1), pp.11–19.
- Friedl, P. & Wolf, K., 2003. Tumour-cell invasion and migration: diversity and escape mechanisms. *Nature reviews. Cancer*, 3(5), pp.362–374.
- Fukata, M. et al., 2002. Rac1 and Cdc42 capture microtubules through IQGAP1 and CLIP-170. *Cell*, 109(7), pp.873–885.
- Gaillard, J. et al., 2011. Differential interactions of the formins INF2, mDia1, and mDia2 with microtubules. *Molecular biology of the Cell*, 22(23), pp.4575–4587.
- Gallant, N.D., Michael, K.E. & Garcı, J., 2005. Cell Adhesion Strengthening : Contributions of Adhesive Area, Integrin Binding, and Focal Adhesion Assembly. *Molecular Biology of the Cell*, 16, pp.4329–4340.
- Ganguly, A. et al., 2012. The Role of Microtubules and Their Dynamics in Cell Migration. *The Journal of biological chemistry*, 287(52), pp.43359–43369.
- Ganguly, A. & Cabral, F., 2011. The arresting action of microtubules in cell motility. *Cell cycle*, 10(16), pp.2614–2615.
- Geiger, B. et al., 2001. Transmembrane extracellular matrix– cytoskeleton crosstalk. *Molecular Cell Biology*, 2, pp.793-805.
- Geraldo, S. et al., 2008. Targeting of the F-actin-binding protein drebrin by the microtubule plus-tip protein EB3 is required for neuritogenesis. *Nature Cell Biology*, 10(10), pp.1181–1189.
- Gierke, S. & Wittmann, T., 2012. EB1-Recruited Microtubule +TIP Complexes Coordinate Protrusion Dynamics during 3D Epithelial Remodeling. *Current Biology*, 22(9), pp.753–762.

- Gimona, M. et al., 2008. Assembly and biological role of podosomes and invadopodia. *Current Opinion in Cell Biology*, 20(2), pp.235–241.
- Gimona, M. et al., 2002. Functional plasticity of CH domains. *FEBS letters*, 513(1), pp.98–106.
- Gimona, M. & Buccione, R., 2006. Adhesions that mediate invasion. *The international journal of biochemistry & cell biology*, 38(11), pp.1875–1892.
- Goldyn, A. et al., 2009. Force-induced cell polarisation is linked to RhoA-driven microtubule-independent focal-adhesion sliding. *Journal of cell science*, 122(20), pp.3644–3651.
- Gomes, E.R., Jani, S. & Gundersen, G.G., 2005. Nuclear movement regulated by Cdc42, MRCK, myosin, and actin flow establishes MTOC polarization in migrating cells. *Cell*, 121(3), pp.451–463.
- Goode, B.L. & Eck, M.J., 2007. Mechanism and function of formins in the control of actin assembly. *Annual review of biochemistry*, 76, pp.593–627.
- Gorovoy M. et al., 2005. LIM Kinase 1 Coordinates Microtubule Stability and Actin Polymerisation in Human Endothelial Cells. *J Biol Cell*, 280(28), pp.26533–26542.
- Hall, A., 2009. The cytoskeleton and cancer. *Cancer metastasis reviews*, 28(1-2), pp.5–14.
- Hamadi, A. et al., 2005. Regulation of focal adhesion dynamics and disassembly by phosphorylation of FAK at tyrosine 397. *Journal of cell science*, 118(19), pp.4415–4425.
- Harburger, D. & Calderwood, D., 2009. Integrin signalling at a glance. *Journal of cell science*, 122(2), pp.159–163.
- Harjanto, D. & Zaman, M., 2010. Matrix mechanics and receptor-ligand interactions in cell adhesion. *Organic & biomolecular chemistry*, 8(2), pp.299–304.
- Hashimoto, Y., Parsons, M. & Adams, J., 2007. Dual actin-bundling and protein kinase C-binding activities of fascin regulate carcinoma cell migration downstream of Rac and contribute to metastasis. *Molecular biology of the cell*, 18(11), pp.4591–4602.
- Hashimoto, Y., Skacel, M. & Adams, J., 2005. Roles of fascin in human carcinoma motility and signaling: prospects for a novel biomarker? *The international journal of biochemistry & cell biology*, 37(9), pp.1787–1804.
- Hayakawa, K., Tatsumi, H. & Sokabe, M., 2012. Mechano-sensing by actin filaments and focal adhesion proteins. *Communicative & integrative biology*, 5(6), pp.572–577.
- Heald, R. & Nogales, E., 2002. Microtubule dynamics. *Journal of cell science*, 115(1), pp.3–4.
- Herrmann, H. et al., 2007. Intermediate filaments: from cell architecture to nanomechanics. *Nature reviews. Molecular cell biology*, 8(7), pp.562–573.
- Hoogenraad, C.C. et al., 2000. Functional analysis of CLIP-115 and its binding to microtubules. *Journal of cell science*, 113(12), pp.2285–2297.

- Hotulainen, P. & Lappalainen, P., 2006. Stress fibers are generated by two distinct actin assembly mechanisms in motile cells. *The Journal of cell biology*, 173(3), pp.383–394.
- Huber, F. et al., 2013. Emergent complexity of the cytoskeleton: from single filaments to tissue. *Advances in Physics*, 62(1), pp.1–112.
- Hynes, R., 2002. Integrins: bidirectional, allosteric signaling machines. *Cell*, 110(6), pp.673–687.
- Ikegami, K. & Setou, M., 2010. Unique post-translational modifications in specialized microtubule architecture. *Cell structure and function*, 35(1), pp.15–22.
- Insall, R.H. & Machesky, L.M., 2009. Actin dynamics at the leading edge: from simple machinery to complex networks. *Developmental cell*, 17(3), pp.310–322.
- Itoh, R.E. et al., 2002. Activation of Rac and Cdc42 Video Imaged by Fluorescent Resonance Energy Transfer-Based Single-Molecule Probes in the Membrane of Living Cells. *Mol. Cell. Biol.,* 22(18), pp. 6582-6591.
- Jansen, S. et al., 2011. Mechanism of actin filament bundling by fascin. *The Journal of biological chemistry*, 286(34), pp.30087–30096.
- Jayo, A. & Parsons, M. , 2010. Fascin: a key regulator of cytoskeletal dynamics. *The international journal of biochemistry & cell biology*, 42(10), pp.1614–1617.
- Jayo, A., Parsons, M. & Adams, J.C., 2012. A novel Rho-dependent pathway that drives interaction of fascin-1 with p-Lin-11/Isl-1/Mec-3 kinase (LIMK) 1/2 to promote fascin-1/actin binding and filopodia stability. *BMC biology*, 10(72), pp.1-19.
- Jefferson, J., Leung, C. & Liem, R., 2004. Plakins: Goliaths that link cell junctions and the cytoskeleton. *Nature Reviews Molecular Cell Biology*, 5(7), pp.542–553.
- Jiang, K. & Akhmanova, A., 2011. Microtubule tip-interacting proteins: a view from both ends. *Current Opinion in Cell Biology*, 23(1), pp.94–101.
- Juwana, J.P. et al., 1999. EB/RP gene family encodes tubulin binding proteins. *International journal of cancer*, 81(2), pp.275–284.
- Kanchanawong, P. et al., 2010. Nanoscale architecture of integrin-based cell adhesions. *Nature*, 468(7323), pp.580–584.
- Kaneko-Kawano, T. et al., 2012. Dynamic regulation of myosin light chain phosphorylation by Rho-kinase. *PloS one*, 7(6), pp.e39269.
- Kavallaris, M., 2010. Microtubules and resistance to tubulin-binding agents. *Nature reviews. Cancer*, 10(3), pp.194–204.
- Kaverina, I, Rottner, K & Small, J. V, 1998. Targeting, capture, and stabilization of microtubules at early focal adhesions. *The Journal of Cell Biology*, 142(1), pp.181–190.
- Keays, D. a et al., 2007. Mutations in alpha-tubulin cause abnormal neuronal migration in mice and lissencephaly in humans. *Cell*, 128(1), pp.45–57.

- Keren, K., 2011. Cell motility: the integrating role of the plasma membrane. *European biophysics journal*, 40(9), pp.1013–1027.
- Van Keymeulen, A. et al., 2006. To stabilize neutrophil polarity, PIP3 and Cdc42 augment RhoA activity at the back as well as signals at the front. *The Journal of cell biology*, 174(3), pp.437–445.
- Khaitlina, S.Y., 2001. Functional specificity of actin isoforms. *International review of cytology*, 202, pp.35–98.
- Kiosses, W.B. et al., 2001. Rac recruits high-affinity integrin alphavbeta3 to lamellipodia in endothelial cell migration. *Nature cell biology*, 3(3), pp.316–320.
- Kirmse, R., Otto, H. & Ludwig, T., 2011. Interdependency of cell adhesion, force generation and extracellular proteolysis in matrix remodeling. *Journal of cell science*, 124(11), pp.1857–1866.
- Kodama, A. et al., 2003. ACF7: an essential integrator of microtubule dynamics. *Cell*, 115(3), pp.343–354.
- Kölsch, V., Charest, P.G. & Firtel, R.A., 2009. The regulation of cell moltility and chemotaxis by phospholipid signaling, *J Cell Sci*, 121(5), pp.551–559.
- Kraning-Rush, C. et al., 2011. The role of the cytoskeleton in cellular force generation in 2D and 3D environments. *Physical biology*, 8(1), pp.15009-15018.
- Kreplak, L. & Fudge, D., 2007. Biomechanical properties of intermediate filaments: from tissues to single filaments and back. *BioEssays : news and reviews in molecular, cellular and developmental biology*, 29(1), pp.26–35.
- Kurosaka S. & Kashina A., 2008. Cell Biology of Embrionic Migration. *Birth Defects Res C Embryo Today*, 84(2), pp.102-122.
- Lai, F.P.L. et al., 2008. Arp2/3 complex interactions and actin network turnover in lamellipodia. *The EMBO Journal*, 27(7), pp.982–992.
- Lai-Cheong, J.E., Parsons, M & McGrath, J.A., 2010. The role of kindlins in cell biology and relevance to human disease. *The international journal of biochemistry & cell biology*, 42(5), pp.595–603.
- Lämmermann, T. & Sixt, M., 2009. Mechanical modes of “amoeboid” cell migration. *Current opinion in cell biology*, 21(5), pp.636–644.
- Lansbergen, G. & Akhmanova, A., 2006. Microtubule plus end: a hub of cellular activities. *Traffic*, 7(5), pp.499–507.
- Lawson, C. et al., 2012. FAK promotes recruitment of talin to nascent adhesions to control cell motility. *The Journal of cell biology*, 196(2), pp.223–232.
- Lee, C.-H. et al., 2012. Structural basis for heteromeric assembly and perinuclear organization of keratin filaments. *Nature structural & molecular biology*, 19(7), pp.707–715.
- Lee, D. et al., 2012. Inositol 1,4,5-trisphosphate 3-kinase A is a novel microtubule-associated protein: PKA-dependent phosphoregulation of

microtubule binding affinity. *The Journal of biological chemistry*, 287(19), pp.15981–15995.

- Lei, W.-L. et al., 2012. Laminin/β1 integrin signal triggers axon formation by promoting microtubule assembly and stabilization. *Cell research*, 22(6), pp.954–972.
- Li, A. et al., 2010. The actin-bundling protein fascin stabilizes actin in invadopodia and potentiates protrusive invasion. *Current biology*, 20(4), pp.339–345.
- Liao, G., Nagasaki, T. & Gundersen, G.G., 1995. Low concentrations of nocodazole interfere with fibroblast locomotion without significantly affecting microtubule level: implications for the role of dynamic microtubules in cell locomotion. *Journal of cell science*, 108 (1), pp.3473–3483.
- Lizárraga, F. et al., 2009. Diaphanous-related formins are required for invadopodia formation and invasion of breast tumor cells. *Cancer research*, 69(7), pp.2792–2800.
- Luo, M. & Guan, J.-L., 2010. Focal adhesion kinase: a prominent determinant in breast cancer initiation, progression and metastasis. *Cancer letters*, 289(2), pp.127–139.
- Machesky, L.M. & Li, A., 2010. Invasive filopodia promoting metastasis. *Communicative & Integrative Biology*, 3(3), pp.263–270.
- MacKay, J.L., Keung, A.J. & Kumar, S., 2012. A genetic strategy for the dynamic and graded control of cell mechanics, motility, and matrix remodeling. *Biophysical journal*, 102(3), pp.434–442.
- Maher, P. a et al., 1985. Phosphotyrosine-containing proteins are concentrated in focal adhesions and intercellular junctions in normal cells. *Proceedings of the National Academy of Sciences of the United States of America*, 82(19), pp.6576–6580.
- Matov, A. et al., 2010. Analysis of microtubule dynamic instability using a plus-end growth marker. *Nature methods*, 7(9), pp.761–768.
- Mejillano, M.R. et al., 2004. of the Actin Nanomachinery : Pivotal Role of the Filament Barbed End. *Cell*, 118, pp.363–373.
- Mellor, H., 2010. The role of formins in filopodia formation. *Biochimica et biophysica acta*, 1803(2), pp.191–200.
- Micalizzi, D., Farabaugh, S. & Ford, H., 2010. Epithelial-mesenchymal transition in cancer: parallels between normal development and tumor progression. *Journal of mammary gland biology and neoplasia*, 15(2), pp.117–134.
- Miller, A. L., 2004. The Abl-related gene (Arg) requires its F-actin-microtubule cross-linking activity to regulate lamellipodial dynamics during fibroblast adhesion. *The Journal of Cell Biology*, 165(3), pp.407–419.
- Mimori-Kiyosue, Y., Shiina, N. & Tsukita, S., 2000. Adenomatous polyposis coli (APC) protein moves along microtubules and concentrates at their growing ends in epithelial cells. *The Journal of Cell Biology*, 148(3), pp.505–518.

- Mitra, S.K. & Schlaepfer, D.D., 2006. Integrin-regulated FAK-Src signaling in normal and cancer cells. *Current opinion in cell biology*, 18(5), pp.516–523.
- Morrison, E.E., 2007. Action and interactions at microtubule ends. *Cellular and molecular life sciences*, 64(3), pp.307–317.
- Myers, K. et al., 2011. Distinct ECM mechanosensing pathways regulate microtubule dynamics to control endothelial cell branching morphogenesis. *The Journal of Cell Biology*, 192(2), pp.321–334.
- Nagano, M. et al., 2012. Turnover of focal adhesions and cancer cell migration. *International journal of cell biology*, 2012, pp.1-10.
- Nagano, M. et al., 2011. ZF21 is a new regulator of focal adhesion disassembly and a potential member of the spreading initiation center. *Cell adhesion & migration*, 5(1), pp.23–28.
- Nobes, C.D. & Hall, A., 1995. Rho, rac, and cdc42 GTPases regulate the assembly of multimolecular focal complexes associated with actin stress fibers, lamellipodia, and filopodia. *Cell*, 81(1), pp.53–62.
- Ono, S., 1996. Phosphorylation of Human Fascin Inhibits Its Actin Binding and Bundling Activities. *Journal of Biological Chemistry*, 271(21), pp.12632–12638.
- Palazzo, A.F. et al., 2004. Localized stabilization of microtubules by integrin- and FAK-facilitated Rho signaling. *Science*, 303(5659), pp.836–839.
- Palmer T.D. et al., 2011. Targeting tumour cell motility to prevent metastasis. *Adv Drug Deliver Rev*, 63(8), pp.568–581.
- Parri, M. & Chiarugi, P., 2010. Rac and Rho GTPases in cancer cell motility control. *Cell communication and signaling*, 8(23), pp.1-14.
- Parsons, M. & Adams, J., 2008. Rac regulates the interaction of fascin with protein kinase C in cell migration. *Journal of cell science*, 121(17), pp.2805–2813.
- Parsons, T., Horwitz, A.R. & Schwartz, M., 2010. Cell adhesion: integrating cytoskeletal dynamics and cellular tension. *Nature reviews. Molecular cell biology*, 11(9), pp.633–643.
- Pellegrin, S. & Mellor, H., 2007. Actin stress fibres. *Journal of cell science*, 120(20), pp.3491–3499.
- Perdiz, D. et al., 2011. The ins and outs of tubulin acetylation: More than just a post-translational modification? *Cellular Signalling*, 23(5), pp.763–771.
- Perez, F et al., 1999. CLIP-170 highlights growing microtubule ends in vivo. *Cell*, 96(4), pp.517–527.
- Perris, R. & Perissinotto, D., 2000. Role of the extracellular matrix during neural crest cell migration. *Mechanisms of development*, 95(1-2), pp.3–21.
- Ponting, C. & Russell, R., 2000. Identification of distant homologues of fibroblast growth factors suggests a common ancestor for all Î^2-trefoil proteins1. *Journal of Molecular Biology*, 302(5), pp.1041–1047.

- Pritchard, C.A. et al., 2004. B-Raf Acts via the ROCKII / LIMK / Cofilin Pathway To Maintain Actin Stress Fibers in Fibroblasts. *Molecular and Cellular Biology*, 24(13), pp.5937–5952.
- Provenzano, P.P. & Keely, P.J., 2009. The role of focal adhesion kinase in tumor initiation and progression. *Cell adhesion & migration*, 3(4), pp.347–350.
- Qin, Z., Kreplak, L. & Buehler, M.J., 2009. Nanomechanical properties of vimentin intermediate filament dimers. *Nanotechnology*, 20(42), p.425101-425110.
- Quinlan, R., Hutchison, C. & Lane, B., 1995. Intermediate filament proteins. *Protein profile*, 2(8), pp.795–952.
- Quintavalle, M. et al., 2010. MicroRNA control of podosome formation in vascular smooth muscle cells in vivo and in vitro. *The Journal of Cell Biology*, 189(1), pp.13–22.
- Redwine, W.B. et al., 2012. Structural basis for microtubule binding and release by dynein. *Science*, 337(6101), pp.1532–1536.
- Reinhart-King, C., 2008. Endothelial cell adhesion and migration. *Methods in enzymology*, 443, pp.45–64.
- Ridley, A.J., 2006. Rho GTPases and actin dynamics in membrane protrusions and vesicle trafficking. *Membrane Dynamics*, 16(10), pp.522–529.
- Ridley, A.J. et al., 2003. Cell migration: integrating signals from front to back. *Science*, 302(5651), pp.1704–1709.
- Ridley, A.J., 2011. Life at the leading edge. *Cell*, 145(7), pp.1012–1022.
- Rodriguez, O.C. et al., 2003. Conserved microtubule-actin interactions in cell movement and morphogenesis. *Nature cell biology*, 5(7), pp.599–609.
- Rohatgi, R. et al., 1999. The interaction between N-WASP and the Arp2/3 complex links Cdc42-dependent signals to actin assembly. *Cell*, 97(2), pp.221–31.
- Rooney, C. et al., 2010. The Rac activator STEF (Tiam2) regulates cell migration by microtubule-mediated focal adhesion disassembly. *EMBO reports*, 11(4), pp.292–8.
- Rørth, P., 2009. Collective cell migration. *Annual review of cell and developmental biology*, 25, pp.407–29.
- Sanz-Moreno, V. et al., 2008. Rac activation and inactivation control plasticity of tumor cell movement. *Cell*, 135(3), pp.510–523.
- Sanz-Moreno, V. et al., 2011. ROCK and JAK1 signaling cooperate to control actomyosin contractility in tumor cells and stroma. *Cancer cell*, 20(2), pp.229–245.
- Sanz-Moreno, V. & Marshall, C. J., 2009. Rho-GTPase signaling drives melanoma cell plasticity. *Cell cycle*, 8(10), pp.1484–1487.
- Schäfer, C. et al., 2010. The key feature for early migratory processes: Dependence of adhesion, actin bundles, force generation and transmission on filopodia. *Cell adhesion & migration*, 4(2), pp.215–225.

- Schober, J.M. et al., 2007. Microtubule-targeting-dependent reorganization of filopodia. *Journal of cell science*, 120(7), pp.1235–1244.
- Schober, M. et al., 2007. Focal adhesion kinase modulates tension signaling to control actin and focal adhesion dynamics. *The Journal of cell biology*, 176(5), pp.667–680.
- Schoumacher, M. et al., 2010. Actin, microtubules, and vimentin intermediate filaments cooperate for elongation of invadopodia. *The Journal of Cell Biology*, 189(3), pp.541–556.
- Scolz, M. et al., 2012. GTSE1 is a microtubule plus-end tracking protein that regulates EB1-dependent cell migration. *PloS one*, 7(12), pp.e51259-51276.
- Seong, J., Wang, N. & Wang, Y., 2013. Mechanotransduction at focal adhesions: from physiology to cancer development. *Journal of cellular and molecular medicine*, 17(5), pp.597-604.
- Shattil, S., Kim, C. & Ginsberg, M., 2010. The final steps of integrin activation: the end game. *Nature reviews. Molecular cell biology*, 11(4), pp.288–300.
- Shoeman, R.L. et al., 2001. Amino-terminal polypeptides of vimentin are responsible for the changes in nuclear architecture associated with human immunodeficiency virus type 1 protease activity in tissue culture cells. *Molecular biology of the Cell*, 12(1), pp.143–154.
- Small, J. V et al., 1998. Assembling an actin cytoskeleton for cell attachment and movement. *Biochimica et biophysica acta*, 1404(3), pp.271–281.
- Small, J. V et al., 1999. Cytoskeleton cross-talk during cell motility. *FEBS letters*, 452(1-2), pp.96–99.
- Small, V., Geiger, B., et al., 2002. How do microtubules guide migrating cells? *Nature reviews. Molecular cell biology*, 3(12), pp.957–964.
- Small, V., Stradal, T., et al., 2002. The lamellipodium: where motility begins. *Trends in cell biology*, 12(3), pp.112–120.
- Stehbens, S. & Wittmann, T., 2012. Targeting and transport: How microtubules control focal adhesion dynamics. *The Journal of Cell Biology*, 198(4), pp.481–489.
- Stradal, T.E.B. et al., 2004. Regulation of actin dynamics by WASP and WAVE family proteins. *Trends in cell biology*, 14(6), pp.303–311.
- Streuli, C. & Akhtar, N., 2009. Signal co-operation between integrins and other receptor systems. *The Biochemical journal*, 418(3), pp.491–506.
- Swiech, L. et al., 2011. CLIP-170 and IQGAP1 Cooperatively Regulate Dendrite Morphology. *The Journal of neuroscience*, 31(12), pp.4555–4568.
- Tamariz, E. & Grinnell, F., 2002. Modulation of Fibroblast Morphology and Adhesion during Collagen Matrix Remodeling. *Molecular Biology of the Cell*, 13, pp.3915–3929.
- Tan V.Y., 2013. Association of fascin-1 with mortality, disease progression and metastasis in carcinomas: systematic review and meta analysis. *BMC Medicine*, 11(1), pp. 1-52.

- Thiery, J.P., 2002. Epithelial-mesenchymal transitions in tumour progression. *Nature reviews. Cancer*, 2(6), pp.442–454.
- Tilghman, R.W. & Parsons, J.T., 2008. Focal adhesion kinase as a regulator of cell tension in the progression of cancer. *Seminars in cancer biology*, 18(1), pp.45–52.
- Tojkander, S., Gateva, G. & Lappalainen, P., 2012. Actin stress fibers--assembly, dynamics and biological roles. *Journal of cell science*, 125(8), pp.1855–1864.
- Tomar, A. et al., 2012. Cortactin as a Target for FAK in the Regulation of Focal Adhesion Dynamics. *PloS one*, 7(8), pp.e44041-4400..
- Tomar, A. & Schlaepfer, D.D., 2009. Focal adhesion kinase: switching between GAPs and GEFs in the regulation of cell motility. *Current opinion in cell biology*, 21(5), pp.676–683.
- Tominaga, T., 2005. The role of mDia in cytoskeletal organization. *Seikagaku. The Journal of Japanese Biochemical Society*, 77(2), pp.133–136.
- Tonami, K. et al., 2011. Calpain-6, a microtubule-stabilizing protein, regulates Rac1 activity and cell motility through interaction with GEF-H1. *Journal of cell science*, 124(8), pp.1214–1223.
- Toriyama, M. et al., 2012. Phosphorylation of doublecortin by protein kinase A orchestrates microtubule and actin dynamics to promote neuronal progenitor cell migration. *The Journal of biological chemistry*, 287(16), pp.12691–12702.
- Tran, A.D.-A. et al., 2007. HDAC6 deacetylation of tubulin modulates dynamics of cellular adhesions. *Journal of cell science*, 120(8), pp.1469–1479.
- Turner, C.E., 2000. Paxillin and focal adhesion signalling. *Nature Cell Biology*, 2(12), pp.231-236.
- Ucar, D.A. et al., 2012. Inhibiting the Interaction of cMET and IGF-1R with FAK Effectively Reduces Growth of Pancreatic Cancer Cells in Vitro and in Vivo. *Anti-cancer agents in medicinal chemistry*, 11(17), pp.3250-3259.
- Ueda, M. et al., 1997. Centrosome positioning and directionality of cell movements. *Proceedings of the National Academy of Sciences of the United States of America*, 94(18), pp.9674–9678.
- Van Rheenen, J., Condeelis, J. & Glogauer, M., 2009. A common cofilin activity cycle in invasive tumor cells and inflammatory cells. *Journal of cell science*, 122(3), pp.305–311.
- Vega, F.M. et al., 2012. RhoB regulates cell migration through altered focal adhesion dynamics. *Open biology*, 2(5), p.120076-120086.
- Vega, F.M. & Ridley, A.J., 2008. Rho GTPases in cancer cell biology. *FEBS letters*, 582(14), pp.2093–2101.
- Vignjevic, D. et al., 2006. Role of fascin in filopodial protrusion. *The Journal of cell biology*, 174(6), pp.863–875.
- Villalonga, P. & Ridley, A.J., 2006. Rho GTPases and cell cycle control. *Growth factors (Chur, Switzerland)*, 24(3), pp.159–164.

- Walcott, S. & Sun, S.X., 2010. Active force generation in cross-linked filament bundles without motor proteins. *Physical review.* 82(5-1), pp.050901-050904.
- Walcott, S. & Sun, S.X., 2010. A mechanical model of actin stress fiber formation and substrate elasticity sensing in adherent cells. *PNAS*, 107(17), pp.7757–7762.
- Wang, Q. et al., 2001. Sites of nucleic acid binding in type I-IV intermediate filament subunit proteins. *Biochemistry*, 40(34), pp.10342–10349.
- Wang, Yu et al., 2011. A direct interaction between the large GTPase dynamin-2 and FAK regulates focal adhesion dynamics in response to active Src. *Molecular biology of the Cell*, 22(9), pp.1529–38.
- Webb, D. et al., 2004. FAK-Src signalling through paxillin, ERK and MLCK regulates adhesion disassembly. *Nature Cell Biology*, 6(2), pp.154–161.
- Webb, D.J., Parsons, J.T. & Horwitz, A.F., 2002. Adhesion assembly, disassembly and turnover in migrating cells -- over and over and over again. *Nature cell biology*, 4(4), pp.E97–100.
- Wehrle-Haller, B. & Imhof, B., 2003. Actin, microtubules and focal adhesion dynamics during cell migration. *The international journal of biochemistry & cell biology*, 35(1), pp.39–50.
- Wen, Y. et al., 2004. EB1 and APC bind to mDia to stabilize microtubules downstream of Rho and promote cell migration. *Nature Cell Biology*, 6(9), pp.820–830.
- Wilson, L. & Jordan, M.A., 2004. New microtubule/tubulin-targeted anticancer drugs and novel chemotherapeutic strategies. *Journal of chemotherapy*, 16 (4), pp.83–85.
- Wittmann, T & Waterman-Storer, C M, 2001. Cell motility: can Rho GTPases and microtubules point the way? *Journal of cell science*, 114(21), pp.3795–3803.
- Wolf, K., Müller, R., et al., 2003. Amoeboid shape change and contact guidance: T-lymphocyte crawling through fibrillar collagen is independent of matrix remodeling by MMPs and other proteases. *Blood*, 102(9), pp.3262–3269.
- Wolf, K., Mazo, I., et al., 2003. Compensation mechanism in tumor cell migration: mesenchymal-amoeboid transition after blocking of pericellular proteolysis. *The Journal of cell biology*, 160(2), pp.267–277.
- Worth, D.C. & Parsons, M., 2010. Advances in imaging cell-matrix adhesions. *Journal of cell science*, 123(21), pp.3629–3638.
- Wu, X. et al., 2011. Skin Stem Cells Orchestrate Directional Migration by Regulating Microtubule-ACF7 Connections through GSK3β. *Cell*, 144(3), pp.341–352.
- Yang, S. et al., 2012. Molecular Mechanism of Fascin Function in Filopodial Formation. *The Journal of biological chemistry*, 288(1), pp. 274-284.

- Yoshigi, M. et al., 2005. Mechanical force mobilizes zyxin from focal adhesions to actin filaments and regulates cytoskeletal reinforcement. *The Journal of cell biology*, 171(2), pp.209–15.
- Zaidel-Bar, R., 2009. Evolution of complexity in the integrin adhesome. *The Journal of Cell Biology*, 186(3), pp.317–321.
- Zalevsky, J. et al., 2001. Different WASP family proteins stimulate different Arp2/3 complex-dependent actin-nucleating activities. *Current biology*, 11(24), pp.1903–1913.
- Zanet, J. et al., 2012. Fascin promotes filopodia formation independent of its role in actin bundling. *The Journal of Cell Biology*. 197(4), pp. 477.486.
- Zanet, J. et al., 2009. Fascin is required for blood cell migration during Drosophila embryogenesis. *Development*, 136(15), pp.2557–2565.
- Zaoui, K. et al., 2010. ErbB2 receptor controls microtubule capture by recruiting ACF7 to the plasma membrane of migrating cells. *Proceedings of the National Academy of Sciences of the United States of America*, 107(43), pp.18517–18522.
- Zhang, F.-R. et al., 2008. Fascin expression in human embryonic, fetal, and normal adult tissue. *The journal of histochemistry and cytochemistry*, 56(2), pp.193–199.
- Zhang, X. et al., 2007. HDAC6 modulates cell motility by altering the acetylation level of cortactin. *Molecular cell*, 27(2), pp.197–213.
- Zhou, F.-Q., Waterman-Storer, C. & Cohan, C., 2002. Focal loss of actin bundles causes microtubule redistribution and growth cone turning. *The Journal of Cell Biology*, 157(5), pp.839–849.
- Van Zijl, F., Krupitza, G. & Mikulits, W., 2011. Initial steps of metastasis: cell invasion and endothelial transmigration. *Mutation research*, 728(1-2), pp.23–34.
-